Enzymatic and Biochemical Analysis of the Hsp90 Chaperone: Regulation by Co-chaperones, SUMOylation, and Interdomain Dynamics

by

Annemarie Wolmarans

A thesis submitted in partial fulfillment of the requirements for the degree of

Doctor of Philosophy

Department of Cell Biology
University of Alberta

Abstract

Hsp90 is an essential eukaryotic molecular chaperone that plays a critical role in protein folding. It regulates the stability, maturation, and activation of numerous client proteins, many of which are involved in oncogenesis. It has been well established that Hsp90 is tightly regulated by co-chaperone proteins and post-translational modifications (PTMs) in the context of an ATP-driven, functional cycle. Although Hsp90 is a homodimeric ATPase, growing evidence suggest that it functions as an asymmetric machine, where each subunit becomes individually functionalized when co-chaperones and clients bind, or when PTMs occur. Much remains to be elucidated about how these asymmetric interactions and modifications influence Hsp90 function.

The goal of my thesis was to define a biochemical and mechanical model for the asymmetric interactions of co-chaperones with Hsp90 and how they regulate the ATPase activity of Hsp90. Various Hsp90 mutants were used in the context of homodimers and heterodimers in ATPase assay to conduct in-depth analyses on how co-chaperones regulate Hsp90 activity. Specifically, I demonstrated that co-chaperones exert different effects on Hsp90 depending on which subunit they bind and proposed a model outlining the mechanism of Aha1p-mediated stimulation of Hsp90 ATPase activity. How asymmetric SUMOylation of Hsp90 influence co-chaperone regulation of the ATPase activity of Hsp90 was also addressed. This was achieved by developing a novel strategy to chemically couple SUMO to Hsp90 *in vitro*. My analysis revealed that chemically

SUMOylated Hsp90 recapitulates the selectivity of co-chaperone binding that is observed *in vivo*, mainly Aha1p-recruitment, but also demonstrated that SUMOylation impairs Sba1p regulation. Lastly, I investigated the conformational dynamics of Hsp90 by restricting interdomain rearrangements of Hsp90 using linker truncation mutants. These analyses brought novel insight into which Hsp90 conformations favor Aha1p and/or Sba1p binding.

My work provides a framework to integrate subunit-specific interactions of co-chaperones and PTMs to further elucidate how the functional cycle of Hsp90 is regulated. It is crucial to understand how Hsp90 functions at a molecular level to advance the development of therapeutics that target the Hsp90 system.

Preface

The work presented in this thesis was conducted in the Department of Cell Biology at the University of Alberta, under the guidance and supervision of Dr. Paul LaPointe. Chapter 3 of this thesis has been published as "Wolmarans, A., Lee, B., Spyracopoulos, L., and LaPointe, P. *The Mechanism of Hsp90 ATPase Stimulation by Aha1*. Sci. Rep. 6, 33179; doi: 10.1038/srep33179 (2016)". With the exception of the NMR experiments that were conducted in collaboration with Dr. Leo Spyracopoulos and Dr. Brian Lee, in the Department of Biochemistry, all the work presented in this thesis is my own.

Acknowledgements

I would first like to sincerely thank my supervisor, Dr. Paul LaPointe, for his guidance and support throughout my graduate degree. His passion and enthusiasm for science and problem solving has led to many stimulating discussions which inspired and motivated me to become a better scientist. Thank you for challenging me in my studies while also encouraging me to pursue all my interests – for that I will always be grateful.

Thank you to the members of my supervisory committee, Dr. Sarah Hughes and Dr. Ing Swie Goping, for their intellectual insights on my projects and their mentorship. Additionally, I want to thank Dr. Gary Eitzen and Dr. Dennis Stuehr for serving on my examining committee and for providing valuable feedback.

Thank you to the Department of Cell Biology along with the Faculty of Medicine and Dentistry, the Faculty of Graduate Studies and Research, and the Graduate Students' Association for financial support. I would also like to express my appreciation to the Cell Biology department– to all the faculty, staff, and students – for establishing such a strong learning environment.

My experience as a graduate student at University of Alberta have been formative to my growth as an academic. I had the honor of working with the members of the LaPointe lab and this enjoyable experience will always be part of my journey. I especially want to thank Rebecca Mercier, Heather Armstrong, and Katie Horvat for their remarkable friendship. Thank you for your valuable feedback and advice on experiments and on my thesis, but also for all our coffee breaks and visits over the years – they have been instrumental in my well-being!

I am blessed with incredible friends and family. Without them, this thesis would not have been possible and I thank you all for supporting me in various way.

To my supportive and loving parents, I cannot say thank you enough for everything you have done for me. You have been in my corner from day one and your unwavering confidence in me has given me the drive to be where I am today.

To my brother and sister-in-law, Siam and Kayleigh, thank you for all the advice, pep talks, and friendship. “Ja nee”… just remember, Siam, I did mention you in my thesis!

I also want to thank my in-laws for their love, support, and encouragement throughout my studies over the last 10 years.

Last, but certainly not least, I would like to thank my husband and best friend, Drikkie. You have been the greatest gift from God to me. Thank you for your never-ending encouragement, patience, and love.

Table of Contents

List of Tables

List of Figures

List of Abbreviations

σ	Standard deviation
ADP	Adenosine diphosphate
AMP	Ampicillin
AMPPNP	Adenylyl-imidodiphosphate
AUC	Analytical Ultracentrifugation
β-ME	β-mercaptoethanol
BMOE	Bismaleimidoethane
BSA	Bovine serum albumin
CFTR	Cystic fibrosis transmembrane conductance regulator
CF	Cystic fibrosis
DMSO	Dimethyl sulfoxide
DNA	Deoxyribonucleic acid
dNTP	Deoxyribonucleotide triphosphate
DPBS	Dulbecco's phosphate buffered saline
DTT	Dithiothreitol
ECL	Enhanced chemiluminescence
E. coli	*Escherichia coli*
EDTA	Ethylene-diamine-tetraacetic acid
EM	Electron microscopy
FPLC	Fast protein liquid chromatography
FRET	Fluorescence resonance energy transfer
GA	Geldanamycin
GHKL	Gyrase, Hsp90, Histidine Kinase, and MutL
GR	Glucocorticoid receptor
HCl	Hydrochloric acid
HexaHis	Histidine tag
HRP	Horseradish peroxidase
Hsp	Heat shock protein
Hsp90	Heat shock protein 90

Hsp70	Heat shock protein 70
Hsp40	Heat shock protein 40
IgG	Immunoglobulin G
IMAC	Immobilized metal affinity chromatography
IMAC A	Immobilized metal affinity chromatography buffer A
IMAC B	Immobilized metal affinity chromatography buffer B
IPTG	Isopropyl-β-D-thiogalactopyranoside
IP	Immunoprecipitation
kDa	Kilodaltons
LB	Luria broth
NADH	Nicotinamide adenine dinucleotide
NaOH	Sodium hydroxide
NEB	New England BioLabs
NMR	Nuclear magnetic resonance
NVP	NVP-AUY922
O.D.	Optical density
PCR	Polymerase chain reaction
PK/LDH	Pyruvate kinase/ lactate dehydrogenase
SDS	Sodium dodecyl sulfate
SDS-PAGE	Sodium dodecyl sulfate polyacrylamide gel electrophoresis
SHR	Steroid hormone receptor
TAE	Tris base, acetic acid, EDTA solution
TBS	Tris-buffered saline solution
TEMED	Tetramethylethylenediamine
ts	Temperature sensitive
TPR	Tetratricopeptide repeat
WT	Wildtype

Chapter 1

Introduction

1.1 Protein folding and stability

Proteins are essential biomolecules that are involved in many cellular processes and carry out a multitude of functions to sustain life. Protein folding is a fundamental process by which proteins adopts their three-dimensional structures from linear chains of amino acids to fulfil their biological functions (Dobson and Ellis, 1998; Hartl, 1996; Hartl, 2011). The question of how proteins fold efficiently, rapidly, and essentially uncatalyzed, has plagued scientists for over 40 years (Dill and MacCallum, 2012). This complex process is thought to be ultimately driven by thermodynamic principles (Anfinsen, 1973). Experimental advances over the past decade have revealed insight into how cells support protein folding, expanding our understanding of protein homeostasis.

The function of a protein is dictated by its three-dimensional structure, which in turn is determined by the primary amino acid sequence (Anfinsen, 1973). A nascent polypeptide chain first acquires fundamental elements of secondary structure according to intramolecular interactions between side chains of adjacent amino acids (Anfinsen, 1973; Dinner et al., 2000). These elements of alpha helices and beta strands spontaneously assemble into higher order tertiary structures that define the native state. In biochemistry, this 'native' state of the protein is known as the fully folded, functional form, but it is more accurately described as an ensemble of distinct states that are in dynamic equilibrium under normal conditions (Dobson and Ellis, 1998). This view of protein folding postulates that the pathway towards the 'native' fold is not linear or deterministic but rather characterized by stochastic sampling of numerous conformations that is guided by the energy landscape (Bryngelson et al., 1995; Bryngelson and Wolynes, 1987).

Acquiring this structure can be a difficult process in many ways. The ensemble of conformations that defines the native state is preceded by numerous intermediate conformations that are often characterized by exposed hydrophobic side chains (Ellis, 2001). Interactions between hydrophobic side chains are very strong and ordinarily form the desolvated core of a folded protein. However, interactions between such hydrophobic surfaces can lead to irreversible aggregation

and loss of protein function (Dobson and Ellis, 1998; Hartl, 1996; Zou et al., 1998). Models for protein folding are based on idealized *in vitro* conditions where protein concentrations are low which disfavors intermolecular interactions. In cells, however, proteins are continuously synthesized in the cytosol of the cell, where intracellular environment protein concentrations are at a steady state of around 200-400 mg/mL (Ellis, 2001; Martin, 2004). In addition to the crowded cellular environment, there are a multitude of factors influencing the energetic landscape of a folding polypeptide chain including environmental factors such as temperature, ionic strength, and pH (Dill and Chan, 1997; Dinner et al., 2000). Thus, the energy landscape has the potential to be completely different for the same protein depending on the various environmental factors.

Cellular stress and environmental insults negatively influences the folding dynamics of proteins and drastically increases the propensity of proteins to make inappropriate hydrophobic interactions (Buchner, 1996; Hartl, 1996). If proteins expose their hydrophobic surfaces, misfolding and aggregation will occur (Zou et al., 1998). Misfolding and aggregation of proteins leads to loss of protein function and toxicity which are heavy burdens on the cells. Protein aggregates are toxic to the cell partly because of their ability to promote misfolding in other proteins, but also because they alter cell signaling by triggering stress response pathways (Ellis and van der Vies, 1991; Morimoto, 2008; Pastore and Temussi, 2012; Whitesell and Lindquist, 2005). In order to maintain the integrity of the proteome, or proteostasis, cells employ extensive quality control networks (Hartl, 1996; McClellan et al., 2005). Cellular proteostasis refers to the numerous quality control networks that collaborate to ensure proper protein synthesis, folding and assembly, unfolding, and turnover. Central components of these quality control networks are molecular chaperones that facilitate protein folding (Kim et al., 2014).

1.2 Molecular chaperones

1.2.1 *Discovery and function of molecular chaperones*

Molecular chaperones are a large and diverse group of proteins that are present in all types of cells and compartments. The term 'molecular chaperone' was first used to describe a nuclear protein (nucleoplasmin) that was found to be required for the folding of nucleosome cores (Laskey et al., 1978). This term was further defined to describe the multitude of roles molecular chaperones have in maintaining proteostasis (Ellis, 1996; Ellis and van der Vies, 1991). Molecular chaperones mediate refolding of misfolded proteins, stabilize protein folding intermediates, prevent inappropriate intramolecular and intermolecular interactions, and help newly synthesized proteins adopt their biologically active conformations (Ellis et al., 2007; Hartl, 2011; Mayer and Bukau, 1999).

The process of protein folding is essential as incorrect folding can lead to protein aggregation or degradation which results in non-functional protein structures (Dobson and Ellis, 1998; Hartl, 1996). Errors in protein folding have been associated with the development of certain disease states including cystic fibrosis and neurodegeneration (Fraser-Pitt and O'Neil, 2015; Knowles et al., 2014; Macario and Conway de Macario, 2005). Molecular chaperones are critical determinants of the balance between folding and degradation and closely cooperate with the ubiquitin-proteasome system to maintain homeostasis (McClellan et al., 2005). When substrate proteins fail to fold correctly due to environmental perturbations, cellular stress, or mutations in the primary sequence, these misfolded proteins are targeted to the proteasome for degradation (Young et al., 2003).

1.2.2 Heat shock proteins; the stress chaperones

A specific class of molecular chaperones, termed heat shock proteins (HSPs), are upregulated during cellular stress (Ellis and van der Vies, 1991). Ferruccio Ritossa was the first to identify HSPs, describing how temperature shock resulted in a characteristic pattern of chromosome puffs in the salivary gland of *Drosophila melanogaster,* suggesting that elevated temperatures induce a specific

change in gene expression (Ritossa, 1962). Ritossa described HSPs as proteins that are dramatically upregulated through the heat shock response (HSR) (Ritossa, 1962). This demonstrates HSPs' important role in preventing misfolding and aiding in refolding of proteins during cellular stress such as heat shock, oxidative stress, and hypoxia (Ellis, 2007). Cells employ HSP chaperones as part of their response network against these stress circumstances but they also play a variety of roles within a normal cell environment.

HSPs are classified into six different groups that are based on their respective molecular weights: Hsp100, Hsp90, Hsp70, Hsp60, Hsp40 and the small Hsps (Verghese et al., 2012). The most well studied family of heat shock proteins is the Hsp70 family whose members collaborate with other chaperones, such as Hsp40 and Hsp90, in distinct functional networks to promote protein folding, transport, and degradation (Kampinga and Craig, 2010; Morano, 2007; Proctor and Lorimer, 2011; Ran et al., 2008; Smith, 1993). Hsp70 functions similar to most canonical chaperones which has a high affinity for short stretches of hydrophobic or aromatic residues that are exposed during synthesis, unfolded under stress conditions, or while native proteins sample intermediate conformations (Rudiger et al., 1997). By reversibly binding hydrophobic regions of unfolded proteins, Hsp70 prevents inappropriate and irreversible intra-and inter-molecular hydrophobic interactions that can occur. Hsp40 assist Hsp70 through recruiting and stabilizing substrate-bound complexes (McCarty et al., 1995; Szabo et al., 1994). Interestingly, both Hsp70 and Hsp90 contain docking motifs that are utilized by regulatory proteins, or co-chaperone proteins, to coordinate their chaperone functions such as substrate transfer from the Hsp70 system to Hsp90 (Scheufler et al., 2000; Young et al., 2003). In contrast to Hsp70, Hsp90 is thought to bind specific secondary or tertiary structures of partially or fully folded proteins after hydrophobic regions have been largely hidden (Figure 1.1) (Pearl and Prodromou, 2000). While all proteins are generally thought to be subject to the Hsp70 chaperone, a small subset of proteins are Hsp90 substrates (Picard, 2002). Hsp90 regulates the folding, maturation, stability, and activation of these non-nascent substrate proteins (Pearl

and Prodromou, 2000; Taipale, M. et al., 2010; Zhao et al., 2005). How Hsp90 activity contributes to client protein activation is not fully understood.

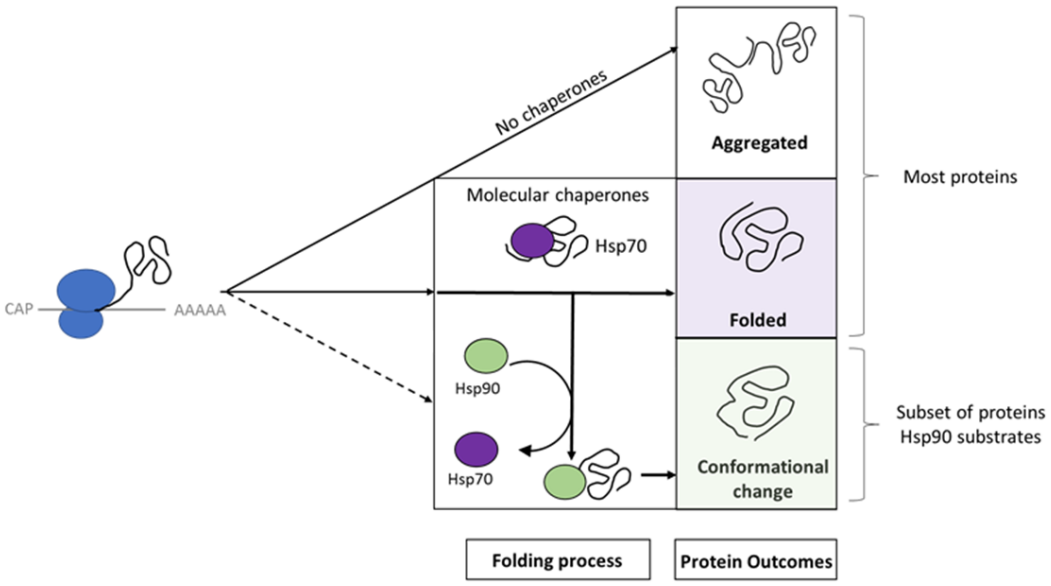

Figure 1.1 The role of molecular chaperones in protein folding. Hsp90 binds to non-nascent proteins, or early folding intermediates. Hsp90 chaperones a subset of proteins while canonical chaperones, such as Hsp70, prevent aggregation and promote folding by binding hydrophobic stretches of newly synthesized proteins (Picard, 2002).

1.3 The 90 kDa Heat shock protein (Hsp90)

Like many chaperone types, Hsp90 is ubiquitously expressed across prokaryotic and eukaryotic species, but is only essential for the viability of eukaryotic cells (Birnby et al., 2000; Borkovich et al., 1989; van der Straten et al., 1997). It is a highly conserved and abundant molecular chaperone that plays a critical role in maintaining cellular homeostasis (Echeverria et al., 2011b; Taipale, M. et al., 2010). Hsp90 accounts for 1-2 % of all cytoplasmic protein under normal physiological conditions and is upregulated during cellular stress (Borkovich et al., 1989; Nathan et al., 1997). There are two highly homologous isoforms of Hsp90 found in the cytosol of most eukaryotes that were once thought to be functionally identical but are now known to be regulated differently at the transcriptional level. Specifically, human cells possess Hsp90β and Hsp90α, which are the constitutively expressed isoform and the heat inducible isoform, respectively (Ammirante et al., 2008). Despite their high degree of conservation (86 % amino acid identity), the fact that Hsp90β is essential, but not Hsp90α, demonstrates their different functions in cells (Grad et al., 2010; Voss et al., 2000; Zuehlke et al., 2015). In *Saccharomyces cerevisiae*, the two homologous genes that code for cytosolic Hsp90 are *HSC82* and *HSP82*, where Hsc82p is the constitutively expressed isoform and Hsp82p is the highly heat-inducible isoform that is markedly upregulated during cellular stress (Borkovich et al., 1989; Csermely et al., 1998; Lindquist and Craig, 1988). Higher eukaryotic species have up to four Hsp90 homologs that are found in different subcellular compartments. These include the two cytosolic Hsp90 homologs along with TRAP1 (tumor necrosis factor receptor-associated protein 1) which is found in the mitochondria and GRP94 (94 kDa glucose-regulated protein) which is found in the endoplasmic reticulum (ER).

Hsp90 was previously thought to be involved in *de novo* folding of proteins, similar to the function Hsp70 has, due to its ability to prevent inappropriate and irreversible interactions of denatured proteins *in vitro* (Hartl, 1996; Jacobs et al., 2007; Matts et al., 2011; Miyata and Yahara, 1992; Morimoto, 2008; Nemoto et al., 2001). Nathan *et al.* postulated, however, that Hsp90 has a more specific role *in*

vivo as it protects difficult to fold substrate proteins (Nathan et al., 1997). It is now understood that Hsp90 regulates the maturation and stability of substrate proteins, termed client proteins, as they require Hsp90 chaperone activity to obtain their active conformation (Borkovich et al., 1989; Nathan et al., 1997; Taipale, H.T. et al., 2010). Hsp90 is a dimeric ATPase and chaperones client proteins through its functional ATPase cycle which will be discussed in further detail in later sections.

Throughout this thesis, I will refer to the protein of interest as Hsp90 when discussing it in general terms, and I will refer to it as Hsp82p (or as another homolog name) when discussing it in more specific terms. These terms (Hsp90/Hsp82p) will be used interchangeably in certain sections.

1.4 Hsp90 client proteins

1.4.1 Classification of Hsp90 clients

Hsp90 interacts with an extensive and diverse set of client proteins. More than 500 clients have been identified, with an up-to-date, and growing list available online: (http://www.picard.ch/downloads/Hsp90interactors.pdf) (Echeverria et al., 2011a; Picard, 2002). Hsp90 client proteins are involved in numerous cellular processes such as receptor activation, cell signal transductions, and cell cycle regulation (Richter et al., 2001; Taipale, M. et al., 2010; Wandinger et al., 2008; Young et al., 2001). Client proteins can be divided into two main classes: protein kinases (such as Src family kinases, ErbB2, and Bcr-Abl) and transcription factors including the steroid hormone receptors (SHR) (such as the glucocorticoid and estrogen receptor) (Roe et al., 2004; Taipale, M. et al., 2010; Wandinger et al., 2008). Although not commonly regarded as a class, there is technically a third class of client proteins, which consists of structurally non-related proteins. The molecular basis of how Hsp90 recognizes this diverse set of clients is unknown despite intense study. Unlike other chaperones that recognize unfolded polypeptides, no unifying sequence or structural similarities have been identified within client proteins that Hsp90 recognizes (Citri et al., 2006; Taipale, M. et al., 2010; Xu et al., 2005; Zhao et al., 2005). In fact, there are many sets of structurally and functionally related

proteins where only some members are subject to Hsp90 regulation, for example Hsp90 binds more strongly to protein tyrosine kinase ErbB2 than EGFR (Xu et al., 2001; Xu et al., 2005). Even with the substrate pool being so diverse, Hsp90 still shows such specificity for its clients which suggests a stringent selection mechanism.

1.4.2 Discovery of Hsp90 clients; kinases

Hsp90 functions in an ATPase driven cycle. It was shown that the ATPase activity of Hsp90 can be inhibited through the use of agents that bind to the nucleotide-binding region (Prodromou et al., 1997; Whitesell et al., 1994). These agents were initially thought to be tyrosine kinase inhibitors because they could reverse cellular transformation induced by kinases v-*Src*, ErbB2, C-raf, and Akt (Banerji et al., 2005; Workman et al., 2007; Xu et al., 2001). It is now, however, understood that these agents target Hsp90 and effectively prevent maturation of client kinases.

Some kinases, such as *Src*, are characterized by stable 'off' conformations and labile 'on' conformations (Xu and Lindquist, 1993). *Src* activity is regulated conformationally by phosphorylation events. *Src* is in its stable conformation when phosphorylated at Tyr527, which is an Hsp90-independent state. The labile 'on' state of *Src* is achieved when Tyr527 is dephosphorylated and Tyr416 is phosphorylated. Hsp90 stabilizes this 'on' conformation and is exemplified by the constitutively active viral form of *Src*, v-*Src*, which is lacking the C-terminal regulatory segment (Falsone et al., 2004). The stability of v-*Src* is completely dependent on Hsp90 and requires Hsp90 to stabilize the 'on' conformation immediately following protein activation, otherwise v-*Src* would be recognized as unfolded by extensive cellular machinery, ubiquitinated, and delivered to the proteasome to be degraded (Whitesell et al., 1994; Xu and Lindquist, 1993).

1.4.3 Other Hsp90 clients

As mentioned earlier, not all Hsp90 clients are kinases. Steroid hormone receptors (SHR) are the most thoroughly studied client proteins of Hsp90 and

include the glucocorticoid and estrogen receptors. The receptors are activated by binding steroid hormones, a process that is Hsp90-dependent. This became evident when Hsp90 was identified to be only in complex with the apo form and not the ligand bound form of a SHR (Sanchez et al., 1988). Hsp90 facilitates the ligand-binding domain of SHR in acquiring a conformation that is capable of binding the ligand. Upon ligand binding, the receptor dissociates from Hsp90, translocates to the nucleus, and regulates target gene expression (Picard, 2006). Another model Hsp90 client is the chloride ion channel, cystic fibrosis transmembrane conductance regulator (CFTR). CFTR was implicated as being Hsp90-dependent when Hsp90 inhibitor drugs prevented proper maturation of CFTR (Loo et al., 1998). Mutations in the CFTR gene causes cystic fibrosis (CF), with the most common form of the disease linked to a single amino acid deletion, ΔF508 (Collins, 1992). The resulting gene product of this mutation fails to fold in the ER, leading to its degradation, and thus, a loss of the functional channel at cell surface is observed (Riordan, 2005). Interestingly, the folding defect of ΔF508 CFTR can be overcome by manipulating the Hsp90 system. By silencing a co-chaperone of Hsp90, Aha1p, ΔF508 is stabilized and cell surface activity is restored (Koulov et al., 2010; Wang et al., 2006a).

Client proteins may reside for a considerable amount of their lifetime in Hsp90 complexes (Mayer and Le Breton, 2015). Recently, it has been shown that the dwell times of clients in specific conformations leads to proper maturation (Zierer et al., 2016). Regulatory proteins called co-chaperones not only mediate the ability of Hsp90 to engage with such diverse clients, but it also influences the conformational dynamics of Hsp90 which lead to client maturation (Hessling et al., 2009; Mickler et al., 2009; Prodromou, 2012; Rohl et al., 2013). Co-chaperone proteins are intricately involved in the regulation of the Hsp90 ATPase cycle which will be discussed in detail in later sections.

1.5 Targeting Hsp90

Many of the client proteins Hsp90 stabilizes are oncoproteins which are involved in cell proliferation as well as the development and progression of cancer (Whitesell and Lindquist, 2005). It was shown that Hsp90 sequesters unstable and mutated oncoproteins, stabilizing and protecting them from being degraded (Taipale, M. et al., 2010; Trepel et al., 2010; Whitesell et al., 1994). Therefore, oncoproteins depend on the chaperone activity of Hsp90 for their maturation and stabilization, making cancer cells highly sensitive to Hsp90 inhibition. Hsp90 has become a promising therapeutic target in the battle against cancer with more than a dozen Hsp90 inhibitors in clinical trials against a range of cancers (Sidera and Patsavoudi, 2014).

The first Hsp90 inhibitor shown to target Hsp90, geldanamycin (GA), was identified in the mid 1990's (Whitesell et al., 1994). Initially, GA was classified as an antitumor agent that showed potent activity in an *in vitro* screen, achieving 50 % growth inhibition at low concentrations against majority of cancer cell lines (DeBoer et al., 1970; Supko et al., 1995). It was thought to be a tyrosine kinase inhibitor because GA was able to reverse the transformed phenotype of fibroblasts that were transformed by oncogenic kinases such as v-*Src* (DeBoer et al., 1970; Uehara et al., 1988). However, GA was unable to inhibit the kinase activity of v-*Src in vitro* (Whitesell et al., 1994). Subsequently, Hsp90 was recognized as the target of GA (Whitesell et al., 1994). GA was later classified as an ATP-competitive inhibitor once GA was crystalized bound to the N-terminal domain of human Hsp90 (Roe et al., 1999; Stebbins et al., 1997). Structural and biochemical studies of the Hsp90 inhibitors have since demonstrated they competitively bind to the N-terminal ATP pocket, which effectively blocks the maturation of client proteins and leads to their degradation via the proteasome pathway (Blagg and Kerr, 2006; Neckers, 2006; Roe et al., 2004; Schneider et al., 1996; Whitesell et al., 1994). The initial Hsp90 ATP-competitive inhibitors were naturally occurring substances (Uehara et al., 1988). For example, both GA and herbimycin-A are benzoquinone ansamycin antibiotics isolated from *Streptomyces hygroscopicus* (Cooper, 2000;

He, W. et al., 2006; Roe et al., 1999; Yang et al., 2006). Although these inhibitors display antitumor effects, they exhibit extremely poor solubility, toxicity, and in the case of radicicol, also show instability and chemical reactivity (Cooper, 2000; He, W. et al., 2006; Roe et al., 1999; Yang et al., 2006). The off-target effects of these naturally occurring products is also problematic. Analysis of the distinctive ATP binding site of Hsp90 has resulted in the development of more potent and specifically designed inhibitors with better toxicology, such as the semisynthetic GA-derivatives, 17-allylamino-17-demethoxygeldanamycin (17-AAG) and 17-dimethylaminoethylamino-17demethocygeldanamycin (17- DMAG) (Smith et al., 2005; Solit et al., 2008; Solit et al., 2002). Semisynthetic analogues showed promising activity in clinical trials with increased affinity for Hsp90 in cancer cells (Kamal et al., 2003; Sydor et al., 2006; Xie et al., 2011). There is a new generation of Hsp90 inhibitors which include small synthetic molecules that were either identified in high-throughput screens or were specifically structure-based designed (Dymock et al., 2005; Proisy et al., 2006). The new generation inhibitors can be classified in various 'scaffold' classes, such as the purine-scaffold derivatives (PU-class). The Hsp90 inhibitor NVP-AUY922 is an optimized small synthetic inhibitor that binds to the ATP binding pocket of Hsp90 with greatly improved specificity and high affinity (Brough et al., 2008). It also proved to have more favorable pharmacological properties such as increased potency and high solubility (Brough et al., 2008).

Drugs targeting Hsp90 have shown to have anticancer properties in many animal models and several of these inhibitors demonstrated selective and high affinity binding to Hsp90 in cancer cells compared to normal cells (He, H. et al., 2006; Kamal et al., 2003). For example, the Hsp90 inhibitors 17-AAG and PU-scaffold derivatives have at least a 100-fold higher affinity for Hsp90 in cancer cells than normal cells (He, H. et al., 2006; Kamal et al., 2003). Moreover, these cancer cells are more sensitive to Hsp90 inhibitors than normal cells. Hsp90 is needed to stabilize the mutated proteins making cancer cells more susceptible to decreased Hsp90 activity, but why Hsp90 inhibitors accumulate in tumor cells is not fully understood (Chiosis and Neckers, 2006).

It is crucial to understand how Hsp90 functions at a molecular level to advance the development of therapeutics that target Hsp90 as potential treatment options for disease (Neckers, 2006; Powers and Workman, 2006). It is also important to study how regulatory proteins, such as co-chaperones, influence Hsp90 drug sensitivity to Hsp90 inhibitors. With the discovery that silencing co-chaperones such as Aha1, p23, or Cdc37 results in an increase in sensitization to Hsp90 inhibitors, more emphasis has been placed on targeting these regulators, in addition to Hsp90, which will be discussed in a later section (Forafonov et al., 2008; Gray et al., 2007; Holmes et al., 2008; McDowell et al., 2009).

1.6 Structural details of Hsp90

Hsp90 is a member of the evolutionary conserved gyrase-Hsp90-hisidine kinase MutL (GHKL) superfamily and functions as an obligate homodimeric ATPase (Panaretou et al., 1998). Hsp90 is a large and flexible protein and can undergo many global conformational rearrangements. Each 90 kDa monomer, or subunit, is comprised of three domains; an N-terminal nucleotide binding domain, a middle client binding domain, and a C-terminal dimerization domain (Prodromou et al., 1997; Richter et al., 2002; Scheibel et al., 1998). The N-terminal and middle domains are joined by a charged linker whose length varies among homologs (Hainzl et al., 2009; Johnson, 2012; Tsutsumi et al., 2012). Due to the large size of Hsp90 and the difficulties crystalizing a flexible protein, crystal structures of the individual domains of Hsp90 were solved prior to the full-length protein. Furthermore, the only full-length structure of Hsp90 is of a highly modified inhibited conformation (Ali et al., 2006). Initial structural homology studies revealed a lot about the mechanics of Hsp90 by comparing crystal structures of the different domains of Hsp90 with the various GHKL superfamily proteins. Detailed characterization of the structure of Hsp90 will be discussed in the following section.

1.6.1 Structure of the N-terminal domain

The amino-terminal (N-terminal) domain of Hsp90 is the most conserved domain, with 41-55 % amino acid sequence identity across homologs (Johnson, 2012). In *S. cerevisiae,* the 23 kDa N-terminal domain of Hsp90 consists of residues 1-210. This domain contains the ATP binding site (Grenert et al., 1997; Prodromou et al., 1997; Stebbins et al., 1997). Specifically, the crystal structure for the isolated Hsp82p N-terminal domain shows extensive interactions with the ADP nucleotide (Prodromou et al., 1997). This nucleotide binding site is a Bergerat ATP-binding fold, formed by structural motifs that are conserved in all members of the GHKL ATPase superfamily (Bergerat et al., 1997; Dutta and Inouye, 2000; Prodromou et al., 1997; Scheibel et al., 1998). The ATP binding pocket is formed by a β sheet as its base while flanking α helices form its walls (Dutta and Inouye, 2000; Prodromou et al., 1997) (Figure 1.2A).

Panaretou and colleagues were the first to show that Hsp90 has ATPase activity *in vitro* (Panaretou et al., 1998). This explicitly identified Hsp90 as an ATP-dependent molecular chaperone. Structural homology and biochemical studies identified multiple residues in the N-terminal domain of Hsp82p that play critical roles in ATP binding and hydrolysis. Asp79 lies at the bottom of the nucleotide binding pocket and makes the only direct hydrogen bond with the bound nucleotide (Panaretou et al., 1998; Prodromou et al., 1997). A mutation of Asp79 to asparagine (D79N) completely disrupts ATP binding and compromises Hsp82p function *in vivo*, as it cannot maintain yeast cell viability (Panaretou et al., 1998). Another critical residue, Glu33, is required for ATP hydrolysis as it coordinates the attacking nucleophilic H_2O molecule in this hydrolysis reaction (Panaretou et al., 1998).

ATPase activity depends on ATP binding and conformational changes that lead to the N-terminal dimerized state (Pearl and Prodromou, 2000; Prodromou et al., 2000; Richter et al., 2001). The N-terminal domain contains two critical structural features that are required for ATP hydrolysis: the ATP lid and the ‘strap’. The ATP lid is of particular importance as it is one of the key structural differences between Hsp82p and the very short lids of the GHKL ATPases MutL and GyrB.

Residues 98-125 act as the lid segment which consists of a helix-loop-helix (Prodromou et al., 1997). Previously published crystal structures of the yeast Hsp90 homolog illustrate the lid in two positions (Figure 1.2). The crystal structure of the isolated N-terminal domain shows the lid in the open state when bound to ADP (Figure 1.2A) (Prodromou et al., 1997). This lid segment has significant mobility as it swings from its 'open' to a 'closed' position to fold over the bound nucleotide (Figure 1.2B) (Ali et al., 2006; Richter et al., 2006). When the lid segment of Hsp82p is deleted, it has no ATPase activity and cannot support yeast cell viability (Richter et al., 2006). The first 24 amino acids of Hsp82p constitute the strap that is also required for ATPase activity. The N-terminal β strand (residues 1-9) swaps over to hydrogen bond with the edge of the main β sheet in the N-terminal domain of the other subunit. This strand swap event occurs during transient N-terminal dimerization and structural rearrangement in the N-terminal domain is evident as the strap is oriented differently when the lid is in the 'open' versus the 'closed' state (Figure 1.2) (Ali et al., 2006; Prodromou et al., 1997). An Hsp82p mutant which has the strap deleted (Δ24-Hsp82p) has significantly reduced ATPase activity (Richter et al., 2002).

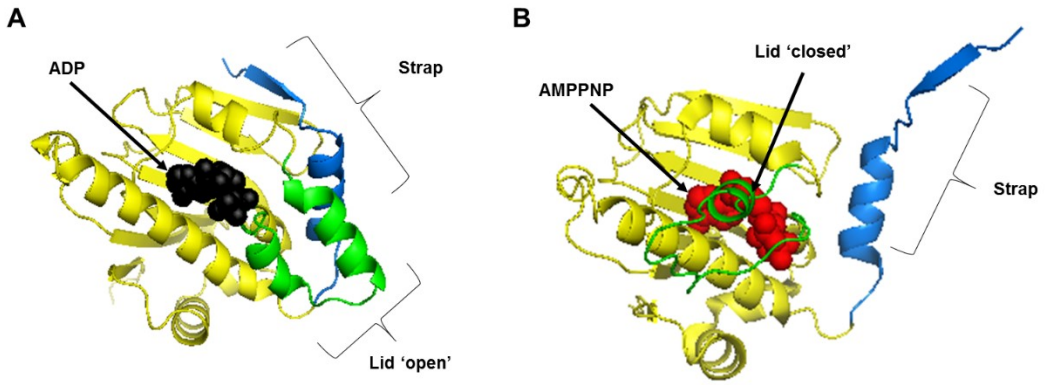

Figure 1.2 Crystal structures of the N-terminal domain of yeast Hsp90 bound to ADP and AMPPNP. The ATP lid is shown in green, the strap is shown in blue, and ADP (**A**) and AMPPNP (**B**) is shown in black and red, respectively. The N-terminal domain bound to ADP reveals the ATP lid 'open' conformation (A) while the N-terminal domain bound to AMPPNP reveals the ATP lid 'closed' conformation (B). These crystal structures were modified using the PDB files 1AMW and 2CG9 for the lid open (A) and the lid closed (B) form, respectively (Ali et al., 2006; Prodromou et al., 1997).

1.6.2 Structure of the middle domain

The middle domain of Hsp90 is the largest of the three domains. It is connected to the N-terminal domain by a flexible, charged linker (residues 211-272 in yeast). Structural analysis of the 33 kDa middle domain of Hsp82p (residues 273-560) identified three main regions that are also shared by members of the GHKL family; two αβα domains linked by an α-helical coil (Figure 1.3A) (Meyer et al., 2004b). Of importance is the highly conserved catalytic loop (residues 370-390; in yellow) found in the first αβα sandwich (Figure 1.3B). The catalytic loop contains a conserved motif: 377 – N(L/I/V)SRExLQ – 384 (Meyer et al., 2004b). Asn377, Arg380, and Gln384 were initially identified as residues capable of interacting with ATP in the N-terminal domain through structural alignments with GyrB and MutL (Meyer et al., 2004b). Interestingly, Ser379, Arg380, and Glu381 are three of the seventeen completely conserved residues present throughout the Hsp90 family (Chen et al., 2006). It was not until the crystal structure of full-length Hsp82p was solved that Arg380 was implicated as being involved with ATP catalysis, as the nucleotide makes direct contact outside of the N-terminal domain with the head group of Arg380 (Ali et al., 2006). Consistent with the structural data, biochemical studies demonstrated that mutations to Arg380 resulted in reduced ATPase activity (Meyer et al., 2004a; Mishra and Bolon, 2014). It is now believed that Arg380 is involved in the catalysis reaction by orienting and stabilizing the γ-phosphate of ATP (Ali et al., 2006; Cunningham et al., 2008; Cunningham et al., 2012).

The middle domain is the binding site for co-chaperones Aha1p and Hch1p, but also serves as a site for client binding (Hawle et al., 2006; Maharaj et al., 2016; Mayer et al., 2009; Panaretou et al., 2002; Pearl et al., 2008). Recently, complementation assays were conducted with yeast cytoplasmic and endoplasmic reticulum paralogs, Hsp82p and Grp94, respectively (Maharaj et al., 2016). Maharaj *et al.* identified a common portion, residues 274-445 (the first αβα domain and the α-helical coil) that supported yeast viability (Maharaj et al., 2016). The authors suggested that this domain constitutes a binding interface for clients and/or co-chaperone proteins. This is consistent with previously described structural data that revealed exposed hydrophobic patches on the middle domain to which client

proteins bind (Ali et al., 2006; Lorenz et al., 2014; Meyer et al., 2003; Vaughan et al., 2006). The kinase Cdk4, which was visualized in complex with Hsp90 and co-chaperone Cdc37 by electron microscopy, interacted mainly with the middle domain of Hsp90 (Vaughan et al., 2006). Also, the glucocorticoid receptor ligand binding domain was similarly visualized to be associated with the outside portion of Hsp90 (Lorenz et al., 2014).

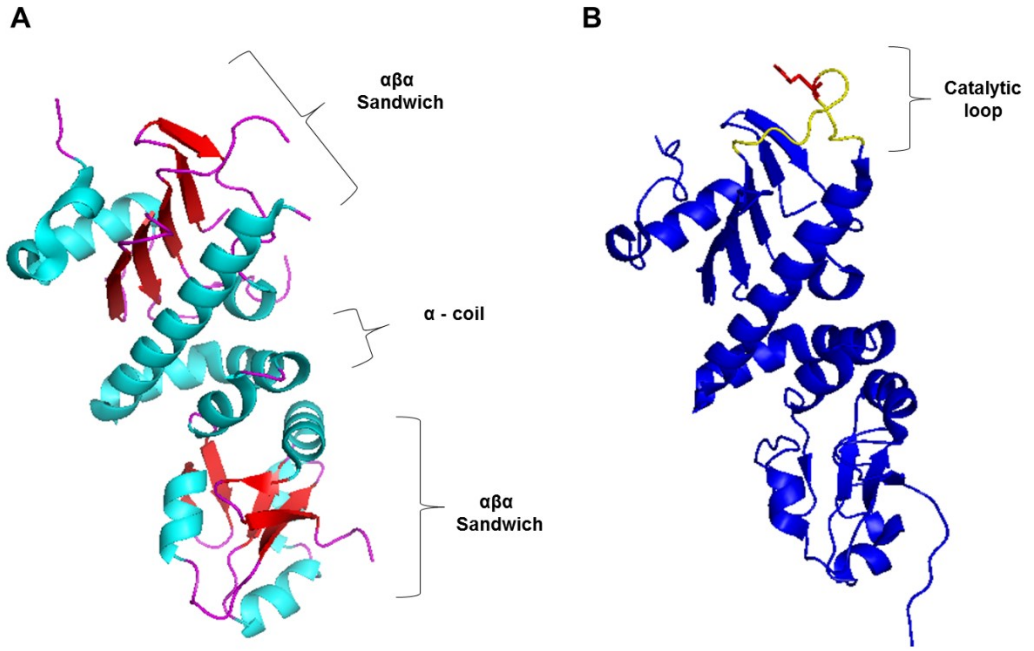

Figure 1.3 Crystal structures of the middle domain of yeast Hsp90. A. Secondary structure is illustrated in different colors to demonstrate the composition of the three regions where helices, sheets, and loops are colored in cyan, red, and magenta, respectively. **B.** The catalytic loop is highlighted in yellow with Arg380 shown as a stick in red. Structures were modified using the PDB file 1USU (A) and 2CG9 (B) (Ali et al., 2006; Meyer et al., 2003).

1.6.3 Structure of the C-terminal domain

The carboxyl-terminal domain is the main dimerization interface for the Hsp90 dimer (Nemoto et al., 1995). C-terminal dimerization is essential for Hsp90 function *in vivo* as it provides correct alignment of the N-terminal domains to undergo transient N-terminal dimerization – a critical conformation required for ATP hydrolysis (Wayne and Bolon, 2007). Dimerized C-terminal domains of the bacterial Hsp90 homolog, HtpG, have previously been solved (Harris et al., 2004) (Figure 1.4A). The dimerized surface is mainly formed by the last two α-helices of each monomer, forming a 4 helix bundle (Harris et al., 2004). This dimerization interface is very similar to yeast Hsp90 (Figure1.4B) (Ali et al., 2006).

The last five amino acids of the C-terminal domain are comprised of a conserved Met-Glu-Glu-Val-Asp (MEEVD) motif (Johnson, 2012; Prodromou et al., 1999; Young et al., 1998). Although the MEEVD motif has not been resolved, as HtpG naturally lacks the C-terminal MEEVD motif and this region was highly disordered in the full-length yeast Hsp90 structure, its role was characterized using MEEVD deletions (Flom et al., 2007; Scheufler et al., 2000; Zuehlke and Johnson, 2012). This MEEVD motif serves as a binding site for various tetratricopeptide repeat (TPR) domain-containing co-chaperone proteins that bind via a carboxylate clamp mechanism (Chen and Smith, 1998; Prodromou et al., 1999; Young et al., 1998). The MEEVD region is of great importance when it comes to understanding the association of Hsp90 with its co-chaperone proteins. For example, co-chaperone Sti1p loads client proteins onto Hsp82p by binding the MEEVD peptide, which will be discussed in more detail in later sections.

While dimerization of Hsp90 is essential for Hsp90 function, the monomers that make up the Hsp90 dimer can dissociate from one another (Richter et al., 2001). Dissociation constants have been calculated to be in the low nanomolar range for different homologs of Hsp90 (Harris et al., 2004; Richter and Buchner, 2001). Experimentally, the fact that these monomers undergo subunit exchange has been exploited in biochemical assays *in vitro* to dissect the mechanism of the ATP hydrolysis which will be discussed in detail in another section.

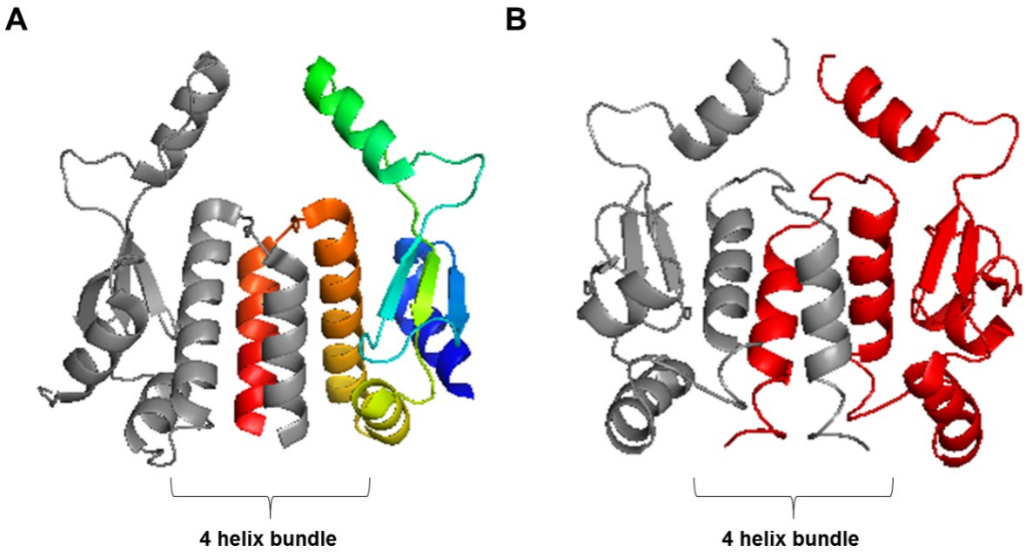

Figure 1.4 Dimerized C-terminal domains of bacterial and yeast Hsp90. **A.** Bacterial Hsp90, HtpG, illustrates the dimerization interface where monomer 1 is rainbow colored from the N- to the C-termini of the C-terminal construct (green to red) and is dimerized with monomer 2 shown in grey. **B.** Dimerized C-terminal domains of yeast Hsp90 is illustrated where monomer 1 and 2 is in red and grey, respectively. These structures show the conserved 4 helix bundle which comprise the dimerization surface. Structures were modified using the PDB file 1SF8 (A) and 2CG9 (B) (Ali et al., 2006; Harris et al., 2004).

1.6.4 Structure of full-length Hsp90 in the inhibited conformation

The crystal structures of the individual domains provided significant insight into each domain, allowing scientists to draw inferences on how Hsp90 relates and functions like other GHKL family proteins (Ali et al., 2006). These individual domains, however, do not provide conformational information of full-length Hsp90 as the domains are independent of each other, and therefore, the structural analyses lacked mechanistic insight on how Hsp90 functions.

Electron microscopy (EM) and small angle X-ray scattering (SAXS) studies, along with crystal structures of Hsp90, demonstrated the dynamic quaternary domain rearrangements Hsp90 can undergo and provided snap shots of the different conformations of Hsp90 (Bron et al., 2008; Lavery et al., 2014; Shiau et al., 2006; Southworth and Agard, 2008). The first crystal structure of the full-length yeast Hsp90 dimer was solved just over a decade ago (Figure 1.5) (Ali et al., 2006). Hsp82p is captured in a closed state, where the N-terminal domains are transiently dimerized with a left-handed twist about the central longitudinal axis of the chaperone (Ali et al., 2006). It was crystalized in the presence of AMPPNP, a non-hydrolyzable ATP analogue, and with Sba1p co-chaperone proteins bound to each N-terminal dimerized surface in a symmetric manner (Ali et al., 2006). This structure was obtained using an engineered form of Hsp82p which lacked its flexible linkers.

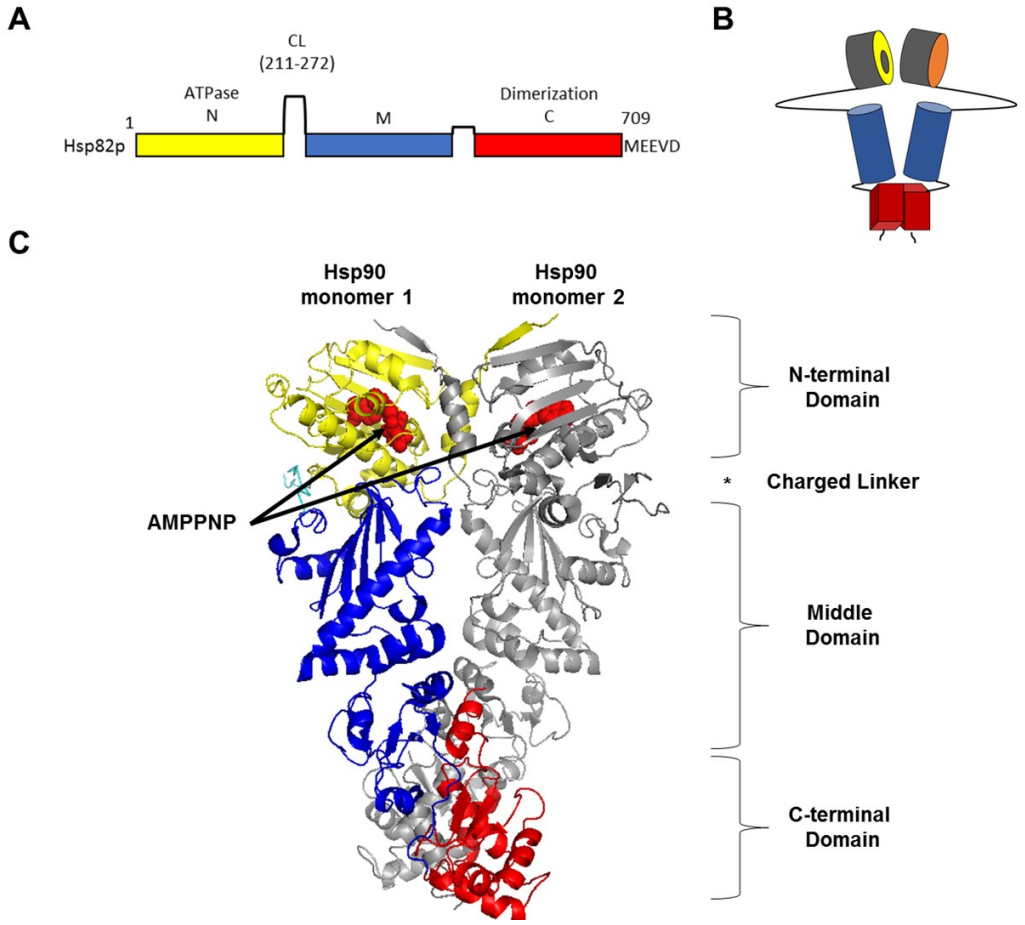

Figure 1.5 Structural representation and crystal structure of yeast Hsp90 in the closed conformation bound to AMPPNP. A. Hsp90 is made up of an N-terminal ATPase domain (N), client binding middle domain (M), and a C-terminal dimerization domain (C). The charged linker (CL) is indicated as residues 211-272 (yeast Hsp90). **B.** Cartoon representation of an Hsp90 dimer. The different 'sides' of the N-terminal domain are illustrated in yellow (with a grey nucleotide binding pocket) and in orange (representing the back side of the domain). **C.** Crystal structure of full-length Hsp82p. Monomer 1 is differentially colored to indicate the N-terminal domain (yellow), middle domain (blue), C-terminal domain (red), and the charged linker (cyan). Monomer 2 is shown in grey with bound AMPPNP in red. Sba1p, which was co-crystalized with Hsp82p, is not shown in this figure. This structure was modified from the PBD 2CG9 file (Ali et al., 2006).

1.7 Conformational dynamics of Hsp90

Hsp90 spontaneously populates different conformational states that are in dynamic equilibrium (Hessling et al., 2009; Mickler et al., 2009; Southworth and Agard, 2008) (Ratzke et al., 2012). The Hsp90 homolog from bacteria, HtpG, was captured in three distinct conformational states by EM (Shiau et al., 2006). The open, closed, and compact conformations were visualized by incubating Hsp90 with no nucleotide, AMPPNP, or ADP, respectively (Shiau et al., 2006). Hsp90 is in the open conformation when the N-terminal domains of Hsp90 are far apart, which is thought to be the 'ground state' where Hsp90 is available to bind client proteins (Shiau et al., 2006). The N-terminal dimerized conformation is the closed conformation which is the conformation competent to hydrolyze ATP (Ali et al., 2006; Prodromou et al., 2000; Richter et al., 2002; Shiau et al., 2006). ATP hydrolysis leads to the compact ADP conformation, which is expected to lead to client release. While structural studies of HtpG indicated that the conformation Hsp90 adopts is significantly influenced by nucleotide occupancy, more recent studies with other paralogs demonstrate that the conformations Hsp90 occupy are nucleotide independent (Southworth and Agard, 2008). EM and SAXS data of full-length mammalian Hsp90 show two distinct conformations of the dimer in apo conditions; one structure is the elongated 'flying seagull' shape (open) and the second distinct structure is a more compact 'v' shape (semi-open) (Bron et al., 2008). The semi-open conformation may represent a transitional state from the open to the closed conformation (Bron et al., 2008). Southworth *et al.* extended this data using different homologs of Hsp90 and demonstrated that nucleotides affected the conformation of Hsp90 very differently depending on the homolog of Hsp90 (Figure 1.6) (Southworth and Agard, 2008). SAXS studies and EM reconstitutions show direct views of the relative population of the various conformations Hsp90 adopts in the presence of different nucleotides (Southworth and Agard, 2008). This established a three-state conformational cycle that is universal to Hsp90 homologs and includes what percentage of the Hsp90 (bacteria, yeast, human) population is found in which conformational states, under different nucleotide conditions (Figure

1.6) (Southworth and Agard, 2008). The differential structural data of Hsp90 homologs model how Hsp90 adopts different conformational states throughout the functional ATPase cycle (Southworth and Agard, 2008). The closed state of Hsp90 is variably adopted depending on the species (yeast>bacterial>human) (Southworth and Agard, 2008). Interestingly, this hierarchy matched the ranking of the rate of ATP hydrolysis, where yeast Hsp90 has the fastest ATPase rate while mammalian Hsp90 has the slowest rate (Southworth and Agard, 2008). This demonstrated that adopting the closed conformation is the rate-limiting step in hydrolysis.

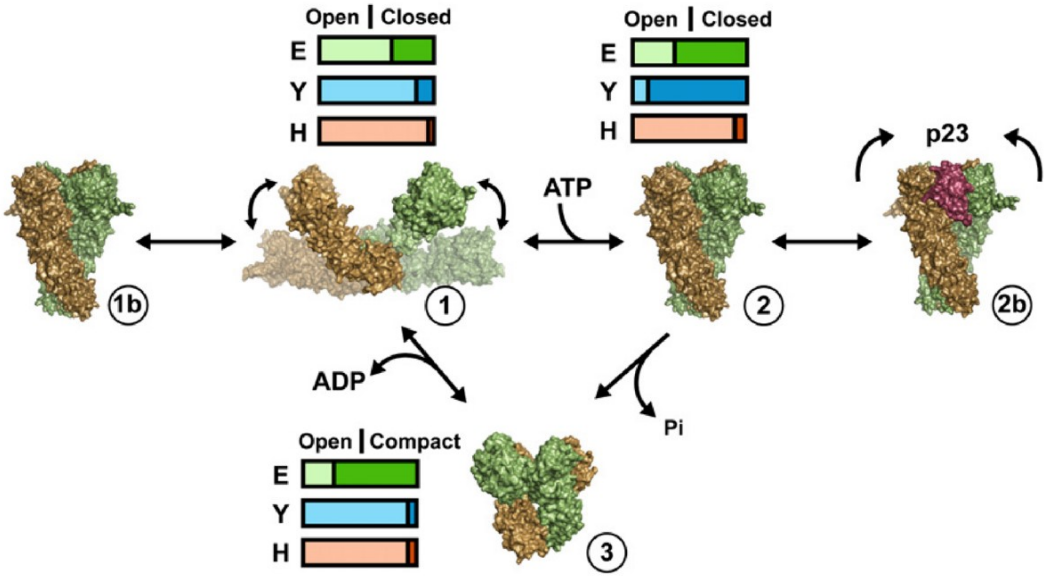

Figure 1.6 Conformational states of Hsp90 are conserved across homologs. Hsp90 populates different conformational states (open, closed, and compact) which is influenced by nucleotide occupancy and dependent on species. The equilibrium between the open (light color) and closed (dark color) conformations was measured and the bars represent the different fractions *E. coli* (E;green), yeast (Y;blue), and human (H;orange) Hsp90 adopt in apo (1), ATP (2), and ADP (3) conditions. The apo and ADP-bound structure is of HtpG (PDB: 1IOQ) and the ATP-bound structure is of Hsp82p (PDB:2CG9). Reprinted from Molecular Cell, Vol 32, Southworth D.R. and Agard D.A., Species-Dependent Ensembles of Conserved Conformational States Define the Hsp90 Chaperone ATPase Cycle, pg. 631-640 (2008), with permission from Elsevier.

Different techniques have been used to probe the dynamic conformational changes within the Hsp90 cycle, including but not limited to nuclear magnetic resonance, fluorescence studies, and mutational analysis (Mickler et al., 2009; Ratzke et al., 2012; Ratzke et al., 2011). Researchers often take advantage of the fact that yeast Hsp90 natively lack cysteine residues. This allows for fluorophores to be attached to cysteine residues that were introduced at specific sites in the N-terminal and middle domains, to detect structural rearrangements within Hsp90 in fluorescent resonance energy transfer (FRET) studies. Using three color FRET analysis, a mechanochemical cycle of Hsp90 was proposed (Ratzke et al., 2011). The Hugel group demonstrated that there is actually no obligate directionality to the acquisition of the different conformational states of Hsp90, either with or without nucleotide. Because of a high free energy barrier that exists between the ATP-bound and hydrolyzed state, binding and release of ATP is much faster than the ATP hydrolysis rate, which means that ATP is bound and released several times before hydrolysis takes place. This is consistent with the findings that nucleotide binding does not necessarily shift the conformational equilibrium to the closed conformation (towards the completion of the cycle), which presents Hsp90 as a *stochastic machine* (Southworth and Agard, 2008). This contrasts with Hsp90 being a *deterministic machine*, which will be discussed in the next section (Section 1.8).

Depending on the species of Hsp90, it has been shown that nucleotide binding may induce directionality to the conformational cycle (Graf et al., 2009; Hessling et al., 2009; Mickler et al., 2009; Shiau et al., 2006). Conformational rearrangements that occur in Hsp90 during ATP hydrolysis have been modeled by using biophysical studies (FRET), from which a minimal set of conformational states have been proposed (Figure 1.7) (Hessling et al., 2009; Mickler et al., 2009). Apo Hsp90 binds a nucleotide quickly, which is followed by the slow acquisition of an open conformation intermediate (I_1) where the ATP lid closes over the bound nucleotide (Hessling et al., 2009; Weikl et al., 2000). This leads to contact between the N-terminal domains (I_2), followed by the acquisition of the closed conformation that is characterized by the repositioning of the middle domains (Hessling et al., 2009). The closed conformation is the ATP hydrolysis competent state, where the

middle domains are correctly oriented and in contact with the N-terminal domains. After ATP hydrolysis, the N-terminal domains dissociate, releasing ADP and inorganic phosphate (P_i), leaving Hsp90 to adopt the open conformation (Hessling et al., 2009).

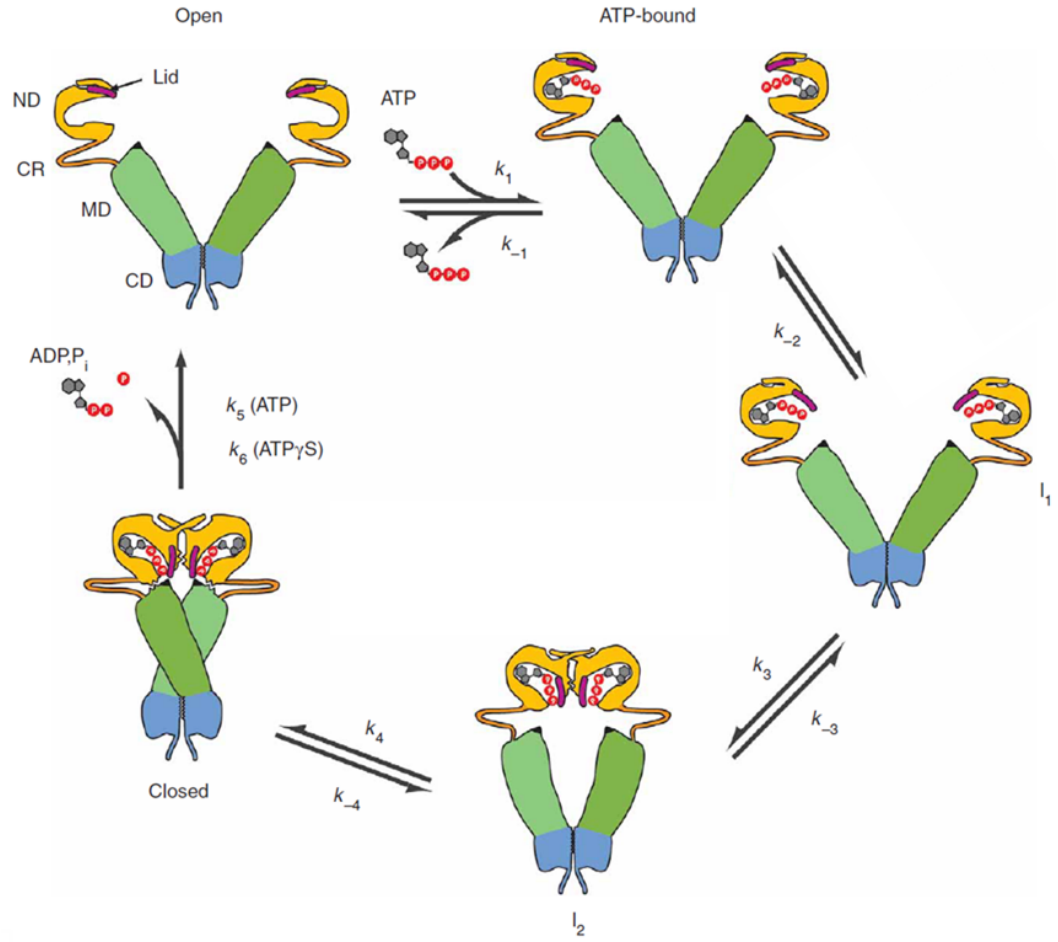

Figure 1.7 Proposed states in the Hsp90 cycle. The Hsp90 cycle was characterized by FRET analysis which revealed 5 conformational intermediates leading to ATP hydrolysis. The cycle involves the binding of ATP, lid closure (I_1), N-terminal dimerization and strand swap (I_2), and communication between the N-M domains to form the closed state. Adapted by permission from Macmillan Publishers Ltd: [Nature Structural and Molecular Biology] Hessling *et al.*, Dissection of the ATP-induced conformational cycle of the molecular chaperone Hsp90, 2009.

1.8 Intra- and inter-protomer interactions required for Hsp90 ATPase activity

ATP binding and subsequent hydrolysis has been the focus of intense study. ATP hydrolysis by Hsp90 is very complex, requiring many intra- and inter-protomer interactions that involve domain rearrangements from both subunits in the dimer structure (Cunningham et al., 2008). Biochemical ATPase studies involving deletions and mutations in the N-terminal domain of Hsp90 has brought insight into which elements are necessary for ATP hydrolysis. Pioneering experiments were performed involving the formation of Hsp90 heterodimers which further dissected the mechanics of ATP hydrolysis. When two forms of Hsp90 are mixed together and incubated, subunit exchange occurs between the subunits and the formation of heterodimers is achieved (Richter et al., 2001). This allowed scientists to uncover the critical intra- and inter-promoter interactions that are required for ATP hydrolysis.

Extensive coordination between numerous elements of the dimer is required to bring the catalytic residues into position to catalyze ATP. This was partly inferred by the fact that the isolated N-terminal domain has negligible ATPase activity (Prodromou et al., 2000). Using heterodimer ATPase assays, it was demonstrated that two N-terminal domains are required to activate the ATPase activity of Hsp90 (Richter et al., 2001). Heterodimers formed from wildtype Hsp82p and D79N (Hsp82p that cannot bind ATP) retained normal ATPase activity *in vitro*, but not heterodimers consisting of wildtype Hsp82p and Hsp82p with the N-terminal domain removed (Richter et al., 2001). This established the requirement for inter-protomer interaction with the opposite subunit, specifically N-terminal dimerization. More importantly, this demonstrated that having only one competent subunit in a dimer is sufficient for ATP hydrolysis and that the nucleotide binding domains bind ATP independently (McLaughlin et al., 2004; Richter et al., 2001). While dimerization of the two N-terminal domains is required, dimerization alone is not sufficient for ATP hydrolysis (Prodromou et al., 2000; Richter et al., 2001; Wandinger et al., 2008).

As previously mentioned, the 'strap' and 'lid' are necessary structural elements that participate in ATPase activity (Richter et al., 2006; Richter et al., 2002). To determine the role of the lid, the ATPase activity of lidless-Hsp82p (where the lid portion, residues 98-121, was replaced by Gly-Ser-Gly) was measured. Lidless-Hsp82p had no ATPase activity and could not support viability in yeast (Richter et al., 2006). Interestingly, ATP binding was greatly enhanced with the lid removed, which suggested that the lid has a role in gating nucleotide binding (Richter et al., 2006). Furthermore, the deletion of the lid in one subunit greatly enhanced the ATPase activity in the opposite subunit in the context of a heterodimer (Richter et al., 2006). This enhanced ATPase activity was attributed to an increase in N-terminal dimerization and also demonstrated that lid closure in one subunit is critical for ATP hydrolysis (Richter et al., 2006). These data show that the lid opens and closes to regulate nucleotide binding and commitment to hydrolysis, and autoinhibits the ATPase activity of Hsp82p (Richter et al., 2006). Similar experiments were conducted with the strap deleted. An increase in ATPase activity above basal intrinsic level of Hsp82p was observed with the removal of the first 8 amino acids (Δ8-Hsp82p) (Richter et al., 2002). Truncations of the first 16 and 24 amino acids, however, severely reduced the ATPase activity of Hsp82p (Richter et al., 2002). Interestingly, heterodimers formed between wildtype Hsp82p and Δ16-Hsp82p had similar ATPase activity as wildtype Hsp82p, but the ATPase activity was greatly reduced when wildtype Hsp82p was mixed with Δ24-Hsp82p instead of Δ16-Hsp82p (Richter et al., 2002). This demonstrated that the first 24 amino acids contribute to the N-terminal dimerization as it is required for ATP hydrolysis (Richter et al., 2002).

ATP binding elicits a succession of conformational changes; first the ATP lid closes, then dimerization of the N-terminal domains and strand swap occur (Figure 1.8). Stabilization of the N-terminal domain dimerized state is in part accomplished by the inter-domain strand swap, but also from critical residues between the N-terminal domain and the opposite middle domain (Cunningham et al., 2008). Residues in the catalytic loop (Leu 372, Leu374, Arg376) interact in *trans* with the opposite subunits' N-terminal domain (Val23 and Thr22)

(Cunningham et al., 2008). Intra-protomer interactions are also important for ATPase activity. As previously mentioned, the crystal structure shows that Arg380 interacts in *cis* with the active site of the same N-terminal domain as it is pointing into the base of the nucleotide binding pocket (Ali et al., 2006). All of these inter- and intra-protomer interactions demonstrate the structural cooperativity between the subunits to promote the closed conformation that is required for hydrolysis of ATP to take place.

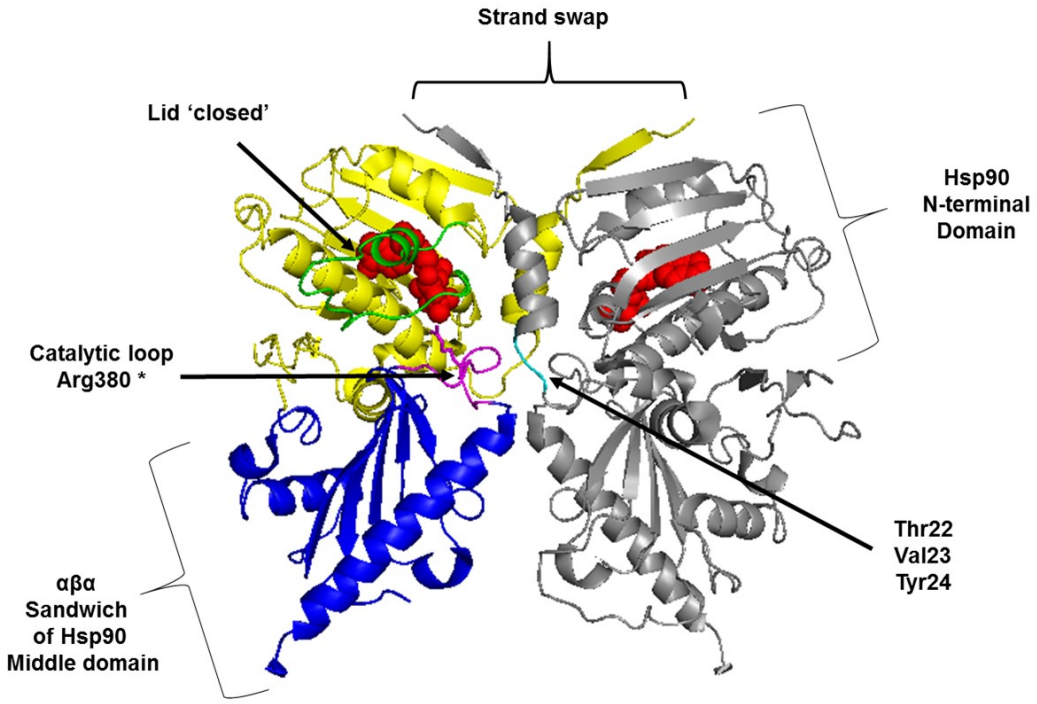

Figure 1.8 Crystal structure of the dimerized N-terminal domains with critical interactions occurring with the opposite middle domains of yeast Hsp90. Strand swap highlights the inter-domain connections, as well as the catalytic loop interacting with Thr22, Val23, and Tyr24. This structure was modified from the PBD 2CG9 file (Ali et al., 2006).

Hsp90 has an extremely low ATPase activity which ranges between 0.1 to 1 molecule of ATP per minute for Hsp90 homologs across prokaryotes and eukaryotes (McLaughlin et al., 2002; McLaughlin et al., 2004; Richter et al., 2001; Wandinger et al., 2008). Slow ATP hydrolysis is thought to be linked to the relatively rare acquisition of the catalytic conformation and presumably inefficient catalysis. This low ATPase rate can be increased by the association of regulatory proteins that also modulate, or fine-tune, the cycle for client protein processing (Calderwood et al., 2006). It remains unclear how exactly clients are activated (Li and Buchner, 2013; Pearl and Prodromou, 2000; Pearl et al., 2008). For almost two decades, it was believed that Hsp90 is dependent on its ATPase activity for *in vivo* function (Panaretou et al., 1998). Numerous studies showed that yeast expressing catalytically dead Hsp90 as the sole source of Hsp90 were not viable (Mishra and Bolon, 2014; Pearl and Prodromou, 2000; Prodromou et al., 1997). Recently, controversy has emerged over this idea based on work from the Buchner group, calling into question whether Hsp90 ATPase activity is essential for its *in vivo* function. They have found that Hsp82p^{E33A} (can bind but not hydrolyze ATP), but not Hsp82p^{D79N} (cannot bind ATP), was able to support yeast cell viability when present as the sole source of Hsp90 (Zierer et al., 2016). Interestingly, Δ8-Hsp82p, which has a higher intrinsic rate than wildtype Hsp82p, also could not support yeast viability (Zierer et al., 2016). Hydrolysis itself may not be necessary for yeast viability, but instead, the distribution of certain conformational states seems to be important. Specifically, the open and the N-terminally dimerized states are each required for a specific duration to allow for client binding (Zierer et al., 2016).

An already complex mechanism of ATP hydrolysis, which is not fully understood, is further complicated as the conformational states of Hsp90 are influenced by other regulatory proteins, post-translational modifications (PTMs), and the clients themselves, which are discussed in detail in the following sections (Dollins et al., 2007; Ratzke et al., 2011). These interactions and modifications have been shown to convert the Hsp90 *stochastic* machine (that undergoes conformational rearrangements randomly) into a *deterministic* machine, as co-chaperone interactions and PTMs modifications *impart directionality* to the cycle

(Li and Buchner, 2013; Mollapour et al., 2014). It is, therefore, necessary to develop an understanding of the link between conformational changes that occur upon co-chaperone binding, PTMs, and client binding.

1.9 The regulatory role of co-chaperone proteins

Co-chaperones are regulatory proteins found within eukaryotic cells that support the function of chaperone proteins. More than 20 Hsp90 co-chaperones have been identified (Matts et al., 2011). During the functional ATPase cycle, co-chaperones sequentially bind to Hsp90 in a conformationally-dependent and ATP-dependent manner to activate clients (Li and Buchner, 2013). Co-chaperones can regulate ATP turnover by inducing or stabilizing structural and conformational changes in Hsp90 (Forafonov et al., 2008; Pirkl and Buchner, 2001; Riggs et al., 2003; Siligardi et al., 2004).

Co-chaperones can be categorized by their effect on ATPase activity or by the manner in which they dock with Hsp90. Figure 1.9 shows a selection of co-chaperones, some of which will be discussed in more detail in this thesis (Wandinger et al., 2008). Co-chaperones that contain a tetracopeptide repeat (TPR) domain are the largest class of co-chaperones, with over 13 TPR co-chaperones interacting with Hsp90 in mammals and 8 in yeast. TPR-domain containing co-chaperones bind to the EEVD motif of Hsp90 by their TPR domain, but may have additional binding sites within the C-terminal, middle, or N-terminal domains of Hsp90. TPR-domain containing co-chaperones in yeast include Sti1p, Ppt1, Cns1p, and peptidyl propyl isomerases such as Cpr6p and Cpr7p (Scheufler et al., 2000; Wandinger et al., 2008). While they all bind to the C-terminus of Hsp90 by means of a TPR domain, most co-chaperones have additional domains. For example, Ppt1p has a protein phosphatase domain to regulate Hsp82p and Cpr6p/Cpr7p contain a peptidyl-propyl isomerase domain that aids in converting cis/trans peptide bonds in proteins (Wandinger et al., 2008). These additional domains highlight the diverse functions TPR co-chaperones have. Some TPR co-chaperones also affect the ATPase activity of Hsp90. Sti1p, for example, forces Hsp82p in the open

conformation, thereby inhibiting the ATPase activity (Hessling et al., 2009; Richter et al., 2002). The non-TPR containing co-chaperones primarily bind to the middle or N-terminal domains of Hsp90. Co-chaperones that bind to the N-terminal domain of Hsp82p, such as Sba1p and Cdc37p, affect the ATPase activity of Hsp90, while only two co-chaperones, Aha1p and Hch1p, have been identified to bind the middle domain of Hsp82p, and they too, impact the ATPase activity of Hsp82p.

It is important to understand how co-chaperones interact and influence the chaperone function because previous studies have suggested that it is the relative levels of co-chaperone proteins that play a role in the kinetics of the Hsp90 cycle, which ultimately affects the fate of the client protein (Wang et al., 2006b). The interplay between the different co-chaperones and domains of Hsp90, as well as the specific requirements for each of their associations with the chaperone, in terms of the ligand binding status and of the conformational state Hsp90 adopts, is discussed in this section. I will focus on certain co-chaperones that either stimulate or inhibit the ATPase activity of Hsp90.

Co-chaperones		Function
Higher Eukaryotes	Yeast Homolog	
TPR co-chaperones		
Hop	Sti1p	Inhibits ATPase activity, recruit clients
FKBP51 / FKBP52		Peptidyl propyl isomerase
Cyp40	Cpr6p ; Cpr7p	Peptidyl propyl isomerase
CHIP		Ubiquitin ligase, interacts with Hsp70
PP5	Ppt1p	Dephosphorylation of Hsp90
Sgt1		Adaptor for clients
TTC4	Cns1p	Essential in yeast
Non TPR co-chaperones		
p23	Sba1p	Inhibits ATPase activity
Aha1	Aha1p ; Hch1p	Stimulates ATPase activity
Cdc37	Cdc37p	Inhibits ATPase activity, recruit client

Figure 1.9 A selection of Hsp90 co-chaperones and their functions. Co-chaperones can be subdivided into two main categories based on the presence of a tetracopeptide repeat (TPR) domain, as listed above. Co-chaperones regulate the chaperone activity of Hsp90 in various ways, such as recruiting clients and stimulating and inhibiting its ATPase activity.

1.9.1 *Aha1p*

The co-chaperone Aha1 (**A**ctivator of **H**sp90 **A**TPase activity) is the most potent stimulator of the ATPase activity of Hsp90 (Lotz et al., 2003; Panaretou et al., 2002). Homologs of Aha1 have been identified within eukaryotes (Lotz et al., 2003; Panaretou et al., 2002). Yeast Aha1 (Aha1p) is a 350 amino acid protein that consists of two domains; a 156 residue N-terminal domain joined by a 40 amino acid linker to a similarly sized C-terminal domain (Koulov et al., 2010). Aha1p stimulates the ATPase activity of Hsp90 through two main interactions with Hsp90. Aha1p binds in an antiparallel fashion: the N-terminal domain of Aha1p binds to the middle domain of Hsp82p while the C-terminal domain binds to the dimerized interface formed by the N-terminal domain of Hsp82p (Koulov et al., 2010; Meyer et al., 2004b; Retzlaff et al., 2010). Although maximal affinity requires full-length Hsp82p as determined by isothermal calorimetry, the main interaction of Aha1p is with the middle domain (Meyer et al., 2004a). The N-terminal domain of Aha1p was co-crystalized with the middle domain of Hsp82p and it was inferred that Aha1p binding aids in aligning Arg380 with the gamma phosphate of ATP (Meyer et al., 2004a) (Figure 1.10). The core interaction of Hsp82p with Aha1p is formed by the hydrophobic interface created by the side chains Leu315, Ile388, and Val391 (Meyer et al., 2004a). Mutation of V391 to glutamate (V391E) on Hsp82p has a significant effect on the binding of Aha1p and subsequent activation of the ATPase, as the V391E mutation decreases Aha1p binding affinity by 10-fold (Retzlaff et al., 2010). Using the Aha1p crystal structure, Asp53 was identified as an important residue within Aha1p for binding to Hsp82p and a charge reversal to lysine (D53K) impairs Aha1p-mediated stimulation of the ATPase activity of Hsp82p (Meyer et al., 2004a). Aha1p contains the RKxK basic motif that is highly conserved in the Aha1/Hch1 family (Meyer et al., 2004a). The RKxK motif (residues 59-62) is part of a flexible loop that is necessary for the remodelling of the catalytic loop in Hsp82p that leads to ATP hydrolysis (Horvat et al., 2014; Meyer et al., 2004a).

In the presence of Aha1p, ATP hydrolysis of Hsp82p is enhanced due to the strong acceleration of rate limiting conformational changes (Hessling et al., 2009). It can robustly stimulate the ATPase activity of Hsp82p up to 12-fold (Lotz et al.,

2003; Panaretou et al., 2002). Hessling *et al.* show that in the absence of nucleotide, Aha1p binding elicits a conformation rearrangement where the N-terminal domains of Hsp82p come closer together to form a closed conformation (Hessling et al., 2009; Retzlaff et al., 2010). One molecule of Aha1p can bridge the subunits of Hsp82p which leads to full stimulation of an Hsp90 dimer, in either *cis* or *trans* (Koulov et al., 2010; Retzlaff et al., 2010). The basis for this asymmetric activation is not fully understood.

Changes in the relative levels of co-chaperones play an important role in the kinetics of the Hsp90 cycle which affects the fate of client proteins and ultimately the outcome of a cell (Holmes et al., 2008). Specifically, the expression levels of Aha1 can greatly influence the maturation of Hsp90 clients. This has also been shown in some cancer cell lines where the silencing of human Aha1 (Ahsa1) expression has been linked to reduced kinase activation and increased sensitivity to Hsp90 inhibitors (Holmes et al., 2008). Aha1 has also been shown to affect changes in the folding of CFTR where over-expression of Aha1 results in increased CFTR degradation (Wang et al., 2006b).

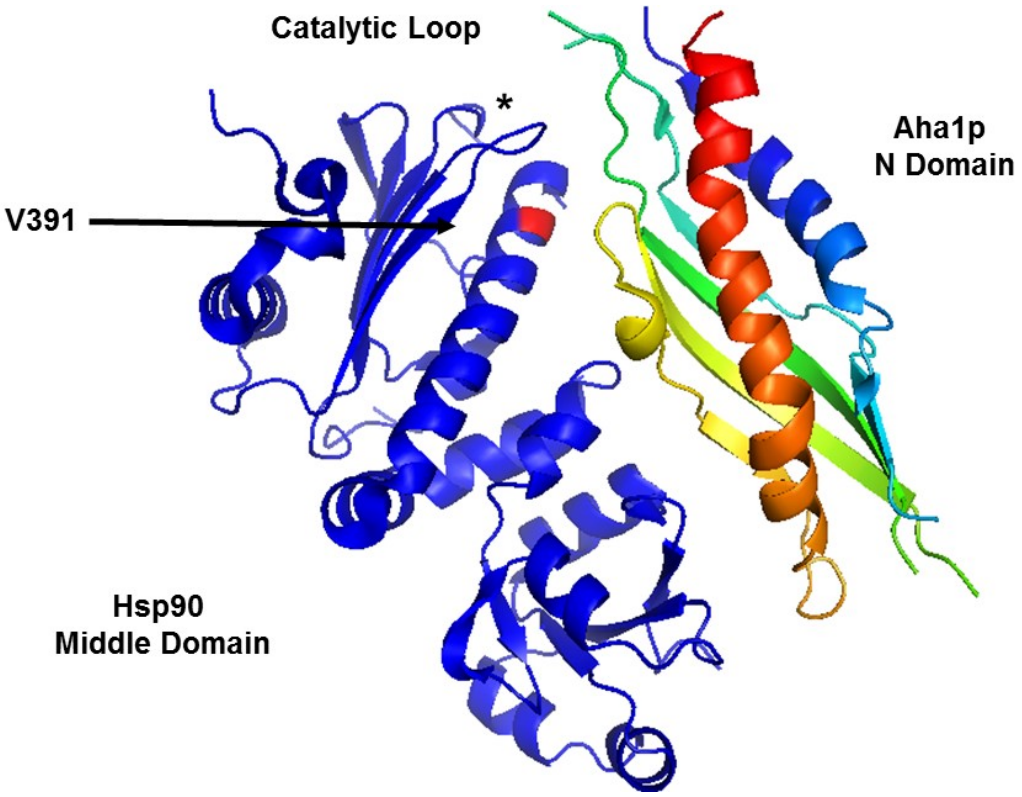

Figure 1.10 Crystal structure of the N-terminal domain of Aha1p bound to the middle domain of Hsp82p. The middle domain of Hsp82p is shown in blue with V391E indicated in red and the catalytic loop indicated with an asterisk. The N-terminal domain of Aha1p is shown in rainbow color, with the amino terminal colored in blue and the carboxy terminal colored in red from which the C-terminal domain of Aha1p continues. The crystal structure was modified using the PDB file 1USV (Meyer et al., 2004a).

1.9.2 *Hch1p*

Yeast possess a co-chaperone named Hch1p that is homologous to Aha1p N-terminal domain (Nathan et al., 1999). Hch1p is only found in some members of the *Saccharomycotina* subphylum and was first identified as a **h**igh **c**opy **H**sp90 suppressor of the *temperature sensitive (ts)* yeast Hsp90 mutant Hsp82p^{E381K} (Horvat et al., 2014; Nathan et al., 1999). While Aha1p and Hch1p competitively bind to the middle domain of Hsp82p, Hch1p can only weakly stimulate the ATPase activity of Hsp82p *in vitro* (Armstrong et al., 2012; Horvat et al., 2014; Lotz et al., 2003; Meyer et al., 2004a; Panaretou et al., 2002). Interestingly, Hch1p and the N-terminal domain of Aha1p (Aha1p$^{1-156}$ or Aha1p^{N}) stimulate the ATPase activity of Hsp82p to a comparable degree while the HA-chimera (fusion of Hch1p and the C-terminus of Aha1p) enhances the ability of Hch1p to stimulate ATPase activity (Horvat et al., 2014).

Earlier studies suggested that Hch1p and Aha1p are functionally homologous. Panaretou *et al.* show that tyrosine phosphorylation of yeast proteins by v-*Src* (a client protein that is highly dependent on the Hsp82p system) is compromised when Aha1p was deleted (Panaretou et al., 2002). Tyrosine phosphorylation by v-*Src* was restored to some degree by the expression of Hch1p (Panaretou et al., 2002). Though some evidence suggests that the N-terminal domains are functionally homologous, our lab has previously shown that Hch1p and Aha1p have different roles in Hsp82p regulation as they differ in their ability to rescue *ts* phenotypes of Hsp82p mutants and their ability to alter sensitivity to Hsp90 inhibitors (Armstrong et al., 2012; Horvat et al., 2014).

While both Hch1p and Aha1p^{N} interact with the catalytic loop of Hsp90, mutations in this loop do not affect these two co-chaperones in the same way. The overexpression of Hch1p rescues growth of the yeast strain expressing Hsp82p^{E381K} (Nathan et al., 1999). Moreover, this mechanism of Hch1p function *in vivo* requires interaction with the middle domain of Hsp82p and the RKxK motif which is necessary to remodel the catalytic loop (Horvat et al., 2014). It was also previously thought that the E381K mutation abolishes Aha1 binding because full ATPase stimulation was not observed (Meyer et al., 2004b). Our lab, however,

demonstrated that the E381K mutation impairs stimulation by Aha1p, but not by Hch1p, indicating that this mutation blocks structural arrangements that allow for full stimulation by Aha1p (Horvat et al., 2014). Furthermore, Hch1p plays an important role in regulating access to the ATP binding pocket in Hsp82p. Overexpression of Hch1p confers hyper-sensitivity to the Hsp90 ATP-competitive inhibitor drug NVP-AUY922 in yeast expressing wildtype Hsp82p (Armstrong et al., 2012). Access to the ATP binding pocket is regulated by the position of this lid segment and its closure over bound ATP results in commitment to hydrolysis.

1.9.3 *Sti1p*

Sti1p is a TPR domain containing co-chaperone that is involved in client recruitment to Hsp82p. In mammalian cells, Sti1p is known as Hop (**H**sp90-Hsp70 **O**rganizing-**P**rotein) which highlights its role and function more specifically as an adaptor protein between the Hsp70 and Hsp90 chaperone systems (Chadli et al., 2000; Chen and Smith, 1998; Smith, 1993). Sti1p binding allows for efficient client transfer from Hsp70, and its co-chaperone Hsp40, to Hsp90 by simultaneously binding both chaperones (Johnson et al., 1998; Pearl and Prodromou, 2006; Scheufler et al., 2000; Wegele et al., 2006). It accomplishes this through the interaction of its TPR domains to the C-terminal motif located at the carboxy terminus of Hsp90 and Hsp70 (Prodromou et al., 1999). Sti1p is composed of three TPR domains (TPR1, TPR2A, and TPR2B) and two domains rich in aspartate and proline (DP domains). TRP1 and TRP2A interact with the C-terminal sequence of the IEEVD motif of Hsp70 and MEEVD motif of Hsp90, respectively (Brinker et al., 2002; Onuoha et al., 2008; Scheufler et al., 2000). Despite binding to the most C-terminal segment of Hsp82p, Sti1p potently inhibits ATP hydrolysis in the N-terminal domains in a non-competitive manner (Flom et al., 2007; Prodromou et al., 1999; Richter et al., 2002). This was the first evidence of a co-chaperone regulating the ATPase activity of Hsp82p (Prodromou et al., 1999). Sti1p is able to inhibit the ATPase activity of Hsp82p because it induces a conformational change that prevents N-terminal domain association and ATP lid closure, thereby stabilizing the open conformation (Hessling et al., 2009; Richter et al., 2006;

Siligardi et al., 2002). Though wildtype Hsc82p bound Sti1p under all conditions, it has weakened interaction with the ATP-bound form and with mutants that favor the closed conformation (A107N, T22I) (Johnson et al., 2007).

1.9.4 *Sba1p*

Sba1p is a small, 23 kDa globular protein that was the first identified co-chaperone found in a stable complex with the SHR (Johnson and Toft, 1994). It was determined that Sba1p binds to the closed, ATP-bound state as mutations that prevent ATP binding to Hsp82p also prevent Sba1p binding to Hsp82p (Grenert et al., 1997; McLaughlin et al., 2006; Obermann et al., 1998; Richter et al., 2002; Sullivan et al., 1997). It was later reported that Sba1p can bind to apo Hsp82p but with a 70-fold lower affinity compared to AMPPNP-bound Hsp82p (Siligardi et al., 2004). Sba1p binding is dependent on the conformational rearrangements that accompany ATP binding which has established Sba1p as a biosensor that recognizes the closed conformation (McLaughlin et al., 2006; Siligardi et al., 2004). Mutations that destabilize the closed, N-terminally dimerized conformation of Hsp82p also have reduced affinity for Sba1p binding. The crystal structure of the Hsp82p-Sba1p-AMPPNP complex confirmed that Sba1p binding requires the dimerized state, thus explaining the biochemical basis for its dependence on nucleotide binding (Ali et al., 2006) (Figure 1.11). The crystal structure in Figure 1.11 demonstrates Sba1p forming interactions mainly with the N-terminal dimerized interface of Hsp82p (Ali et al., 2006). Binding of Sba1p has been speculated to block rearrangement of the catalytic loop in the middle domain of Hsp82p thus, inhibiting the its ATPase activity (Ali et al., 2006; Martinez-Yamout et al., 2006; Panaretou et al., 2002). More recently, however, it was determined that Sba1p inhibits the release of product (ADP) by protecting the ATP lid (Graf et al., 2014). Thus, Sba1p inhibits the ATPase activity of Hsp82p by prolonging the closed conformation and delaying the start of a new Hsp82p cycle (Ali et al., 2006; Prodromou, 2012). Sba1p associates with Hsp82p late within its cycle and is thought to stabilize the client-bound complex, slowing dissociation of the N-

terminal domains and ADP release to facilitate client maturation (Ali et al., 2006; Freeman et al., 2000; McLaughlin et al., 2006).

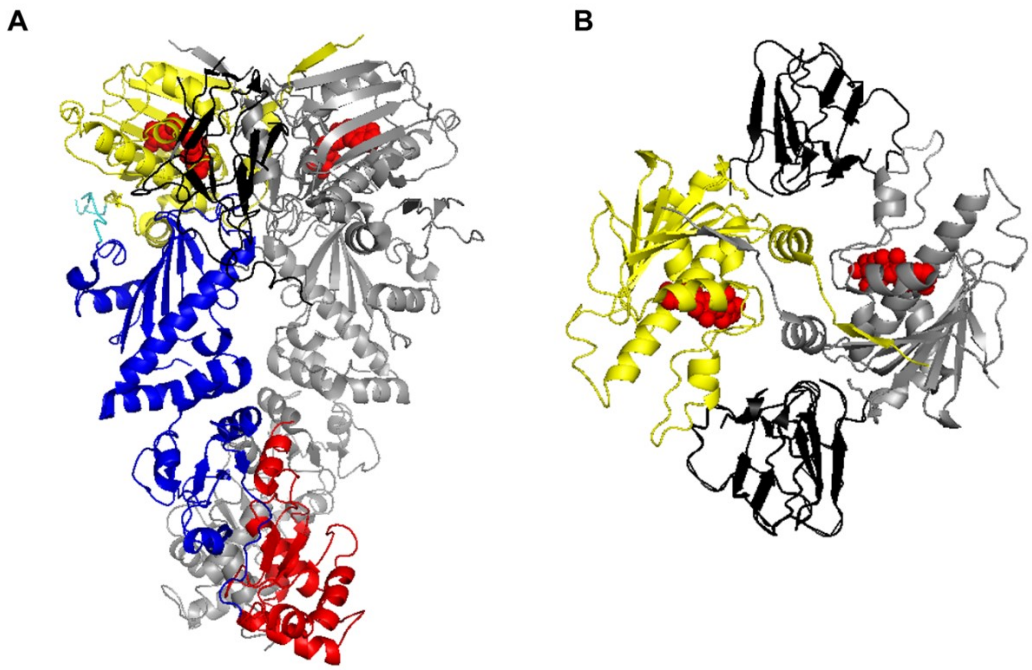

Figure 1.11 Crystal structures of Sba1p bound to the N-terminal domains of full-length Hsp82p. **A.** Hsp82p dimer showing Sba1p bound to the dimerized interface created by the two N-terminal domains. **B.** Top view of the Hsp82p dimer (A) showing two Sba1p molecules bound to the dimerized N-terminal domains of Hsp82p. Monomer 1 of Hsp82p has the N-terminal, middle, and C-terminal domains illustrated in yellow, blue, and red, respectively, while monomer 2 is shown in grey. Sba1p molecules are shown in black. These crystal structures were modified from the PBD 2CG9 file (Ali et al., 2006).

1.10 The Hsp90 ATPase cycle: Co-chaperone cycling and client activation

The activation of Hsp90 clients occurs via progression through a complex, but poorly understood, ATPase cycle that requires the stepwise assembly of chaperone-client heterocomplexes (Eckl and Richter, 2013; Hawle et al., 2006; Hessling et al., 2009; Li and Buchner, 2013; Pearl et al., 2008). The Hsp90 cycle begins with the binding of Sti1p, which induces an open conformation (Richter et al., 2002). Li *et al.* demonstrated that Cpr6p, a TPR domain containing co-chaperone that competes with Sti1p for binding, cannot displace Sti1p efficiently on its own, but can through the cooperative action of either Sba1p or Aha1p (Li et al., 2012). Aha1p and Sba1p are involved in progression through the end stages of the Hsp90 cycle. It is not known whether it is Sba1p or Aha1p which is primarily responsible for advancing the Hsp90 cycle past the Sti1p-bound conformation, however, it likely depends on the client bound.

The best characterized groups of client proteins, the steroid hormone receptors (SHRs) and the protein kinases, fall into two main models of the ATPase driven Hsp90 cycle (Figure 1.12). SHRs are one of the best characterized examples of client maturation (Pearl and Prodromou, 2006). At least five co-chaperone proteins are required for the maturation of SHRs. The “early” chaperone complex is characterized by the presence of Hsp40, Hsp70, and the client protein (Smith, 1993). The adaptor protein Sti1p bridges the Hsp70 system to Hsp90 by means of interacting with their EEVD motifs (Chadli et al., 2000; Chen et al., 1998; Scheufler et al., 2000). This complex (Hsp70-Sti1-Hsp90) marks the beginning of the Hsp90 cycle and is known as the “intermediate” complex (Chen and Smith, 1998; Johnson et al., 1998). The binding of Sti1p induces a conformational change that inhibits the ATPase activity of Hsp90 in a non-competitive manner by preventing N-terminal dimerization in order to ensure client transfer (Richter et al., 2002; Rohl et al., 2013). “Late” chaperone complexes are characterized by the presence of co-chaperones Sba1p and an immunophilin, such as Cpr6p, with Hsp90 (Freeman et al., 2000; Johnson and Toft, 1994). Sba1p has a role in stabilizing the steroid receptor complexes by inhibiting the ATPase activity of Hsp90 (Richter et al.,

2004). The cycle is thought to end with the hydrolysis of ATP and release of a mature client, which 'resets' the Hsp90 cycle (Obermann et al., 1998; Panaretou et al., 1998).

Alternatively, the activation of protein kinases differs from the cycle in which SHR are matured, as it involves the co-chaperone Cdc37 which plays a critical role in recruitment of client protein kinases to Hsp90 (Stepanova et al., 1996). Hundreds of protein kinases have been identified as being dependent on the interaction of Cdc37 and Hsp90, and Cdc37 exclusively recruits kinases to Hsp90 (Taipale, M. et al., 2010). Hsp70 and Hsp40 first interact with the newly synthesized protein kinase (Caplan et al., 2007). Sti1p and the kinase-specific co-chaperone Cdc37p recruit the protein kinases to Hsp90, where they both stabilize the kinase-Hsp90 complex (Lee et al., 2004; Lee and Tsai, 2005). Aha1p stimulates the ATPase activity of Hsp90, which is followed by the release of the activated kinase client (Gaiser et al., 2010).

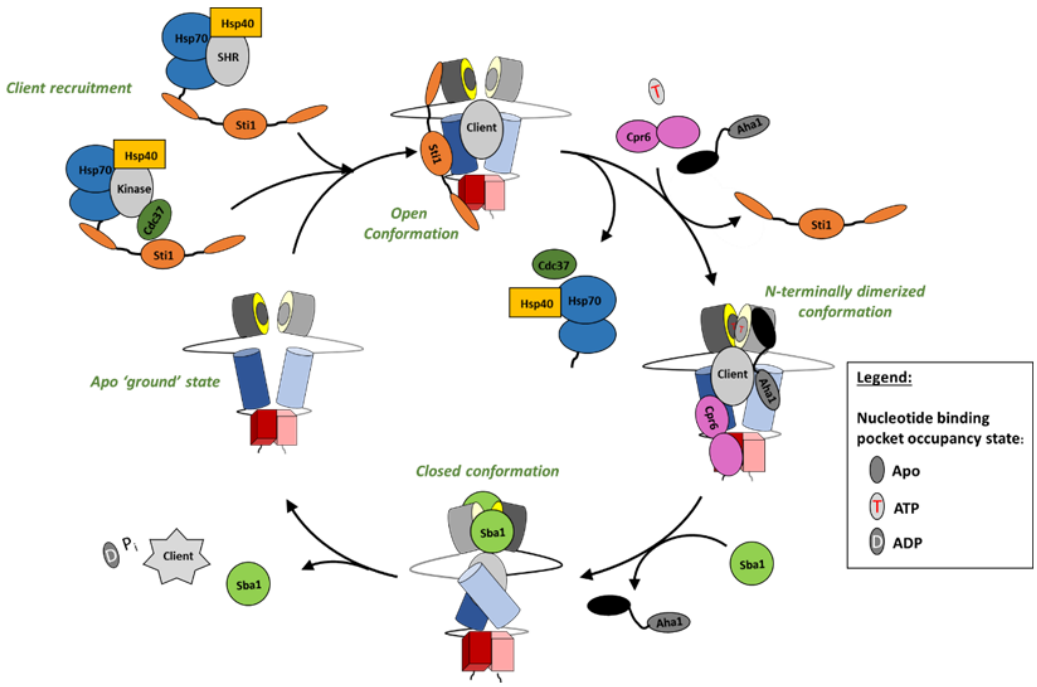

Figure 1.12 A simplified Hsp90 ATPase cycle with co-chaperones. Clients are recruited to Hsp90 by Sti1p or Cdc37p, depending on the client. Sti1p stabilizes the open conformation of Hsp90 and inhibits the ATPase activity. Cpr6p and Aha1p, along with ATP, displaces Sti1p, resulting in the acquisition of an N-terminally dimerized state. Sba1p stabilizes the closed conformation. ATP hydrolysis results in the release of a mature client, ADP, inorganic phosphate (P_i), and Sba1p, leaving Hsp82p to adopt the open, apo, conformation.

1.11 Asymmetric Hsp90 model

To add to the complexity of Hsp90 regulation, recent evidence suggests Hsp90 is an asymmetric machine. This model postulates that each subunit of Hsp90 becomes individually functionalized either through PTM, co-chaperones binding, or client binding. Indeed, Hsp90 interacts asymmetrically with clients and some co-chaperones despite subunits being identical in protein sequence (Lorenz et al., 2014; Mollapour et al., 2014; Retzlaff et al., 2010).

It has long been known that ATP hydrolysis can occur in one protomer of the dimer, independent of the other protomer (McLaughlin et al., 2004; Richter et al., 2001; Wegele et al., 2004). Work by Mishra and Bolon show support for the asymmetric model. Yeast strains expressing engineered heterodimers of wildtype Hsp82p and E33A (WT:E33A), but not WT:D79N, could complement yeast viability, which demonstrates that both subunits need to bind ATP but hydrolysis is only necessary in one subunit (Mishra and Bolon, 2014). Recently, the Agard group brought more insight into the structural mechanics of ATP hydrolysis. They solved the crystal structure of TRAP1, revealing that Hsp90 acquires an asymmetric closed conformation (Lavery et al., 2014). ATP binding results in the acquisition of a closed, asymmetric conformation. Due to strain in adopting the closed conformation, asymmetry is induced as the middle domain of one subunit 'buckles' out (Lavery et al., 2014). This was proposed to prevent simultaneous ATP hydrolysis in both subunits (Lavery et al., 2014).

It has also been proposed that co-chaperone binding to an Hsp90 dimer results in a loss of subunit independence. In other words, co-chaperone binding to one subunit results in allosteric conformational changes that alter binding properties elsewhere in the chaperone. Asymmetric co-chaperone binding has been demonstrated for multiple co-chaperones. Two Sti1p molecules can bind Hsp82p simultaneously, each to a MEEVD motif present at the C-terminus of the subunit, but binding to one subunit results in a significant reduction in affinity for Sti1p at the second site (Alvira et al., 2014; Ebong et al., 2011). This demonstrates that the binding of one Sti1p molecule to Hsp82p induces asymmetry in the dimer.

Furthermore, heterocomplexes seem to be favored as one of the Sti1p molecules can be displaced by Cpr6p (Li et al., 2011; Li et al., 2012). Other co-chaperones show 1:2 binding stoichiometry as well, including Sba1p, Aha1p, and Cdc37p. Asymmetric binding is very fitting when considering Hsp90 biology *in vivo*, as co-chaperone concentration levels are substoichiometric to the ubiquitously expressed Hsp90 (Ghaemmaghami et al., 2003). Sba1p was crystalized in a 2:2 complex with Hsp82p but isothermal titration calorimetry (ITC) showed Sba1p binding in a 1:2 stoichiometry (Siligardi et al., 2004). Similarly, Aha1p stimulates the ATPase activity of Hsp82p from one subunit of the dimer and Cdc37 was visualized to interact asymmetrically with Hsp90 when a kinase client was bound (Retzlaff et al., 2010; Vaughan et al., 2006).

Asymmetry may be induced by client binding, as described above with Hsp90-Cdc37-kinase complex (Vaughan et al., 2006). Another example of the formation of an asymmetric complex involves the glucocorticoid hormone receptor (GR) (Lorenz et al., 2014). Although two molecules of GR can interact with a single Hsp90 dimer, the addition of either Sti1p or Sba1p results in an asymmetric complex. How asymmetric interactions or modifications affect Hsp90 action is not fully understood and has not been incorporated into the Hsp90 cycle.

1.12 Hsp90 regulation by post-translational modifications

Hsp90 is subject to many post-translational modifications (PTM) including phosphorylation, acetylation, SUMOylation, methylation, ubiquitination, and oxidation (Mollapour and Neckers, 2012; Prodromou, 2016). There are over 150 PTMs in Hsp90α detected within the Phosphosite database and they overlap with client and co-chaperone binding sites. It is interesting that although the PTMs are detected over all three domains of Hsp90, there is a higher concentration of modification sites on the first half of the protein (N-terminal and middle domains of Hsp90) (Figure 1.13). With Hsp90 being abundantly more prominent than co-chaperones, PTMs serve as a mechanism to control the interaction of co-chaperones and a way to modulate chaperone function. The functional consequences of these

modifications are only starting to become apparent. Similar to the involvement of the relative expression levels of co-chaperones, it is clear that PTMs add another layer of regulation on the Hsp90 system to tightly control its chaperone function (Scroggins and Neckers, 2007). These modifications affect the conformations Hsp90 adopts, as well as co-chaperone and client binding. Just as co-chaperone binding affects Hsp90 conformation rearrangement and ATPase activity, evidence has shown PTMs propagate signals allosterically from different domains as well (Retzlaff et al., 2010). Due to the dynamic nature of PTMs, they may allow for adaptation to specific and changing environmental conditions, and thus, Hsp90 can be fine-tuned for specific clients. It is unknown under which conditions and during what part of the cycle all these modifications occur. It is also unknown whether all these modifications occur on one or both subunits. In this thesis, I will be discussing SUMOylation and phosphorylation in more detail.

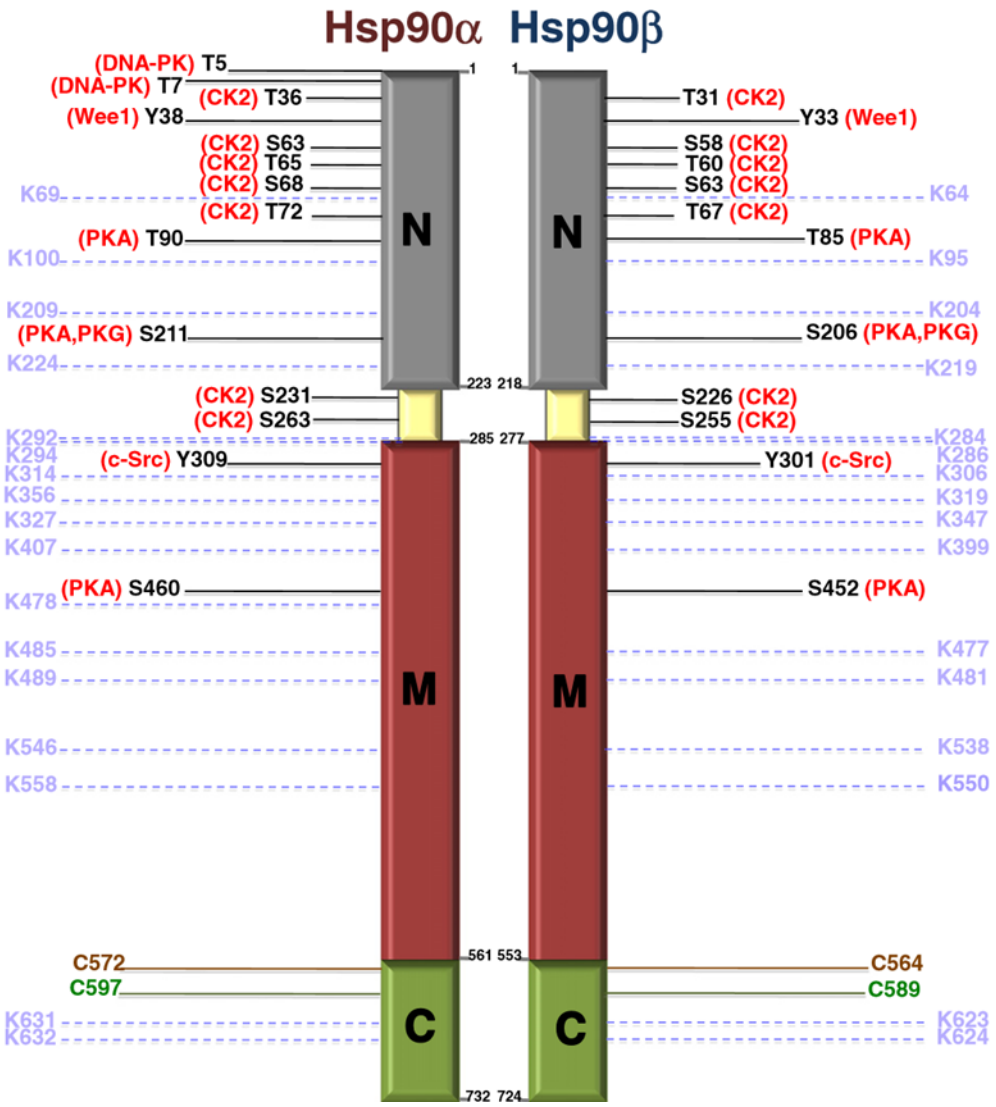

Figure 1.13 Post-translational modifications of Hsp90. The various PTMs of Hsp90α and Hsp90β are shown in a schematic representation, highlighting in which domain the modifications occur. Phosphorylation residues are shown in black where modifications made by known kinases are labelled in red. Acetylation residues are in purple, nitrosylated residue in green, and oxidation residue in brown. Figure from Mollapour and Neckers 2017. Reprinted from Biochimica et Biophysica Acta (BBA) – Molecular Cell Research, Vol 1823, Mollapour M. and Neckers L., Post-translational modifications of Hsp90 and their contributions to chaperone regulation, pg. 648-655 (2012) with permission from Elsevier.

1.12.1 SUMOylation

SUMOylation, a reversible PTM, has been the focus of intense research since its discovery over two decades ago, as it has been found to be an essential process for most eukaryotic organisms (Matunis et al., 1996). This PTM was first discovered in budding yeast upon the identification of the SUMO gene (SMT3). SUMO is a 12kDA **s**mall **u**biquitin-like **mo**difier (**SUMO**) protein that is covalently attached to a lysine residue of a target protein (Gareau and Lima, 2010; Hecker et al., 2006). SUMO proteins are part of the ubiquitin like protein (Ubls) family which all share a β-grasp fold that can be conjugated to target proteins post-translationally. Yeast SUMO, Smt3p, is conjugated to target proteins through a cycle involving the maturation, activation, conjugation, and ligation of Smt3p (Figure 1.14) (Zhou et al., 2004). Although conjugation of SUMO is mediated by similar machinery responsible for the conjugation of ubiquitin, it does not target proteins for degradation like ubiquitin but rather plays a regulatory role in activating target proteins by altering proteins' conformation, subcellular localization, and interactions with known binding partners (Flotho and Melchior, 2013; Gareau and Lima, 2010; Hickey et al., 2012; Matunis et al., 1996; Ulrich, 2009). Furthermore, target proteins are SUMOylated and deSUMOylated during rapid cycles which results in a low steady state level of SUMOylation (Geiss-Friedlander and Melchior, 2007). This steady state can be shifted with environmental or metabolic stresses (Bettermann et al., 2012; Enserink, 2015; Zungu et al., 2011).

SUMO is synthesized as a pro-protein which is then activated when proteases cleave the C-terminal peptide to expose a diglycine motif. The function of SUMO proteases is two-fold. Firstly, they are involved in producing the mature form of SUMO by cleaving a short peptide from the C-terminus of the protein to reveal a diglycine motif (Hay, 2007). Secondly, they have a critical role in deSUMOylating target proteins, as the same proteases are also responsible for its removal from its substrate proteins (Mukhopadhyay and Dasso, 2007). Thus, proteases play a critical role in the steady state of SUMOylated proteins. Through

an E1, E2, E3 enzyme cascade, SUMO is attached to a lysine residue of a target protein as illustrated in the SUMOylation cycle in Figure 1.14.

Characterization of SUMOylated proteins has been difficult due to their low abundance compared to non-modified counterparts (Nie and Boddy, 2015). It has also been extremely difficult to identify due to the difficulty in detecting SUMOylation experimentally. A growing number of proteins have been identified as SUMOylation substrates, with more than two-thirds of them having the SUMOylation consensus motif ΨKxE/D (where Ψ is a large hydrophobic residue and x is any residue) (Denison et al., 2005; Rodriguez et al., 2001; Vertegaal et al., 2006). SUMOylation of many proteins is stimulated by cell stress and several stress proteins have been linked to modification of substrates (Brunet Simioni et al., 2009; Enserink, 2015; Guo and Henley, 2014; Yang et al., 2013). Interestingly, Hsp90 has recently been identified as a target for SUMOylation at the conserved lysine residue (K178 in yeast and K191 in humans) in the N-terminal domain (Mollapour et al., 2014). The authors reported that yeast Hsp90 is asymmetrically SUMOylated and moreover, that this SUMOylated Hsp90 facilitates the recruitment of Aha1 (Mollapour et al., 2014). They also show that SUMOylated Hsp90 appears to limit chaperone activity towards its clients such as GR and CFTR *in vivo* (Mollapour et al., 2014). This is possibly due to increased Aha1 recruitment, leading to acceleration of the cycle and reduced dwell time for maturation of the client because this result is consistent with increased CFTR maturation upon Aha1 knockdown (Koulov et al., 2010; Wang et al., 2006b). How SUMOylation affects the ATPase activity of Hsp90 has not been investigated.

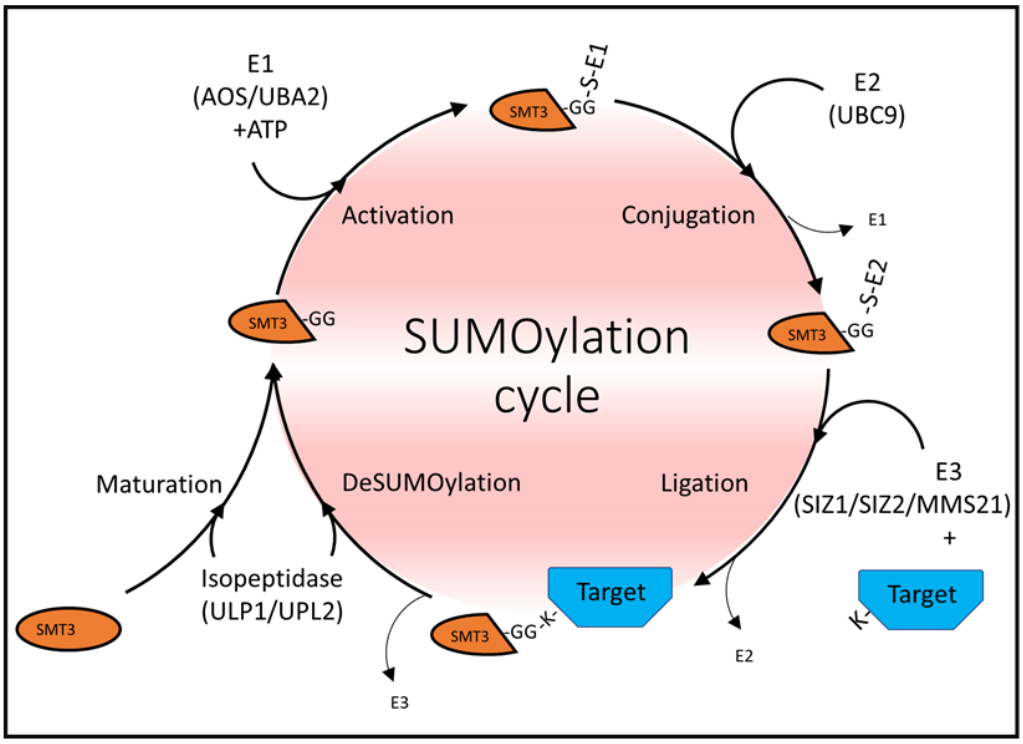

Figure 1.14 The SUMOylation cycle. A C-terminal peptide from SUMO is cleaved by Ulp1/Upl2 to reveal a di-glycine motif. Mature SUMO is activated when bound to the E1 heterodimer Aos1-Uba2. SUMO is then passed to an Ubc9, an E2 conjugation enzyme. E3 ligases (Siz1/Siz2/Mms21) mediate the ligation of SUMO to its target protein. SUMO can be recycled by deSUMOylation enzymes Ulp1/Upl2 that remove SUMO from its target protein.

1.12.2 Phosphorylation

Phosphorylation of Hsp90 has been extensively reported, but the role the distinct phosphorylation modifications have on chaperone function is not fully understood. Serine, threonine, and tyrosine phosphorylation sites have been identified (Figure 1.15), and those for which the kinases are known, are shown on Figure 1.13. Experiments to determine the role individual phosphorylation sites have on Hsp90 activity have been carried out and they demonstrate that phosphorylation is a powerful regulator of ATPase activity and chaperone function. The consequence of phosphorylation at any one site is very complex. The example of casein kinase 2 (CK2) phosphorylation of T22 demonstrates this complexity (Mollapour and Neckers, 2011). CK2 is a serine/threonine kinase, whose activity is also dependent on Hsp90. When phosphorylated at T22, Hsp82p chaperoned GR, while chaperoning of v-*Src* and Ste11 was reduced (Mollapour and Neckers, 2011). With Hsp90 having such a diverse clientele, it is likely that PTMs, such as phosphorylation at T22 in yeast, mediate the different conformational states Hsp90 adopts to accommodate different clients. This would result in the formation of specific client-Hsp90 complexes under certain conditions (Street 2011). Comparing the *in vitro* and *in vivo* data, however, further complicates the understanding of the functional consequence of the T22 modification. The phosphomimetic mutant, T22E, has a 2-fold lower intrinsic ATPase activity, but is stimulated normally by Aha1p *in vitro* (Mollapour and Neckers, 2011). Furthermore, the recruitment of Aha1p to Hsp90 is prevented when CK2 phosphorylation of Hsp82p at T22 is blocked, but also when it is mimicked by the T22E substitution (Mollapour and Neckers, 2011). Although association with Aha1p (and Cdc37p) is affected, phosphorylation of T22 does not affect Sti1p or Sba1p binding (Mollapour et al., 2011b). This highlights the specific requirements that different clients may need for activation.

Additional PTMs also influence Aha1p co-chaperone recruitment besides phosphorylation of T22. Phosphorylation of tyrosine 24 by Swe1 is required for Aha1p association (Mollapour et al., 2010). In mammalian studies, phosphorylation of tyrosine 313 induces structural rearrangements that favor Aha1 binding, while

phosphorylation of Y627 contributes to the release of Aha1 and an activated client (Xu et al., 2012). The succession of phosphorylation and dephosphorylating seems to imprint directionality to the Hsp90 cycle. This raises questions about how these PTMs in Hsp90 regulate chaperone activity and co-chaperone recruitment together. Coordination between the different modifications that leads to recruitment of Aha1p alone is complex, requiring at least SUMOylation of lysine 178 and phosphorylation of threonine 22 and tyrosine 24 (Mollapour et al., 2014; Mollapour et al., 2010; Mollapour et al., 2011b). The functional consequences of the other PTM sites remains unknown and it is unclear if these modifications occur simultaneously, or in different 'pools' (or subpopulations) of Hsp90. It is also not known if phosphorylation of Hsp90 occurs asymmetrically or symmetrically, or if phosphorylation occurs on the same subunit as SUMOylation.

Phosphorylation of co-chaperones has also been identified to impact the Hsp90 system by changing co-chaperone function (Bansal et al., 2004; Dunn et al., 2015; Kobayashi et al., 2005; Vaughan et al., 2008). The co-chaperones Cdc37, Hop, and p23 are phosphorylated in cells but the significance of these modifications is only beginning to be explored (Longshaw et al., 2009; Millson et al., 2009; Shao et al., 2003). For example, CK2-mediated phosphorylation of Cdc37 on serine 13 is required for kinase recruitment by Cdc37 to Hsp90 (Bandhakavi et al., 2003; Miyata, 2009; Shao et al., 2003). The phosphomutant S13A (non-phosphorylated form) results in increased Hsp90 inhibitor sensitivity, and overexpression of the phosphatase (Ppt1) responsible for dephosphorylating Cdc37 results in synthetic lethality with GA in yeast (Vaughan et al., 2008).

The phosphorylation status of Hsp90, and of its co-chaperones, greatly influences client activation and efficacy of Hsp90 inhibitor drugs (Kurokawa et al., 2008; Piper and Millson, 2011). Therefore, understanding the functional consequence of each modification, and the interplay between the different modifications that occurs on Hsp90 and the co-chaperones, is of critical importance.

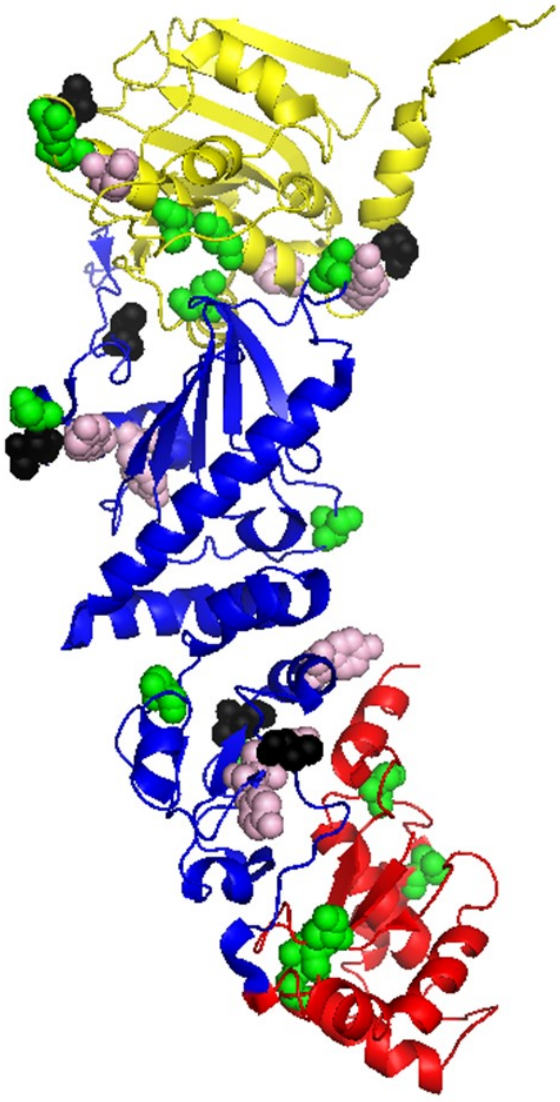

Figure 1.15 Identified phosphorylation residues in yeast Hsp90. Ribbon cartoon structure of one yeast Hsp82p subunit (N-terminal domain in yellow, middle domain in blue, and C-terminal domain in red), with phosphorylation residues presented as spheres. Serine residues are illustrated in green, tyrosine residues in light pink, and threonine residues in black. This structure was modified from the PBD 2CG9 file (Ali et al., 2006).

1.13 Targeting co-chaperones in cancer and disease

While Hsp90 N-terminal domain inhibitors have very promising therapeutic potential, a common cellular response ensuing treatment with ATP-competitive Hsp90 inhibitors is the upregulation of the heat shock proteins Hsp27 and Hsp70 (McCollum et al., 2008). Upon inhibition of Hsp90, heat shock factor-1 (HSF1) is activated which binds to the heat shock elements of multiple HSPs promotors (McCollum et al., 2008). Hsp27 and Hsp70 are then upregulated which influences the Hsp90 system to facilitate the activation and maturation of oncoproteins (Frydman et al., 1994; Wegele et al., 2006). Upregulation of Hsp27 and Hsp70 is also associated with strong antiapoptotic activity and cellular proliferation (Koay et al., 2014; Sarto et al., 2000). The overproduction of Hsp27 and Hsp70, which promotes cancer cell survival, has led researchers in search of other targets within the Hsp90 system, such as co-chaperones, that prevent this stress response.

Considering the plethora of co-chaperones and their specific roles in client maturation, there are many attractive targets within the Hsp90 system including Cdc37, Sti1/Hop, and Aha1. Cdc37 and Hop are responsible for client recruitment and loading onto Hsp90, making them ideal targets. An inhibitor of Hop activity, C9, prevents Hsp90-Hop interaction, and thus, clients are not transferred to Hsp90 (Pimienta et al., 2011). This compound does not induce the transcriptional upregulation of Hsp70, like the Hsp90 inhibitor 17-AAG, in BT-474 ductal carcinoma breast cells (Pimienta et al., 2011). More importantly, C9 not only obliterates the compensatory response cancer cells have to these Hsp90 inhibitors, it also makes the cells more sensitive towards Hsp90 inhibitors (Pimienta et al., 2011). Drugs against Cdc37 may be beneficial to specifically target kinase addicted cancers, as Cdc37 been implicated in oncogenic transformations (Pearl, 2005).

Modulating Aha1 also has a biological consequence on client protein folding, such as the oncogenic Hsp90 client C-raf. C-raf is a key signal transduction protein that supports malignant transformation and is stabilized and protected against degradation by Hsp90 (Grbovic et al., 2006). Its stability leads to the phosphorylation of downstream targets Mek1/2 and Erk1/2 (Grbovic et al., 2006;

Paraiso and Smalley, 2012). Aha1 overexpression leads to hyper-phosphorylation of Erk1/2 and conversely, decreasing the levels of Aha1 reduced client kinase activation and attenuated the phosphorylation of Erk1/2 in a concentration dependent manner (Holmes et al., 2008). This was not due to an increase in total protein levels, as Erk and C-raf protein levels remained the same, but due to the increased involvement of the Hsp90 system chaperoning oncogenic clients. Another example involves the silencing of Aha1 expression which caused an increase in cellular sensitivity to the Hsp90 inhibitor, 17-AAG, in human cancer cell lines (Holmes et al., 2008).

Aha1 has not only been linked to kinase activation, but also hormone receptor function, and quality control of CFTR (Harst et al., 2005; Wang et al., 2006b). Specifically, the expression level of Aha1 have been shown to regulate the balance between folding and degradation of CFTR (Loo et al., 1998; Wang et al., 2006b). Downregulation of Aha1 results in increased stability of the most common, disease-associated variant of CFTR (Δ508) and allows for modest amounts of export to the cell surface (Wang et al., 2006b). Conversely, Aha1 overexpression results in the degradation of ΔF508 CFTR and the wildtype CFTR (Wang et al., 2006b).

All these observations illustrate how the Hsp90 system might be manipulated – by altering the co-chaperone level or co-chaperone interaction with Hsp90 – to mitigate the folding of oncogenic proteins or to restore the folding and activation of proteins like ΔF508 CFTR.

1.14 Objectives

Hsp90 is a dimeric molecular chaperone that must be able to bind and hydrolyze ATP to carry out its essential functions (Obermann et al., 1998; Panaretou et al., 1998). Hsp90 facilitates the activation of numerous client proteins in the context of an ATP-driven functional cycle (Pearl, 2005). To maintain aberrant client protein activation in cancer cells, an increase in Hsp90 activity is required (Xu and Neckers, 2007). Co-chaperone proteins regulate the Hsp90 system

to fine-tune its activity to support increased Hsp90 demand in diseased states (Holmes et al., 2008; Koulov et al., 2010; McLaughlin et al., 2006; Siligardi et al., 2004; Wang et al., 2006b). It is well established that co-chaperones levels affect Hsp90 activity, as it was specifically shown that Aha1 modulates Hsp90 function in malignant cell types (Holmes et al., 2008). The exact mechanism underlying the Hsp90 ATPase activity is not fully elucidated and there remains a significant gap in our knowledge on how this activity is regulated by Aha1.

One objective of my thesis was to characterize asymmetric interactions of co-chaperones, and more specifically, how they regulate the ATPase activity of Hsp90. The results detailed in chapter 3 presents a clear mechanistic advance in our understanding of Aha1p-mediated stimulation, describing how Aha1p binding to one subunit results in specific conformational changes in Hsp82p leading to ATP hydrolysis. Another objective of my thesis was to analyse how post-translational modifications affect Hsp82p–co-chaperone interactions and ATPase activity. SUMOylation of Hsp82p at K178 was shown to recruit Aha1p, but how this post-translational modification affects the ATPase activity of Hsp90 cannot be determined without a means to generate Hsp90 quantitatively modified at that specific site. Chapter 4 outlines a novel strategy that was designed for examining SUMOylated Hsp82p *in vitro*, by covalently linking the yeast SUMO, Smt3p, to Hsp82p with a homobifunctional maleimide crosslinker. This modification recapitulated *in vivo* findings, mainly Aha1p-recruitment, but also revealed that SUMOylation of Hsp82p alters Sba1p regulation of its ATPase activity. Lastly, chapter 5 contains the analysis of how constraining Hsp90 conformational dynamics, by shortening the N-M linker of Hsp82p, alters co-chaperone regulation. Many different rearrangements must occur within the Hsp90 dimer to acquire the ATP-hydrolysis competent state, and this type of investigation revealed that Aha1p preferentially binds to a constrained conformation of Hsp82p and that Aha1p binding induces a conformation primed for Sba1p association.

Results from this thesis provide a more in depth understanding of the specific protein-protein interactions that are involved in regulating Hsp90 function. Understanding how the various Hsp90 conformations influence the progression of

the Hsp90 cycle, and elucidating how these conformations are regulated by co-chaperone proteins and PTMs is essential to improving our understanding of client protein maturation. Because many clients of Hsp90 have been implicated in the development and progression of various diseases, increasing our understanding of these interactions and how they are related to drug sensitivity is important for the ongoing development of clinical agents targeting Hsp90 and its regulatory proteins.

Chapter 2

Materials and methods

2.1 Materials

2.1.1 Reagents

The following reagents were used according to manufactures' guidelines and recommendations, and in adherence to procedures outlined by the Environmental Health and Safety of the University of Alberta and Workplace Hazardous Materials Information Systems (WHIMIS).

Table 2.1 Chemicals, materials, and reagents

Reagent	Supplier
ß-Mercaptoethanol	BioShop Canada Inc.
Acetic acid; glacial	Thermo Fisher Scientific
Acetone	Thermo Fisher Scientific
Acrylamide (30 %; 29:1)	BioRad Laboratories
Adenosine Di-Phosphate (ADP)	MP Biomedicals, LLC
Adenosine Tri-Phosphate (ATP)	Fisher BioReagents
Adenylyl-imidodiphosphate (AMPPNP)	Sigma-Aldrich Life Sciences
Agar	Thermo Fisher Scientific
Agarose (UltraPure™)	Thermo Fisher Scientific
Ammonium Sulphate	Thermo Fisher Scientific
Ampicillin	Sigma-Aldrich Life Sciences
Bovine serum albumin (BSA)	Hoffmann-La Roche Ltd.
Brilliant Blue R-250	Fisher BioReagents
Bromophenol Blue	BDH Laboratory Sciences
Butanol	Thermo Fisher Scientific

Complete, EDTA-free protease inhibitor cocktail tablets	Hoffmann-La Roche Ltd.
Coomassie Blue Stain	BioRad Laboratories
Delbecco's phosphate buffered saline (DPBS)	Mediatech Inc.
Deoxyribonucleotide triphosphate (dNTP)	Roche Diagnostics
Dithiothreitol (DTT)	Roche Diagnostics
Dimethyl sulfoxide (DMSO)	Thermo Fisher Scientific
Ethanol	Thermo Fisher Scientific
Ethylenediamine-tetraacetic acid (EDTA)	Thermo Fisher Scientific
Glycerol	Thermo Fisher Scientific
HALT Protease Inhibitor	Thermo Fisher Scientific
Hepes	Brand BioReagents
Hydrochloric acid	Thermo Fisher Scientific
Hydrogen Peroxide	Thermo Fisher Scientific
Imidazole	Thermo Fisher Scientific
Isopropanol	Thermo Fisher Scientific
Isopropyl-β-D-thiogalactopyranoside (IPTG)	OmniPur
Luria Broth (LB), Miller	Thermo Fisher Scientific
Methanol	Thermo Fisher Scientific
Magnesium chloride ($MgCl_2$)	Thermo Fisher Scientific
NaCl (Sodium chloride)	Thermo Fisher Scientific
Nickel Sulphate	Thermo Fisher Scientific

Nicotinamide Adenine Dinucleotide (NADH)	Sigma-Aldrich Life Sciences
Nitrocellulose membranes	BioRad Laboratories
NVP-AUY922	Chemie Tek
p-Coumaric Acid	Sigma-Aldrich Life Sciences
PCR Primers	Integrated Device Technology
Phosphoenol Pyruvate (PEP)	Sigma-Aldrich Life Sciences
Potassium Chloride (KCl)	Thermo Fisher Scientific
Pyruvate Kinase/Lactate Dehydrogenase enzyme from Rabbit muscle (PK/LDH)	Sigma-Aldrich Life Sciences
Sodium Dodecyl Sulphate (SDS)	Thermo Fisher Scientific
Sodium Chloride (NaCl)	Thermo Fisher Scientific
Sodium Hydroxide (NaOH)	Thermo Fisher Scientific
Sodium Phosphate (NaH_2PO_4)	Thermo Fisher Scientific
SYBR Safe DNA Gel Stain	Invitrogen - Life Technologies
Tetramethylethylenediamine (TEMED)	Thermo Fisher Scientific
Tris (tris-(hydrocymethyl)aminomethane) (Tris-Base)	Thermo Fisher Scientific
Triton X-100	Thermo Fisher Scientific
Tween 20	Thermo Fisher Scientific

Table 2.2 Molecular standards

Standard	Supplier
GeneRuler 1 kb DNA Ladder	Fermentas – Thermo Fisher Scientific
PageRuler™ Protein Ladder Plus	Fermentas – Thermo Fisher Scientific

Table 2.3 DNA modifying enzymes and buffers

Enzyme or Buffer	Supplier
PfuTurbo DNA polymerase	Agilent Technologies
Restriction Digest Enzymes	New England BioLabs (NEB)
Restriction Digest Enzymes Buffer	New England BioLabs (NEB)
TopTaq DNA Polymerase	QIAGEN
TopTaq DNA Polymerase Buffer	QIAGEN
T4 DNA Ligase	New England BioLabs (NEB)
T4 DNA Ligase Buffer	New England BioLabs (NEB)

Table 2.4 Commercial kits

Kit	Supplier
QIAquick Gel Extraction Kit	QIAGEN
QIAGEN PCR Purification Kit	QIAGEN
QIAGEN Plasmid Midi Kit	QIAGEN
QIAprep Spin Miniprep Kit	QIAGEN
QuikChange Mutagenesis	Agilent Technologies

2.1.2 Laboratory media and buffers

The following media and buffers were prepared using the reagents and supplies listed in Section 2.1.1.

Table 2.5 Media and buffers

Buffer	Contents
4X ATPase Assay Reaction Buffer	11 mM Hepes, pH 7.2 4 mM PEP

1X Coomassie Stain	25 g Brilliant Blue R-250 500 mL Methanol
Destain	2.105 L 95 % Ethanol 15.895 L ddH_2O 2.0 L Glacial Acetic Acid
6X DNA Loading Dye	0.3 % (w/v) Bromophenol Blue 30 % (v/v) Glycerol 0.3 % (w/v) Xylene cyanol Up to 10 mL ddH_2O
ECL Solution #1	0.45 mM p-Coumaric Acid 3.75 mL DMSO 2.5 mM Luminol Up to 250 mL 0.1 M Tris, pH 8.8
ECL Solution #2	0.02 % (v/v) 250 mL 0.1 M Tris Base, pH 8.8
10X Electrode	2880 g Glycine 600 g Tris Base 200 g SDS Up to 20 L ddH_2O
Gel Filtration Buffer (Co-Chaperone)	25 mM Hepes 50 mM NaCl 5 mM β-Mercaptoethanol Up to 1 L ddH_2O, pH 7.2
Gel Filtration Buffer (Hsp90)	25 mM Hepes 10 mM NaCl 5 mM β-Mercaptoethanol Up to 1 L ddH_2O, pH 7.2
Immobilized Metal Ion Affinity Chromatography (IMAC) Buffer A (Resuspension Buffer)	25 mM NaH_2PO_4 500 mM NaCl 20 mM Imidazole 1 mM $MgCl_2$ 5 mM β-Mercaptoethanol Up to 1 L ddH_2O, pH 7.2

Immobilized Metal Ion Affinity Chromatography (IMAC) Buffer B	25 mM NaH_2PO_4 500 mM NaCl 1 M Imidazole 1 mM $MgCl_2$ 5 mM β-Mercaptoethanol Up to 1 L ddH_2O, pH 7.2
Luria Broth, Miller's	25 g LB powder 1 L ddH20
10X PBS	1600 g NaCl 40 g KCl 48 g KH_2PO_4 432 g Na_2HPO_4 Up to 20 L ddH_2O
4X Running Gel Buffer	363.4 g Tris Base 1600 mL ddH_2O 8 g SDS Up to 2 L ddH_2O, pH 8.8
SDS-PAGE Sample Buffer (6X)	30 % (v/v) Glycerol 120 mM Tris Base pH 7.0 6 % (w/v) SDS 0.6 % (w/v) Bromophenol Blue Drop
Stacking Gel Buffer	33.92 g Tris Base 1800 mL ddH_2O 2.2 g SDS Up to 2 L ddH_2O, pH 6.8
50X TAE	242 g Tris Base 57.1 mL Glacial Acetic Acid 100 mL 0.5 M EDTA Up to 1 L ddH_2O, pH 8.0
10X TBS (tris-buffered saline)	320 g NaCl 8 g KCl 120 g Tris Base Up to 4 L ddH_2O, pH 8.0
10X Western Transfer Buffer	605 g Tris Base 2880 g Glycine Up to 20 L ddH_2O

2.1.3 Primers

The following primers were used in polymerase chain reactions (PCR) to construct genes of interest, add tags, and insert mutations.

Table 2.6 Primers

Primer ID #	Primer Name	Sequence
22	NScHsp82NdeI	gagagacatatggctggtgaaacttttg
23	CScHsp82BamHI	gagagaggatcctcactaatctacctcttccatttcggtg
28	NScAha1NdeI	gagagacatatggtcgtgaataacccaaataactggc
29	CScAha1BamHI	gagagaggatcctcactataatacggcaccaaagccg
289	sQCHsp82V391E	gttacaacaaaataagatcatgaaggagattagaaag aacattgtcaaaaag
290	aQCHsp82V391E	ctttttgacaatgttctttctaatctccttcatgatcttatttt gttgtaac
339	sQCHsp82D79N	gagcaaaaagttttggaaatcagaaattctggtattggtat gaccaaggctg
340	aQCHsp82D79N	cagccttggtcataccaataccagaatttctgatttccaaa actttttgctc
402	sQCHsp82E33A	caaggaaattttcttgagagcactgatatctaatgcctc
403	aQCHsp82E33A	gaggcattagatatcagtgctctcaagaaaatttccttg
668	sQCHsp82K178C	ggggtaccatcttgaggttattcttgtgcgatgaccaattgg agtacttggaag
669	aQCHsp82K178C	cttccaagtactccaattggtcatcgcacaagaataacctc aagatggtacccc
665	sSMT3Nde1	gagagacatatgtcggactcagaagtcaatcaagaagc
666	aSMT3GGCysBamH1	tctctcggatcctcactagcaaccaccaatctgttctctgt gag

667	aSMT3GCysBamH1	tctctcggatcctcactagcaaccaatctgttctctgtgag
491	sNde1Cpr6	gagagacatatgactagacctaaaacttttttgatatttc
492	aBamH1Cpr6	gagagaggatcctcactaggagaacatcttcgaaagagac
578	sAha1del157-206	gctggccacccatggtaatgacattcaggtgcaaaacggaagcggcaatagtac
579	aAha1del157-206	gtactattgccgcttccgttttgcacctgaatgtcattaccatgggtggccagc
580	sAha1del157-181	gctggccacccatggtaatgacattcaggtgtcaaagccaaaaaagaatgcac
581	aAha1del157-181	gtgcattctttttggctttgacacctgaatgtcattaccatgggtggccagc
582	sAha1del182-206	ctttaccgaaatcaaggactccgctcaaaacggaagcggcaatagtac
583	aAha1del182-206	gtactattgccgcttccgttttgagcggagtccttgatttcggtaaag
584	sHsp82del211-263	gtggcctacccaatccaattagtcgtcaccgttcaagagatagaagaactaaacaagactaagc
585	aHsp82del211-263	gcttagtcttgtttagttcttctatctcttgaacggtgacgactaattggattgggtaggccac
483	sNcoIHisMycNdeISba1	gagagaccatgggccatcaccatcaccatcacgaacaaaaattgatttctgaagaggatttgcatatgtccgataaagttattaaccctcaagttgc
616	sNcoIHisFlagNdeISba1	gagagaccatgggccatcaccatcaccatcacgattacaaggatgacgacgataagcatatgtccgataaagttattaaccctcaagttgc
617	sNcoIHisHANdeISba1	gagagaccatgggccatcaccatcaccatcactacccatacgatgttccagattacgctcatatgtccgataaagttattaaccctcaagttgc
45	CScSba1BamHI	gagagaggatcctcactaagctttcacttccggctc

2.1.4 Plasmid vectors

All vectors listed are ampicillin selectable with an HexaHis (6xHis) epitope tag placed at the amino-terminal of the protein of interest. pET11dHis vectors containing Hsp82p, Sba1p, Sti1p, Aha1p, Aha1p^{N}, HA-chimera, and Hch1p were previously constructed by graduate students in the LaPointe Lab (Armstrong et al., 2012; Horvat et al., 2014). Myc, HA, and Flag tags were engineered downstream of the His tags with primers to Sba1p, and were added onto the specified vectors by sub-cloning. Hsp82p^{LL} was kindly provided by Dr. Johannes Buchner in a pET24a vector. Refer to Section 2.2.7 for plasmid construction information.

Table 2.7 Plasmids used and constructed

Plasmid Name	Derived from / Provided by	Primers	Sub-cloning
pET11dhisHsp82			
pET11dhisMycHsp82	pET11dhisHsp82		✓
pET11dhisHsp82^{V391E}	pET11dhisHsp82	289, 290	
pET11dhisMycHsp82^{V391E}	pET11dhisHsp82^{V391E}		✓
pET11dhisHsp82^{D79N}	pET11dhisHsp82	339, 340	
pET11dhisHAHsp82^{D79N}	pET11dhisHsp82^{D79N}		✓
pET11dhisHsp82^{E33A}	pET11dhisHsp82	402, 403	
pET11dhisHAHsp82^{E33A}	pET11dhisHsp82^{E33A}		✓
pET11dhisHsp82^{LL}	pET24aHsp82lidless		✓
pET11dhisHsp82$^{V391E/LL}$	pET11dhisHsp82^{LL}	289, 290	✓
pET11dhisHsp82^{K178C}	pET11dhisHsp82	668, 669	
pET11dhisMycHsp82^{K178C}	pET11dhisHsp82^{K178C}		✓
pET11dhisFlagHsp82^{K178C}	pET11dhisHsp82^{K178C}		✓
pET11dhisHsp82$^{\Delta 211\text{-}263}$	pET11dhisHsp82	22, 584, 23, 585	
pET11dhisAha1			
pET11dhisMycAha1	pET11dhisAha1		✓

pET11dhisAha1$^{\Delta 156\text{-}206}$	pET11dhisAha1	28, 578	
		29, 579	
pET11dhisAha1$^{\Delta 156\text{-}181}$	pET11dhisAha1	28, 580	
		29, 581	
pET11dhisAha1$^{\Delta 182\text{-}206}$	pET11dhisAha1	28, 582	
		29, 583	
pET11dhisHch1			
pET11dhisMycHch1	pET11dhisHch1		✓
pET11dhisSba1			
pET11dhisMycSba1	pET11dhisSba1	483, 45	
pET11dhisHASba1	pET11dhisSba1	617, 45	
pET11dhisFlagSba1	pET11dhisSba1	616, 45	
pET11dhisSti1			
pET11dhisMycSti1	pET11dhisSti1		✓
pET11dhisCpr6		91, 92	
pET11dhisMycCpr6	pET11dhisCpr6		✓
pET11dhisSmt3pGG		665, 666	
pET11dhisSmt3pG		665, 667	
pET11dhisHAchimera			
pET11dhisAha1^{N}			

2.1.5 Protein Sequences

Expression vectors all contained 6xHis tags that were placed at the amino-terminal of the protein of interest, with additional Myc, Flag, or HA tags downstream of the His tag, where specified in Section 2.1.4.

Table 2.8 Epitope tag sequences

Tag	Sequence
His	HHHHHH
Myc	EQKLISEEDL
HA	YPYDVPDYA
Flag	DYKDDDK

Yeast proteins were used throughout this thesis work, and protein sequences for Sti1p, Cpr6, Hch1p, Sba1p can be found on www.yeastgenome.org. Hsp82p, Aha1p, and Smt3p sequences were modified in the following ways outlined below.

Full-length Hsp82p sequence consists of the following 709 amino acids:

MASETFEFQAEITQLMSLIINTVYSNKEIFLRELISNASDALDKIRYKSLSDP
KQLETEPDLFIRITPKPEQKVLEIRDSGIGMTKAELINNLGTIAKSGTKAFM
EALSAGADVSMIGQFGVGFYSLFLVADRVQVISKSNDDEQYIWESNAGGS
FTVTLDEVNERIGRGTILRLFLKDDQLEYLEEKRIKEVIKRHSEFAYPIQLV
VTKEVEKEVPIPEEEKKDEEKKDEEKKDEDDKKPKLEEVDEEEEKKPKTK
KVKEEVQEIEELNKTKPLWTRNPSDITQEEYNAFYKSISNDWEDPLYVKH
FSVEGQLEFRAILFIPKRAPFDLFESKKKKNNIKLYVRRVFITDEAEDLIPEL
SFVKGVVDSEDLPLNLSREMLQQNKIMKVIRKNIVKKLIEAFNEIAEDSEQ
FEKFYSAFSKNIKLGVHEDTQNRAALAKLLRYNSTKSVDELTSLTDYVTR
MPEHQKNIYYITGESLKAVEKSPFLDALKAKNFEVLFTDPIDEYAFTQLKE
FEGKTLVDITKDFELEETDEEKAEREKEIKEYEPLTKALKEILGDQVEKVV
VSYKLLDAPAAIRTGQFGWSANMERIMKAQALRDSSMSSYMSSKKTFEIS
PKSPIIKELKKRVDEGGAQDKTVKDLTKLLYETALLTSGFSLDEPTSFASRI
NRLISLGLNIDEDEETETAPEASTAAPVEEVPADTEMEEVD

Residues highlighted in red indicate point mutations that were inserted using Quickchange^{TM} Mutagenesis. To construct Hsp82p^{LL} and Hsp82p$^{\Delta 211\text{-}263}$, the following sequences were modified:

Table 2.9 Design of Hsp82p deletion constructs

Construct	Sequence	Modification
Hsp82p^{LL}	KSGTKAFMEALSAGADVSMIGQFG	Replaced with GSG
Hsp82p$^{\Delta 211\text{-}263}$	KEVEKEVPIPEEEKKDEEKKDEEKK DEDDKKPKLEEVDEEEEKKPKTKKVKEE	Deleted

Full-length Aha1p consists of the following 350 amino acids:
MVVNNPNNWHWVDKNCIGWAKEYFKQKLVGVEAGSVKDKKYAKIKSV
SSIEGDCEVNQRKGKVISLFDLKITVLIEGHVDSKDGSALPFEGSINVPEVA
FDSEASSYQFDISIFKETSELSEAKPLIRSELLPKLRQIFQQFGKDLLATHGN
DIQVPESQVKSNYTRGNQKSSFTEIKDSASKPKKNALPSSTSTSAPVSSTN
KVPQNGSGNSTSIYLEPTFNVPSSELYETFLDKQRILAWTRSAQFFNSGPK
LETKEKFELFGGNVISELVSCEKDKKLVFHWKLKDWSAPFNSTIEMTFHE
SQEFHETKLQVKWTGIPVGEEDRVRANFEEYYVRSI KLTFGFGAVL

To construct Aha1p$^{\Delta 156\text{-}206}$, Aha1p$^{\Delta 156\text{-}181}$, Aha1p$^{\Delta 181\text{-}206}$, the Aha1p sequence was modified in the following manner:

Table 2.10 Design of Aha1p deletion constructs

Construct	Sequence	Modification
Aha1p$^{\Delta 156\text{-}206}$	PESQVKSNYTRGNQKSSFTEIKDSASKP KKNALP SSTSTSAPVSSTNKVP	Deleted
Aha1p$^{\Delta 156\text{-}181}$	SQVKSNYTRGNQKSSFTEIKDSA	Deleted
Aha1p$^{\Delta 182\text{-}206}$	SKPKKNALP SSTSTSAPVSSTNKVP	Deleted

Full-length Smt3p consists of the following 101 amino acids:
MSDSEVNQEAKPEVKPEVKPETHINLKVSDGSSEIFFKIKKTTPLRRLMEA
FAKRQGKEMDSLRFLYDGIRIQADQTPEDLDMEDNDIIEAHREQIGGATY

This sequence of Smt3p represents SUMO as a pro-protein, before it is activated upon cleavage by a protease that removes the C-terminal peptide to expose a diglycine motif. To construct Smt3pGG-Cys and Smt3pG-Cys, the Smt3p sequence was modified in the following manner:

Table 2.11 Design of Smt3p constructs

Construct	Sequence	Modification
Smt3pGG-Cys	ATY	Replaced with C
Smt3pG-Cys	GATY	Replaced with C

2.1.6 Antibodies

The following antibodies were used in western blotting experiments. Secondary antibodies, which were acquired from Jackson Labs, were used at a dilution of 1:2000.

Table 2.12 Primary antibodies

Primary Antibody	Dilution	Type	Secondary	Supplier
anti-Myc (4A6)	1:1000	Monoclonal	Mouse	Millipore
anti-Tetra-His (34670)	1:1000	Monoclonal	Mouse	Qiagen
anti-HA (3F10)	1:1000	Monoclonal	Rat	Roche
anti-Flag (F3165)	1:1000	Monoclonal	Mouse	Sigma

2.2 Methods

2.2.1 Polymerase chain reaction

DNA was amplified using Platinum TopTaq polymerase PCR kit with template DNA, primers listed in Table 2.6. Reactions contained 50 ng plasmid

DNA, 200 nM sense and antisense primers, 500 nM dNTPs, and 1 U of Platinum TopTaq in 50 µL reactions. Reactions were carried out with a QIAGEN PCR protocol on an Eppendorf Mastercyler.

2.2.2 QuikChange™ mutagenesis

Site-directed mutagenesis was used to introduce mutations into Hsp82p using QuikChange™ mutagenesis. Reactions contained 100 ng of template DNA, 4 mMol dNTP, 5 µL 10X Pfu Buffer, 1 µL Pfu, 10 pmol sense primer, 10 pmol antisense primer, and distilled water to a total volume of 50 µL. Reactions were carried out with a PCR protocol on an Eppendorf Mastercyler, after which the 50 µL reaction was digested with 2 µL of Dpn1 enzyme and incubated for four hours at 37°C.

2.2.3 Agarose gel electrophoresis

PCR samples and restriction endonuclease digests were separated on a 0.8 % agarose gel by gel electrophoresis. Samples were run beside a 1 Kb DNA ladder until the bands were separated enough to resolve inserts from plasmid DNA. Using the Cell Biosciences FluorChemQ system to visualize the gels, desired bands were excised from the gel and then gel purified.

2.2.4 Purification of DNA fragments

To purify PCR products, the purification kit and protocol from QIAGEN was used. PCR product sample was diluted into five times the volume of Buffer PB, placed in a QIAquick spin column, and centrifuged using an Eppendorf 5417C centrifuge with an F45-30-11 rotor set at 14,000 rpm for one minute. Flow-through was discarded and 750 µL Buffer PE was added and spin column and centrifuged for one minute. Flow-through was discarded and spin column was centrifuged for two minutes to dry sample of ethanol (contained in the PE Buffer). By adding 50 µL dH_2O to the column, DNA was eluted in a clean 1.5 mL microcentrifuge tube by centrifugation for one minute.

To purify excised gel fragments, QIAGEN QIAquick gel extraction kit and protocol was used. Gel fragments containing excised DNA bands from agarose gel were melted in five times volume of Buffer QG at 50 °C for 10 minutes. Liquid samples were centrifuged through QIAquick spin columns using an Eppendorf 5417C centrifuge with an F45-30-11 rotor set at 14,000 rpm for one minute. Flow-through was discarded before adding 500 µL of Buffer QG to the spin column and centrifuged for one minute. Flow-through was discarded before adding 750 µL of Buffer PE to the spin column and centrifuged again for one minute. Flow-through was discarded and spin column was centrifuged for two minutes to dry sample of ethanol (contained in the PE Buffer). By adding 30 µL dH_2O to the column, DNA was eluted in a clean 1.5 mL microcentrifuge tube by centrifugation for one minute.

2.2.5 Restriction endonuclease digestion

For plasmid construction, DNA was digested with restriction endonucleases following New England Biolabs protocols. Reactions were set up to contain 2 µL NEB restriction enzymes, 5 µL NEB 10X reaction buffer, 5 µL 10X BSA, 1 µg of DNA, and distilled water to a final volume of 50 µL. Reactions were incubated at 37 ºC for three hours. For diagnostic purposes to verify successful cloning and also for subcloning of PCR products or plasmid inserts into vector DNA backbones, small scale reactions were set up. Reactions contained 0.5 µL NEB restrictive digestive enzyme, 2 µL NEB 10X reaction buffer, 2 µL 10X BSA, 0.25-0.5 µg DNA, and distilled water to a final volume of 20 µL. Reactions were incubated at 37 ºC for one hour. Diagnostic digest samples were run on agrose gels to verify successful cloning, prior to being transformed into *Escherichia coli.*

Table 2.13 Restriction endonucleases used in molecular cloning

Restriction Endonuclease	Buffers	Application
*Nde*I-*Bam*HI	NEB 4 + BSA	Plasmid isolation
*Nco*I-*Bam*HI	NEB 3 + BSA	Plasmid isolation
*Dpn*1	NEB4	Quikchange mutagenesis

2.2.6 Ligation

Ligation reactions contained 1:3 molar ratio of similarly cut vector DNA to insert DNA in 20 µL reaction volumes. 50 ng of vector DNA was combined with the corresponding amount of insert DNA, and 4 µL 10X T4 ligase buffer, 1 µL (1 U) T4 Ligase, and distilled water was mixed together to reach a final reaction volume of 20 µL. Control samples included distilled water instead of insert DNA. Reactions were incubated at room temperature for 1-3 hours. After incubation, DNA was transformed into DH5α or BL21 *Escherichia coli.*

2.2.7 Plasmid construction

Expression vectors encoding Hsp82p, Aha1p, Aha1p^{N}, Hch1p, HA-chimera, Sti1p, and Sba1p were used throughout my thesis, and were constructed as previously described (Armstrong et al., 2012; Horvat et al., 2014). Using these vectors as templates, site directed mutagenesis was conducted. All genes were cloned to introduce *Nde*I and *Bam*HI restriction sites at the 5' and 3', respectively.

The CPR6 and SMT3 coding sequencing were amplified by PCR with primers designed to introduce *Nde*I and *Bam*HI restriction sites at the 5′ and 3′ ends, respectively. The PCR products were digested with *Nde*I and *Bam*HI for ligation into similarly cut pET11dHis. The lidless-mutant of Hsp82p was constructed and kindly provided by Johannes Buchner in a pET28a vector (Richter et al., 2006). The lidless Hsp82p (Hsp82p^{LL}) construct was digested with *Nde*1 and *Bam*H1 for ligation into similarly cut pET11dhis vector. Site directed mutagenesis was carried out to construct Hsp82p variants (Hsp82p^{K178C}, Hsp82p^{V391E}, Hsp82p^{D79N}, Hsp82p^{E33A}, Hsp82p^{LL}, Hsp82p$^{V391E/LL}$, Hsp82p$^{V391E/D79N}$, and Hsp82p$^{V391E/E33A}$) using QuikChange mutagenesis (Agilent). The coding sequences contained in all mutagenized plasmids were verified by sequencing.

Constructing linker deletions

The coding sequence of Hsp82p$^{\Delta 211-263}$, Aha1p$^{\Delta 156-206}$, Aha1p$^{\Delta 156-181}$, and Aha1p$^{\Delta 182-206}$, was constructed in a two-step PCR process using an overlapping PCR strategy. The first PCR reaction amplified the N-terminal domain of the

Hsp82p coding sequence prior to the linker region, and also the remaining Hsp82p coding sequence after the linker region. The N-terminal domain was amplified using sense primer 22 and antisense primer 584, where the primer 584 contained a short segment of the coding sequence of Hsp82p after the deletion region. This was also completed for the remaining part of Hsp82p, using primers sense 23 and antisense 585, where the primer 585 contained the nucleotides of prior to the deletion region. The second PCR step used the two overlapping gene fragments as the template DNA with the sense primer 22 and antisense primer 23. Aha1p linker truncation variants were constructed similarly using the primers outlines in Table 2.6. These PCR products were then cloned into the pET11dhis vector as described above.

Introduction of Myc, HA, and Flag tags

All bacterial expression plasmids were constructed using pET11dhis to produce recombinant proteins harboring an N-terminal 6xHis tag, downstream of the *Nde*I site, for purification purposes (Armstrong et al., 2012). The Myc, HA, and Flag epitope was fused in-frame with the 6xHis-tag sequence, upstream of the *Nde*I site of the pET11dhis vector, by using sense primers designed to introduce the *NcoI* restriction site at the 5' end, followed by the His-tag and the Myc, HA, or Flag tags, the *Nde*1 site, and the beginning of the Sba1p sequence. Sba1p was amplified with the tags using the sense primer containing the Myc, Flag, or HA tags as described (primers 483, 616, and 617) and the antisense primer 45. Engineering the *Nde*I restriction site after the tags enabled me to sub-clone all genes sequences from the pET11dhis vectors into the HisMyc, HisFlag, and HisHA vectors.

2.2.8 *Escherichia coli* transformation

2 µL plasmid DNA was incubated with 100 µL of thawed competent *Escherichia coli* cells. DH5α cells were used for molecular cloning purposes. Reactions were incubated on ice for 20 minutes, heat shocked 45 seconds on a 42 ºC heat block, and set on ice for another 2 minutes. 1 mL of LB media was added to the cells and placed in the 37 ºC incubator for a 30-minute recovery. The cells

were pelleted down at 13600 rpm for 20 seconds using an Eppendorf 5417C centrifuge (F45-30-11 rotor). Supernatant was decanted, cells resuspended in 100 µL LB media, and plated on LB agar plates containing 100 ug/ml ampicillin. Plates were incubated at 37 ºC overnight.

When transforming ligated DNA, 5 µL of the ligation reactions was incubated with the competent cells. For protein expression purposes, competent BL21(DE3) *Escherichia coli* strain was used instead.

2.2.9 Glycerol stocks

Glycerol stocks were made by inoculating a 5 mL LB culture containing 0.5 mg ampicillin with a single colony from a LB agar plate. The culture was incubated overnight at 37 ºC while shaking at 200 rpm. 500 µL 30 % sterilized glycerol and 500 µL of culture was mixed in sterile eppendorf tubes and stored in a -80 ºC freezer.

2.2.10 Isolation of plasmid DNA from *Escherichia coli*

QIAprep spin mini prep kits were used to extract plasmid DNA for *E. coli* DH5α bacteria following manufacturer's protocol. A single colony of DH5α bacteria was picked from an LB Amp plate to inoculate a 5 mL LB culture. Alternatively, a 50 mL starter culture was inoculated with DH5α bacteria transformed with plasmid of interest from a glycerol scrape. The culture was grown overnight at 37 ºC while shaking at 200 rpm. The following day, culture was pellets by centrifugation at 5000 x g for 10 minutes. Supernatant was discarded, pellet was resuspended in ~200 µL LB media, transferred to a 1.5 mL centrifuge tube, and subject to centrifugation for one minute at 13600 rpm using an Eppendorf 5417C centrifuge with a F45-30-11 rotor (used for all further centrifugation steps). Supernatant was removed and 250 µL of Buffer P1 was added to resuspend pellet. 250 µL Buffer P2 was added and tube was inverted 6 times and incubated at room temperature for <5 minutes. Chilled Buffer N3 was added and tube was inverted 6 times before being subject to centrifugation for 10 minutes. Supernatant was transferred to QIAprep spin column and centrifuged for one minute, removing

flow-through thereafter. The column was washed with 500 µL Buffer PB and centrifuged for one minute, removing the flow-through thereafter. The column was washed by adding 750 µL Buffer PE and centrifuged for one minutes. Column was placed in a new 1.5 centrifuge tube to elute DNA, which was achieved by adding 50 µL of dH_2O to the column and centrifugation for one minute.

2.2.11 Protein expression

A single BL21 (DE3) colony was picked to inoculate a 50 mL starter culture containing 5 mg ampicillin. Alternatively, the glycerol stock was scraped to inoculate multiple starter cultures. The cultures were grown overnight at 37 ºC while shaking at 200 rpm. The following day, 10-15 mL of the starter culture was used to inoculate 750 mL LB media flasks with 75 mg ampicillin. Large scale expression involved growing 8-12 750 mL flasks. These cultures were grown to an OD_{600} of 0.8-1.2 and then induced with 1 mM isopropyl-1-thio-D-galactopyranoside (IPTG), and then incubated at 37 °C for co-chaperone proteins or 30 °C for Hsp90 cultures. Cells expressing co-chaperone proteins Aha1p, Hch1p, HA-chimera, $Aha1p^{N}$, and $Smt3p^{Cys}$, were harvested after 8 hours of growth, while cells expressing Hsp82p (and variants), Sti1p, Sba1p, and Cpr6p were harvested after overnight growth. Cultures were harvested at 4 °C using a Beckman Coulter Avanti J-26XP1 with a JLA-8.1 rotor for 15 minutes at 7,000 rpm. Supernatants were removed, pellets resuspended in 1x PBS, and transferred to 50 mL falcon tubes. Cells were centrifuged for 15 minutes at 4,150 rpm using a Thermo Scientific Sorval Legend T+ (7500 6445 swinging bucket rotor). Supernatant was removed and pellets were stored in − 80 °C freezer.

2.2.12 Protein purification

All protein purifications were performed at 4 °C using an AKTA Explorer Fast Protein Liquid Chromatography (FPLC) system with a Frac-950 collector (GE Healthcare). Buffers used are listed in section 2.1.2 and Nickel columns (HisTrap FF 5 mL and 1 mL columns) were stripped and cleaned before every protein purification following the following protocol. Solutions listed in Table 2.14 were

pushed through the columns manually. Each step was followed by pushing through the same amount of filtered water as the amount of column volumes the previous step listed, with the exception of step 6 and 7 which received double the amount of filtered water.

Table 2.14 Solutions for cleaning and charging HisTrap columns

Step	Solution	Column Volumes
1	200 mM EDTA	1
2	1 M NaCl	5
3	1 M NaOH	5
4	20 % EtOH	5
5	30 % Isopropanol	5
6	50 mM EDTA	5
7	10 mM NiSO4	5

- All solutions must be filtered before use

2.2.12.1 Pellet resuspension and mechanical lysis

Bacterial pellets were thawed on ice and resuspended in Resuspension buffer, supplemented with 1X HALT EDTA-free protease inhibitor (Thermoscientific) and 5 mM βMe. Cells were lysed 6 times using Avestin Emulsiflex C3 (Avestin, Ottawa, Ontario, Canada) at 4 °C. Lysates were clarified by ultracentrifugation using a Beckman Coulter Optima L-100K centrifuge with a Ti60 rotor at 36,000 rpm for 30 minutes to separate cell debris from the cytoplasm.

2.2.12.2 Immobilized metal affinity chromatography (IMAC)

Supernatant containing the cytoplasmic protein from section 2.2.12.1 was loaded onto the FPLC and His-tagged proteins were isolated on a 5 mL HisTrap FastFlow (FF) Nickel column (GE Healthcare). Weakly bound proteins were washed off in a 5 % IMAC B step over 4 column volumes, collecting eluted proteins in 1 mL fractions. Next, proteins were eluted by running a 5-100 % gradient of IMAC B over 4-6 column volumes, and a final step of a 100 % IMAC B for 1 -2

column volumes. The FPLC absorbance chromatograms were used to determine in which 1 mL fractions the protein of interest was collected in. 10 µL of each 1mL fraction were run on an 8-12 % SDS-PAGE gel to verify protein clarity and concentration. Isolated 6xHis-tagged containing protein fractions were pooled and concentrated in a 15 mL Amicon Ultra Centrifugal Filter Device. 10k cutoff was used for Hsp82p (and variants), Cpr6p, Aha1p, HA-chimera, and Sti1p, and a 3k Cutoff was used for Sba1p, Hch1p, $Aha1p^{N}$ and $Smt3p^{Cys}$. Protein samples were centrifuged for 3-5 minutes at a time, using a Thermo Scientific Sorval Legend T+ (7500 6445 swinging bucket rotor), mixing the sample carefully between spins. Concentrated protein samples were then transferred to Eppendorf tubes, centrifuged for 1 minutes, at 13,600 rpm in an Eppendorf Centrifuge 5417C (F45-30-11 rotor) to pellet insoluble particulates. Supernatant was transferred to a new Eppendorf tube and stored at 4 °C.

2.2.12.3 Gel filtration (GF)

Protein samples were further purified by size exclusion chromatography on either a Superdex 200, Superose 6, or a Superdex75 column (GE Healthcare). 100-250 µL samples were injected into FPLC loading port when using Superdex 75 and Superose 6 columns, and 1 mL- 3 mL samples were injected into FPLC loading port when using the Superdex 200 column. Hsp82p (and variants) were eluted in a final GF buffer consisting of 25 mM Hepes pH 7.2, 10 mM NaCl, and 5 mM ß-mercaptoethanol, and all other proteins were eluted in co-chaperone GF buffer (25 mM Hepes pH 7.2, 50 mM NaCl, and 5 mM ß-mercaptoethanol). No reducing agents were added when protein was made for crosslinking purposes.

2.2.13 Protein concentration determination

The absorbance of light at a specific wavelength (280 nM for protein) is directly proportional to the concentration of a protein according to Beer-Lambert Law:

$$A = \varepsilon cl$$

where ***A*** is the absorbance, ***ε*** is the extinction coefficient or the molar absorptivity, ***c*** is the concentration and ***l*** is the path length of the light through the sample in cm. The final concentration of the purified protein was determined by using a NanoDrop Spectrophotometer to measure the absorbance at 280 nm (A_{280}) where *l* was 1 cm and then the concentration was calculated by using the following formula:

$$\textbf{Concentration (µM)} = A_{280} / \varepsilon \times 1{,}000{,}000$$

Buffer was used as the blank prior to protein samples were measured. For each protein sample, multiple readings were made and the average A_{280} was calculated. When necessary, a 1 in 5 or 1 in 10 dilution of the protein sample was prepared to ensure that the absorbance reading was within the working range (between 0.1 and 2 absorbance units) of the NanoDrop. The extinction coefficient (ε) for each protein, listed in Table 2.15, was calculated using Vector NTI as it is dependent on size and amino acid composition. HA and Flag tags influence the extinction coefficient of the protein, and thus it was also calculated for those select proteins when purifying HA- and Flag-tagged proteins (not shown).

Table 2.15 Extinction coefficients of Hsp82p and co-chaperone proteins

Protein	Extinction Coefficient (ε) M^{-1} cm^{-1}
Hsp82p	54050
Aha1p	50430
Hch1p	21030
Sti1p	49430
Cpr6p	18760
Sba1p	28710
$Hsp82p^{\Delta LL}$	54050
$Hsp82p^{\Delta 211\text{-}263}$	54050
$Aha1p^{N}$	22430
$Aha1p^{\Delta 156\text{-}206}$	49150

Aha1p $^{\Delta 156\text{-}181}$	49150
Aha1p $^{\Delta 182\text{-}206}$	50430
Smt3p	2560
HA-chimera	50310

- The extinction coefficient of was calculated with the His tag, and the presence of the Myc-tag (His-Myc) does not change it.

2.2.14 Snap freezing

Protein samples were aliquoted into 50, 100, and 150 µL small eppendorf tubes and snap frozen in liquid nitrogen. Before using in any assays, the protein purity, quality, and concentration was assessed by running various different concentrations on an appropriate SDS-PAGE gel and also compare to previous protein preps if available.

2.2.15 Sodium dodecyl sulfate polyacrylamide gel electrophoresis (SDS-PAGE)

SDS PAGE was used to detect in which fractions proteins were eluted in and also to assess protein quality and quantity during purification steps. Different percentage of gels (5,8,10,12 %) allowed for resolving different molecular mass proteins.

Protein samples were prepared by adding 2 µL of 6x Sample buffer containing negatively charged SDS, which denatures and charges the protein uniformly. Samples in eppendorf tubes were heated for 5-10 minutes at 100°C before loading 10 µL aliquots onto the gel. All gels were run using 1X Gel Running Buffer at 120 V for 1 hour and 15 min.

2.2.16 Coomassie blue staining

All SDS-PAGE gels were stained with Coomassie Blue staining dye. Coomassie Blue staining dye was added to a container with gel(s), heated for 30 seconds in a microwave, followed by rocking for 10-30 minutes. Background dye

was removed by immersion in destain solution after 20 seconds heating in a microwave. Gels were visualized using Cell Biosciences FluorChemQ system.

2.2.17 ATPase assays

All ATPase assays were carried out using the PK/LDH regenerating system as previously described where the regeneration of ATP is coupled to the oxidation of NADH (Armstrong et al., 2012; Horvat et al., 2014; Panaretou et al., 1998). Every experiment was done in triplicate (n=3), unless specified, and reactions within experiments were carried out three times in 100 µL volumes using a 96-well plate. Absorbance at 340 nm (absorbance of NADH) was measured at 30 ºC every minute for 90 minutes using a BioTek Synergy 4, with the path-length correction function enabled. All ATPase assay was started by the addition of the regenerating system consisting of $MgCl_2$, DTT, NADH, ATP, PEP, and PK/LDH.

Data was then exported by the Gen5 software program to Excel. To calculate Hsp90 activity, the decrease in NADH absorbance at 340 nm was converted to micromoles of ATP using Beer's Law and expressed as a function of time (min^{-1}). Average values of the experiments are shown with error expressed as standard error of the mean using Prism GraphPad. The ATPase rates are either shown as µM ATP hydrolyzed per minute per µM of Hsp90 (1/min) or as a fold ATPase stimulated rate of the starting Hsp90 or heterodimer intrinsic rate.

Fit lines were calculated according to the following equation:

$$(Y =))B_{MAX}*X)/(K_{APP} + X)) + X_0)$$

The final conditions of all the reactions in Chapter 3 and 5 are 25 mM Hepes (pH 7.2), between 1–25 mM NaCl, 5 mM $MgCl_2$, 1 mM DTT, 0.3-0.6 mM NADH, 2 mM ATP, 1 mM phosphoenol pyruvate (PEP), 2.5 µL of pyruvate kinase/lactate dehydrogenase (PK/LDH) (Sigma), and 0.5 % DMSO. Chapter 4 reaction conditions were similar to the reactions described above, but contained increased DTT levels as part of the crosslinking quenching protocol. In all experiments, identical reactions were set up and quenched with 50 µM or 100 µM NVP-AUY922

and then subtracted from unquenched reactions to correct for contaminating ATPase activity.

2.2.17.1 Hsp90 heterodimer ATPase assays

Heterodimer ATPase Assays were performed as described in Retzlaff *et al*. 2010. We allowed equilibration of heterodimers by mixing two samples of Hsp90 (one being a functional, ATPase-competent Hsp90 and the other, an ATPase-dead Hsp90 variant) at a specific concentration ratio for 15 minutes at room temperature. Hsp82p^{LL} was titrated into 2 μM wildtype Hsp82p or Hsp82p^{V391E} and Hsp82p$^{V391E/LL}$ was titrated into 2 μM Hsp82p to determine at which ratio we have to mix the ATPase competent with the ATPase dead Hsp90 to ensure > 80 % heterodimer formation (based on resulting ATPase rate). We determined that a 2:10 ratio (or 1:5 ratio of ATPase competent to ATPase dead) results in > 80 % heterodimer formation, and used this 1:5 ratio in the following co-chaperone titration experiments. Heterodimers were first formed by incubating them separately for 15 minutes prior to adding them to specific wells. Co-chaperones were then added to the wells containing the heterodimer mix. ATPase-dead variants Hsp82p^{E33A}, Hsp82p^{D79N}, Hsp82p$^{V391E/E33A}$ or Hsp82p$^{V391E/D79N}$ were titrated into reactions containing functional, ATPase-competent, wildtype Hsp82p or Hsp82p^{V391E}, and a defined concentration of co-chaperone. First, the ATPase competent Hsp82p was added to wells, followed by the addition of the ATPase-dead variants of a specific concentration. Co-chaperones were then added to the wells after allowing heterodimers to form for 15 minutes.

2.2.17.2 Cycling ATPase assays

For the Sti1p displacement ATPase assay, 4 μM Aha1p, HA-chimera, Hch1p, or Aha1p^{N} were added to the designated wells first, followed by 4 μM Sti1p and Cpr6p. Lastly, 2 μM wildtype Hsp82p was added to these reactions. Statistical significance was measured using one-way ANOVA analysis.

2.2.17.3 Crosslinking ATPase assays

To achieve crosslinking of Hsp82p^{K178C} to Smt3p^{Cys}, and not to itself, 32 µM Hsp82p^{K178C} must be derivitized which is achieved by incubating it with 200 µM BMOE (short-arm homo-bifunctional maleimide crosslinker) for one hour at room temperature. Smt3p^{Cys} is then added to a final concentration of 250 µM, mixed, and incubated at room temperature for another hour. To stop the crosslinking reaction and to quench all unreacted reactive groups, 30 mM DTT is added and incubated for 15 minutes. Control reactions use the same amount of DMSO instead of BMOE.

2.2.18 Immunoprecipitation assays

In vitro immunoprecipitation (IP) assays were conducted using Ultralink Protein G beads (Pierce Thermo Fisher) that had been coupled to anti-myc monoclonal antibodies (clone 9E10) at a concentration of 5 µg antibody per 1 µL of beads. All recombinant proteins used in these assays harbor N-terminal 6xHis tags, and where specified, the additional Myc-tag, HA-tag, or Flag-tag. The final buffer conditions for all IP reactions consisted of 25 mM Hepes (pH 7.2), 10–15 mM NaCl, 5 mM $MgCl_2$, and 0.1 % tween-20. For chapter 4, varying concentrations of DTT (1-3 mM) is present in the IP reactions depending on the volume of Hsp82p^{K178C}-Smt3p^{Cys} added.

2.2.18.1 Co-chaperone immunoprecipitation assays

To assess Aha1p binding in chapter 3 and 4, equimolar Aha1p and Hsp90 was mixed. Specifically in chapter 3, 5 µM Hsp82p (wildtype or mutant – Hsp82p^{V391E}, Hsp82p^{D79N}, Hsp82p^{E33A}, Hsp82p^{LL}) was mixed with 5 µM 6xHisMyc-tagged Aha1p, while in chapter 4, 5 µM Hsp82p^{K178C}, Hsp82p^{K178C}-Smt3p^{Cys}, or an equal mix of 2.5 µM Hsp82p^{K178C} and 2.5 µM Hsp82p^{K178C}-Smt3p^{Cys} was mixed with 5 µM 6xHisMyc-tagged Aha1p. To assess binding of co-chaperones to SUMOylated and non-SUMOylated Hsp82p^{K178C}, 5 µM of 6xHisMyc-tagged co-chaperones were mixed with 5 µM Hsp82p^{K178C} or Hsp82p^{K178C}-Smt3p^{Cys}, in the presence of 5 mM ADP or AMPPNP.

To assess Sti1p displacement from Hsp82p, 5 μM Hsp82p was incubated with 5 μM 6xHisMyc-tagged Sti1p in the presence of 5 μM Cpr6p, with and without 10 μM Aha1p or 50 μM of Aha1p^{N}, and 5 mM AMPPNP.

10 μL of Ultralink Protein G beads coupled to anti-Myc monoclonal antibodies to all these 50 μL reactions and then incubated on a rotator at room temperature for 60-90 minutes. Beads were then pelleted, washed once in 250 μL of binding buffer, resuspended in 50 μL SDS sample buffer, and run on SDS-PAGE. Complexes were analyzed by coomassie blue staining or western blotting. Band intensities of Hsp82p and MycSti1p from coomassie stained gels were measured using the multiplex band analysis function of AlphaView software (FluorChemQ, Protein Sample). The ratio of Hsp82p to MycSti1p was used to measure the efficiency of recovery in each condition. The percent displacement represents the average relative reduction in this ratio from three independent experiments. Statistical significance was measured using one-way ANOVA analysis.

2.2.18.2 Hsp82p immunoprecipitation assays

To assess heterodimer formation in chapter 3, 5 μM Myc-tagged Hsp82p or Hsp82p^{V391E} was incubated with 5 μM HA-tagged Hsp82p^{D79N} or Hsp82p^{E33A} for 15 minutes. 10 μL of Ultralink Protein G beads coupled to anti-Myc monoclonal antibodies was added to all these 50 μL reactions and then incubated on a rotator at room temperature for 90 minutes. Beads were then pelleted, washed once in 250 μL of binding buffer, resuspended in 50 μL SDS sample buffer, and run on SDS-PAGE. Complexes were analyzed by western blotting. Myc-tagged proteins were detected with mouse anti-Myc monoclonal antibody (4A6, Millipore), His-tagged proteins were detected with mouse anti-Tetra-His monoclonal antibody (34670, Qiagen), and HA-tagged proteins were detected with rat anti-HA monoclonal antibody (3F10, Roche).

To test whether SUMOylated Hsp82p could undergo heterodimerization chapter 4, Myc-tagged and Flag-tagged Hsp82p^{K178C} was SUMOylated, following the same protocol as outlined in section 2.2.17.3. Samples containing crosslinker

BMOE was treated with 10mM DTT and incubated for 30 minutes to quench all reactive groups before adding Myc-tagged and Flag-tagged Hsp82p^{K178C}-Smt3p^{-Cys} to IP reactions. 10 µL of Ultralink Protein G beads coupled to anti-Myc monoclonal antibodies was added to all these 50 µL reactions and then incubated on a rotator at room temperature for 60 minutes. Beads were then pelleted, washed once in 250 µL of binding buffer, resuspended in 50 µL SDS sample buffer, and run on SDS-PAGE. Complexes were analyzed by western blotting. Myc-tagged proteins were detected with mouse anti-Myc monoclonal antibody (4A6, Millipore) and Flag-tagged proteins were detected with mouse anti-Flag monoclonal antibody (F3165, Sigma).

2.2.19 Western blot analysis

Following SDS-PAGE, samples were transferred to pure nitrocellulose membrane, using 1X western buffer. Protein transfer was achieved using BioRad Tran-Blot Electrophoresis transfer cell apparatus at 100V, for 90 minutes. To minimize non-specific binding to the membrane, membranes were blocked overnight in 2 % BSA-0.1 % TBS-tween (Tris-buffered saline (TBS), 0.1 % tween, and 2 % Bovine Serum Albumin), while rocking at 4 ºC.

Membranes were incubated with primary antibodies for 3 hours at room temperature, or overnight at 4 ºC. Membranes were washed three times with 0.1 % TBS-tween at the 10-, 20-, and 25-minute timepoint at room temperature. Membranes were then incubated with secondary antibodies for 45 minutes at room temperature. Bands were visualized using electrochemiluminescence (ECL) and images using the FluorChemQ system.

Chapter 3

The asymmetric mechanism of Hsp90 ATPase stimulation by Aha-type co-chaperones

A version of this chapter has been published in

"Wolmarans, A. et al. The Mechanism of Hsp90 ATPase Stimulation by Aha1. Sci. Rep. 6, 33179; doi: 10.1038/srep33179 (2016)

3.1 Introduction

Co-chaperones are critical regulators of the Hsp90 system but how these co-chaperones regulate Hsp90 is not fully understood. Aha1p is the most potent stimulator of the ATPase activity of Hsp82p (Meyer et al., 2004a; Panaretou et al., 2002). Biochemical and structural studies have shown that Aha1p-mediated stimulation of Hsp82p is characterized by two main interactions: Aha1p^{N} interacts with the middle domain of Hsp82p while Aha1p^{C} interacts with the dimerized N-terminal domains of the Hsp82p dimer (Figure 3.1 A and B) (Horvat et al., 2014; Koulov et al., 2010; Meyer et al., 2004a; Retzlaff et al., 2010). The relative contributions of these co-chaperone interactions in relation to Hsp82p ATPase stimulation or to the underlying mechanism leading to stimulation are not fully understood. Hch1p is a yeast co-chaperone that is homologous to Aha1p^{N} and is used as a tool for interrogating Hsp82p domain rearrangements that occur upon interaction with the middle domain of Hsp82p (Figure 3.1A) (Ali et al., 2006; Meyer et al., 2004a; Prodromou et al., 1999; Richter et al., 2003). Hch1p shares 36.6 % sequence identity and 50 % similarity with Aha1p^{N}, and although both Hch1p and Aha1p^{N} interact with the catalytic loop of Hsp82p, our lab has shown that mutations in this loop do not affect these two co-chaperones in the same way (Horvat et al., 2014; Lotz et al., 2003; Nathan et al., 1999). Furthermore, our group has shown that the significant difference between Hch1p and Aha1p is not the C-terminal domain that is present on Aha1p, but the consequence of their interaction with the middle domain of Hsp82p (Horvat et al., 2014). Hch1p and Aha1p^{N} can stimulate the ATPase activity of Hsp82p to a similar degree and the fusion of Aha1p^{C} to Hch1p (HA-chimera) enhances ATPase stimulation but to a lesser extent than that achieved by full-length Aha1p (Figure 3.1A) (Horvat et al., 2014; Lotz et al., 2003; Meyer et al., 2004a; Panaretou et al., 2002).

Hsp82p is a highly dynamic, allosteric machine and accumulating research has further classified it as an asymmetric machine (Mollapour et al., 2014; Retzlaff et al., 2010). Retzlaff *et al.* defined a model for the asymmetric action of Aha1p as follows: only one Aha1p molecule is required to fully stimulate ATP hydrolysis

and Aha1p can stimulate the ATPase activity from either subunit of an Hsp82p dimer (Retzlaff et al., 2010). This model, however, does not provide mechanistic insight into how Aha1p drives the process of ATPase stimulation.

There are many Hsp82p mutants that result in increased intrinsic ATPase rates because these mutations somehow promote the closed, N-terminal dimerized state that is necessary for ATP hydrolysis. This led me to hypothesize that Aha1p stimulation occurs simply through tethering the N-terminal domains together. By first examining the modular nature of Aha1p binding and action through utilizing different Aha-type constructs (Figure 3.1 A-B), I will be able to dissect the underlying conformational changes that Aha1p binding impart on Hsp82p to regulate its ATPase activity. Combining the Aha-type constructs with specific Hsp82p mutants that restrict hydrolysis and co-chaperone binding to one of the subunits, will allow for interrogation of Aha1p action in the context of an asymmetric Hsp82p dimer. The different Hsp82p mutants that I will be utilizing are the ATPase-dead mutants (ATP-binding deficient mutant Hsp82p^{D79N}, ATP-hydrolysis deficient mutant Hsp82p^{E33A}, and lidless-Hsp82p) and Hsp82p^{V391E} which blocks Aha-type co-chaperones from binding to the middle domain of Hsp82p (Figure 3.1C). Comparing the effects that Hch1p and Aha1p has on the ATPase activity of Hsp82p will reveal biological insight into the mechanics of Hsp82p regulation by these co-chaperones.

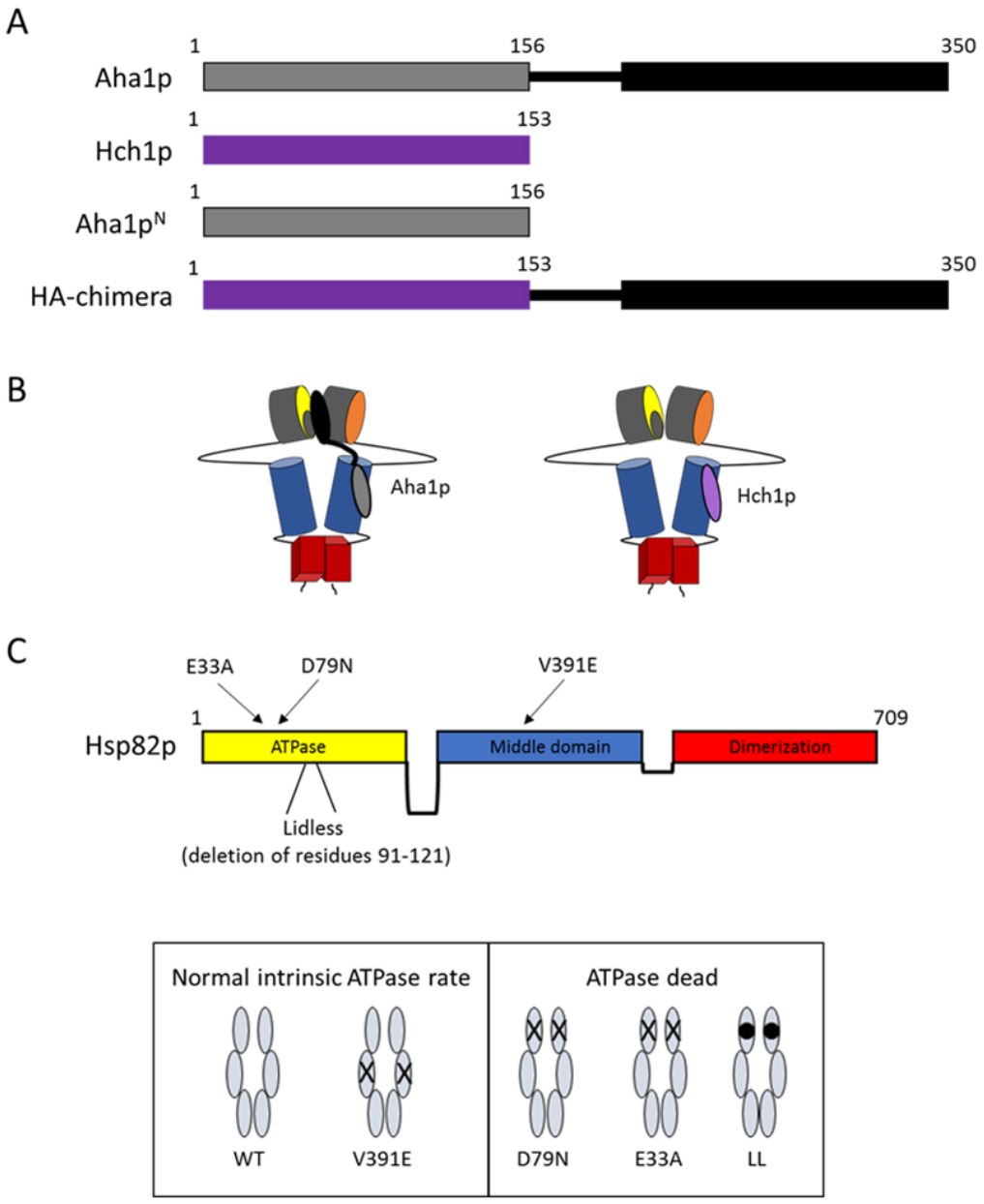

Figure 3.1 Aha-type co-chaperone constructs and Hsp82p mutants used in this study. A. Co-chaperone constructs used in this thesis. Aha1p is a 350-amino acid protein, Aha1p^{N} is 156 amino acids and corresponds to the 153 amino acid Hch1p. The HA-chimera is comprised of Hch1p fused to the C terminal domain of Aha1p. **B.** Cartoon representation of Aha1p and Hch1p binding to the middle domain of Hsp82p. **C.** Schematic depicting location and type of Hsp82p mutants used in this chapter.

3.2 Results

3.2.1 Regulation of Hsp82p lid dynamics by Aha1p and Hch1p

The conformational changes that occur in the Hsp82p dimer during an ATPase cycle have been analyzed in attempt to de-convolute the events coupled to the hydrolysis reaction (Hessling et al., 2009). Using fluorescence resonance energy transfer (FRET), at least 5 conformational transitions were identified that occur within Hsp82p upon ATP binding. Importantly, the progression through these conformational states was found to be altered in a similar manner upon the addition of Aha1p or the deletion of the lid segment (residues 98-121) in one subunit of Hsp82p in a heterodimer context (Hessling et al., 2009). This suggested that the 'lidless' mutant of Hsp82p, as well as Aha1p, accelerated the cycle in the same way. Altogether, this led me to hypothesize that ATPase stimulation by Aha1p occurs by influencing the dynamics of the lid segment of Hsp82p, leading to the N-terminal dimerized conformation and accelerating ATP hydrolysis.

To investigate this, I predicted that Aha1p would be unable to stimulate heterodimers formed between wildtype and lidless-Hsp82p ($Hsp82p^{LL}$) because the deletion of the lid segment bypasses Aha1p-mediated ATPase stimulation. I first confirmed that $Hsp82p^{LL}$ had no ATPase activity by itself (Figure 3.2A), and that the addition of this ATPase dead mutant to wildtype Hsp82p stimulated the intrinsic rate (Figure 3.2B). Consistent with previous reports, $Hsp82p^{LL}$ potently stimulated the ATPase activity of the wildtype subunit (Richter et al., 2006). However, upon titration of Aha1p into Hsp82p:$Hsp82p^{LL}$ heterodimers, Aha1p was able to further stimulate the ATPase activity, almost 10-fold over the Hsp82p:$Hsp82p^{LL}$ intrinsic rate (Figure 3.2C - black triangles). To further interrogate the mechanism of Aha1p stimulation, I also questioned which domain of Aha1p is responsible for this additional stimulation and set out to compare the contribution of the N-terminus of Aha1p ($Aha1p^{N}$) alone. Consistent with results of full-length Aha1p, $Aha1p^{N}$ was also able to stimulate the ATPase activity of Hsp82p:$Hsp82p^{LL}$ heterodimers, although only with a 2-fold increase (Figures 3.2C - blue squares). This result

suggests that Aha1p does not act at the level of lid opening by alleviating auto-inhibition of the ATPase activity, but rather by some other mechanism.

Hch1p and Aha1p^{N} can stimulate the ATPase activity of Hsp82p to similar levels (Lotz et al., 2003; Meyer et al., 2004a; Panaretou et al., 2002), and although they both interact with the catalytic loop, our lab has shown that mutations in this loop do not affect these two co-chaperones in the same way *in vivo* (Horvat et al., 2014). We have also shown that Hch1p plays an important role in regulating access to the ATP binding pocket in Hsp82p by ATP-competitive inhibitor drugs like NVP-AUY922, as overexpression of Hch1p, but not Aha1p, in yeast increases the cellular sensitivity to specific Hsp90 inhibitors (Armstrong et al., 2012). Consequently, I hypothesized that the mechanism of Hch1p stimulation is mediated by influencing the structure of the ATP lid. Interestingly, upon Hch1p titration, the ATPase activity was inhibited in a manner that was gradually overcome at higher co-chaperone concentrations (Figure 3.2C – red circles). Hch1p had an inhibitory effect on the ATPase activity of Hsp82p until Hch1p concentrations exceeded the concentration of Hsp82p (6 μM) that was present in these assays, suggesting that inhibition was likely due to Hch1p binding to one subunit of the heterodimer. This revealed the first significant difference between the mechanism of Hsp82p stimulation by Aha1p^{N} and Hch1p, *in vitro*.

The stimulation of wildtype Hsp82p homodimers by Aha1p, Aha1p^{N}, and Hch1p is shown in Figure 3.2D for comparison. The corresponding maximal ATPase rates (V_{MAX}) for Hsp82p stimulation by each of these co-chaperones are 3.8 ± 0.4 min^{-1} (Aha1p), 0.4 ± 0.1 min^{-1} (Hch1p), and 0.8 ± 0.1 min^{-1} (Aha1p^{N}).

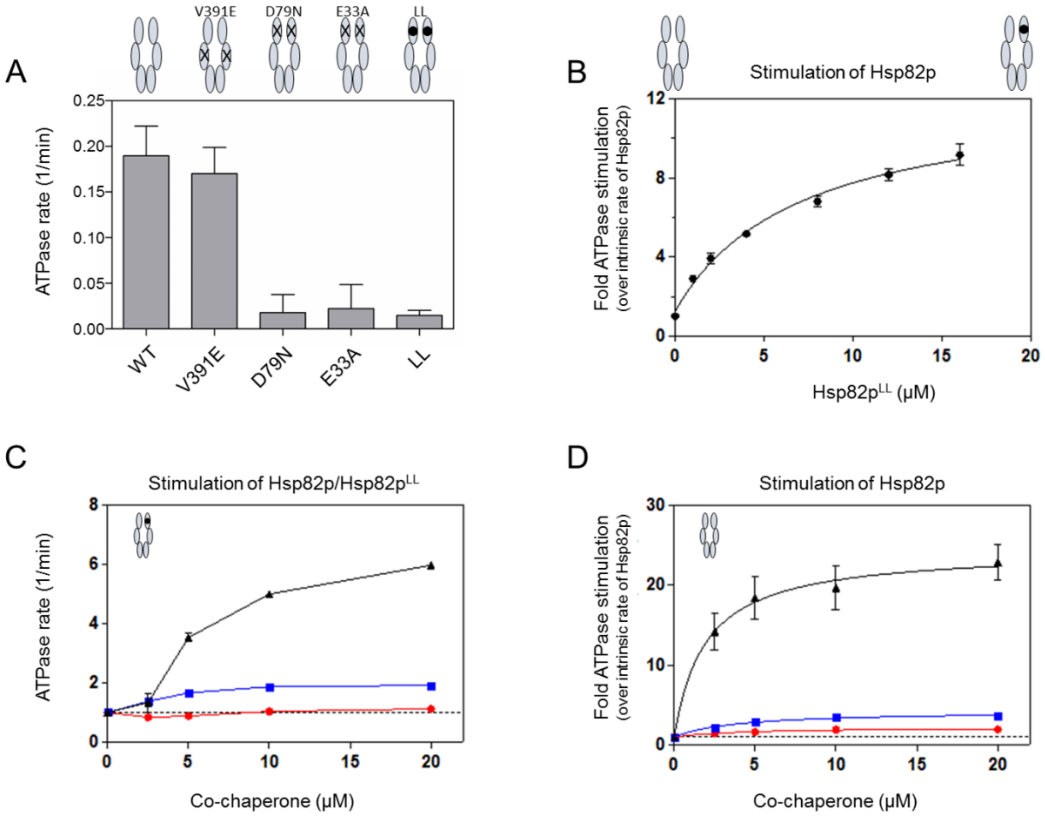
A
V391E
D79N
E33A
LL
ATPase rate (1/min)
0.25
0.20
0.15
0.10
0.05
0.00
WT
V391E
D79N
E33A
LL
B
Stimulation of Hsp82p
Fold ATPase stimulation
(over intrinsic rate of Hsp82p)
12
8
4
0
0
5
10
15
20
Hsp82p^LL (μM)
C
Stimulation of Hsp82p/Hsp82p^LL
ATPase rate (1/min)
8
6
4
2
0
0
5
10
15
20
Co-chaperone (μM)
D
Stimulation of Hsp82p
Fold ATPase stimulation
(over intrinsic rate of Hsp82p)
30
20
10
0
0
5
10
15
20
Co-chaperone (μM)

Figure 3.2 ATPase stimulation of Hsp82p:Hsp82p^{LL} heterodimers. **A.** Bar graph showing the intrinsic ATPase rates of wildtype Hsp82p, Hsp82p^{V391E}, Hsp82p^{D79N}, Hsp82p^{E33A}, and Hsp82p^{LL}. Reactions contained 4 μM of Hsp82p or Hsp82p mutants. ATPase rate shown in micromolar ATP hydrolyzed per minute per micromolar of enzyme (1/min). **B.** Hsp82p^{LL} titration into reactions containing 2 μM of wildtype Hsp82p results in ATPase stimulation. ATPase rate is shown as a fold stimulation of the intrinsic Hsp82p rate. **C.** Titration of Aha1p (black) and Aha1p^{N} (blue) stimulated the ATPase activity of Hsp82p:Hsp82p^{LL} heterodimers, while Hch1p (red) inhibited the ATPase activity of Hsp82p:Hsp82p^{LL} heterodimers at low concentrations (by ~16 % at 2.5 μM Hch1p and ~11 % at 5 μM Hch1p). Heterodimers are formed by mixing 1 μM Hsp82p and 5 μM of Hsp82^{LL}. ATPase rates are shown as a fold stimulation the intrinsic rate of Hsp82p:Hsp82p^{LL} heterodimers (stippled line). **D.** ATPase stimulation of wildtype Hsp82p by Aha1p (black), Aha1p^{N} (blue), and Hch1p (red). Reactions contained 2 μM of Hsp82p with indicated concentrations of co-chaperones. The ATPase rate is shown as a fold stimulation of the intrinsic Hsp82p rate (stippled line). V_{MAX} for Hsp82p stimulation by each of these co-chaperones are 3.8 ± 0.4 min^{-1} (Aha1p), 0.4 ± 0.1 min^{-1} (Hch1p), and 0.8 ± 0.1 min^{-1} (Aha1p^{N}). Figure and legend are modified from (Wolmarans et al., 2016).

3.2.2 Aha-type co-chaperones exert different effects when bound to specific subunits in the context of Hsp82p heterodimers

Hsp90 is an obligate dimer and thus, there are two potential binding sites – one on each subunit – to which co-chaperones and clients can bind. Aha-type co-chaperones can bind to either the intact, wildtype subunit or the ATPase-dead, lidless subunit of the Hsp82p:Hsp82p^{LL} heterodimer in these assays. Introducing a V391E mutation that severely impairs the binding of the Aha-type co-chaperones to the middle domain of Hsp82p is a strategy I employed to determine to which Hsp82p subunit Hch1p is exerting its inhibitory effect (Retzlaff et al., 2010). I first confirmed that homodimers harboring the V391E mutation have a normal intrinsic rate (Figure 3.3A) and that they cannot be readily stimulated by Aha1p (Figure 3.3A) (Retzlaff et al., 2010). This demonstrated that this mutation effectively reduces Aha1p-mediated stimulated of V391E when compared to Aha1p-mediated stimulation of wildtype Hsp82p. By forming Hsp82p^{V391E}:Hsp82p^{LL} heterodimers, the binding of co-chaperones will preferentially occur on the lidless subunit. Next, I verified that Hsp82p^{V391E} is also potently stimulated by the addition of Hsp82p^{LL} (Figure 3.3B). Interestingly, Aha1p and Aha1p^{N} were both less effective in stimulating the ATPase activity of Hsp82p^{V391E}:Hsp82p^{LL} heterodimers (Figure 3.3C). This very weak stimulation that is evident, is likely due to the weak binding of Aha1p and Aha1p^{N} to the V391E subunit of the heterodimer, since the V391E mutation does not restrict co-chaperone binding completely (Retzlaff et al., 2010). Thus, this result suggests that neither Aha1p nor Aha1p^{N} appear to be able to stimulate the ATPase activity of the heterodimer from the non-hydrolyzing, lidless subunit. Moreover, Hch1p inhibited the ATPase rate of the Hsp82p^{V391E}:Hsp82p^{LL} heterodimers which suggests that binding to the Hsp82p^{LL} subunit antagonized the enzymatic activity of the Hsp82p^{V391E} subunit (Figure 3.3C).

From the data, thus far, the deletion of the lid segment interferes with co-chaperone mediated stimulation when bound to that subunit. I predicted that all Aha-type co-chaperones would stimulate the ATPase activity of Hsp82p heterodimers if co-chaperone binding is restricted to the wildtype subunit by introducing the V391E mutation to the ATPase-dead, lidless subunit. To test my

hypothesis, I carried out parallel ATPase assays using Hsp82p/Hsp82p$^{V391E/LL}$ heterodimers. The addition of Hsp82p$^{V391E/LL}$ stimulated the ATPase activity in wildtype Hsp82p, consistent with previous lidless titrations (Figure 3.3D). Aha-type co-chaperones will preferentially bind to the wildtype subunit of the Hsp82p:Hsp82p$^{V391E/LL}$ heterodimers due to the V391E mutation on the other subunit. In contrast to Hsp82p^{V391E}:Hsp82p^{LL} heterodimers, Aha1p, Aha1p^{N}, and Hch1p stimulated the ATPase activity of Hsp82p:Hsp82p$^{V391E/LL}$ heterodimers (Figure 3.3E). Simply, the resulting effect of the Aha-type co-chaperones on the ATPase activity of Hsp82p was dependent on which subunit the co-chaperone bound. Lid cooperation is needed on the subunit to which the co-chaperones bind to, as the ATPase rate was not robustly stimulated by either Aha1p or Aha1p^{N} when bound to the lidless subunit. More intriguingly, Hch1p antagonized the intact Hsp82p ATPase when bound to the lidless subunit. Taking these results together suggest that Aha1p is most likely enhancing the conformational changes in the Hsp82p dimer that are driven by deletion of the lid segment.

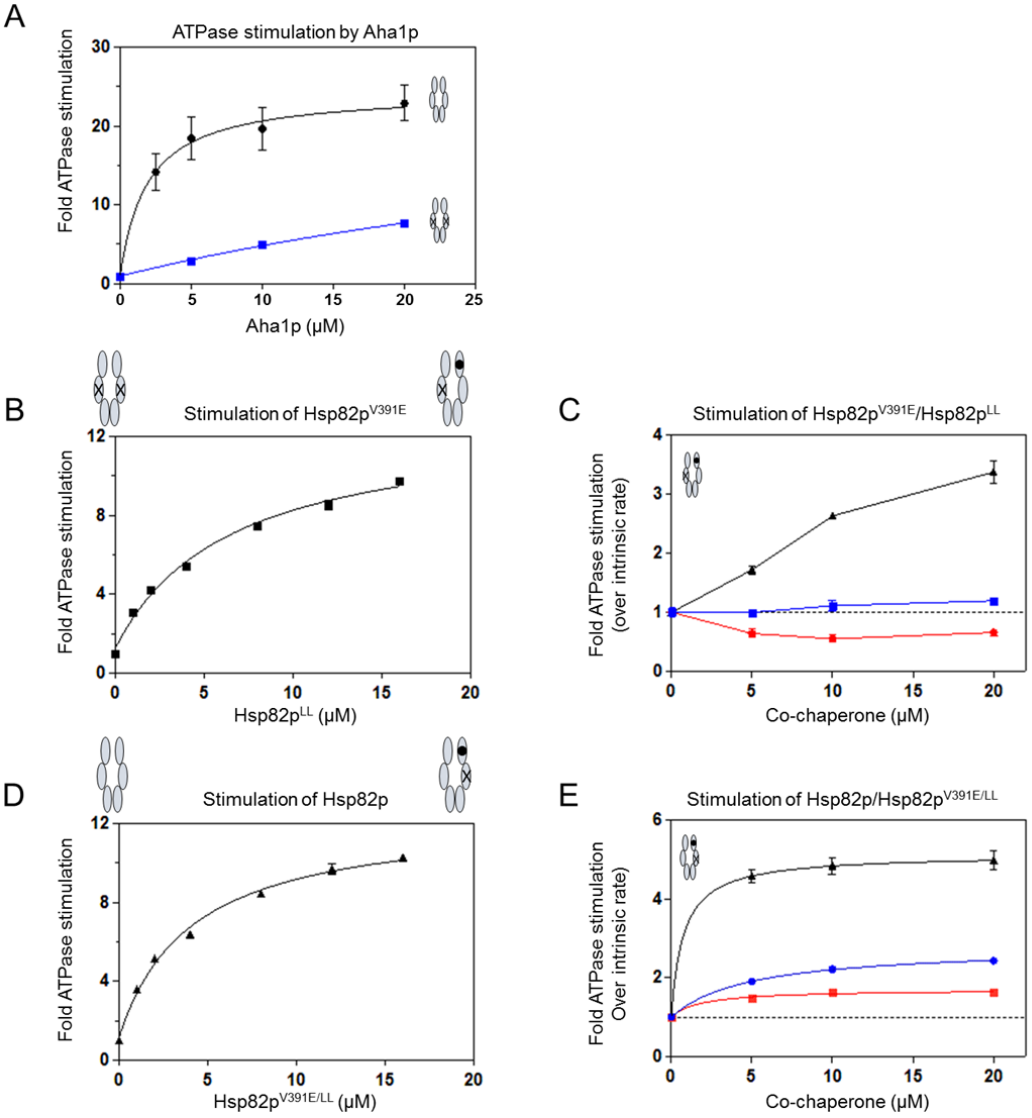
A
ATPase stimulation by Aha1p
Fold ATPase stimulation
Aha1p (μM)
B
Stimulation of Hsp82p^V391E
Fold ATPase stimulation
Hsp82p^LL (μM)
C
Stimulation of Hsp82p^V391E/Hsp82p^LL
Fold ATPase stimulation (over intrinsic rate)
Co-chaperone (μM)
D
Stimulation of Hsp82p
Fold ATPase stimulation
Hsp82p^V391E/LL (μM)
E
Stimulation of Hsp82p/Hsp82p^V391E/LL
Fold ATPase stimulation Over intrinsic rate)
Co-chaperone (μM)

Figure 3.3 Co-chaperones exert different effects from different subunits. **A.** Aha1p stimulates wildtype Hsp82p (black) robustly but does not readily stimulate Hsp82p^{V391E} (blue). Reactions contained 2 μM Hsp82p or Hsp82p^{V391E} with indicated Aha1p concentrations. ATPase rate shown as a fold stimulation of Hsp82p or Hsp82p^{V391E} intrinsic rate. **B.** Hsp82p^{LL} titration into reactions containing 2 μM of Hsp82p^{V391E} results in ATPase stimulation. ATPase rate is shown as a fold stimulation of the intrinsic Hsp82p^{V391E} rate. **C.** Aha1p (black) and Aha1p^{N} (blue) do not robustly stimulate the ATPase activity of Hsp82p^{V391E}:Hsp82p^{LL} heterodimers, and Hch1p (red) inhibited the ATPase activity of Hsp82p^{V391E}:Hsp82p^{LL} heterodimers. Heterodimers are formed by mixing 1 μM Hsp82p^{V391E} and 5 μM Hsp82p^{LL}. ATPase rates are shown as a fold stimulation of the intrinsic rate of Hsp82p^{V391E}:Hsp82p^{LL} heterodimers (stippled line). **D.** Hsp82p$^{V391E/LL}$ titration into reactions containing 2 μM of wildtype Hsp82p results in ATPase stimulation. Hsp82p$^{V391E/LL}$ was titrated into reactions containing 2 μM of Hsp82p results in ATPase stimulation. ATPase rate is shown as a fold stimulation of the intrinsic Hsp82p$^{V391E/LL}$ rate. **E.** Aha1p (black), Aha1p^{N} (blue), and Hch1p (red) stimulates the ATPase activity of Hsp82p:Hsp82p$^{V391E/LL}$ heterodimers. Heterodimers are formed by mixing 1 μM Hsp82p and 5 μM of Hsp82p$^{V391E/LL}$. ATPase rates are shown as a fold stimulation the intrinsic rate of Hsp82p: Hsp82p$^{V391E/LL}$ heterodimers (stippled line). Figure and legend modified from (Wolmarans et al., 2016).

3.2.3 Aha1- and Hch1-mediated ATPase stimulation of heterodimers harboring Hsp82p ATP hydrolysis mutants

Aha1p and Hch1p clearly exerted different effects from the hydrolyzing and non-hydrolyzing subunit of the heterodimer harboring a lidless subunit. To further examine the conformational remodeling and the role the catalytic subunit has on ATPase stimulation, I employed ATP binding deficient (D79N) and ATP hydrolysis deficient (E33A) Hsp82p mutants that are otherwise structurally intact and can bind Aha1p (Obermann et al., 1998; Panaretou et al., 1998; Retzlaff et al., 2010; Richter et al., 2006). A previous study of engineered Hsp82p heterodimers found that heterodimers harboring an E33A subunit, but not a D79N subunit, supported yeast viability (Mishra and Bolon, 2014). To explore the nature of catalytic activity for Hsp82p heterodimers where only one subunit can hydrolyze ATP, Hsp82p^{D79N} or Hsp82p^{E33A} was titrated into ATPase reactions containing Hsp82p^{V391E} and Aha1p. In these assays, co-chaperone binding will preferentially occur on the ATPase dead subunit, although some binding of Aha1p to the V391E subunit is evident as stimulation is seen at 0 μM D79N and E33A (Figure 3.4A). Consistent with previous reports, the addition of Hsp82p^{D79N} restores Aha1p-mediated ATPase stimulation of Hsp82p^{V391E} to comparable wildtype stimulated rates (Figure 3.4A – green circles) (Retzlaff et al., 2010). In contrast, the addition of Hsp82p^{E33A} did not restore Aha1p-mediated ATPase stimulation to Hsp82p^{V391E} (Figure 3.4A – blue squares). This indicates that Aha1p can stimulate the ATPase activity of the ATPase-competent Hsp82p^{V391E} subunit when it is bound to Hsp82p^{D79N}, and not to Hsp82p^{E33A}. This demonstrates that the E33A mutation ablates the ability of Aha1p to act asymmetrically from the ATPase-dead subunit. Interestingly, when conducting the reciprocal assay by titrating in the double mutant Hsp82p$^{V391E/D79N}$ or Hsp82p$^{V391E/E33A}$ into wildtype Hsp82p, the Aha1p stimulated rate of wildtype Hsp82p was not diminished (Figure 3.4B). This demonstrates that binding of Aha1p to the ATPase-competent subunit can stimulate ATP hydrolysis of that subunit regardless of whether the D79N or E33A mutation is present in the opposite subunit. In other words, Aha1p-mediated stimulation is only blocked by E33A when Aha1p is bound to that subunit.

The N-terminal domain of Aha1p makes an important interaction with the middle domain of the catalytically active subunit of the Hsp82p dimer, leading to ATPase stimulation by full-length Aha1p. This raised the question whether Aha1p^{N} and Hch1p elicit the same conformational remodeling when bound to the middle domain of the catalytic subunit. I employed the HA-chimera to test whether Hch1 can fulfill the role of Aha1p^{N} in this same assay (Horvat et al., 2014). Consistent with Aha1p results, chimera-mediated stimulation of Hsp82p^{V391E} is restored with the addition of Hsp82p^{D79N}, but again, not with the addition of Hsp82p^{E33A} (Figure 3.4C). Unexpectedly, the addition of Hsp82p$^{V391E/E33A}$ greatly diminished the chimera-mediated ATPase stimulation of wildtype Hsp82p while the addition of Hsp82p$^{V391E/D79N}$ did not (Figure 3.4D). This result suggests that the HA-chimera cannot stimulate Hsp82p:Hsp82p^{E33A} heterodimers from either subunit. I also confirmed that Hsp82p:Hsp82p^{E33A} and Hsp82p:Hsp82p^{D79N} heterodimers form equally well (Figure 3.5A) and that Aha1p interacted with each of our Hsp82p mutants except Hsp82p^{V391E} (Figure 3.5B).

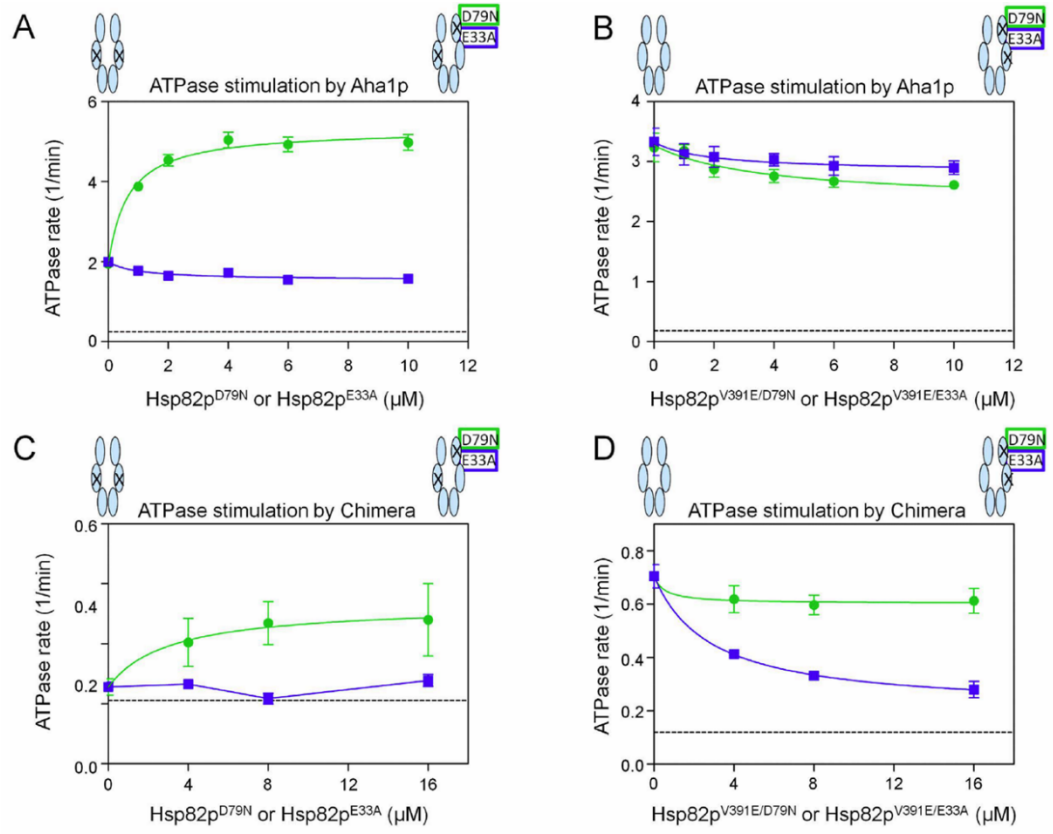
A
D79N
E33A
ATPase stimulation by Aha1p
ATPase rate (1/min)
Hsp82p^D79N or Hsp82p^E33A (μM)
B
D79N
E33A
ATPase stimulation by Aha1p
ATPase rate (1/min)
Hsp82p^V391E/D79N or Hsp82p^V391E/E33A (μM)
C
D79N
E33A
ATPase stimulation by Chimera
ATPase rate (1/min)
Hsp82p^D79N or Hsp82p^E33A (μM)
D
D79N
E33A
ATPase stimulation by Chimera
ATPase rate (1/min)
Hsp82p^V391E/D79N or Hsp82p^V391E/E33A (μM)

Figure 3.4. The E33A mutation blocks Aha1p^{N}-mediated conformational changes in *cis*. **A.** Aha1p-mediated ATPase stimulation of Hsp82p^{V391E} was restored in *trans* with Hsp82p^{D79N} (green) but not Hsp82p^{E33A} (blue). Reactions contained 1 μM Hsp82p^{V391E}, 10 μM Aha1p and indicated concentrations of Hsp82pD79N or Hsp82pE33A. Intrinsic rate of Hsp82p^{V391E} shown as black stippled line. **B.** Aha1p-mediated ATPase stimulation of Hsp82p:Hsp82p$^{V391E/D79N}$ (green) and Hsp82p:Hsp82p$^{V391E/E33A}$ (blue) heterodimers. Reactions contained 1μM Hsp82p, 10 μM Aha1p and indicated concentrations of Hsp82p$^{V391E/D79N}$ or Hsp82p$^{V391E/E33A}$. Intrinsic rate of wildtype Hsp82p shown as black stippled line. **C.** Chimera-mediated ATPase stimulation of Hsp82p^{V391E} was restored in *trans* with Hsp82p^{D79N} (green) but not Hsp82p^{E33A} (blue). Reactions contained 1 μM Hsp82p^{V391E}, 10 μM HA-chimera, and indicated concentrations of Hsp82p^{D79N} or Hsp82p^{E33A}. Intrinsic rate of Hsp82p^{V391E} shown as black stippled line. **D.** HA-chimera-mediated ATPase stimulation of Hsp82p:Hsp82p$^{V391E/D79N}$ (green) heterodimers but not of Hsp82p:Hsp82p$^{V391E/E33A}$ (blue) heterodimers. Reactions contained 1μM Hsp82p, 10 μM HA-chimera and indicated concentrations of Hsp82p$^{V391E/D79N}$ or Hsp82p$^{V391E/E33A}$. Intrinsic rate of wildtype Hsp82p shown as black stippled line. All ATPase rates are shown in micromolar ATP hydrolyzed per minute per micromolar of enzyme (1/min). Figure and legend from (Wolmarans et al., 2016).

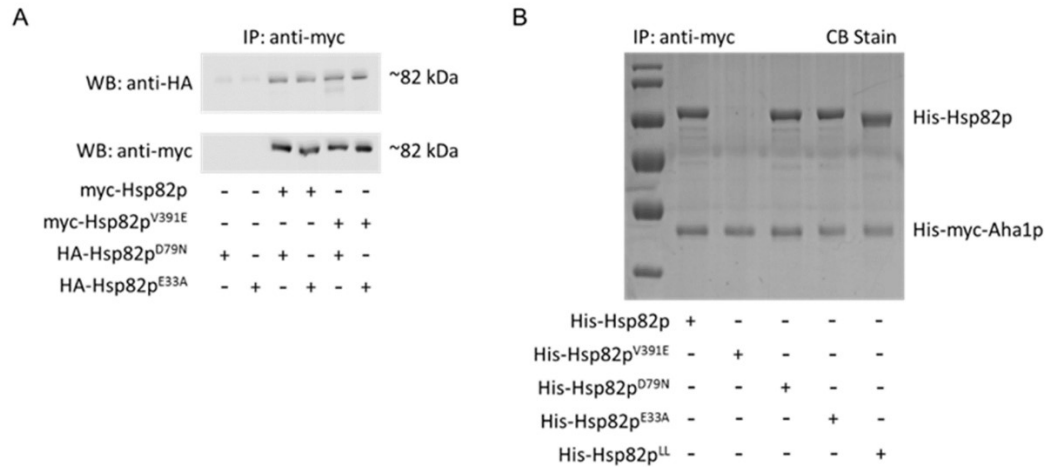

Figure 3.5 Heterodimers form between wildtype Hsp82p, Hsp82p^{V391E}, Hsp82p^{D79N} and Hsp82p^{E33A} and all Hsp82p variants bind Aha1p. A. Hsp82p and Hsp82p^{V391E} both form heterodimers with Hsp82p^{D79N} and Hsp82p^{E33A} as HA-tagged Hsp82p^{D79N} and Hsp82p^{E33A} co-IP with MycHsp82p and MycHsp82p^{V391E}. 5 µM purified Myc-tagged Hsp82p or Hsp82p^{V391E} was incubated with 5 µM purified Flag-tagged Hsp82p^{D79N} or Hsp82p^{E33A} for 15 minutes. These reactions were incubated on a rotator at RT for 90 min. Beads were pelleted, washed once in 250 µL of binding buffer, run on SDS-PAGE, and analyzed by western blotting. **B.** Wildtype Hsp82p, Hsp82p^{D79N}, Hsp82p^{E33A}, and Hsp82p^{LL} all form a stable complex with Myc-tagged Aha1p *in vitro*. Hsp82p^{V391E} harbors a mutation that prevents the formation of a stable complex with Aha1p. 5 µM of Hsp82p variants were incubated with 5 µM 6xHisMyc-tagged Aha1p. Complexes were isolated with beads coupled to anti-Myc monoclonal antibody 9E10, run on SDS-PAGE and analyzed by Coomassie blue staining (CB). Figures and legends are modified from (Wolmarans et al., 2016).

A possible reason to explain why the HA-chimera cannot stimulate Hsp82p:Hsp82p^{E33A} heterodimers from either subunit is because Hch1 cannot stimulate these heterodimers. To determine whether Hch1p and Aha1p^{N} have the ability to stimulate Hsp82p:Hsp82p^{E33A} heterodimers, I titrated Hsp82p^{E33A} into reactions containing Hsp82p^{V391E} and the co-chaperone in question. Interestingly, both Aha1p^{N} and Hch1p promoted ATPase stimulation of Hsp82p^{V391E} upon titration of Hsp82p^{E33A} (Figure 3.6A). Furthermore, titration of Hsp82p$^{V391E/E33A}$ did not impair ATPase stimulation of Hsp82p by either co-chaperone construct (Figure 3.6B). This result suggests that Aha1p^{C} domain of the HA-chimera is unable to participate in the ATPase stimulation of Hsp82p:Hsp82p^{E33A} heterodimers. Taken together, these results reveal that the action of Aha1p^{C} in the stimulation of a heterodimer harboring an E33A mutation can only be restored when Aha1p^{N} interacts with middle domain of the opposite subunit.

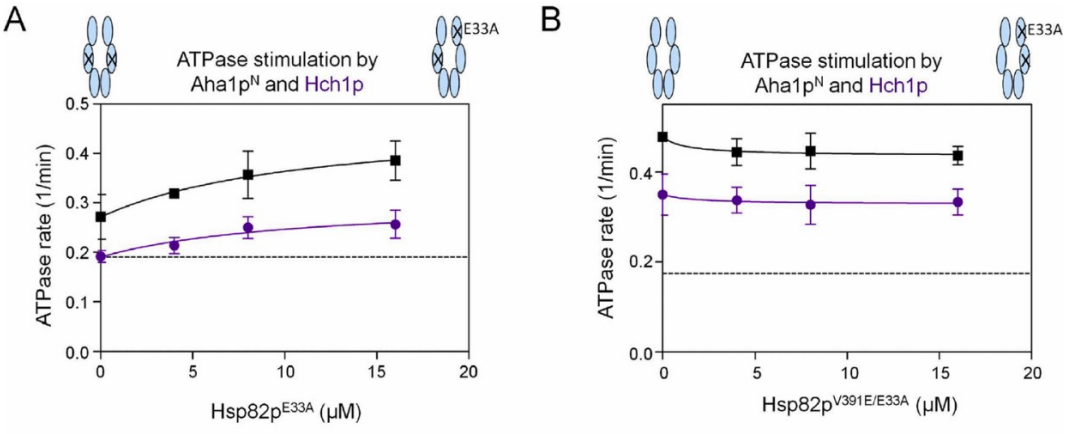

Figure 3.6 Hch1p and Aha1p^N stimulate Hsp82p ATPase activity from either catalytic or non-catalytic protomer. A. Hch1p- and Aha1p^N-mediated ATPase stimulation of Hsp82p^{V391E}:Hsp82p^{E33A} heterodimers. Reactions contained 4 μM Hsp82p^{V391E}, 20 μM Hch1p (purple) or Aha1p^N (black), and indicated concentrations of Hsp82p^{E33A}. Intrinsic rate of Hsp82p^{V391E} shown as black stippled line. **B.** Hch1p- and Aha1p^N-mediated ATPase stimulation of Hsp82p:Hsp82p$^{V391E/E33A}$ heterodimers. Reactions contained 4 μM Hsp82p, 20 μM Hch1p (purple) or Aha1p^N (black), and indicated concentrations of Hsp82p$^{V391E/E33A}$. Intrinsic rate of wildtype Hsp82p shown as black stippled line. ATPase rates are shown in micromolar ATP hydrolyzed per minute per micromolar of enzyme (1/min). Figure and modified legend from (Wolmarans et al., 2016).

3.2.4 Hch1p interaction with the middle domain of Hsp82p drives N-M communication

Co-chaperone binding to one subunit results in allosteric conformational changes that alter binding properties elsewhere in the chaperone. Analysis of various ATPase assays led me to hypothesize that Hch1p and Aha1p must drive different conformational changes, outside the middle domain of Hsp82p, to influence the ATPase cycle in different ways. To test this hypothesis, our lab collaborated with the laboratory of Dr. Leo Spyracopoulos from the Department of Biochemistry (University of Alberta) to carry out NMR analysis. By employing an NMR strategy, we were able to examine the conformational changes that occur in Hsp82p upon co-chaperone interaction. To study the difference between Aha1p and Hch1p interaction with Hsp82p, we added Aha1p^{N} or Hch1p, with or without ATP, to an Hsp82p construct comprised of the middle and N-terminal domains (Hsp82p^{N-M}). The chemical shift changes in the Hsp82p^{N-M} spectra were then examined. Analysis of this Hsp82p^{N-M} construct gave well dispersed peaks and we were able to detect large peak shifts corresponding to the Hsp82p N-terminal domain upon addition of near saturating concentrations of ATP binding, consistent with previous reports (Figure 3.7A – top panel). Also, consistent with previous observations, the addition of the Aha1p^{N} resulted in chemical shifts localized primarily in the middle domain and the C-terminal end of the N-terminal domain of Hsp82p (Figure3.7A – middle panel). The addition of Hch1p, however, resulted in very different NMR spectra. Although, a similar pattern of chemical shift changes to the middle domain are observed upon the addition of Hch1p to Hsp82p^{N-M}, suggesting it binds in a similar fashion as Aha1p^{N}, Hch1p also causes significant changes in residues ~20–50 of the N-terminal domain. This indicates that Hch1p either interacts with this region directly, or it indirectly affects the conformation of the N-terminal domain. The addition of ATP to either Aha1p^{N}- or Hch1p-bound Hsp82p^{N-M} causes chemical shift changes identical to those for ATP alone, occurring mainly within the N domain (Figure 3.7).

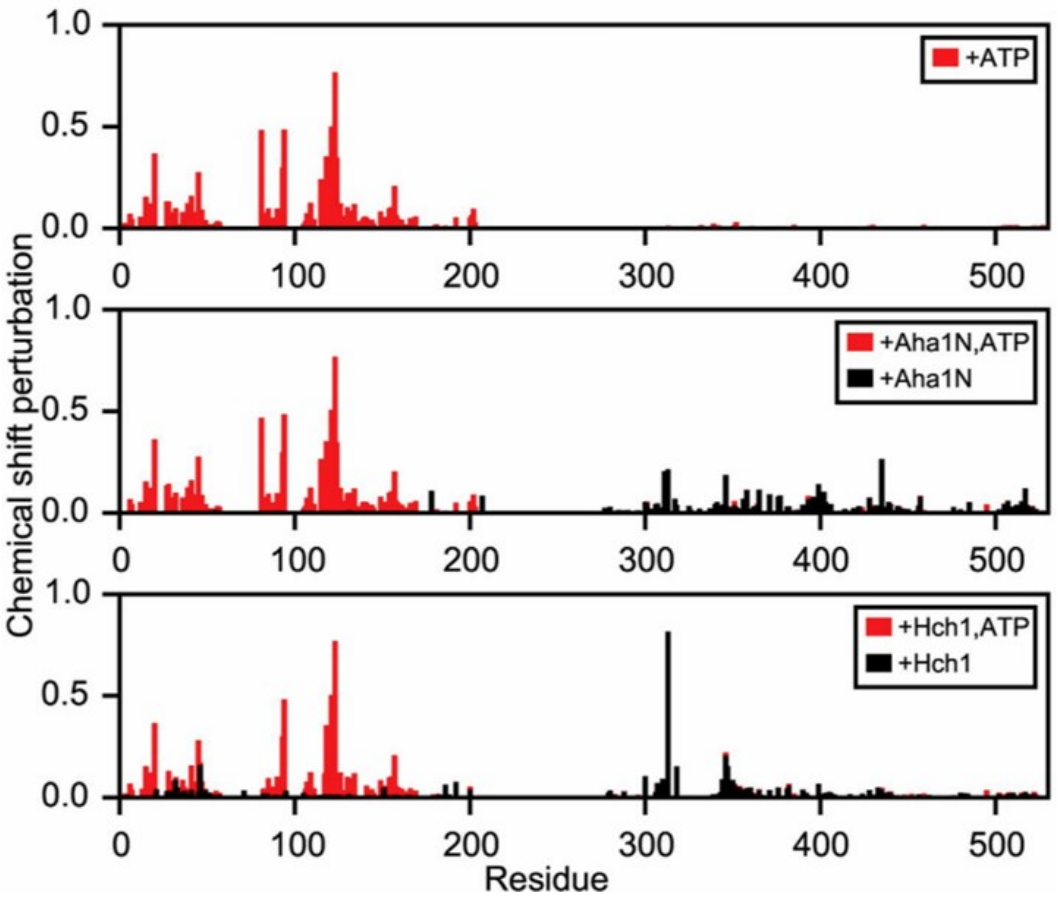

Figure 3.7 Chemical shift analysis in an Hsp82p^{N-M} construct upon ATP, and co-chaperone binding. Chemical shift changes for Hsp82p^{N-M} construct upon addition of ATP (red, top panel), Aha1p^{N} (black, middle panel), Aha1p^{N} and ATP (red, middle panel), Hch1p (black, lower panel), or Hch1p and ATP (red, lower panel). NMR was conducted by Dr. Brian Lee from Dr. Leo Spyracopoulos' Lab (Department of Biochemistry). Figure and legend were modified from (Wolmarans et al., 2016).

Another way to analyze the interactions or conformational changes that occur within a protein is to look at changes in peak intensity of the NMR spectra upon addition of ligands and binding partners. The normalized intensities of the peaks between free-state Hsp82p^{N-M} and ATP is shown in black in Figure 3.8 (top panel). Upon the addition of Aha1p^{N} (red) and Hch1p (blue), the intensities decreased overall compared to those with ATP alone, with a larger decrease observed in the middle domain peaks (Figure 3.8 – top panel). Lower intensity peaks represent larger molecular-weight species tumbling more slowly, which is an indication that both Aha1p^{N} and Hch1p are in fact binding to the middle domain of Hsp82p. Interestingly, the addition of Hch1p resulted in a uniform decrease of all the peaks in Hsp82p^{N-M}. Consistent with the chemical shift data, this suggests that Hch1p binding results in a strong interaction of the N-terminal domain with either Hch1p or the middle domain, which is not observed with Aha1p^{N}.

I was curious to examine how the presence of Aha1p^{C} would affect the NMR spectra and preceded to test how full-length Aha1p influences the Hsp82p^{N-M} construct. Peak assignments were difficult to make as the addition of Aha1p resulted in significant peak broadening of many peaks, specifically of the middle domain. The addition of Aha1p results in a large peak intensity decrease in the N-terminal domain along with similar chemical shifts to the middle domain (Figure 3.8 - bottom panel). This indicates that there is a stronger interaction between the full-length Aha1p and Hsp82p^{N-M} compared to Aha1p^{N}, and that Aha1p^{N} binds to the middle domain primarily and only weakly interacts with the N-terminal domain of Hsp82p. Moreover, Aha1p^{C} interacts and restricts the motion of the N-terminal domain of Hsp82p.

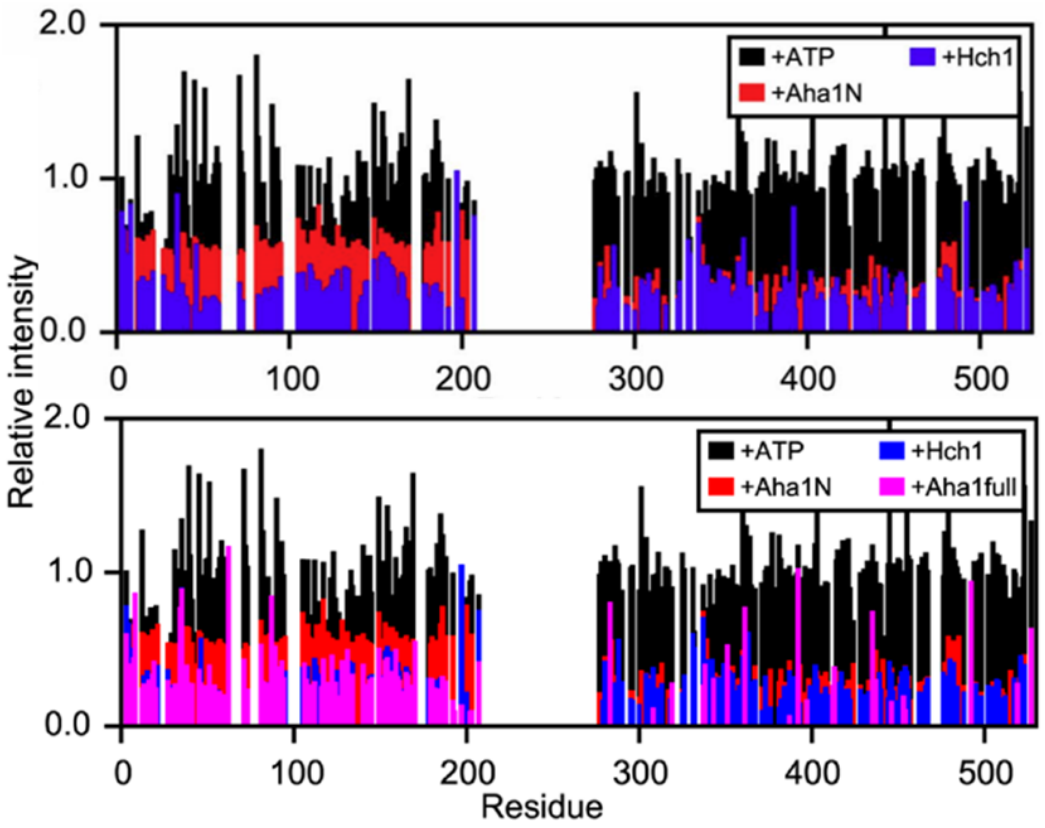

Figure 3.8 Peak intensity analysis in an Hsp82p^{N-M} construct upon ATP, and co-chaperone binding. Peak intensity changes in Hsp82p^{N-M} construct NMR spectra upon addition of ATP (black), Aha1p^{N} (red), or Hch1p (blue) plotted on the top panel. Bottom panel shows the top panel results with an overlay of full-length Aha1p (pink) peak intensity changes. NMR was conducted by Dr. Brian Lee from Dr. Leo Spyracopoulos' Lab (Department of Biochemistry). Figure and legend were modified from (Wolmarans et al., 2016).

Analysis of the NMR peak shift data shows that Hch1p and Aha1p^{N} cause different changes within the middle domain of Hsp82p, which is consistent with their different biological activities which our lab has previously observed (Horvat 2014, Armstrong 2012). The addition of Aha1p^{N} to the Hsp82p^{N-M} construct caused the peaks of 21 residues within the middle domain of Hsp82p to shift by more than one standard deviation (σ) from the average shift. These residues are relatively spread out throughout the binding interface between Hsp82p and Aha1p^{N}, as highlighted on the crystal structure (Figure 3.9- green residues). Only eight residues shift to this extent upon Hch1p binding and they are concentrated to the N-terminal segment of middle domain of Hsp82p, from residues 300-350 (Figure 3.9 – purple residues). Interestingly, only two residue-specific chemical shift changes in the middle domain of Hsp82p^{N-M} (Gly313 and Arg346) are shared between Aha1p^{N} and Hch1p (Figure 3.9 – yellow residues). The chemical peak of Gly313 shifted by 2 σ upon Aha1p binding, but shifted by more than 15 σ upon Hch1p binding.

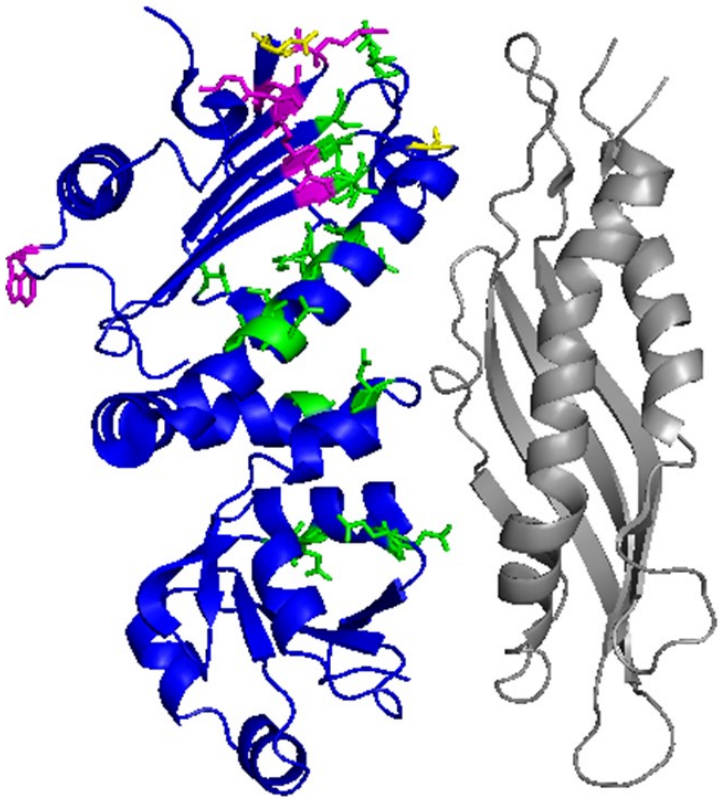

Figure 3.9 Residues that shift in the middle domain of Hsp82p upon Aha1p^{N} and Hch1p binding. Crystal structure of the middle domain of Hsp82p (blue) bound to Aha1p^{N} (grey) with highlighted residues that shifted upon Aha1p^{N} (green) and Hch1p (purple) association. Modified PDB file 1USU (Meyer et al., 2004a).

The chemical shift changes in the NMR spectra of the N-terminal domain of Hsp82p are less in magnitude, compared to the changes observed in the middle domain, however, they reveal striking differences between the addition of Aha1p^{N} and Hch1p. The addition of Hch1p to the Hsp82p^{N-M} construct caused 16 residues to shift 1/3 σ from the average shift upon Hch1p interaction (Figure 3.10A). Thirteen of these residues are concentrated around the nucleotide binding pocket, specifically, the long flanking helix that is downstream of the N-terminal strand (residues 21-49 highlighted in red) (Figure 3.10A). Three residues that shifted more than 1/3 σ from the average upon Hch1p interaction are residues that are oriented towards the middle domain suggesting that Hch1p interacts directly with the N-terminal domain of Hsp82p (Glu186, Glu192, Phe200 -highlighted in cyan) (Figure 3.10A). Aha1p^{N} interaction caused slight chemical shifts as only 2 residues were identified to shift by more than 1/3 σ from the average shift upon Aha1p^{N} interaction (Figure 3.10B – black residues). It is important to note, however, that these 2 residues – Lys178 and Leu207 – shifted by more than 2 σ and 1 σ, respectively, and are located in the back of the N-terminal domain of Hsp82p relative to the binding site, suggesting an allosteric conformational change. Interestingly, Lys178 is the site of SUMOylation that recruits Aha1p to the Hsp82p dimer (Mollapour et al., 2014). Taken together, these NMR spectra data suggest that binding of Hch1p influences the nucleotide binding pocket in a way that Aha1p cannot, which is consistent with our previous work where we have shown that Hch1p regulates the ability of Hsp90 inhibitors to bind *in vivo* (Armstrong et al., 2012; Horvat et al., 2014).

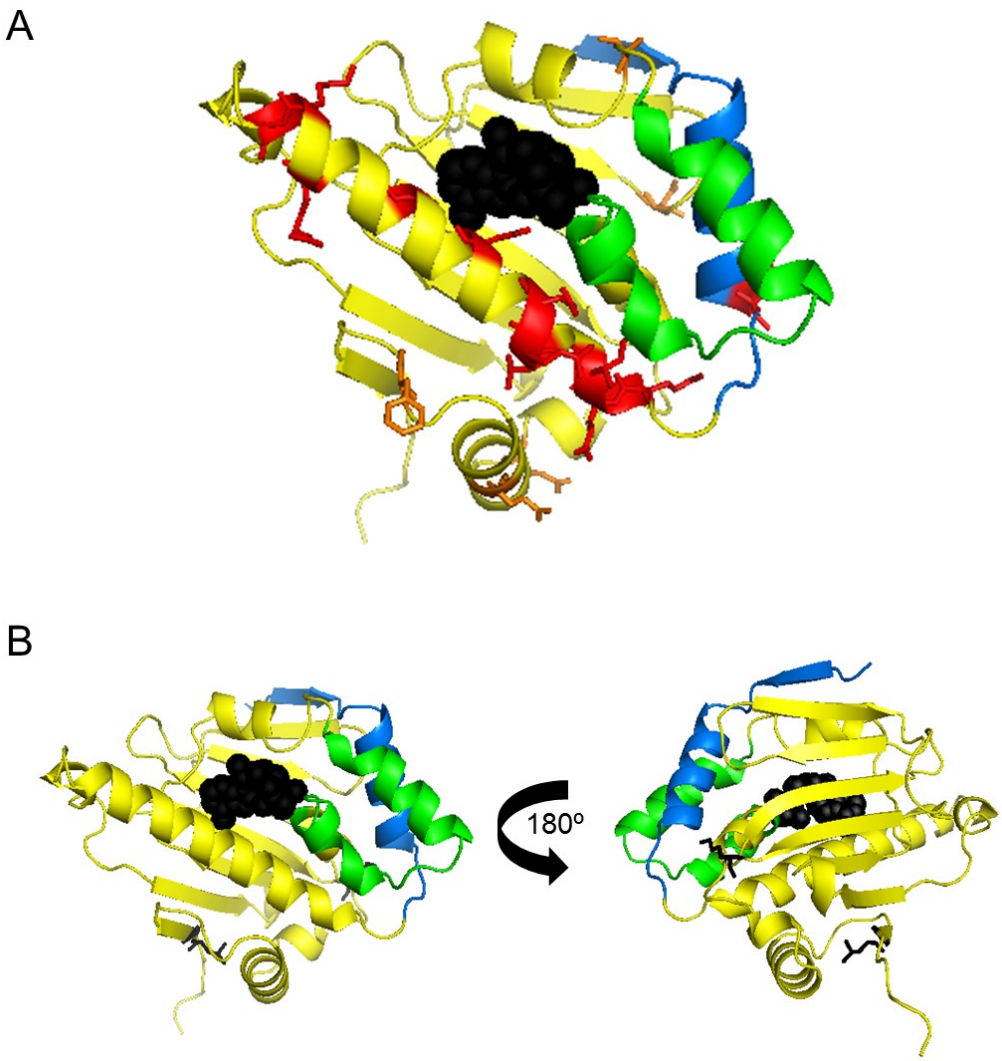

Figure 3.10 Residues that shift in the N-terminal domain of Hsp82p upon Aha1p^{N} and Hch1p binding. Crystal structure of the N-terminal domain of Hsp82p (yellow) bound to AMPPNP (black) with highlighted residues that shift upon Hch1p and Aha1p^{N} association. **A.** Hch1p binding to the middle domain of Hsp82p^{N-M} resulted in chemical shifts of 13 residues concentrated within the nucleotide binding region (red), and 3 residues that are oriented towards the middle domain of Hsp82p (oranges). **B.** Aha1p^{N} binding to the middle domain of Hsp82p^{N-M} resulted in chemical shifts of Lys178 and Leu207, which are located to the back of the N-terminal domain of Hsp82p (black). Modified PDB file 1AMW (Prodromou et al., 1997).

3.2.5 C-terminal domain of Aha1p is required for co-chaperone switching

The functional cycle of Hsp82p requires the sequential interaction of co-chaperones with Hsp82p to modulate progression through numerous conformations (Li 2011). How late-acting co-chaperones like Aha1p displace early-acting co-chaperones like Sti1p is only now being revealed (Li et al., 2011; Li et al., 2013). Sti1p is a potent inhibitor of Hsp82p ATPase activity but can be displaced by the cooperative action of Cpr6p with either Aha1p or Sba1p (Eckl and Richter, 2013; Li et al., 2013). This provided an explanation for how this so-called 'co-chaperone switching' can take place to allow cycle progression, however, the mechanism of co-chaperone switching is not fully understood. Since both Sba1p and Aha1p interact with the N-terminal domain of Hsp82p, displacement may be mediated by co-chaperone association with the N-terminal domains of Hsp82p. With the modular nature of Aha1p, I questioned how each domain of Aha1p might contribute to displacement of Sti1p from the Cpr6p-Hsp82p-Sti1p ternary complex. I hypothesized that Aha1p^{C} allows for cycle progression via co-chaperone switching. To examine this, I tested Aha1p, Aha1p^{N}, Hch1p, and the HA-chimera for the ability to stimulate the ATPase activity of the Cpr6p-Hsp82p-Sti1p ternary complex. Sti1p completely inhibited the stimulated rates of Hsp82p ATPase activity regardless of the presence of Aha1p or Hch1p co-chaperone constructs, consistent with previous reports (Figure 3.11A - blue). The addition of Cpr6p had a mild stimulatory effect on both the intrinsic Hsp82p ATPase rate as well as the stimulated rates mediated by the Aha1p and Hch1p co-chaperone constructs (Figure 3.11A - purple). This data demonstrate that Sti1p overcomes, while Cpr6p enhances, the ATPase stimulation mediated by all the Aha1p and Hch1p constructs. If the Aha1p^{C} is required for co-chaperone switching, then only full-length Aha1p and the HA-chimera would be able to stimulate the ATPase rate of reactions containing both Cpr6p and Sti1p. Consistent with this hypothesis, the addition of only full-length Aha1p and HA-chimera resulted in a statistically significant increase in ATPase activity in reactions containing both Sti1p and Cpr6p. This suggests that Aha1p^{C} was able to cooperate with Cpr6p to overcome Sti1p inhibition and restore stimulation (Figure 3.11B). The addition of Hch1p and

Aha1p^{N} to reactions containing both Sti1p and Cpr6p, however, resulted in a decrease in ATPase activity, which suggests neither Hch1p or Aha1p^{N} are able to displace Sti1p (Figure 3.11B).

To further investigate this displacement more directly, I employed immunoprecipitation assays to measure the physical displacement of Hsp82p from Sti1p. N-terminally Myc-tagged version of Sti1p was constructed, expressed, and purified for co-immunoprecipitation experiments. Hsp82p was readily recovered in complex with Myc-Sti1p in a Myc-IP when equimolar amounts of Hsp82p and Myc-Sti1p (5 μM) were incubated together (Figure 3.12A - lane 3). The addition of equimolar amounts of Cpr6p (5 μM) resulted in a small decrease (~20 % of the total – Figure 3.12B) in Hsp82p recovery with Myc-Sti1p (Figure 3.12A – lane 4). This result is consistent with previous studies showing that these two co-chaperones compete for binding to the MEEVD motif at the C terminus of Hsp82p and that they can form a ternary complex with Hsp82p (Li et al., 2013). The addition of both Crp6p (5 μM final) and Aha1p (10 μM final) displaced approximately 50 % of Hsp82p from Myc-Sti1p (Figure 3.12A – lane 6), while the addition of Aha1p alone resulted in negligible displacement of Hsp82p from Myc-Sti1p (Figure 3.12A – lane 5). This confirms our ATPase data, that Sti1p is displaced by the cooperative action of Cpr6p and Aha1p. Also, consistent with our ATPase data, the addition of a large excess of Aha1p^{N} (50 μM final) did not result in displacement of Hsp82p from Myc-Sti1p on its own (Figure 3.12A – lanes 7 & 8). Moreover, the addition of Aha1p^{N} together with Cpr6p did not result in any further displacement of Hsp82p compared to Cpr6p alone (Figure 3.12 A-B).

Taken together, I have reconstituted a robust Hsp82p ATPase cycle, *in vitro*, in the presence of Sti1p as the concerted actions of Aha1p and Cpr6p overcome Sti1p ATPase inhibition. The C-terminal domain of Aha1p is required for Sti1p displacement, as the addition of full-length Aha1p and HA-chimera was able to cooperate with Cpr6p to overcome Sti1p inhibition and restore stimulation.

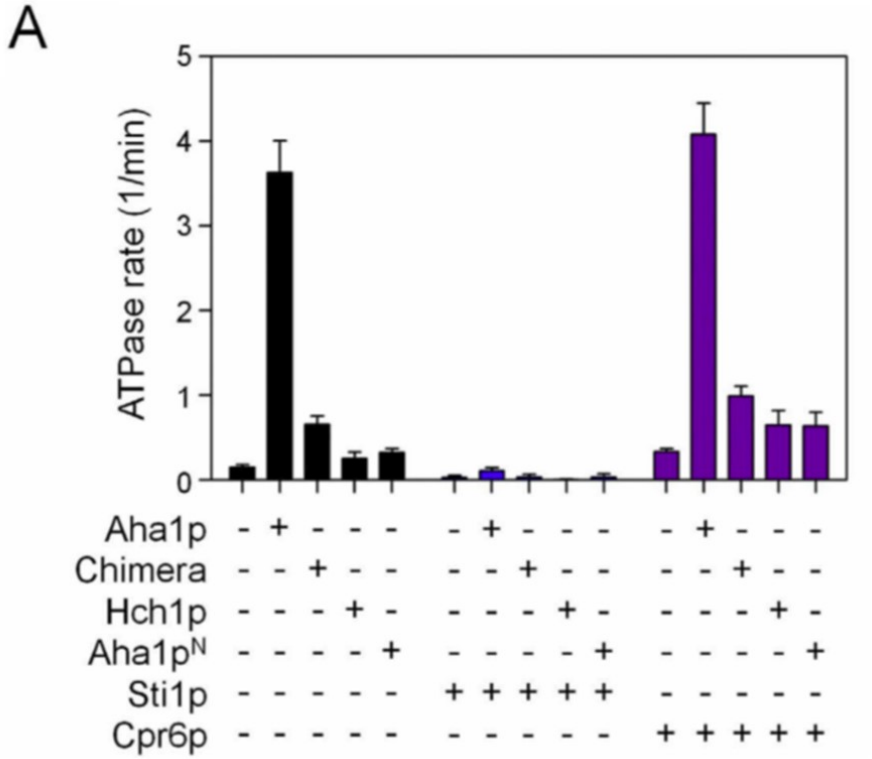
A
ATPase rate (1/min)
5
4
3
2
1
0
Aha1p - + - - - - + - - - - + - - -
Chimera - - + - - - - + - - - - + - -
Hch1p - - - + - - - - + - - - - + -
Aha1p^N - - - - + - - - - + - - - - +
Sti1p - - - - - + + + + + - - - - -
Cpr6p - - - - - - - - - - + + + + +

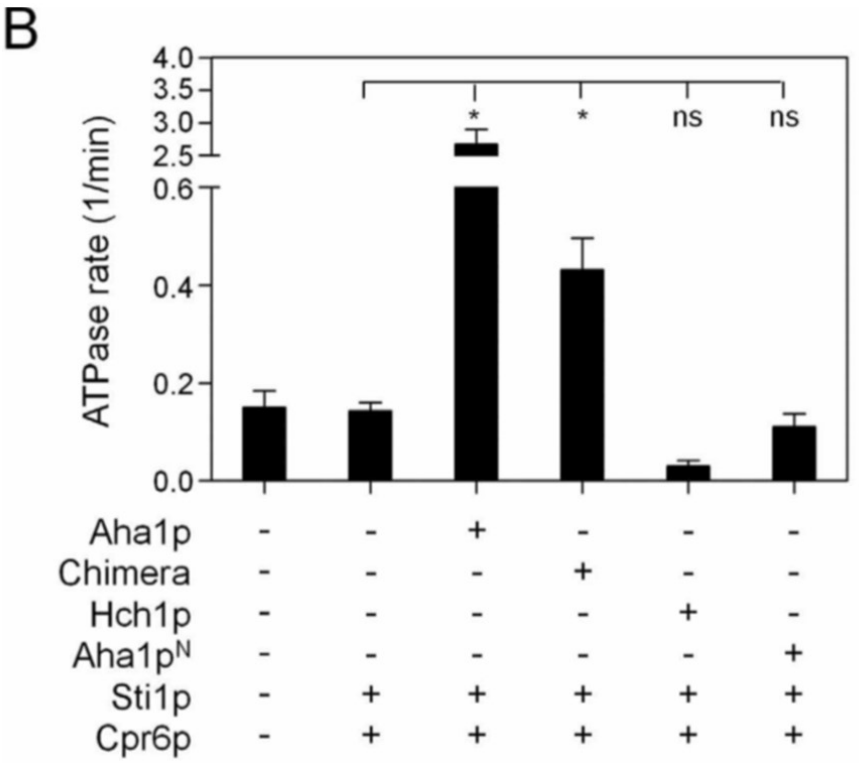
B
ATPase rate (1/min)
4.0
3.5
3.0
2.5
0.6
0.4
0.2
0.0
*
*
ns
ns
Aha1p - - + - - -
Chimera - - - + - -
Hch1p - - - - + -
Aha1p^N - - - - - +
Sti1p - + + + + +
Cpr6p - + + + + +

Figure 3.11 The C-terminal domain of Aha1p cooperate with Cpr6p to overcome Sti1p inhibition of the ATPase activity of Hsp82p. A. Each co-chaperone construct (Aha1p, HA-chimera, Hch1p, and Aha1p^{N}) stimulated Hsp82p ATPase activity (black bars). Addition of Sti1p inhibited both intrinsic and stimulated Hsp82p ATPase activity (blue bars). Addition of Cpr6p enhanced both intrinsic and stimulated Hsp82p ATPase activity (purple bars). **B.** Only the addition of Aha1p and the HA-chimera to reactions containing both Sti1p and Cpr6p resulted in a statistically significant (* - one-way ANOVA, $p< 0.05$) increase in ATPase activity compared to the Sti1p plus Cpr6p condition while the addition of Hch1p or Aha1p^{N} did not (n = 4). ATPase reactions (in A and B) contained 2 μM Hsp82p and 4 μM co-chaperones. ATPase rates are shown in micromolar ATP hydrolyzed per minute per micromolar of enzyme (1/min). Figure and legend modified from (Wolmarans et al., 2016).

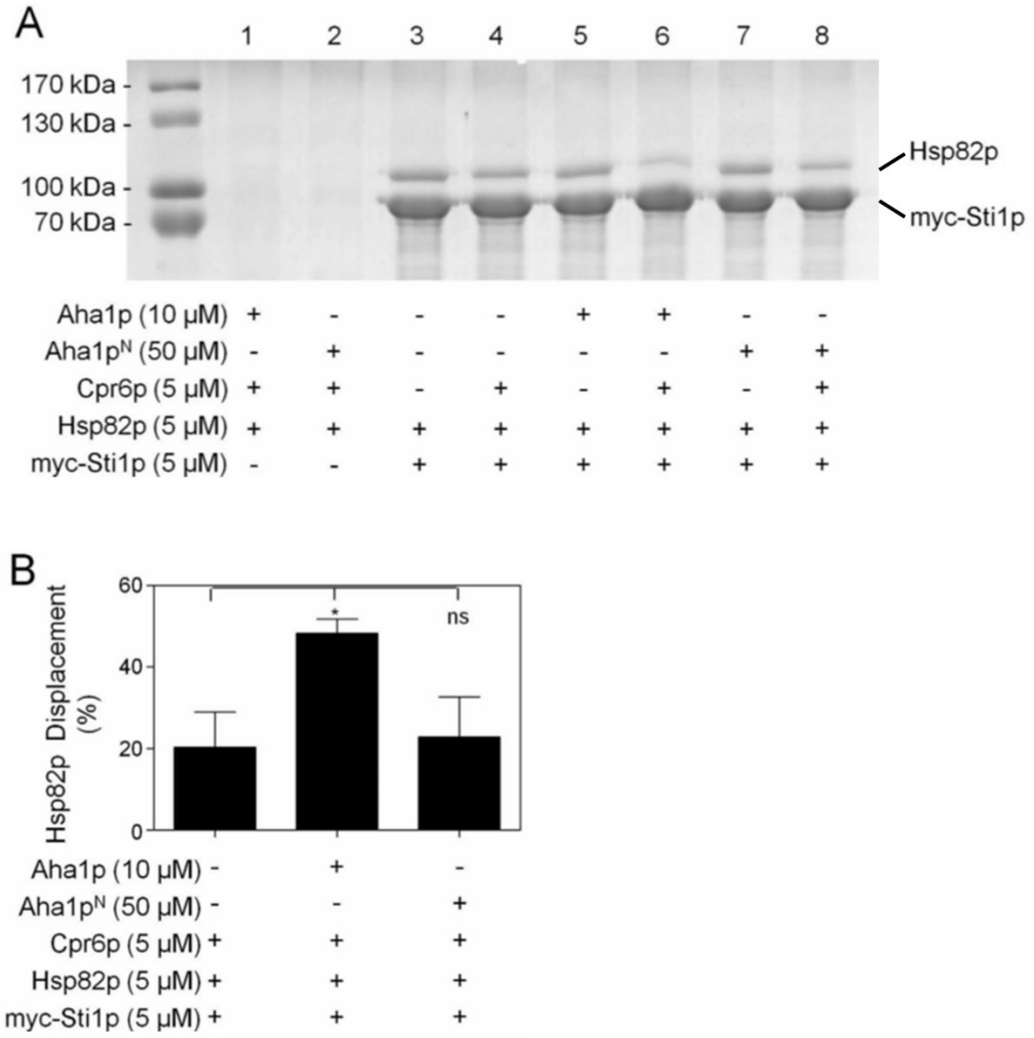

Figure 3.12 The C-terminal domain of Aha1p is required for the cooperative displacement of Sti1p from Hsp82p. A. Co-immunoprecipitation of Hsp82p with MycSti1p in the presence of different combinations of co-chaperones. Gel is a representative view of 3 replicates conducted in AMPPNP nucleotide conditions. **B.** Quantification of Hsp82p displacement from MycSti1p (n = 3). A statistically significant (* - one-way ANOVA, Tukey's HSD, $p < 0.05$) displacement of Hsp82p compared to the addition of Cpr6p alone was observed upon the addition of Aha1p but not a 5-fold excess of Aha1p^N. Figure and legend modified from (Wolmarans et al., 2016).

3.3 Summary and model

Overview

This study provides further illustration of the different mechanisms by which Hch1p and Aha1p regulate Hsp82p (Armstrong et al., 2012; Horvat et al., 2014). Hch1p exerts opposite effects from the catalytic and non-catalytic protomers of an Hsp82p/Hsp82p^{LL} heterodimer. ATPase activity was inhibited when Hch1p bound to the lidless protomer of Hsp82p/Hsp82p^{LL} heterodimers but was stimulated when it bound to the wildtype protomer. NMR analysis revealed extensive peak shifts in the N domain of the Hsp82p^{N-M} construct upon Hch1p binding that did not occur when Aha1p^{N} was added. Reconstitution of the cycling reaction revealed that the C-terminal domain of Aha1p is required for the cooperative displacement of Sti1p from Hsp82p.

Aha1p acts at a different stage of Hessling's model

It is well-established that Aha1 stimulates the ATPase activity of Hsp90 *in vitro* and that this property is conserved between Aha1 paralogs across species. However, the mechanistic understanding of Hsp82p stimulation remained elusive. The purpose of this study was to dissect the molecular mechanism of ATPase stimulation of Hsp82p by Aha1p. I initially hypothesized that Aha1p acts by alleviating lid-mediated inhibition of Hsp82p's ATPase activity, for the deletion of the lid segment in one subunit promotes N-terminal dimerization and increased ATPase stimulation (Richter et al., 2006). Moreover, the conformational dynamics of Hsp82p are altered in a similar manner by Aha1p binding or lid deletion (Hessling et al., 2009; Richter et al., 2006). The addition of Aha1p, however, led to a further increase in ATPase stimulation of Hsp82p/Hsp82p^{LL} heterodimers, thus, ATPase stimulation of Hsp82p by Aha1p is not mediated by alleviation of auto-inhibition by the lid. This Aha1p-mediated stimulation was greater than stimulation by Aha1p^{N} alone, further demonstrating that neither domain of Aha1p acts to alleviate lid-inhibition. The FRET analysis by Hessling *et al.* demonstrated that the transitions between the conformational states of the intrinsic ATPase cycle are

augmented in the same way when the lid of one segment is deleted or upon the addition of Aha1p (Hessling et al., 2009). However, in the lidless heterodimer experiments, lid deletion in one subunit and Aha1p binding contributed to the ATPase stimulation independently. These results suggest that Aha1p action is at least partly independent of the five global conformational rearrangements identified in a previous study (Hessling et al., 2009).

Protomer-specific effect of Hch1p

Our work has previously unveiled that Aha1p and Hch1p regulate Hsp82p differently *in vivo* (Armstrong et al., 2012; Horvat et al., 2014). In this study, I show the first evidence of how these two co-chaperones are mechanistically different *in vitro*. While Aha1p^{N} functioned in a similar manner to full-length Aha1p in the lidless heterodimer assays (except for stimulating to a lesser degree), Hch1p gave very different results. Hch1p exert opposite effects from the catalytic and non-catalytic subunits of an Hsp82p/Hsp82p^{LL} heterodimer: ATPase activity was inhibited when Hch1p bound to the lidless subunit of Hsp82p/Hsp82p^{LL} heterodimers but was stimulated when restricted to bind to the wildtype subunit. Based on our NMR data, we reasoned that the lid deletion may be antagonizing Hsp82p N-M communication that Hch1p binding induces. The observation that none of the Aha-type co-chaperones stimulated the ATPase activity when forced to bind to the lidless subunit suggested that deleting the lid blocks necessary intra-protomer conformational events that would lead to ATPase stimulation. These results with Hch1p illustrated how co-chaperones can exert subunit specific effects depending on the subunit they are bound to. My results show support for a different 'asymmetric' model, where it matters to which side the co-chaperone binds to, as opposed to binding to either subunit in an asymmetric fashion.

Mechanism of ATPase stimulation of Hsp82p

The result of my work led to the proposal of the following model involving three different steps of Aha1p-mediated ATPase stimulation (Figure 3.12A). The first interaction is characterized by Aha1p^{N} binding to the middle domain of one of

the Hsp82p subunits. This interaction results in a small stimulatory effect of Hsp82p ATPase activity in an asymmetric manner, meaning that Aha1p^{N} can stimulate the ATPase activity regardless of which subunit it binds to, *i.e.* in *cis* or *trans* to the hydrolyzing subunit. The second step induces *cis* conformational changes in the N-terminal domain, likely occurring through Aha1p^{N} interaction with the catalytic loop of Hsp82p. This step was revealed from findings from Hsp82p heterodimer assays with D79N, E33A, and V391E, that uncovered that the E33A mutation – which is widely used in the Hsp90 field – actually blocks the action of Aha1p^{C} in *cis* to the Aha1p^{N} interaction (Figure 3.12B) (Johnson et al., 2007; Mishra and Bolon, 2014). Because Aha1p^{N} can stimulate from either subunit of a heterodimer harboring an Hsp82p^{E33A} subunit, my results suggest that the E33A mutation blocks the rearrangement of the Hsp82p N-terminal domains which is required for the action of Aha1p^{C}. This *cis* conformational rearrangement is critical for the action of Aha1p^{C}, as the introduction of E33A in *cis* abolishes further ATPase stimulation altogether. This second step drives a final rearrangement of both N-terminal domains (step 3), which provides the dimerized N-terminal domain interface to which Aha1p^{C} binds, leading to further stimulation of Hsp82p's ATPase activity.

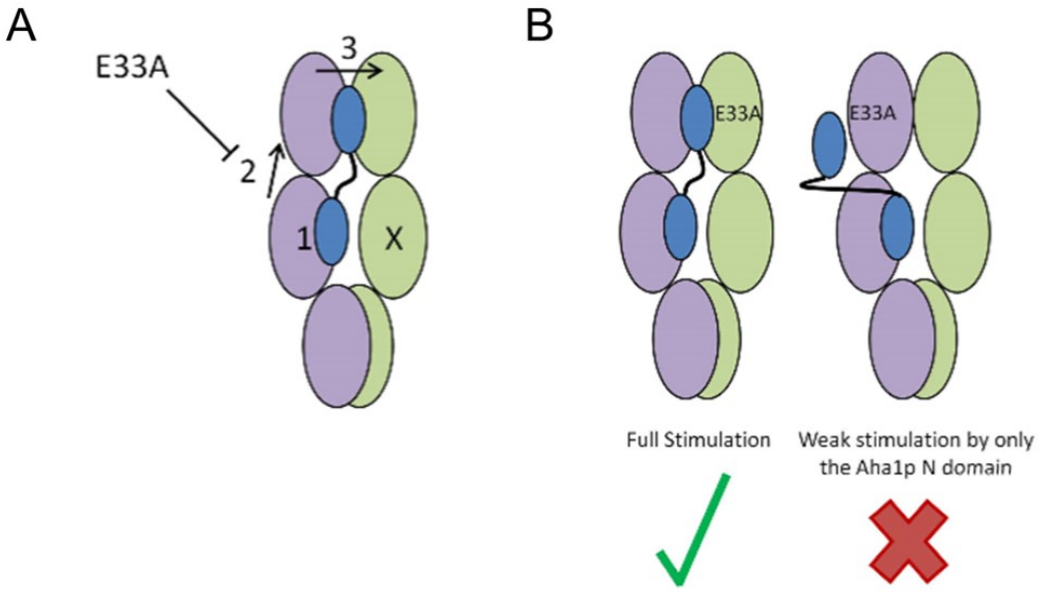

Figure 3.13 A mechanistic model for Aha1p-mediated stimulation of the ATPase activity of Hsp82p. A. The first step occurs when the Aha1p^{N} interacts with the middle domain Hsp82p middle domain, driving a small increase in ATPase activity (1). The second step is the *cis* rearrangement of the Hsp82p N-terminal domain (2) which can be blocked by the E33A mutation. The third step is a final rearrangement of one or both N-terminal domains of Hsp82p that allows for the participation of the Aha1p^{C} in full ATPase stimulation (3). **B.** The E33A mutation blocks ATPase stimulation by the Aha1p^{C} only in *cis* to the Aha1p^{N} interaction. Figure and legend from (Wolmarans et al., 2016).

Chapter 4

A novel strategy to chemically conjugate SUMO to Hsp90 *in vitro*

4.1 Introduction

Post-translational modifications (PTMs) play a critical role in regulating the chaperone activity and co-chaperone association with Hsp90 (Li et al., 2012; Mollapour et al., 2014; Mollapour and Neckers, 2012; Mollapour et al., 2010; Mollapour et al., 2011b). Recently, the first SUMOylation site of Hsp90 was reported (Mollapour et al., 2014). The small ubiquitin-like modifier protein (SUMO) is synthesized as a pro-protein which is activated when proteases cleave a short peptide from the C terminus of the protein, revealing a diglycine motif (Hay, 2007). Mature SUMO is then covalently attached to a lysine residue of a target protein through the action of E1, E2, and E3 ligases (Hay, 2007; Hecker et al., 2006; Minty et al., 2000). Although conjugation of SUMO is mediated by similar machinery responsible for the conjugation of ubiquitin, it does not target proteins for degradation like ubiquitin but rather plays a regulatory role in activating target proteins or directing them to multiprotein complexes (Gareau and Lima, 2010). SUMOylation has important functions in normal cell homeostasis but also during cellular stress, as SUMOylation of many proteins is known to be stimulated by cell stress (Enserink, 2015). SUMOylation has been shown to modify protein activity through altering conformation, localization, and interactions (Flotho and Melchior, 2013).

Recently, SUMOylation of a conserved lysine (K178 in yeast and K191 in humans) located in the N-terminal domain of Hsp90 was identified (Mollapour et al., 2014). This SUMOylation event facilitates the recruitment of Aha1 and limits Hsp90 chaperone activity towards its clients, such as the glucocorticoid hormone receptor (GR) and the cystic fibrosis transmembrane conductance regulator (CFTR) *in vivo* (Mollapour et al., 2014). Furthermore, there is an increase in SUMOylated Hsp90 species during cellular transformation which sensitizes yeast and mammalian cells to Hsp90 inhibitors (Mollapour et al., 2014). How SUMOylation alters the function of target proteins, such as the ATPase activity of Hsp90, has not been investigated due to technical challenges of studying SUMOylated proteins *in vitro*.

The effects of other PTMs, such as phosphorylation of Hsp90, have been more broadly studied. Through molecular means, one codon in the gene sequence can often be changed to mimic the phosphorylated version of the protein, but there is no easy way to study SUMOylation *in vitro.* Isolating SUMOylated proteins from cells is difficult because the relative stoichiometry of the modified proteins to the non-modified is extremely low (Nie and Boddy, 2015). Strategies have been employed to increase the proportion of SUMOylated proteins in the cell by over expressing SUMO or by stimulating the pathways that drive SUMOylation of a substrate protein *in vivo* (Mollapour et al., 2014). Although other methods that have yielded some success, including in-frame insertion of the SUMO coding sequence into the target protein or SUMOylating target proteins *in vitro* using purified ligases, these methods are not site-specific (Babic et al., 2006; Tan et al., 2008).

The goal of this project was to interrogate how SUMOylation regulates the function of Hsp90 by examining how it effects the enzymatic ATPase activity of Hsp90 as well as the co-chaperone interactions and their subsequent regulation of Hsp90. Understanding the dynamics of co-chaperone regulation of SUMOylated Hsp90, by themselves or in combination with other co-chaperones, will help pinpoint where in the ATPase cycle SUMOylation may affect the activity of Hsp90. This project required the development of an improved strategy to produce SUMOylated Hsp90 *in vitro*, of which a chemical coupling approach was devised. Using this methodology, SUMOylated Hsp90 could be made efficiently for *in vitro* study.

4.2 Results

4.2.1 Experimental strategy of chemical crosslinking

Yeast Hsp90 and SUMO (Hsp82p and Smt3p, respectively) natively lack cysteine residues. By taking advantage of the fact that both Hsp82p and Smt3p are cysteine-less, I introduced a single cysteine residue in Smt3p and a cysteine in place of a target lysine in Hsp82p to allow for efficient and specific crosslinking of Hsp90

and SUMO using a homo-bifunctional maleimide crosslinker that conjugates sulfhydryl groups.

To this end, I constructed a plasmid encoding Hsp82p that harbors a cysteine residue instead of a lysine residue at position 178 ($Hsp82p^{K178C}$) and also constructed the mature form of Smt3p, either harboring a cysteine downstream of the diglycine motif ($Smt3pGG^{Cys}$) or where the cysteine replaces one of the glycine residues ($Smt3pG^{Cys}$) (Figure 4.1A). The addition of a cysteine after the last glycine residue does further lengthen the chemical linkage of Smt3p to Hsp82p by one amino acid, and thus, I also constructed Smt3p where the last glycine was replaced with a cysteine residue. Mature SUMO is produced when the diglycine motif is revealed after cleavage by a C-terminal hydrolase, allowing for the formation of an isopeptide bond to form between the C-terminal glycine of SUMO and the lysine on the target protein. The di-glycine motif may be important *in vivo,* to be recognized by the ATP dependent E1 enzyme for activation, but because this is an *in vitro* crosslinking reaction, I hypothesize that both $Smt3pG^{Cys}$ and $Smt3pGG^{Cys}$ would crosslink to $Hsp82p^{K178C}$. These proteins were expressed and purified from bacteria.

I selected the short arm homo-bifunctional maleimide crosslinker, bismaleimidoethane (BMOE), to couple the cysteine residues of $Smt3p^{Cys}$ ($Smt3pG^{Cys}$ and $Smt3pGG^{Cys}$) and $Hsp82p^{K178C}$, to keep the length of the artificial linkage as close to the native covalent addition of SUMO to target proteins as possible (Figure 4.1B).

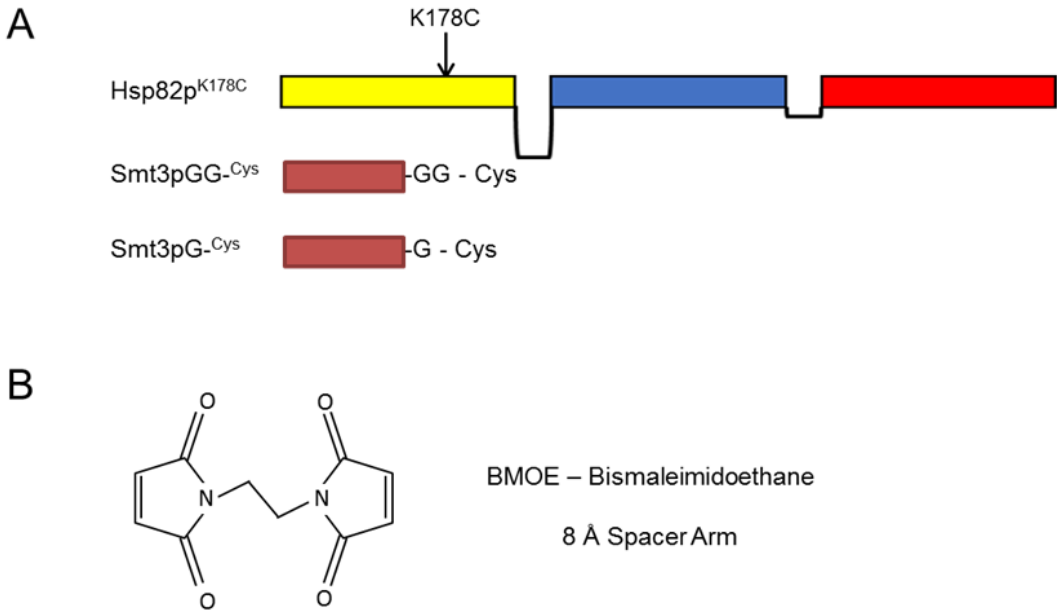

Figure 4.1 Constructs and reagents used in the SUMOylation of Hsp82p study. **A.** Full-length Hsp82p construct harboring a cysteine in place of lysine at residue 178, and two Smt3p constructs, harboring a cysteine downstream of either a diglycine motif or single glycine, was constructed. The N-terminal domain, middle domain, and C-terminal domain of Hsp82p is shown in yellow, blue, and red, respectively. **B.** Short-arm homo-bifunctional maleimide crosslinker BMOE, with a spacer arm of 8 Angstroms (Å), was used to chemically crosslink $Smt3p^{Cys}$ to $Hsp82p^{K178C}$.

4.2.2 Covalent addition of Smt3p^{Cys} to Hsp82p^{K178C}

Following the manufacturers protocol for the BMOE crosslinker, Hsp82p^{K178C} was pre-incubated with > 6-fold excess of BMOE crosslinker. If all cysteines reacted with a separate molecule of BMOE, the formation of crosslinked Hsp82p^{K178C} dimers would be limited (Figure 4.2A). I determined that an hour incubation of Hsp82p^{K178C} with BMOE alone effectively 'derivatized' all reactive groups on Hsp82p^{K178C} which resulted in no significant intermolecular (Hsp82p^{K178C}-Hsp82p^{K178C}) crosslinking (Figure 4.2B). The free reactive group of BMOE on the derivitized Hsp82p^{K178C} can then be crosslinked to another cysteine residue through a second incubation. Smt3p^{Cys} incubation will result in Smt3p^{Cys} coupling with the unreacted end of the BMOE present on Hsp82p^{K178C} but will also react with unreacted, free BMOE that is not coupled to Hsp82p^{K178C} to form Smt3p^{Cys}-Smt3p^{Cys} dimers (Figure 4.2A). The presence of either of these products will indicate that the crosslinking reaction was successful, and will be evident on a coomassie gel through the appearance of a higher molecular weight band than Hsp82p and/or Smt3p.

The two different Smt3p^{Cys} proteins was tested for their ability to crosslink to Hsp82p^{K178C}, by titrating Smt3pG^{Cys} and Smt3pGG^{Cys} into derivatized Hsp82p^{K178C}. At lower concentrations of Smt3pGG^{Cys}, I first observed an appearance of a prominent band corresponding to a dimer of Smt3pGG^{Cys} (Figure 4.2C). A shift of Hsp82p^{K178C} to a higher molecular weight corresponding to crosslinked Hsp82p^{K178C}-Smt3pGG^{Cys} was observed at higher concentrations of Smt3pGG^{Cys} (Figure 4.2C). Smt3p^{Cys} with a single glycine before the cysteine, Smt3pG^{Cys}, did not crosslink to Hsp82p^{K178C} to any significant degree nor was it able to readily form Smt3pG^{Cys} –Smt3pG^{Cys} homodimers compared to Smt3pGG^{Cys} (Figure 4.2D). For all further experiments, hereinafter, Smt3pGG^{Cys} was used and will be referred to as Smt3p^{Cys}.

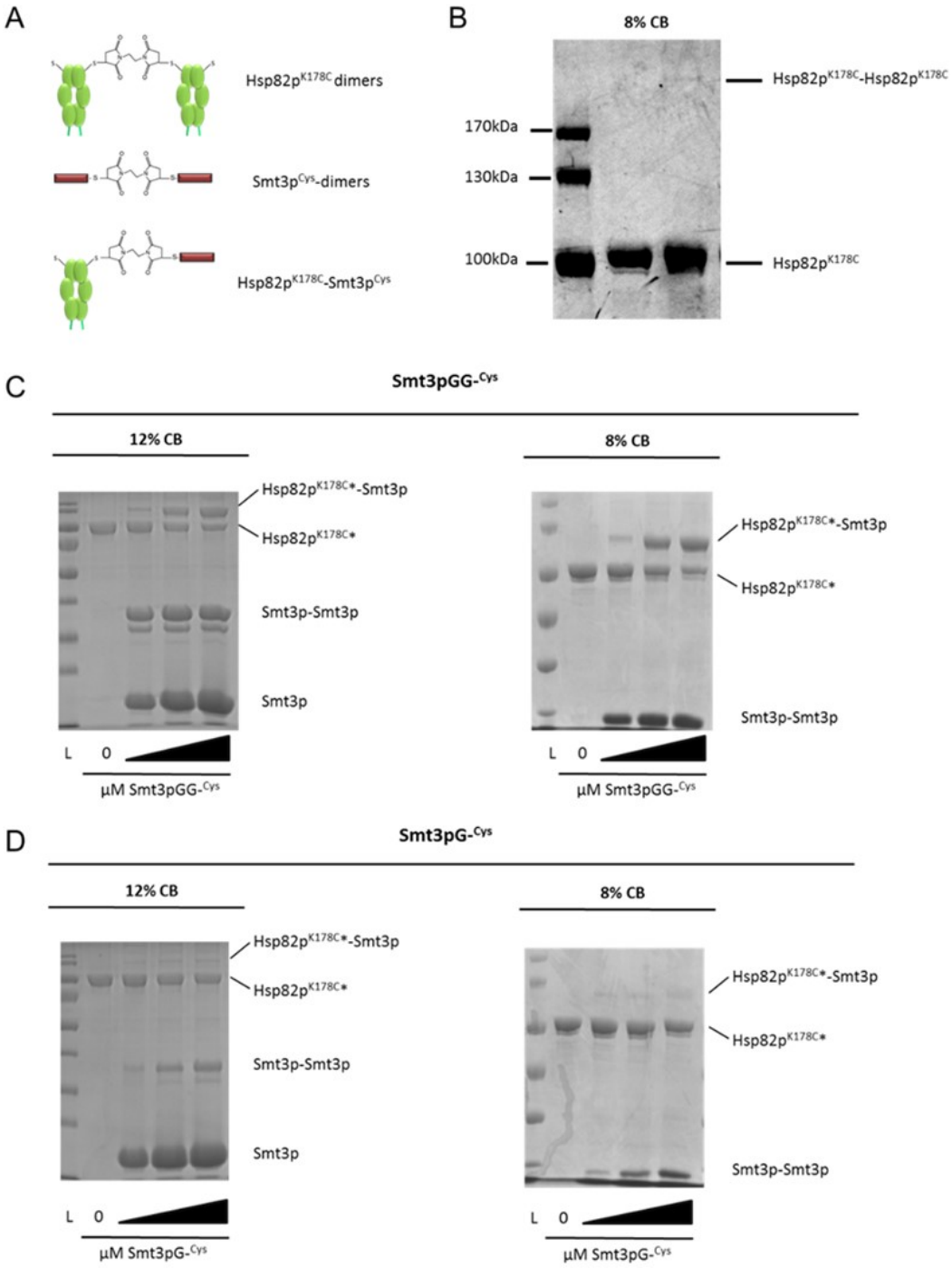
A
Hsp82p^K178C dimers
Smt3p^Cys-dimers
Hsp82p^K178C-Smt3p^Cys
B
8% CB
170kDa
130kDa
100kDa
Hsp82p^K178C-Hsp82p^K178C
Hsp82p^K178C
C
Smt3pGG-^Cys
12% CB
8% CB
Hsp82p^K178C*-Smt3p
Hsp82p^K178C*
Smt3p-Smt3p
Smt3p
L 0
µM Smt3pGG-^Cys
D
Smt3pG-^Cys
12% CB
8% CB
Hsp82p^K178C*-Smt3p
Hsp82p^K178C*
Smt3p-Smt3p
Smt3p
L 0
µM Smt3pG-^Cys

Figure 4.2 Testing crosslinking strategy of Hsp82p^{K178C} with Smt3pGG^{Cys} and Smt3pG^{Cys}. **A.** Potential protein-crosslinker products that can be made through the addition of the homo-bifunctional maleimide crosslinker, BMOE: Both Hsp82p^{K178C} and Smt3p^{Cys} can crosslink to themselves to form Hsp82p^{K178C}-Hsp82p^{K178C} and Smt3p^{Cys}-Smt3p^{Cys} dimers, respectively, and Hsp82p^{K178C} can crosslink to Smt3p^{Cys} to form SUMOylated Hsp82p (Hsp82p^{K178C}-Smt3p^{Cys}). The derivatization of Hsp82p^{K178C} and the crosslinking of Smt3p to Hsp82p^{K178C} is shown only on one protomer of the dimer for simplicity, but experimentally, Hsp82p will be dually derivitized and SUMOylated. **B.** No significant intermolecular (Hsp82p^{K178C}–Hsp82p^{K178C}) crosslinking was observed in the presence of BMOE. Crosslinking reactions contained 32 μM Hsp82p^{K178C} and 200 μM BMOE (lane 2) or DMSO (lane 1). **C-D.** Titration of Smt3pGG^{Cys} (C), but not Smt3pG^{Cys} (D), into derivatized Hsp82p^{K178C}, results in an observed shift of Hsp82p^{K178C} to a higher molecular weight. Reactions contained 32 μM Hsp82p^{K178C}, 200 μM BMOE, and 0, 40, 100, or 200 μM Smt3pGG^{Cys} (C) or Smt3pG^{Cys} (D). * Denotes derivatization of Hsp82p^{K178C}. 10μL of the 40μL reactions were visualized on 8 % and 12 % SDS gels, stained with CB.

Smt3p^{Cys} was titrated into derivitized Hsp82p^{K178C} to establish the optimal crosslinking reaction. I observed maximal crosslinking of Smt3p^{Cys} to Hsp82p^{K178C} upon addition of 250 µM Smt3p^{Cys}, but a small proportion of non-SUMOylated Hsp82p^{K178C} remained (Figure 4.3A). This non-SUMOylated Hsp82p^{K178C} pool may exist due to a lack of full derivatization, insufficient amount of Smt3p^{Cys}, or may simply be a degradation product that cannot be SUMOylated. I tested whether increasing the concentration of crosslinker would increase the amount of crosslinked Hsp82p^{K178C}-Smt3p^{Cys} product, however, an increase in crosslinker concentration only affected the rate of Hsp82p^{K178C}-Smt3p^{Cys} formation, as free BMOE formed Smt3p^{Cys} dimers more readily (Figure 4.3B). The greatest crosslinking efficiency occurred when derivatizing Hsp82p^{K178C} for one hour with 200 µM BMOE prior to addition of Smt3p^{Cys} (Figure 4.3B). Adding a concentration much higher than 250 µM Smt3p^{Cys} may result in higher crosslinking efficiency, as crosslinking is concentration dependent, but this is not experimentally feasible due to limited reaction volumes to maintain a concentration of 32 µM of Hsp82p^{K178C}.

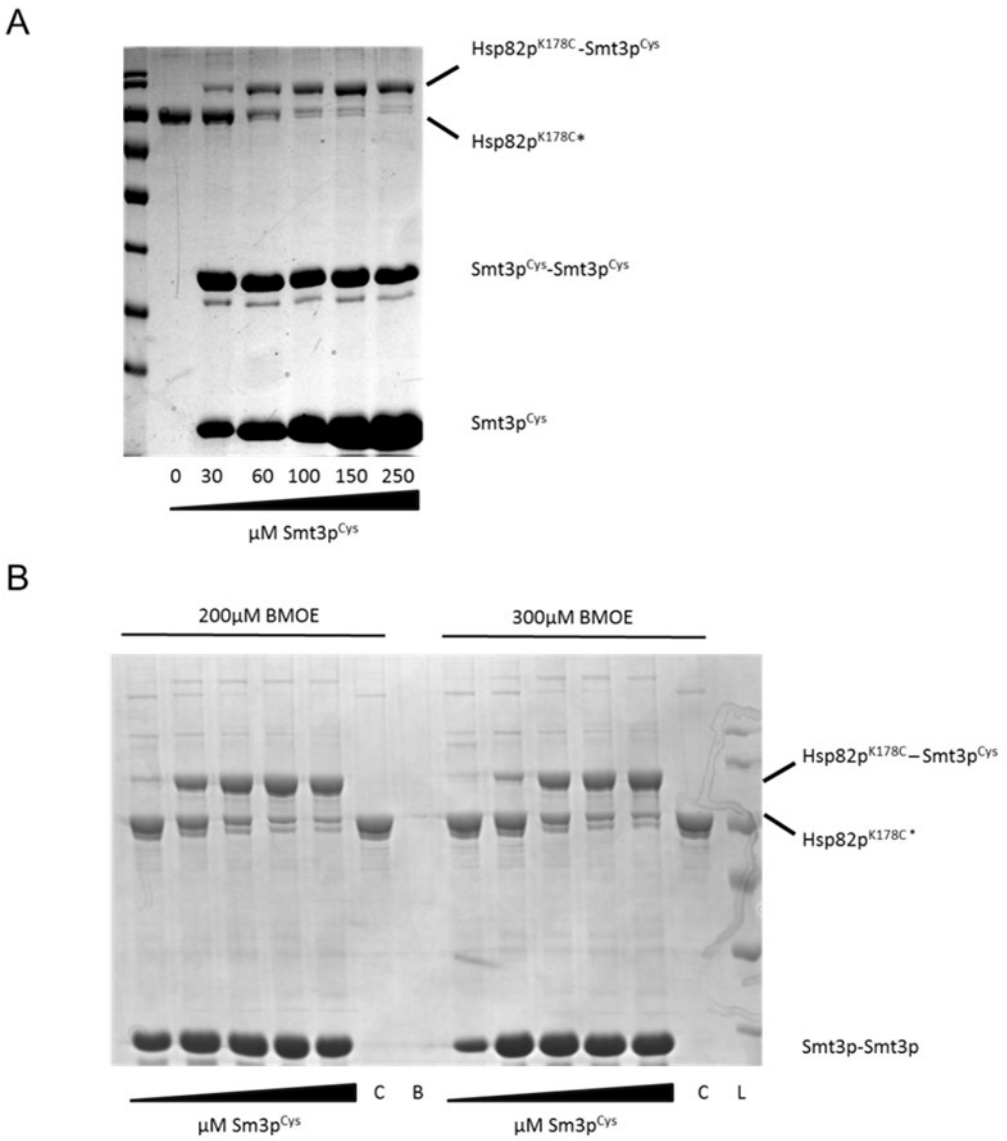

Figure 4.3 Covalent addition of Smt3p^{Cys} to Hsp82p^{K178C}. **A.** Maximal crosslinking of Smt3p^{Cys} to Hsp82p^{K178C} occurred upon the addition of 250 µM Smt3p^{Cys}. Crosslinking reactions contained 32 µM Hsp82p^{K178C}, 200 µM BMOE, and indicated concentration of Smt3p^{Cys} **B.** Crosslinking of Smt3p^{Cys} to Hsp82p^{K178C} is optimal using 200 µM BMOE. Hsp82p^{K178C} was derivitized (*) in the presence of 200 µM or 300 µM BMOE for an hour prior to incubation with Smt3p^{Cys}. Final reactions contained 2µM derivitized Hsp82p^{K178C} and 0, 20, 40, 60, 80, 100 µM Smt3p^{Cys}. "C" denotes derivatized Hsp82p^{K178C} control with 0 µM Smt3p^{Cys} and "L" denotes ladder. 10µL of the 40µL reactions were visualized on 12 % (A) or 8 % (B) SDS gels, stained with CB.

4.2.3 Characterization of the intrinsic ATPase activity of Hsp82p^{K178C} and SUMOylated Hsp82p^{K178C}

Increased N-terminal domain SUMOylation of Hsp90 was evident in cells transformed with v-*Src*, which rendered these cells more sensitive to the Hsp90 inhibitor, ganetespib (Mollapour et al., 2014). Furthermore, Hsp90 isolated from clinical tumor samples revealed an increase in both ATPase activity and affinity for Hsp90 inhibitors compared to Hsp90 isolated from normal, non-transformed tissue sample (Kamal et al., 2003). These results suggest that SUMOylated Hsp90 may be more active, which led me to hypothesize that SUMOylated Hsp90 will have a higher intrinsic ATPase rate relative to non-modified Hsp90.

I first tested the intrinsic ATPase rate of Hsp82p^{K178C}, which retained wildtype ATPase activity of ~0.16 μM ATP/min (Figure 4.4A). This confirmed that the point mutation (K178C) did not affect the intrinsic rate of Hsp82p^{K178C}. The addition of Smt3p^{Cys}, without the presence of the crosslinker, did not affect the ATPase rate of either wildtype or mutant Hsp82p (Figure 4.4A). The addition of BMOE alone, resulted in a statistically significant increase in the intrinsic ATPase activity of Hsp82p^{K178C} (~2.5-fold increase), but did not affect the rate of wildtype Hsp82p (Figure 4.4B). This is consistent with the cysteine in Hsp82p^{K178C} reacting with the BMOE crosslinker. This increase in ATPase activity may be due to the hydrophobic properties of the added crosslinker to the N-terminal domain of Hsp82p^{K178C}. The acquired hydrophobicity in the N-terminal domain would result in an increase in ATPase rate because the closed state of Hsp82p may be favored or more frequently sampled. Indeed, it has previously been shown that when hydrophobic side chains are introduced near the N-terminal dimerization interface, an increase in ATPase activity is observed (Hawle et al., 2006; Vaughan et al., 2009). Furthermore, the addition of Smt3p^{Cys} to this derivitized Hsp82p^{K178C} (which results in the crosslinked Hsp82p^{K178C}-Smt3p^{Cys} product) decreased that ATPase rate slightly (Figure 4.4B). The addition of Smt3p^{Cys} presumably 'masks' the previously exposed hydrophobic crosslinker, effectively protecting it from the aqueous environment. Interestingly, this increase in the intrinsic ATPase activity, compared to wildtype, is statistically significant. This suggests that the increase

may not be due to the hydrophobic crosslinker, but that the SUMO modification is responsible for the increase in ATPase rate. Therefore, consistent with my hypothesis, these data suggest that SUMOylation mildly enhances the ATPase activity of $Hsp82p^{K178C}$ (approximately 2-fold). The addition of BMOE and $Smt3p^{Cys}$ to wildtype Hsp82p did not result in a significant increase (Figure 4.4B)

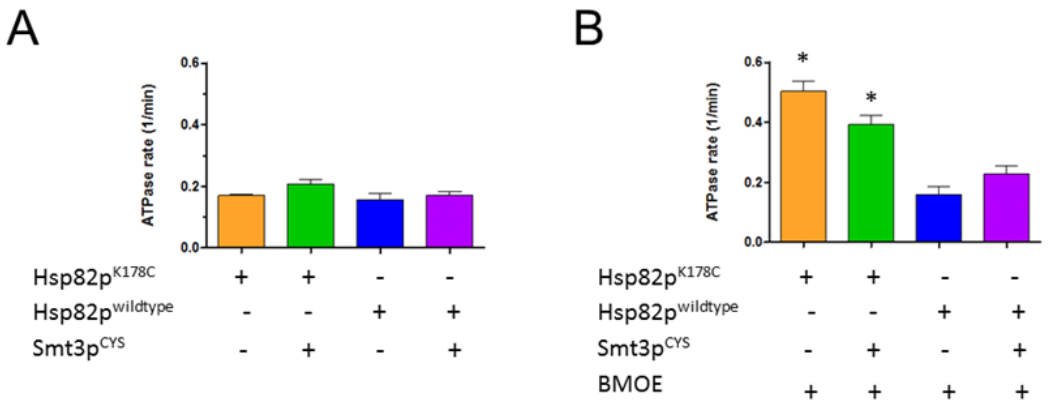

Figure 4.4 Intrinsic ATPase activity of Hsp82p, Hsp82p^{K178C}, and SUMOylated Hsp82p^{K178C}. A. The intrinsic ATPase activity of Hsp82p^{K178C} is similar to wildtype Hsp82p, with and without Smt3p^{Cys}. **B.** The chemical coupling of Smt3p to Hsp82p^{K178C} causes an increase in the intrinsic ATPase rate compared to wildtype Hsp82p. ATPase rates are shown as µM ATP hydrolyzed per minute per µM of Hsp82p (1/min). Reactions of (A) and (B) are identical, except for the addition of 200 µM BMOE. Reactions contained 2 µM Hsp82p^{K178C} or Hsp82p^{WT}, and either DMSO (A) or 200 µM BMOE (B). A statistical significant (* - one-way ANOVA, Tukey's HSD, $p<0.05$) increase in the intrinsic ATPase rate is observed when Hsp82p^{K178C} is derivitized and conjugated to Smt3p^{Cys}.

The crosslinking reaction is not 100 % efficient (based on gels in Figure 4.3), as there is approximately a 90 % band shift from the derivitized Hsp82p^{K178C} to the chemically-coupled Hsp82p^{K178C}-Smt3p^{Cys} band. This made me question what species of Hsp82p is contributing to the ATPase activity in Figure 4.4. Is the increased ATPase rate due to the Hsp82p^{K178C} dimers that are SUMOylated on each subunit (dually SUMOylated) or is it remaining derivitized Hsp82p^{K178C} population producing the altered ATPase rate? To address this concern, I tested the ATPase activity of hemi-SUMOylated Hsp82p^{K178C} against the dually-SUMOylated Hsp82p^{K178C} (>90 % SUMOylation). I determined that a 50 % band shift to the higher molecular weight band resulted when 30 μM Smt3p^{Cys} was incubated with derivitized Hsp82p^{K178C}, which represents hemi-SUMOylated Hsp82p^{K178C} (data not shown). I am assuming that majority of derivitized Hsp82p^{K178C} would exist in a heterodimeric state (hemi-SUMOylated Hsp82p^{K178C}), rather than consisting of two pools of either type of homodimer. It must be considered, however, that under these substoichiometric SUMOylation conditions, not all of the derivitized Hsp82p^{K178C} dimers will be hemi-SUMOylated but a small amount will be dually-SUMOylated and a small amount with be unmodified. The ATPase activity of hemi-SUMOylated (50 %) and dually-SUMOylated (>90 %) Hsp82p^{K178C} was measured and the results indicate that there is a small difference between their intrinsic ATPase rates (Figure 4.5). Therefore, the small pool of derivitized (non-SUMOylated) Hsp82p^{K178C} has a negligible influence on the ATPase readout of what I consider the ATPase activity of dually-SUMOylated Hsp82p.

Hsp82p^{K178C} will be used as the control in all subsequent ATPase assays because it has identical intrinsic ATPase activity to wildtype Hsp82p (Figure 4.4). Crosslinking of Smt3p^{Cys} to Hsp82p^{K178C} was confirmed in every experiment by checking the band shift from ~100kDa to ~130kDa on SDS gels stained with coomassie blue.

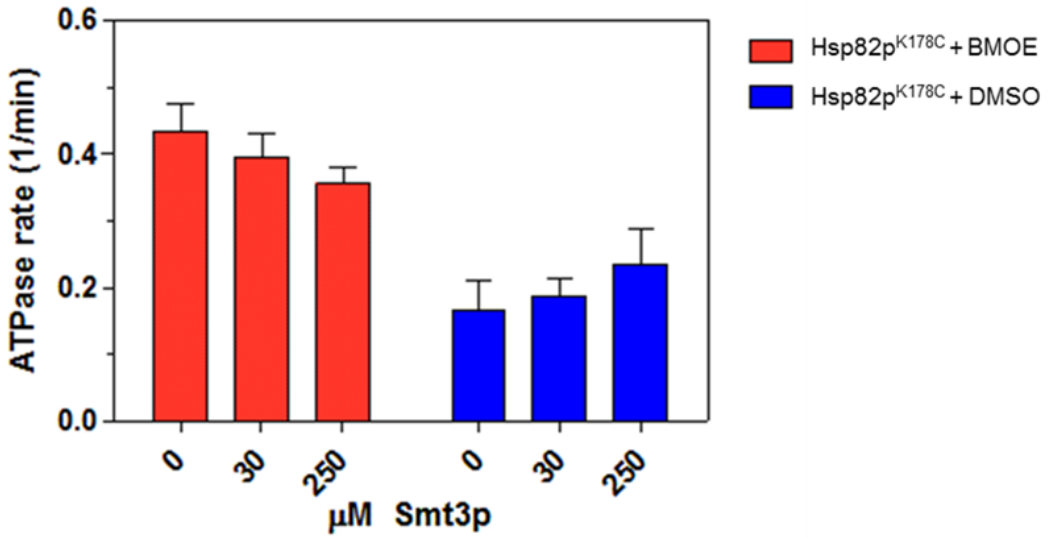

Figure 4.5 Intrinsic ATPase rate of hemi- and dually-SUMOylated Hsp82p^{K178C}. The intrinsic ATPase activity of derivitized Hsp82p^{K178C} (red) decreases slightly with increasing SUMOylation (0 to 250 µM Smt3p^{Cys}), while the intrinsic ATPase activity of DMSO treated Hsp82p^{K178C} (blue) remained unaffected by the addition of Smt3p^{Cys}. ATPase rate is shown as µM ATP hydrolyzed per minute per µM of Hsp82p (1/min). Reactions contained 2 µM Hsp82p^{K178C} in the presence of DMSO or BMOE, and the indicated amount of Smt3p^{Cys}. ATPase rates are shown as µM ATP hydrolyzed per minute per µM of Hsp82p (1/min) with standard deviation plotted as error bars.

The SUMO modification occurs very infrequently and it is not known to what extent Hsp90 is SUMOylated in cells under normal conditions. Given the sparsity of the modification, it is reasonable to assume a small population of Hsp90 would be modified, and if modified, most likely on only one subunit. Because the same proteases that generate mature SUMO are also responsible for removal of SUMO from target proteins (Mukhopadhyay and Dasso, 2007), to overcome the result of enzymes deSUMOylating target proteins *in vivo*, SMT3 must be overexpressed to shift the balance toward SUMOylation. In this recent study, SUMOylation was either blocked through mutating lysine, at position 178, to arginine, or was enhanced through overexpression of SMT3, *in vivo* (Mollapour et al., 2014). Interestingly, only asymmetrically SUMOylated Hsp82p was observed *in vivo* (Mollapour et al., 2014).

Next, I wanted to investigate if asymmetric SUMOylated Hsp82p can be obtained through subunit exchange, *in vitro*. Mixing dually-SUMOylated Hsp82p^{K178C} with a non-modified Hsp82p would allow for the formation of heterodimers that are asymmetrically SUMOylated if subunit exchange occurs. I assessed whether SUMOylated Hsp82p^{K178C} can form heterodimers by conducting an immunoprecipitation (IP) of differentially tagged Hsp82p mutants. Myc-Hsp82p was immunoprecipitated from samples containing equimolar Flag-tagged Hsp82p^{K178C} (non-modified and SUMOylated). Western blot analysis revealed that SUMOylated or non-SUMOylated Hsp82p^{K178C} can undergo subunit exchange to the same degree as wildtype Hsp82p (Figure 4.6). Asymmetrically SUMOylated Hsp82p^{K178C} can be formed through subunit exchange, as a non-SUMOylated Hsp82p^{K178C} subunit readily dimerized with both non-SUMOylated and SUMOylated Hsp82p^{K178C} subunits (Figure 4.6).

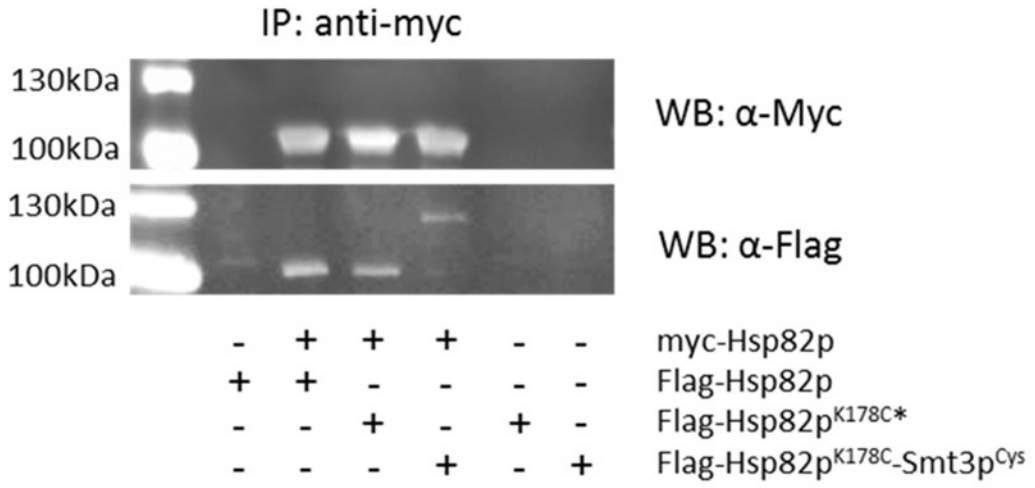

Figure 4.6 Heterodimer formation between wildtype Hsp82p and non- and SUMOylated-Hsp82p^{K178C}. SUMOylated Hsp82p^{K178C} and non-SUMOylated Hsp82p^{K178C} both form heterodimers with wildtype Hsp82p. Flag-tagged Hsp82p^{K178C}* and Flag-tagged Hsp82p^{K178C}-Smt3p^{Cys} co-IP with Myc-tagged Hsp82p to a similar degree as Flag-tagged Hsp82p co-IP with Myc-Hsp82p. 5 µM purified Myc-tagged Hsp82p was incubated with 5 µM Flag-tagged Hsp82p, Hsp82p^{K178C*}, and Hsp82p^{K178C}-Smt3p^{Cys} for 30 minutes to allow heterodimer formation. These reactions were incubated on a rotator at room temperature for 60 minutes with beads coupled to anti-Myc monoclonal antibody 9E10. Beads were pelleted, washed once in 250 µL of binding buffer, run on SDS-PAGE, and analyzed by western blotting. (*) Denotes derivatization with crosslinker.

4.2.4 ATPase regulation of SUMOylated Hsp82p^{K178C} by co-chaperones

It is not known how co-chaperones affect the ATPase activity of SUMOylated Hsp82p. Mollapour *et al.* demonstrated that SUMOylated Hsp82p recruits Aha1p association (Mollapour et al., 2014). SUMOylation may also influence how other co-chaperones interact with the Aha1p-recruited Hsp82p complex, and therefore, I will determine how the SUMO modification affects Aha1p ATPase regulation and interaction as well as Sti1p and Sba1p regulation of the Aha1p-Hsp82p complex.

4.2.4.1 Regulation by the ATPase stimulator, Aha1p

It is thought that Aha1p regulates Hsp82p function by robustly stimulating the intrinsically low ATPase activity (Lotz et al., 2003; Meyer et al., 2004a; Panaretou et al., 1998). Preventing SUMOylation of Hsp82p by replacing K178 with arginine *in vivo* reduces the interaction between Hsp82p and Aha1p. Therefore, I hypothesized that SUMOylated Hsp82p would be more robustly stimulated by Aha1p or would have a higher affinity for SUMOylated Hsp82p. To test this, I titrated Aha1p into SUMOylated Hsp82p^{K178C} and DMSO incubated Hsp82p^{K178C} in the presence of Smt3p^{Cys}. In the presence of saturating levels of Aha1p, Aha1p stimulated the ATPase rate of Hsp82p^{K178C}-Smt3p^{Cys} to a slightly lower degree than of Hsp82p^{K178C} (Figure 4.7A). A decrease in the overall maximal stimulation was observed for SUMOylated Hsp82p^{K178C} as the maximum velocity (V_{MAX}) of the ATPase reaction was 3.2 min^{-1} and 2.6 min^{-1} for non-SUMOylated and SUMOylated Hsp82p^{K178C}, respectively. Interestingly, there is a statistically significant increase in the apparent Aha1p binding affinity for SUMOylated Hsp82p^{K178C} (0.30 ± 0.08 μM) compared to non-SUMOylated Hsp82p^{K178C} (0.57 ± 0.22 μM) (unpaired *t*-test $p<0.05$) (Figure 4.7B). These results indicate that there is a relationship between SUMOylated Hsp82p^{K178C} and Aha1p binding affinity, and suggests that the apparent requirement of SUMOylated Hsp82p for Aha1p binding *in vivo* is indeed linked to the conjugation of Smt3p to Hsp82p.

In vivo, SUMOylation of Hsp90 was reported to occur on only one protomer of the Hsp90 dimer (Mollapour et al., 2014). In my experiments, dimers were

predominantly SUMOylated on both subunits of Hsp82p^{K178C}. This led me to question if Aha1p stimulation would be different for asymmetrically SUMOylated Hsp82p^{K178C}. To test this, I measured the stimulated ATPase activity of hemi- and dually-SUMOylated Hsp82p^{K178C}. Hsp82p^{K178C} was derivatized and incubated in the presence of 30 μM or 250 μM Smt3p^{Cys} to yield hemi-SUMOylated and dually-SUMOylated Hsp82p^{K178C}, respectively. When stimulated by Aha1p, the ATPase activity of hemi-SUMOylated Hsp82p^{K178C} was slightly higher than dually-SUMOylated Hsp82p^{K178C} (Figure 4.7C). Overall, the ATPase activity of Hsp82p is affected equally by symmetric and asymmetric SUMOylation.

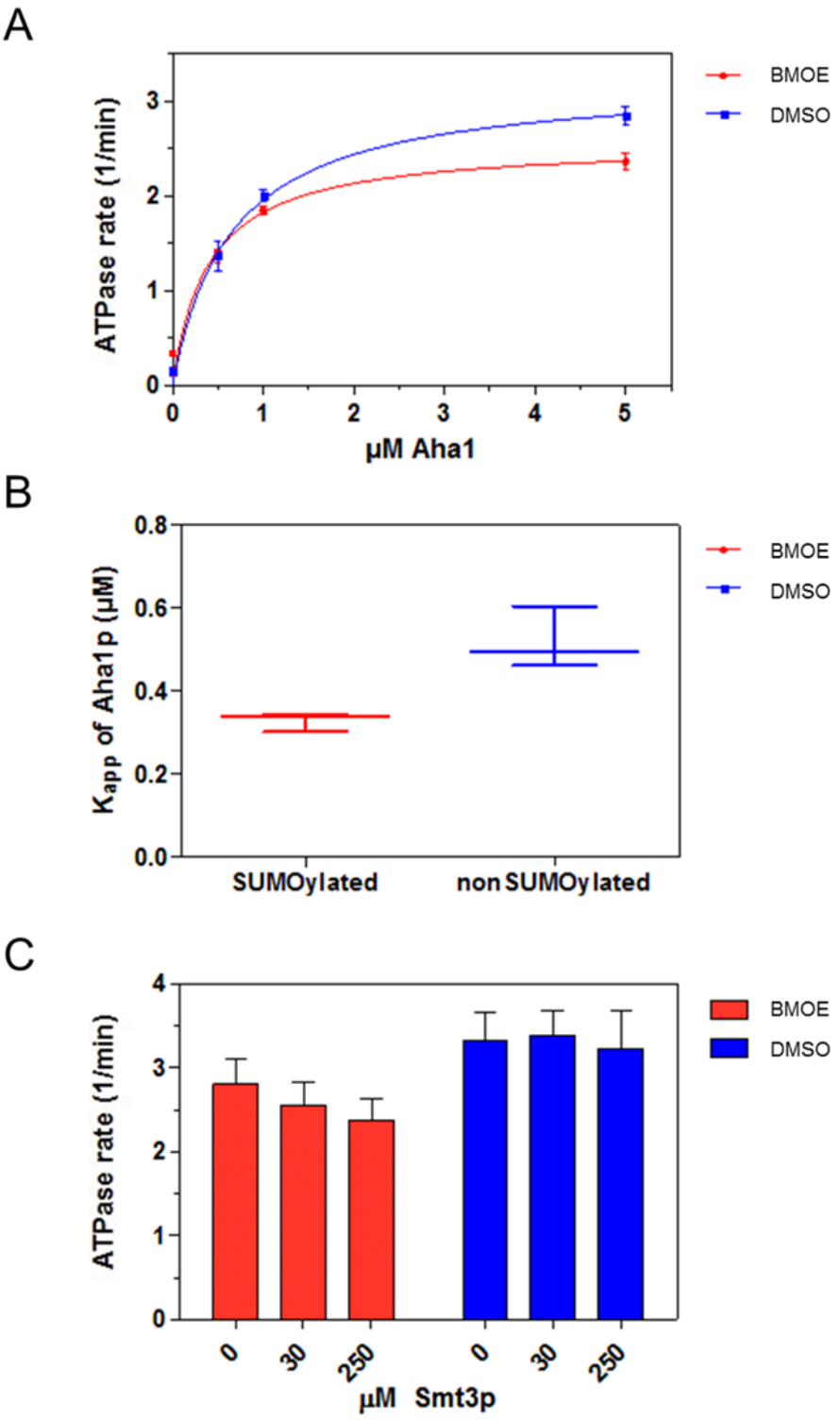
A
ATPase rate (1/min)
μM Aha1
BMOE
DMSO
B
K_{app} of Aha1 p (μM)
SUMOylated
non SUMOylated
BMOE
DMSO
C
ATPase rate (1/min)
μM Smt3p
BMOE
DMSO

Figure 4.7 Aha1p-mediated stimulation of SUMOylated Hsp82p^{K178C}. **A.** Aha1p titration into Hsp82p^{K178C}-Smt3p^{Cys} and Hsp82p^{K178C}. All reactions contained 1 μM SUMOylated Hsp82p^{K178C} (Hsp82p^{K178C}-Smt3p^{Cys}) or non-SUMOylated Hsp82p^{K178C}, and the indicated concentration of Aha1p. The V_{max} values for Hsp82p stimulation by Aha1p was calculated to be 2.6 ± 0.15 min^{-1} for SUMOylated (red) and 3.2 ± 0.12 min^{-1} for non-SUMOylated (blue). Reactions contained 1 μM Hsp82p^{K178C} or Hsp82p^{K178C}-Smt3p^{Cys} and the indicated amount of Aha1p. **B.** The binding constant (K_{app}) of Aha1p for SUMOylated and non-SUMOylated Hsp82p^{K178C} was calculated to be 0.30 ± 0.08 μM and 0.57 ± 0.22 μM, respectively, indicating that Aha1p has a higher apparent affinity for SUMOylated Hsp82p^{K178C}. The apparent affinity (K_{APP}) for Aha1p was calculated from ATPase assays, similar to those conducted in (A), using Michaelis-Menton kinetic analysis on Prism GraphPad. Reactions contained 0.25 μM Hsp82p^{K178C} or Hsp82p^{K178C}-Smt3p^{Cys} and the indicated concentration of Aha1p. DMSO represents non-modified Hsp82p^{K178C} while BMOE represents SUMOylated Hsp82p^{K178C}. **C.** The stimulated ATPase activity of derivitized Hsp82p^{K178C} (red) decreases slightly with increasing SUMOylation (0 to 250 μM Smt3p^{Cys}), while the stimulated ATPase activity of DMSO treated Hsp82p^{K178C} (blue) remained unaffected by the addition of Smt3p^{Cys}. Reactions contained 1 μM Hsp82p^{K178C}, 10 μM Aha1p, DMSO or BMOE, and the indicated amount of Smt3p^{Cys}. The ATPase activity and K_{APP} of Hsp82p^{K178C} and Hsp82p^{K178C}-Smt3p^{Cys} is shown in blue and red, respectively, and the ATPase rates are shown as μM ATP hydrolyzed per minute per μM of Hsp82p (1/min).

To investigate the stability of the interaction between Aha1p and SUMOylated Hsp82p^{K178C}, I conducted a Myc immunoprecipitation assay with Myc-Aha1p and equimolar concentration of non-SUMOylated, dually-SUMOylated, and hemi-SUMOylated Hsp82p^{K178C}. In this experiment, hemi-SUMOylated Hsp82p^{K178C} was formed by mixing and incubating equimolar amounts of non-SUMOylated and SUMOylated Hsp82p^{K178C} for 60 minutes. I hypothesized that Myc-Aha1p would stably interact with hemi-SUMOylated Hsp82p^{K178C} which would result in an increased recovery of Hsp82p^{K178C}-Smt3p^{Cys} with Myc-Aha1p compared to the recovery of non- or dually-SUMOylated Hsp82p^{K178C}. Myc-Aha1p was able to interact with non-, dually-, and hemi-SUMOylated Hsp82p^{K178C} equally (lanes 2, 4, and 6 respectively) (Figure 4.8).

I am assuming subunit exchange is not altered between the modified Hsp82p^{K178C} variants based on the heterodimer western blot that indicates heterodimers can be formed with SUMOylated Hsp82p. The stability of Hsp82p dimers was previously investigated by FRET by measuring the half-life of subunit exchange (Li et al., 2013), and thus, 60 minutes allotted time should provide ample time for subunit exchange to occur (Figure 4.8).

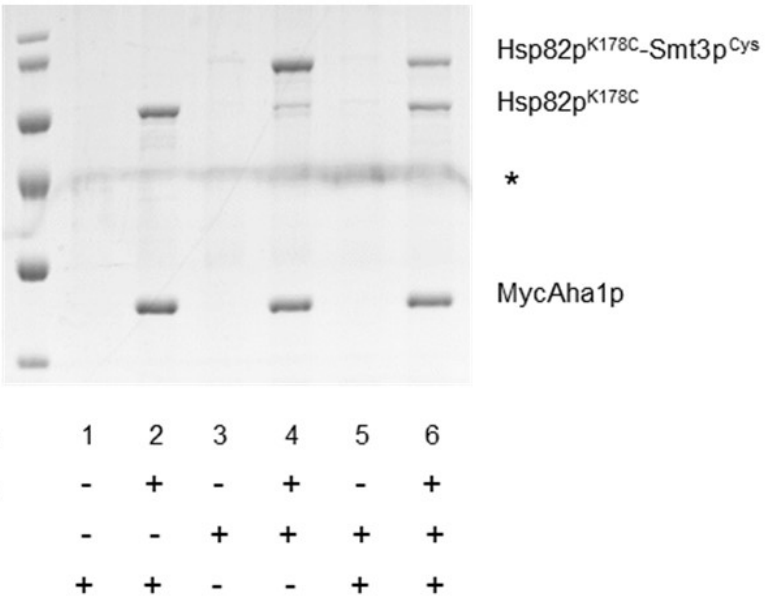

Lane	1	2	3	4	5	6
MycAha1p	-	+	-	+	-	+
Hsp82p^{K178C}-Smt3p^{Cys}	-	-	+	+	+	+
Hsp82p^{K178C}	+	+	-	-	+	+

Figure 4.8 Aha1p stably interacts with both non-SUMOylated and SUMOylated Hsp82p^{K178C} species. Myc-Aha1p immunoprecipitate non-SUMOylated, dually-SUMOylated, and hemi-SUMOylated Hsp82p^{K178C} equally. Reactions contained 5 µM Myc-Aha1p and 5 µM Hsp82p^{K178C}, Hsp82p^{K178C}-Smt3p^{Cys}, or an equal mix of 2.5 µM Hsp82p^{K178C} and 2.5 µM Hsp82p^{K178C}-Smt3p^{Cys}. 10 µL of bead slurry coupled to anti-Myc monoclonal antibody 9E10 were added to the 50 µL reactions and were incubated on a rotator at room temperature for 60 minutes. Beads were pelleted, washed once in 250 µL of binding buffer, and 10 µL of sample was visualized on an 8 % SDS-PAGE gel, stained with CB. (*) Denotes non-specific CB staining of the gel.

4.2.4.2 Regulation by ATPase inhibitors, Sti1p and Sba1p

Sti1p is a known inhibitor of the ATPase activity of Hsp82p and preferentially binds to Hsp82p in the absence of nucleotide (Johnson et al., 2007; Prodromou et al., 1999; Richter et al., 2003). Sti1p stabilizes the open conformation of Hsp82p through binding to the C-terminal MEEVD motif and other regions in the N-terminal and middle domains of Hsp82p (Richter et al., 2003; Southworth and Agard, 2011). Sba1p is also an inhibitor of the ATPase activity of Hsp82p, but in contrast to Sti1p, it binds exclusively to the closed, ATP-bound conformation and can be used as a conformation-dependent sensor (Ali et al., 2006; McLaughlin et al., 2006). Sti1p and Sba1p have the potential to form ternary complexes with Hsp82p and Aha1p, and can inhibit the Aha1p stimulated ATPase activity of Hsp82p (Retzlaff et al., 2010; Richter et al., 2004). Sba1p and Sti1p associated with both SUMOylated and non-SUMOylated Hsp82p *in vivo*, which led me to hypothesize that these co-chaperones would inhibit the Aha1p-mediated stimulation of SUMOylated Hsp82p^{K178C} in the same manner as non-modified Hsp82p (Mollapour et al., 2014). Titration of Sti1p revealed that Sti1p can inhibit the Aha1p-mediated stimulated rates of both non-SUMOylated and SUMOylated Hsp82p, decreasing the stimulated rates down to wildtype intrinsic rates (Figure 4.9A). Sba1p, however, was not able to inhibit the Aha1p-mediated stimulation of SUMOylated Hsp82p^{K178C} to the same extent as it decreased the stimulated non-SUMOylated Hsp82p^{K178C} ATPase rate (Figure 4.9B). I performed *t*-tests and established that there is a statistically significant difference between Sba1p inhibition of SUMOylated Hsp82p^{K178C} compared to non-SUMOylated Hsp82p^{K178C} in the presence of Aha1p (unpaired *t*-test $p<0.05$). There was, however, no significant difference between Sti1p inhibition of SUMOylated and non-SUMOylated Hsp82p^{K178C}. This indicates that the SUMO modification on Hsp82p affects Sba1p inhibition but not Sti1p inhibition of the Aha1p stimulated rate.

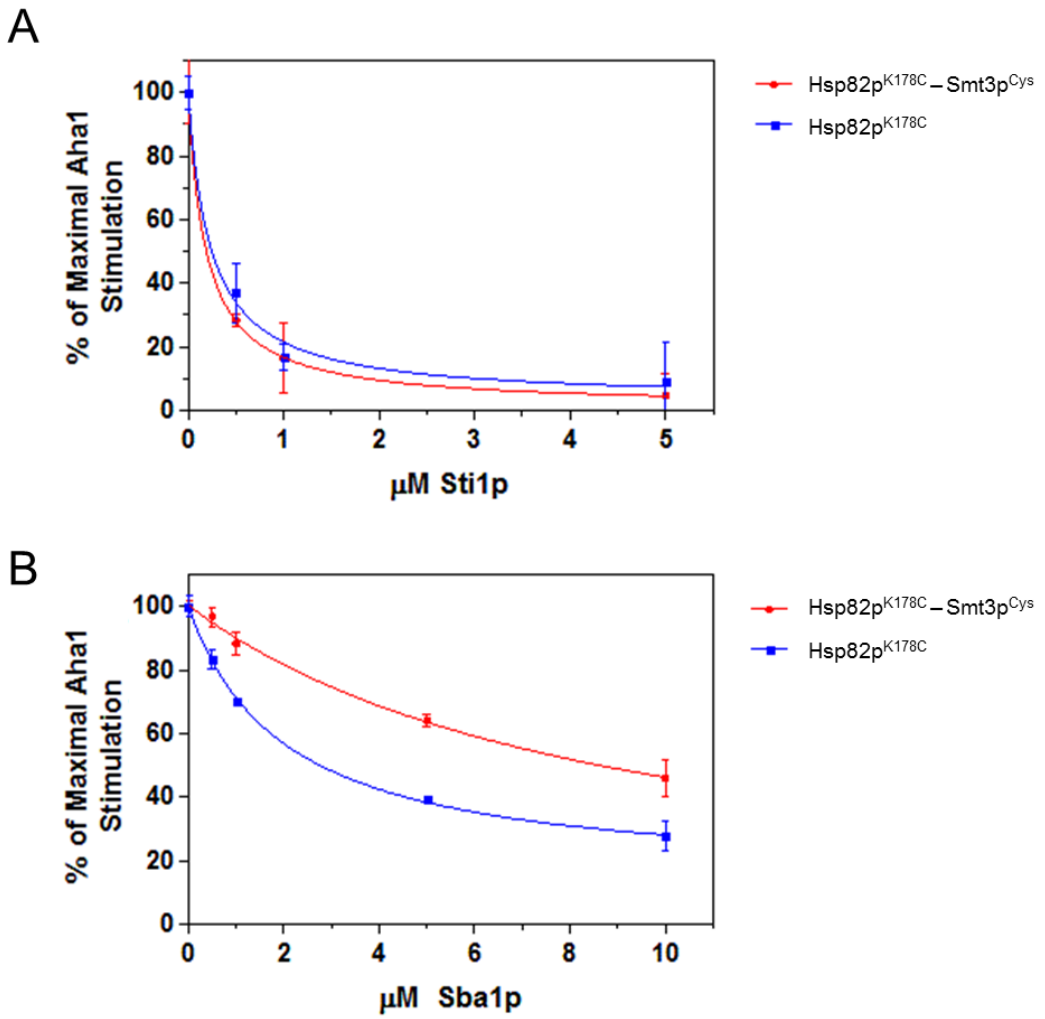

Figure 4.9 SUMOylation of Hsp82p^{K178C} affects Sba1p, but not Sti1p, inhibition of the Aha1p stimulated ATPase rate. Sti1p **(A)** and Sba1p **(B)** inhibition of the maximally Aha1p-mediated stimulation of SUMOylated (Hsp82p^{K178C}-Smt3p^{Cys}) and non-SUMOylated Hsp82p^{K178C}. All reactions contained 1 µM Hsp82p^{K178C} or Hsp82p^{K178C}-Smt3p^{Cys}, 5 µM Aha1p and the indicated concentration of co-chaperone Sti1p (A) or Sba1p (B). The ATPase activity of Hsp82p^{K178C} and Hsp82p^{K178C}-Smt3p^{Cys} is shown in blue and red, respectively. The ATPase rates are shown as the percent of the maximal Aha1p-mediated stimulated rate of Hsp82p (1/min).

4.2.5 Co-chaperone interactions with SUMOylated Hsp82p^{K178C}

PTMs of Hsp90 can inhibit or enhance interactions with co-chaperone proteins (Mollapour and Neckers, 2012). In cells where SUMOylation of Lys178 is enhanced, more Aha1p is recovered in complex with Hsp82p while the amounts of the co-chaperones Sba1p and Sti1p remained the same (Mollapour et al., 2014). Conversely, Sba1p and Sti1p, were recovered in complex with Hsp82p^{K178R}, but Aha1p was not (Mollapour et al., 2014). To further characterize co-chaperone interactions, I performed IP assays with Myc-tagged co-chaperones in AMPPNP and ADP conditions, as different nucleotide conditions affect co-chaperone interactions with Hsp82p (Johnson et al., 2007). Also, differential binding of co-chaperones is linked to conformational changes in Hsp82p as it binds and hydrolyzes ATP (Pearl et al., 2008).

Although SUMOylated and non-SUMOylated Hsp82p associated with both Sti1p and Sba1p *in vivo* (Mollapour et al., 2014), my ATPase results suggested Sba1p binding may be affected (Figure 4.9B). I hypothesized a difference would be evident between the stable interactions of Sba1p with SUMOylated compared to non-SUMOylated Hsp82p^{K178C} *in vitro.* To assess co-chaperone interactions, equimolar Myc-tagged co-chaperones were incubated with either non-SUMOylated or SUMOylated Hsp82p^{K178C}. Interestingly, the same amount of Hsp82p^{K178C} co-immunoprecipitated with Myc-tagged Aha1p, Cpr6p, Hch1p, and Sti1p, regardless of the SUMOylation modification, in either AMPPNP and ADP conditions (Figure 4.10). Sba1p only bound to Hsp82p in AMPPNP conditions, as expected (Figure 4.10A). Moreover, all co-chaperones, except Hch1p, immunoprecipitated Hsp82p in a 1:1 ratio, as the bands of the co-chaperone are the same in intensity to the amount of Hsp82p recovered. Markedly low Hsp82p recovery is expected due to Hch1p binding with a lower affinity to Hsp82p compared to Aha1p (Figure 3.2) (Lotz et al., 2003; Panaretou et al., 2002).

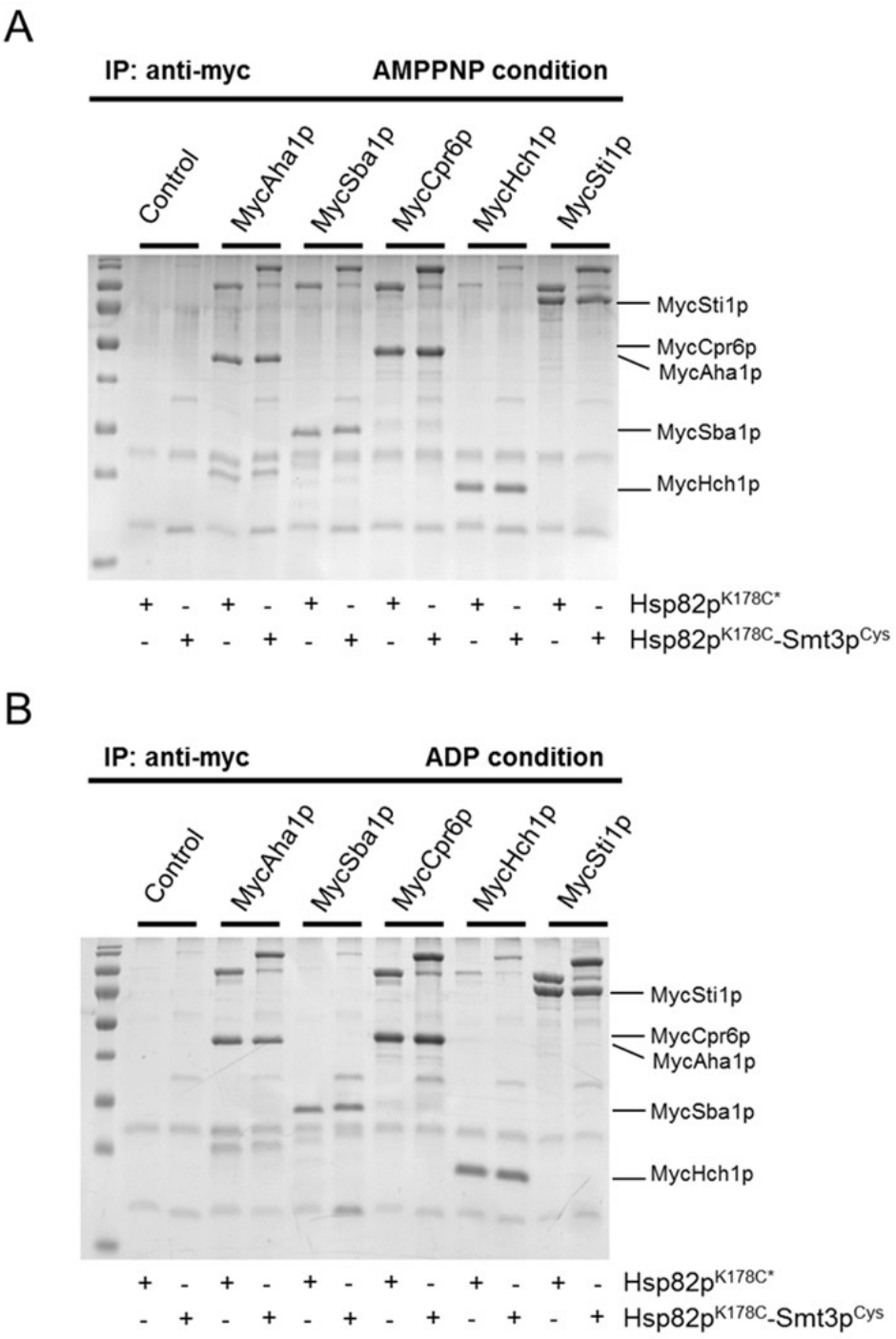
A
IP: anti-myc
AMPPNP condition
Control
MycAha1p
MycSba1p
MycCpr6p
MycHch1p
MycSti1p
MycSti1p
MycCpr6p
MycAha1p
MycSba1p
MycHch1p
+ - + - + - + - + - + - Hsp82p^K178C*
- + - + - + - + - + - + Hsp82p^K178C-Smt3p^Cys
B
IP: anti-myc
ADP condition
Control
MycAha1p
MycSba1p
MycCpr6p
MycHch1p
MycSti1p
MycSti1p
MycCpr6p
MycAha1p
MycSba1p
MycHch1p
+ - + - + - + - + - + - Hsp82p^K178C*
- + - + - + - + - + - + Hsp82p^K178C-Smt3p^Cys

Figure 4.10 Co-chaperones interact with non- and SUMOylated-Hsp82p^{K178C}. Myc-tagged Aha1p, Sba1p, Cpr6p, Hch1p, and Sti1p immunoprecipitated non- and SUMOylated Hsp82p^{K178C} to the same degree in both AMPPNP (**A**) and ADP (**B**) conditions. Control lanes show the amount of Hsp82p species sticking to the beads, indicating non-specific binding of SUMOylated Hsp82p^{K178C} to the beads in, specifically in (B). Reactions contained 5 µM of Myc-tagged co-chaperones and 5 µM Hsp82p^{K178C} or Hsp82p^{K178C}-Smt3p^{Cys}. 10 µL of Ultralink Protein G beads coupled to anti-Myc monoclonal antibodies were added to these 50 µL reactions and then incubated on a rotator at room temperature for 60 minutes. Beads were then pelleted, washed once in 250 µL of binding buffer, resuspended in 50 µL SDS sample buffer, and run on SDS-PAGE. Complexes were analyzed by CB staining.

4.2.6 SUMOylation of Hsp82p does not affect co-chaperone switching

Evident from the analysis of the ATPase assays, SUMOylation of Hsp82p^{K178C} resulted in an increased binding affinity for Aha1p and does not interfere with the interaction of known binding partners, except for Sba1p. Hsp82p cycle progression requires the sequential interaction of co-chaperones with Hsp82p. Co-chaperones interact dynamically with Hsp82p, forming binary and ternary complexes, to regulate the function of Hsp82p during the maturation of clients (Li and Buchner, 2013; Richter et al., 2003). I previously have reconstituted a robust Hsp82p ATPase cycle, *in vitro*, showing the concerted actions of Aha1p and Cpr6p overcome Sti1p inhibition of the ATPase activity of Hsp82p (Wolmarans et al., 2016). I used this assay to query how SUMOylation will affect this cycle. SUMOylation of Hsp82p at Lys178 appears to limit chaperone activity towards clients like the glucocorticoid hormone receptor (GR) and the difficult to fold client, cystic fibrosis transmembrane conductance regulator (CFTR) (Mollapour et al., 2014). This suggests that SUMOylation of Hsp82p accelerates the chaperone cycling, and thus, I hypothesized that under *in vitro* cycling conditions, SUMOylated Hsp82p^{K178C} will show a greater restoration of ATPase activity from the Sti1p inhibited rate in the presence of Aha1p and Cpr6p, compared to non-SUMOylate Hsp82p^{K178C}. A very small increase in the ATPase activity is evident in the restorative conditions with SUMOylated Hsp82p^{K178C} compared to non-SUMOylated Hsp82p^{K178C} (Figure 4.11A – lanes 5 and 10) (77.4 % compared to 74.1 %). Sti1p is a non-competitive inhibitor and in my assays, Sti1p was able to inhibit the Aha1p stimulated ATPase rates of SUMOylated Hsp82p^{K178C} fully (Figure 4.9A) (Richter et al., 2003). Thus, it not likely that the small increase in ATPase restoration is due to the increased affinity for Aha1p binding. I confirmed that Sti1p inhibited while Cpr6p stimulated the intrinsic ATPase activity of SUMOylated Hsp82p^{K178C} in the same manner that they regulated non-SUMOylated Hsp82p^{K178C} (Figure 4.11B). Interestingly, the additive effect of Aha1p and Cpr6p stimulation of SUMOylated Hsp82p^{K178C} is not observed (Figure 4.11A – lanes 4 and 9), even though Cpr6p had a stimulatory effect on the intrinsic ATPase rate (Figure 4.11B).

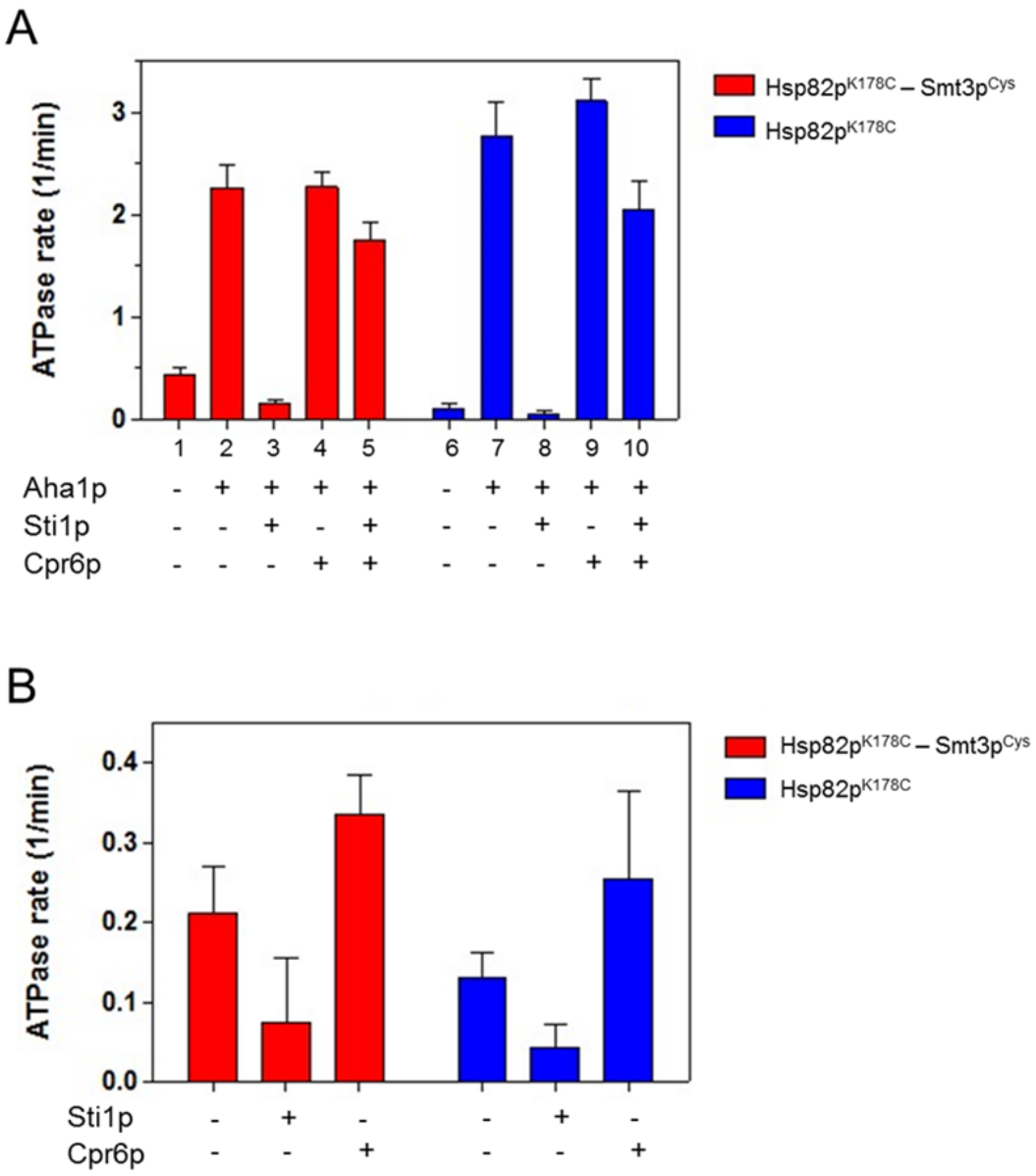
A
ATPase rate (1/min)
0
1
2
3
1 2 3 4 5 6 7 8 9 10
Aha1p - + + + + - + + + +
Sti1p - - + - + - - + - +
Cpr6p - - - + + - - - + +
Hsp82p^K178C – Smt3p^Cys
Hsp82p^K178C
B
ATPase rate (1/min)
0.0
0.1
0.2
0.3
0.4
Sti1p - + - - + -
Cpr6p - - + - - +
Hsp82p^K178C – Smt3p^Cys
Hsp82p^K178C

Figure 4.11 Cooperative displacement of Sti1p from SUMOylated and non-SUMOylated Hsp82p^{K178C} by Aha1p and Cpr6p. A. Effective displacement of Sti1p by Cpr6p and Aha1p results in a slightly higher restorative ATPase rate when Hsp82p^{K178C} is SUMOylated (Hsp82p^{K178C}-Smt3p^{Cys}). Reactions contained 1 μM Hsp82p^{K178C} or Hsp82p^{K178C}-Smt3p^{Cys} and 4 μM co-chaperones where indicated (Aha1p, Sti1p, and Cpr6p). **B.** Sti1p and Cpr6p regulate the ATPase activity of SUMOylated Hsp82p^{K178C} in a similar manner as non-SUMOylated Hsp82p^{K178C}. Reactions contained 1 μM Hsp82p^{K178C} or Hsp82p^{K178C}-Smt3p^{Cys} and 5 μM Sti1p or Cpr6p. The ATPase rates are shown as μM ATP hydrolyzed per minute per μM of Hsp82p (1/min). SUMOylated and non-SUMOylated Hsp82p^{K178C} is shown in red and blue, respectively.

4.2.7 SUMOylation does not increase drug sensitivity of Hsp82p to NVP-AUY922 *in vitro*

Mollapour *et al.* demonstrated that following SMT3 overexpression in cells expressing wildtype Hsp82p, the cells displayed greater sensitivity to Hsp90 inhibitors (Mollapour et al., 2014). Additionally, the binding of ATP-competitive drugs and association of Aha1 with Hsp90 is mutually exclusive, as drug binding prevents N-terminal dimerization and traps SUMOylated Hsp82p in an open conformation (Mollapour et al., 2014). Titration of NVP-AUY922 into SUMOylated and non-SUMOylated Hsp82p^{K178C} revealed that SUMOylation does not increase inhibition of ATPase activity by Hsp90 inhibitor drugs (Figure 4.12). One caveat of this experiment is that it is was not conducted with hemi-SUMOylated Hsp82p^{K178C}. I cannot rule out the possibility that asymmetrically SUMOylated Hsp82p^{K178C} is more susceptible to drug inhibition based on my findings reported here. From this data, SUMOylation of Hsp82p^{K178C} does not increase the affinity of Hsp90 inhibitor drug, NVP-AUY922.

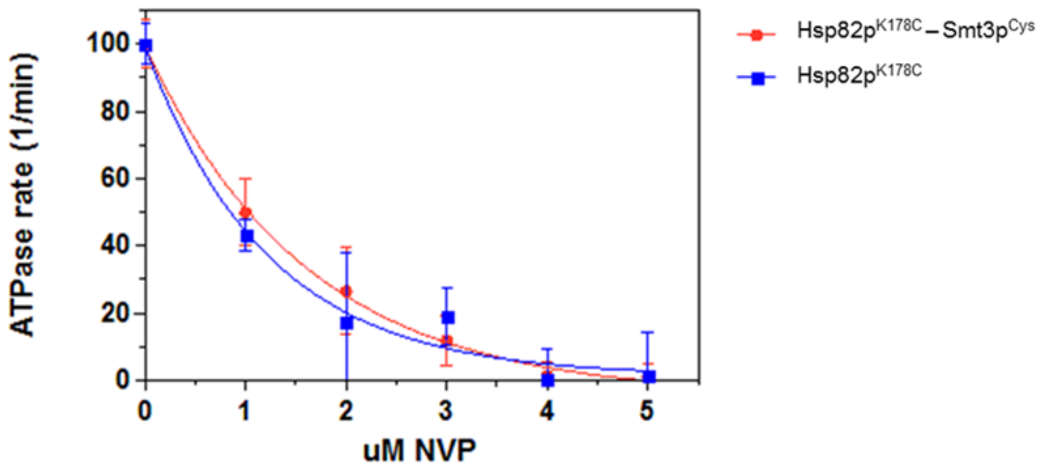

Figure 4.12 Inhibition of SUMOylated and non-SUMOylated Hsp82p^{K178C} ATPase activity with Hsp90 inhibitor drug NVP-AUY922. NVP-AUY922 was titrated into 2 µM Hsp82p^{K178C} or Hsp82p^{K178C}-Smt3p^{Cys}. The specific ATPase activity is shown as a percentage of the intrinsic rates (n=4).

4.3 Summary and model

Crosslinking methodologies developed to study proteins

Protein-protein interactions occur throughout the cell in numerous organelles and pathways. Characterization of protein-protein interactions *in vitro* provides valuable insight into how their association effects function, which is of growing importance to further our understanding of the role each protein has. Many of these interactions are transient in nature, and that is where crosslinkers have become useful tools in a variety of techniques and studies. Many different types of crosslinkers are available for use, which bind or attach to specific functional groups, making their use easy and specific. For example, crosslinkers have been used to study interactions by linking them to a purified "bait" proteins and identifying interacting "prey" proteins in lysates of cells (Chien et al., 1991; Fields and Song, 1989; Fields and Sternglanz, 1994; Rain et al., 2001; Uetz et al., 2000). They have also been used in structural studies to identify amino acids or to determine the number of subunits present in a protein (Sato et al., 1994). In detection procedures, crosslinker have been used to prepare antibody-enzyme conjugates (Brinkley, 1992; Porstmann and Kiessig, 1992) as probes for ELISA (Grunow et al., 1994) and western blotting protocols (Blaser et al., 1995).

PTMs have been shown to alter protein function. The effect of the phosphorylation status of a protein has been studied *in vitro* by expressing phosphomimetic and non-phosphomimetic versions of the protein (Thorsness and Koshland, 1987). Little is known about how SUMOylation alters a protein's interactions or modify its activity, as there is no easy way to study it *in* vitro (Flotho and Melchior, 2013; Nie and Boddy, 2015). This chapter outlines a novel crosslinking methodology to SUMOylate Hsp82p in a site-specific manner, which can be applied in other disciplines to dissect the effects of this PTMs *in vitro.*

Overview of results

The future of Hsp90 research lies in the detailed characterization of how PTMs alter Hsp90 chaperone dynamics. Therefore, it is crucial to gain insight into

the different dynamics of Hsp90, which can be achieved through *in vitro* studies. In this study, I outline the procedure to chemically SUMOylate Hsp82p. This strategy involves the covalent linking of the yeast SUMO, Smt3p, to Hsp82p^{K178C} using a homo-bifunctional maleimide crosslinker BMOE. I demonstrated that this SUMO modification does not interfere with dimerization or with ATP hydrolysis. My results reveal that Aha1p binds with higher affinity to SUMOylated Hsp82p^{K178C}, consistent with the finding that SUMOylated Hsp90 recruits Aha1 (Mollapour et al., 2014). My results also reveal that Sba1p regulation of the ATPase activity of SUMOylated Hsp82p^{K178C} is altered when stimulated by Aha1p.

SUMOylated Hsp82p^{K178C} has a higher intrinsic ATPase activity

SUMOylation of Hsp82p^{K178C} results in a 2-fold, statistically significant increase in the intrinsic ATPase rate *in vitro*. Many Hsp82p mutations that were either engineered or discovered through genetic screens, have been found to affect the ATPase activity of Hsp82p (Nathan and Lindquist, 1995). A mutation which increases the intrinsic ATPase rate, such as Hsp82p^{T22I}, has been shown to favor a closed conformational state (Hawle et al., 2006; Nathan and Lindquist, 1995; Vaughan et al., 2009). Thus, the increased ATPase rate of SUMOylated Hsp82p^{K178C} is consistent with the idea this modification may favor the closed conformation.

Chemical SUMOylation of Hsp82p^{K178C} recapitulates in vivo data

This study demonstrates that *in vitro* SUMOylation of Hsp82p^{K178C} recapitulates *in vivo* data. The apparent binding affinity of Aha1p for SUMOylated Hsp82p^{K178C} is higher than for non-modified Hsp82p^{K178C} (Figure 4.7), consistent with the findings that SUMOylated Hsp90 recruits Aha1 (Mollapour et al., 2014). Aha1p was still able to robustly stimulate SUMOylated Hsp82p^{K178C} in my ATPase assays, though a small decrease in the magnitude of stimulation by Aha1p compared to non-SUMOylated Hsp82p^{K178C} is observed. The significance of the magnitude of ATPase stimulation, however, is not fully understood.

Binding of co-chaperones to SUMOylated Hsp82p^{K178C} was assessed by showing Sti1p, Hch1p, Sba1p, and Cpr6p were recovered in complex with both SUMOylated and non-modified Hsp82p^{K178C}. This result is consistent with data presented by the Neckers group, who report SUMOylation was a prerequisite for Hsp82p recovery of Aha1p (Mollapour et al., 2014). They also reported that Aha1p is only recruited to asymmetrically SUMOylated Hsp82p. In my *in vitro* immunoprecipitation assays, however, there was no difference in the amount of Aha1p recovered between non-SUMOylated and SUMOylated Hsp82p^{K178C}. It is well known that non-modified Hsp82p can bind and be stimulated by Aha1p, thus, it is no surprise to see Aha1p coming down in complex with non-modified Hsp82p^{K178C}. Also, while binding of Aha1p to K178R (non-SUMOylatable Hsp82p) was not detected in their *in vivo* IPs, strong overexpression of Aha1p did result in Aha1p association with K178R (Mollapour et al., 2014). My *in vitro* results show that although the apparent binding affinity for Aha1p is increased, SUMOylation of Hsp82p^{K178C} does not increase the stable association of Aha1p to Hsp82p.

SUMOylation slightly enhances Aha1p-driven co-chaperone switching in vitro

The client activation cycle of Hsp90 involves the sequential recruitment and displacement of co-chaperones which is likely regulated by PTMs like SUMOylation. To examine whether SUMOylation would interfere with the cooperative displacement of Sti1p by Aha1p and Cpr6p, I tested Aha1p and Cpr6p for the ability to overcome Sti1p inhibition of ATPase activity of SUMOylated and non-SUMOylated Hsp82p^{K178C}. SUMOylation of Hsp82p^{K178C} slightly enhanced the restoration of ATPase activity by the cooperative action of Aha1p and Cpr6p in the presence of Sti1p. But because no significant difference is observed between SUMOylated and non-SUMOylated Hsp82p^{K178C} recovery ATPase rates, the data suggests that the role of SUMOylation is not at the level of regulating Sti1p displacement.

SUMO modification affects Sba1p regulation in vitro

Sba1p inhibition of the Aha1p stimulated ATPase rate, however, is affected for SUMOylated Hsp82p^{K178C}. For SUMOylated Hsp82p^{K178C}, when Sba1p is placed in direct competition with Aha1p *in vitro*, Sba1p inhibition of its ATPase activity is decreased. This could be explained by the increase in affinity that Aha1p has for SUMOylated Hsp82p^{K178C}, which diminishes the ability of Sba1p to compete for binding. It is important to note that, Hsp82p is in vast excess to the relative levels of co-chaperones *in vivo*, which is not the case in the *in vitro* conditions (Ghaemmaghami et al., 2003). Furthermore, *in vivo* immunoprecipitations demonstrate that Sba1p was in complex with both SUMOylated or non-SUMOylated Hsp82p (Mollapour et al., 2014). This may suggest that Sba1p and Aha1p associate with different Hsp82p pools *in vivo*, or that there may be additional modifications that influence the binding of these co-chaperones.

The fact remains that Sba1p inhibition is greatly diminished in the presence of Aha1p when Hsp82p^{K178C} is SUMOylated. In the functional ATPase cycle of Hsp82p, PTMs are known regulate co-chaperone interactions in order to facilitate proper maturation of client proteins. What my ATPase assays reveal is that SUMOylation results in the recruitment of Aha1p while it disfavors Sba1p binding. SUMOylation of Hsp82p may act to influence the kinetics of the Hsp82p ATPase cycle, which results in an accelerating past the Sba1p inhibited conformation. It is also possible that for Sba1p to bind to efficiently and to displace Aha1p, either Hsp82p must first be de-SUMOylated or only asymmetrically SUMOylated.

Hsp82p drug sensitivity

Mollapour *et al.* show that Hsp82p was more sensitive to ATP-competitive inhibitors when SUMOylated (Mollapour et al., 2014). My results, however, show that upon titration of Hsp90 inhibitor NVP-AUY922, both SUMOylated and non-SUMOylated Hsp82p^{K178C} was inhibited similarly. Because the affinity for the drug did not increase, as predicted from *in vivo* studies, perhaps SUMOylation affects the affinity for ATP. If SUMOylated Hsp82p^{K178C} has a decreased affinity for ATP,

it may be more sensitive to drug inhibition since ATP and the Hsp90 inhibitor drugs compete for binding to the N-terminal ATP-binding pocket. Testing whether the affinity for ATP (K_M) of SUMOylated Hsp82p^{K178C} is altered compared to non-SUMOylated Hsp82p^{K178C} will test this hypothesis, and I predict an increase in K_M will be observed for SUMOylated Hsp82p^{K178C}.

Co-chaperone regulation of asymmetrically SUMOylated Hsp82p ATPase activity

SUMOylation of Hsp82p *in vivo* was reported to occur on only one subunit of the Hsp82p dimer (Mollapour et al., 2014). This method outlining how to SUMOylate Hsp82p^{K178C} *in vitro,* produces dually-SUMOylated Hsp82p SUMOylated Hsp82p^{K178C} where both subunits are modified. I confirmed that the chemical coupling of Smt3p^{Cys} to Hsp82p^{K178C} does not interfere with subunit exchange, which means that the formation of heterodimers is possible, where the SUMO modification can be introduced to one subunit of the dimer. To further investigate the consequence of this asymmetric modification I will be able to generate heterodimers where each subunit is differentially modified/mutated. By mixing SUMOylated Hsp82p^{K178C} with other Hsp82p mutants such as V391E and D79N, will allow me to decipher to which subunit Aha1p binds – the SUMOylated Hsp82p subunit, or the non-modified subunit.

The role SUMOylation has on the functional ATPase cycle of Hsp82p

SUMOylation, in its physiological purpose, seem to have a role in recruiting Aha1p to Hsp82p – which was first published by the Neckers group and supported by my *in vitro* data (Figure 4.7) (Mollapour et al., 2014). My analysis of how the ATPase activity of SUMOylated Hsp82p^{K178C} is regulated by co-chaperones reveal that the SUMO modification does not interfere with Sti1p displacement (Figure 4.11B), but did interfere with Sba1p inhibition (Figure 4.9B). Taking all the data together, my results suggests that SUMOylation may have a significant role in influencing the kinetics of the ATPase cycle as cycling of late-acting co-chaperone (Sba1p), but not of early-acting co-chaperone (Sti1p), is altered (Figure 4.13). If SUMOylation specifically alters the kinetics of the Aha1p-bound to Sba1p-bound

transition, then the ATPase cycle is presumably accelerated past the Sba1p-bound conformation, which I can speculate may lead to immature client protein release.

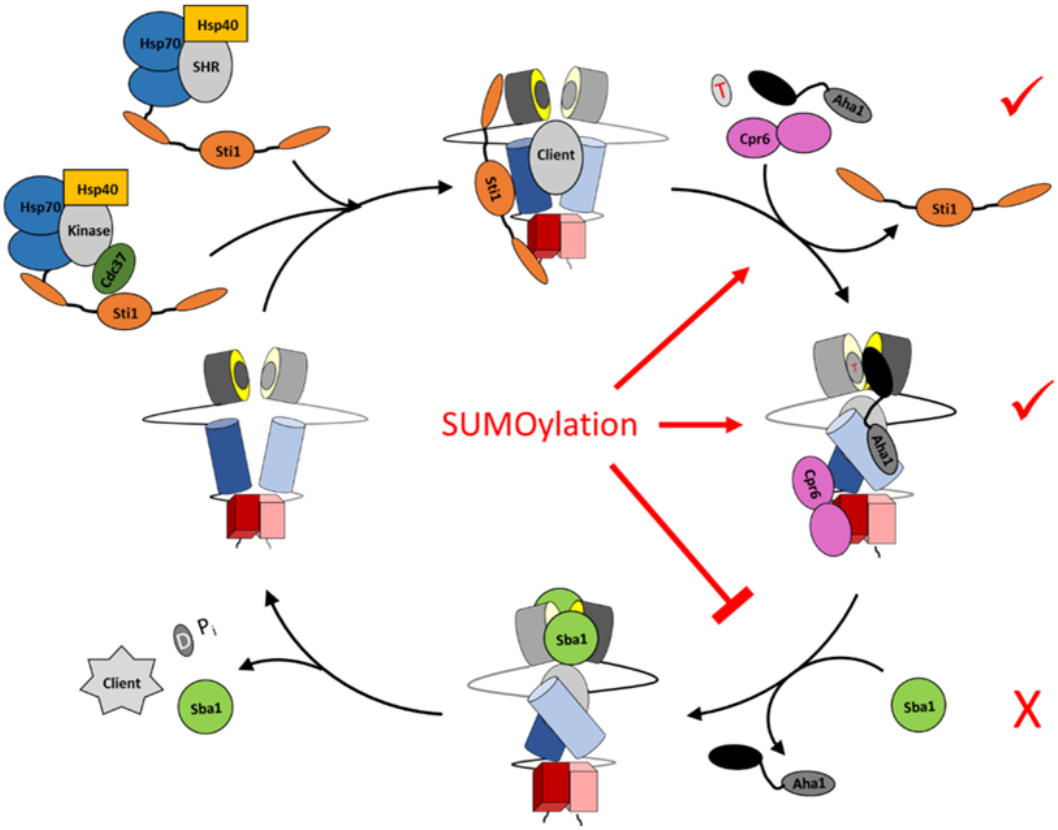

Figure 4.13 A model of the role SUMOylation has on the ATPase cycle of Hsp82p. SUMOylation at Lys178 does not interfere with Sti1p displacement but results in Aha1p recruitment, which disfavors the Sba1p-bound conformation and presumably lead to an acceleration of the functional Hsp82p ATPase cycle.

Chapter 5

Analysis of the linker region of Hsp90: How it influences conformational dynamics and co-chaperone regulation

5.1 Introduction

Hsp90 is a highly flexible protein that can undergo global conformational rearrangements during its functional cycle (Shiau et al., 2006). These rearrangements result in numerous intermediate conformations which are associated with ATP hydrolysis and client activation (Richter et al., 2008; Shiau et al., 2006; Vaughan et al., 2009). The N-terminal and middle domains in each Hsp82p subunit are separated by a long, charged linker which tethers these domains together and presumably provides the conformational flexibility required for adopting the ATPase competent state (Tsutsumi et al., 2012). The inherent flexibility of Hsp82p has made structural studies of the full-length chaperone extremely difficult.

The linker of Hsp82p is considered to be residues 211-272 according to structural data and sequence analysis (Ali et al., 2006; Hainzl et al., 2009). Initial analysis of the amino acid sequence shows the linker has a low sequence complexity and largely takes on a coiled-coil conformation based on secondary structure prediction software (Hainzl et al., 2009). Since then, multiple groups have analyzed the significance of the length and composition of the charged linker on yeast cell viability and Hsp82p chaperoning function (Hainzl et al., 2009; Scheibel et al., 1999; Tsutsumi et al., 2012; Wayne and Bolon, 2010). It was previously demonstrated that a region of the linker (residues 211-259) is dispensable, while truncations past residue 259 affected client maturation and/or viability (Hainzl et al., 2009; Louvion et al., 1996). Yeast expressing Hsp82p with progressive linker truncations (Δ211-266 and Δ211-272) are not viable (Hainzl et al., 2009). FRET analysis demonstrated that these Hsp82p linker truncations could not undergo N-terminal dimerization, thereby preventing ATP hydrolysis (Hainzl et al., 2009). The biological activity of Hsp90 can be maintained when the native linker is replaced by small uncharged linkers (Gly-Ser stretches), which implies that the length of the linker, and not the composition, is important (Hainzl et al., 2009).

Hsp82p is a split ATPase, where the catalytic residues from different domains must come together for ATP hydrolysis to occur. Specifically, Arg380, in

the catalytic loop of the middle domain, contacts the γ phosphate of ATP in the nucleotide binding pocket in the N-terminal domain and has been implicated in stabilizing the closed state (Cunningham et al., 2012; Mishra and Bolon, 2014). Although the structure of the ATP hydrolysis-competent state has not been solved, an inhibited conformation of Hsp82p has been resolved in complex with Sba1p, which has provided some insight in the role of the linker (Ali et al., 2006). It is important to note that this Hsp82p structure lacks linker residues 214-261, which means that the N-terminal and middle domains are held close together by the remaining linker sequence (residues 262-272), presumably limiting conformational dynamics and favoring crystallization (Ali et al., 2006). There is no clear understanding of how the N-terminal domains are brought into contact with their respective middle domain, so that the catalytic residues can facilitate ATP hydrolysis, when the entire linker is present.

Theoretically, by shortening the distance between the N-terminal and the middle domains of Hsp82p, N-M communication is more favorable, as they are in closer proximity with each other. It is, therefore, also conceivable that this will enhance ATPase activity because it brings the Arg380 residue in the middle domain into proximity to ATP in the N-terminal domain. However, this is not the case as the linker truncation mutant, Hsp82p$^{\Delta 211\text{-}263}$, has a reduced ATPase rate, which is not due to decreased N-terminal dimerization or affinity for ATP (Hainzl et al., 2009). Previous studies have also investigated how co-chaperone regulation is affected when the linker region of Hsp82p is deleted. Analytical ultracentrifugation (AUC) experiments indicate that Hsp82p linker truncations that do not support viability in yeast (Hsp82p$^{\Delta 211\text{-}266}$ and Hsp82p$^{\Delta 211\text{-}272}$) were unable to bind Sba1p, or be stimulated by Aha1p, while inhibition by Sti1p was retained (Hainzl et al., 2009). In this chapter, I investigate the significance of shortening the distance between the N-M domains of Hsp82p by analyzing how co-chaperone regulation is altered.

5.2 Results

5.2.1 Truncation of the N-M linker decreases ATPase activity

The charged linker region of yeast Hsp90 (amino acids 211-272) is 62 amino acids long and contains 18 positively charged and 28 negatively charged amino acids (Figure 5.1A). I began this project by constructing the linker deletion construct Hsp82p$^{\Delta 211\text{-}263}$, where 53 amino acids were deleted (Figure 5.1A). This linker mutant supports cell viability but has reduced chaperone activity *in vivo* (Hainzl et al., 2009). I confirmed the intrinsic ATPase rate of Hsp82p$^{\Delta 211\text{-}263}$ to be approximately 2-fold lower than wildtype Hsp82p (Hsp82p^{WT}), similar to previous observations (Hainzl et al., 2009) (Figure 5.1B). The reason for the decreased ATPase activity is not understood as the affinity for ATP (K_M) and N-terminal dimerization is similar to the wildtype protein according to FRET analysis (Hainzl et al., 2009). This suggests that besides N-terminal dimerization, another rearrangement within the N-terminally dimerized state is necessary for wildtype ATPase activity.

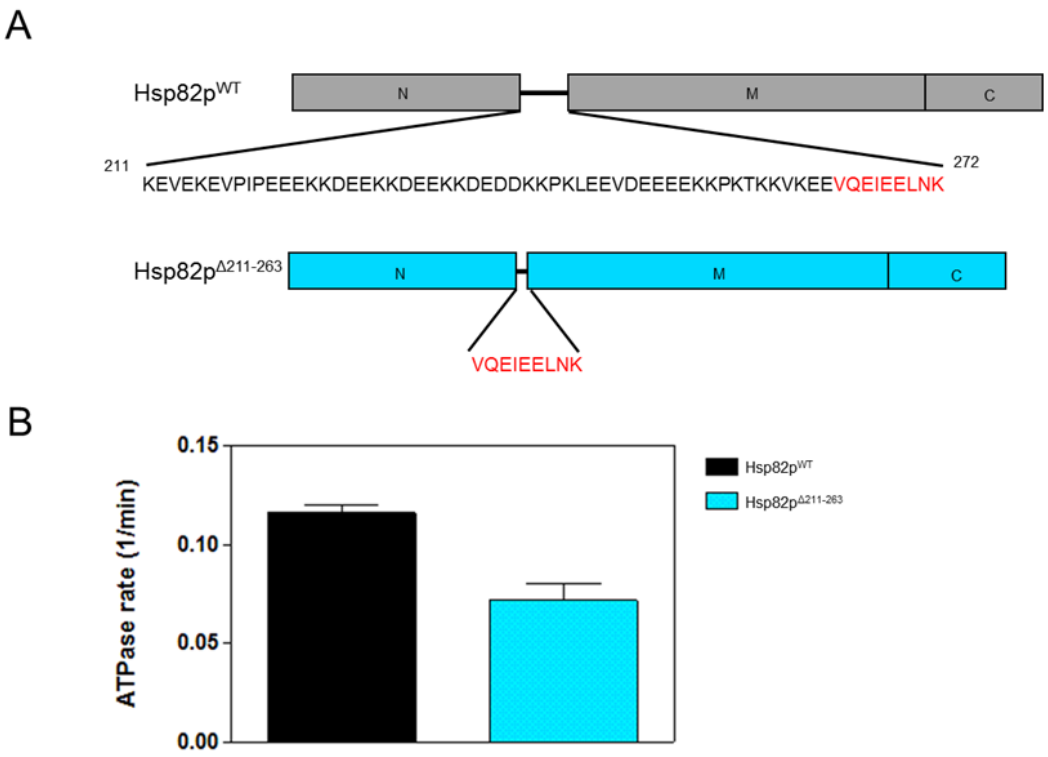

Figure 5.1 Structure and intrinsic ATPase rate of wildtype Hsp82p and Hsp82p$^{\Delta 211-263}$ A. Schematic representation of the domain structure of wildtype (Hsp82p^{WT} – grey) and linker deletion mutant (Hsp82p$^{\Delta 211-263}$- cyan) of yeast Hsp82p. The full linker sequence is written below Hsp82p^{WT}. The sequence in red indicates the remaining linker sequence which is required to support viability *in vivo.* **B.** Intrinsic rate of Hsp82p^{WT} and Hsp82p$^{\Delta 211-263}$. Each reaction contained 2 µM Hsp82p^{WT} (black) or Hsp82p$^{\Delta 211-263}$ (cyan). ATPase rates are shown as µM ATP hydrolyzed per minute per µM of Hsp82p (1/min). This ATPase assay was conducted in triplicate and error bars indicate standard deviation.

5.2.2 N-M linker required for optimal Aha1p and Sba1p regulation

Investigating how co-chaperone regulation is affected with Hsp82p$^{\Delta 211\text{-}263}$ allows us to further scrutinize the function of the linker region. Because the deletion of the linker segment in Hsp82p results in lower ATPase activity, I hypothesized that this is due to Hsp82p adopting a different, less active, dimerized conformation which will affect subsequent co-chaperone regulation.

Hainzl *et al.* reported the catalytic activity (K_{CAT}) for Hsp82p$^{\Delta 211\text{-}266}$ to be 0.2 min^{-1}, which is lower than the K_{CAT} of Hsp82p$^{\Delta 211\text{-}263}$, which was reported to be 0.3 min^{-1} (Hainzl et al., 2009). Interestingly, while both linker truncations could bind Aha1p, Hsp82p$^{\Delta 211\text{-}263}$, but not Hsp82p$^{\Delta 211\text{-}266}$, could be stimulated by Aha1p (Hainzl et al., 2009). This suggests that the linker region past residue 263 is required for the acquisition of the ATPase competent conformation in Hsp82p which is driven by Aha1p binding (Hainzl et al., 2009). Interestingly, the intrinsic and Aha1p stimulated rates of Hsp82p$^{\Delta 211\text{-}263}$ is approximately 50 % of the intrinsic and stimulated rates of Hsp82p^{WT} (Hainzl et al., 2009). Upon titration of Aha1p into Hsp82p^{WT} and Hsp82p$^{\Delta 211\text{-}263}$, I obtained similar results as Aha1p could stimulate Hsp82p$^{\Delta 211\text{-}263}$ to 75 % of the stimulated ATPase rate of Hsp82p^{WT} (Figure 5.2A). While a decrease in the overall velocity of the reaction (V_{MAX}) was evident, the apparent binding affinity for Aha1p increased, as the K_{APP} changed from 1.19 ± 0.07 μM to 0.49 ± 0.15 μM (Figure 5.2A). The higher binding affinity of Aha1p for Hsp82p$^{\Delta 211\text{-}263}$ indicates that Aha1p prefers binding to a constrained conformation where the N-terminal and middle domains of Hsp82p are in close proximity, although this conformation of Hsp82p appears to be less catalytically active.

Co-chaperones Sti1p and Sba1p inhibit the ATPase activity of Hsp82p by different mechanisms and during different stages of the Hsp82p functional cycle through binding and/or inducing specific conformations (Richter et al., 2003; Richter et al., 2004). If the inhibition of ATPase activity by either of these co-chaperones is affected, then I can infer that the linker has a role in acquiring or inducing a certain conformation. Sba1p acts as a conformational sensor, as it exclusively binds to a closed, ATP-bound conformation (McLaughlin et al., 2006;

Richter et al., 2004). Sba1p binds to the dimerized N-terminal domains of Hsp82p, which is a similar binding interface that Aha1p^{C} binds, and inhibits the steady state ATPase activity of Hsp82p by primarily preventing nucleotide release (Ali et al., 2006; Graf et al., 2014; Koulov et al., 2010; Li and Buchner, 2013; Retzlaff et al., 2010). In a previous study, Sba1p was shown to have about half the affinity for Hsp82p$^{\Delta 211\text{-}263}$ compared to Hsp82p^{WT}, but its regulation of Hsp82p activity was not addressed (Hainzl et al., 2009). If the lack of linker limits the twisted, closed conformation from forming, then the binding of Sba1p will be affected, and thus, Sba1p's ability to inhibit the ATPase activity of Hsp82p may be compromised as well. Surprisingly, Sba1p was better at inhibiting the Aha1p stimulated rate of Hsp82p$^{\Delta 211\text{-}263}$ than wildtype Hsp82p, indicating that Sba1p binding is not affected as previously reported, or at least not when Aha1p is present (Figure 5.2B). This indicates that the closed, ATP-bound conformation is able to form and that Sba1p has a higher apparent binding affinity for the Aha1p-Hsp82p$^{\Delta 211\text{-}263}$ complex than the Aha1p-Hsp82p^{WT} complex. This suggest that the constrained Hsp82p conformation where the N-M are closer in proximity, is also a conformation Sba1p binds more readily.

Sti1p is a potent, non-competitive inhibitor of the ATPase activity of Hsp82p which can reduce the intrinsic and Aha1p stimulated rate (Richter et al., 2003). Aha1p binding occurs after Sti1p association with Hsp82p in the functional ATPase cycle of Hsp82p, as these two co-chaperones form different complexes and do not co-immunoprecipitate together (Li et al., 2011). Previous reports have shown that the ATPase activity of Hsp82p$^{\Delta 211\text{-}263}$ can be inhibited by Sti1p, and thus, I hypothesized that the mechanism of Sti1p inhibition will not be altered in the presence of Aha1p, even though Aha1p has a higher binding affinity for Hsp82p$^{\Delta 211\text{-}263}$ (Figure 5.2A). Consistent with this hypothesis, Sti1p was able to inhibit the stimulated ATPase rate of Hsp82p$^{\Delta 211\text{-}263}$ completely, displacing Aha1p entirely as no ATPase activity was evident (Figure 5.2C). There was no difference between Sti1p inhibition of stimulated Hsp82p^{WT} and Hsp82p$^{\Delta 211\text{-}263}$.

Hsp82p can form a ternary complex with Cpr6p and Sti1p, and also with Cpr6p and Aha1p (Li and Buchner, 2013; Li et al., 2011). Thus, in the functional

cycle of Hsp82p, Cpr6p association occurs after Sti1p, but before Aha1p binding. Addition of Cpr6p to Aha1p-containing reactions results in additional ATPase stimulation of Hsp82p (Li et al., 2013). With Sti1p inhibition not being altered in any of the linker truncation mutants, I do not expect ATPase regulation by other TPR domain containing co-chaperones to be altered and thus hypothesized that Cpr6p regulation of Hsp82p$^{\Delta 211\text{-}263}$ will not be affected. Aha1p cooperatively binds with Cpr6p-bound Hsp82p complexes, and thus Cpr6p and Aha1p resulted in a higher stimulated rate, as expected (Figure 5.2D – 0 μM Sti1p). Upon Sti1p titration into the Hsp82p-Cpr6p-Aha1p complexes, it is evident that the presence of Cpr6p greatly diminishes the potency of Sti1p inhibition of the stimulated rate compared to Figure 5.2C (Figure 5.2D). Consistent with my hypothesis, however, Sti1p was able to inhibit the Cpr6p/Aha1p-mediated stimulation of both Hsp82p^{WT} and Hsp82p$^{\Delta 211\text{-}263}$ to the same degree at higher concentrations of Sti1p. It is interesting that with the Hsp82p linker deletion, the rate at which Sti1p inhibited the Cpr6p-Aha1p stimulated rate decreased. Because Sti1p inhibited the Aha1p stimulated rate of Hsp82p$^{\Delta 211\text{-}263}$ and Hsp82p^{WT} similarly (Figure 5.2C), the decrease in inhibition by Sti1p cannot be explained by the higher apparent binding affinity of Aha1p to Hsp82p$^{\Delta 211\text{-}263}$. Instead, this could suggest that the conformation that Hsp82p$^{\Delta 211\text{-}263}$ acquires when Cpr6p and Aha1p bind is a complex that disfavors Sti1p inhibition, as Hsp82p-Cpr6p-Aha1p complexes have increased stability when the linker is deleted. This result also suggests that Cpr6p preferentially bind to a compact Hsp82p where the N-M domains are in close proximity to each other. This could be confirmed by conducting a titration of Cpr6p alone into Hsp82p$^{\Delta 211\text{-}263}$ and Hsp82p^{WT} to reveal the higher apparent binding affinity of Cpr6p to a compact Hsp82p conformation.

Overall, it appears that the linker deletion in Hsp82p affected Aha1p, Sba1p, and Cpr6p regulation of Hsp82p's ATPase activity in a way that increases their association with Hsp82p. These data indicate that the linker region of Hsp82p is likely required for rearrangements in the N-terminal domains to the closed dimerized conformation, that are associated with optimum ATP hydrolysis.

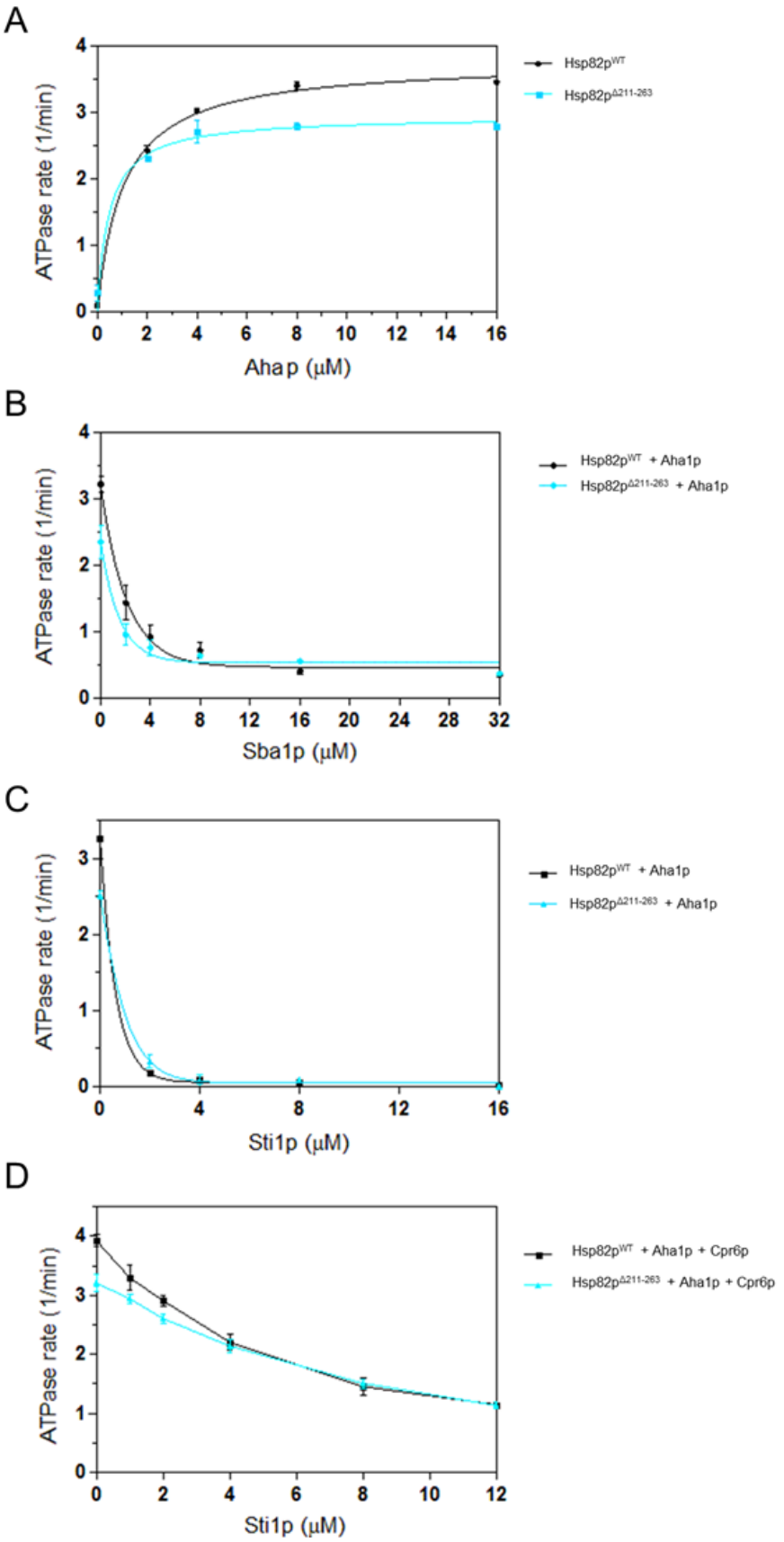
A
ATPase rate (1/min)
Aha p (μM)
Hsp82p^WT
Hsp82p^Δ211-263
B
ATPase rate (1/min)
Sba1p (μM)
Hsp82p^WT + Aha1p
Hsp82p^Δ211-263 + Aha1p
C
ATPase rate (1/min)
Sti1p (μM)
Hsp82p^WT + Aha1p
Hsp82p^Δ211-263 + Aha1p
D
ATPase rate (1/min)
Sti1p (μM)
Hsp82p^WT + Aha1p + Cpr6p
Hsp82p^Δ211-263 + Aha1p + Cpr6p

Figure 5.2 Aha1p, Sba1p, Cpr6p, and Sti1p regulation of the ATPase activity of Hsp82p$^{\Delta 211\text{-}263}$. A. Aha1p-mediated stimulation of wildtype Hsp82p and Hsp82p$^{\Delta 211\text{-}263}$. Reactions contained 2 μM Hsp82p variant with the indicated concentration of Aha1p. **B.** Sba1p inhibition of Aha1p stimulated Hsp82p^{WT} and Hsp82p$^{\Delta 211\text{-}263}$. Reactions contained 2 μM of Hsp82p variants, 4 μM Aha1p^{WT} and the indicated concentration of Sba1p. **C.** Sti1p inhibition of Aha1p stimulated Hsp82p^{WT} and Hsp82p$^{\Delta 211\text{-}263}$. Reactions contained 1 μM of Hsp82p variants, 4 μM Aha1p^{WT}, and the indicated concentration of Sti1p. **D.** Sti1p inhibition of Aha1p- and Cpr6p-mediated stimulated Hsp82p^{WT} and Hsp82p$^{\Delta 211\text{-}263}$. Reactions contained 1 μM of Hsp82p variants, 4 μM Aha1p^{WT}, 4 μM Cpr6p, and the indicated concentration of Sti1p. ATPase rates are shown in μM ATP hydrolyzed per minute per μM of enzyme (1/min). ATPase activity of Hsp82p^{WT} is shown in black and Hsp82p$^{\Delta 211\text{-}263}$ is shown in cyan.

5.2.3 Shortening the linker between the Aha1p N and C domain enhanced affinity for Hsp82p but diminishes stimulated ATPase rate

Aha1p plays an important role in mediating conformational changes in Hsp82p that are required for ATP hydrolysis (Hessling et al., 2009). In the previous sections, my results show that Aha1p preferentially bind to a constrained conformation when the N-M domains of Hsp82p are in close proximity to each other, as the binding affinity for Aha1p increased with Hsp82p$^{\Delta 211\text{-}263}$. This may indicate that Aha1p may also adopt a more compact conformation when it is bound to the N-terminal and middle domains which are closer together.

Structurally, Aha1p is a two-domain protein where the N-terminal domain is joined to the C-terminal domains by a 40-amino acid linker (Koulov et al., 2010; Lotz et al., 2003; Meyer et al., 2004a). For full-stimulation, Aha1p^{N} must bind the middle domain and Aha1p^{C} must interact with the N-terminally dimerized interface of Hsp82p (Koulov et al., 2010; Retzlaff et al., 2010; Wolmarans et al., 2016). To further investigate the Hsp82p conformation to which Aha1p binds and to assess whether Aha1p binds to more constrained Hsp82p conformation, I constructed three Aha1p linker truncation variants. I hypothesized that Aha1p linker truncations will have a higher binding affinity than wildtype Aha1p, as binding of these Aha1p linker variants will mimic the compact conformation as it induces the N-M constrained conformation in Hsp82p upon binding.

I constructed and purified three Aha1p linker truncation variants, either deleting the first half (Aha1p$^{\Delta 156\text{-}181}$), second half (Aha1p$^{\Delta 182\text{-}206}$), or the entire linker (Aha1p$^{\Delta 156\text{-}206}$) (Figure 5.3A). The primary binding site for Aha1p on Hsp82p is the middle domain, which promotes N-terminal domain rearrangement (Meyer et al., 2004a; Retzlaff et al., 2010; Wolmarans et al., 2016). Aha1p^{N} interaction with the middle domain should not be affected by shortening the linker of Aha1p, and thus, the resulting stimulated ATPase activity rate will reflect the role of the linker and the C-terminus of Aha1p as well as the conformation Aha1p binding induces in Hsp82p. I hypothesized that Aha1p with a shorter linker will result in an increase in binding affinity, while decreasing the Aha1p stimulated ATPase rate of Hsp82p. Titration of the Aha1p linker variants revealed that both Aha1p$^{\Delta 156\text{-}181}$ and

Aha1p$^{\Delta 182\text{-}206}$ stimulated wildtype Hsp82p ATPase activity to ~80 % of the maximal stimulated rate by wildtype Aha1p while Aha1p$^{\Delta 156\text{-}206}$ showed a more pronounced defect in stimulating Hsp82p^{WT}, resulting in only ~55 % of the maximal stimulated rate by wildtype Aha1p (Figure 5.3B). Consistent with my hypothesis, the apparent binding affinity of the Aha1p linker truncation variants increased 2-fold for Hsp82p compared to the binding affinity of wildtype Aha1p to Hsp82p (Figure 5.3C). Because the binding affinity is similar between all three Aha1p linker truncation variants, but the stimulated ATPase rate of Hsp82p is further decreased when the linker of Aha1p is completely removed (Aha1p$^{\Delta 156\text{-}206}$), suggests that the action of the C-terminal domain of Aha1p$^{\Delta 156\text{-}206}$ is not effective in this conformation.

Furthermore, when Aha1p linker truncation variants were titrated into Hsp82p$^{\Delta 211\text{-}263}$, a compounding effect was observed. By shortening the linkers of both Aha1p and Hsp82p, the magnitude of the stimulated ATPase rates decreased further (Figure 5.3D), while the apparent binding affinity increased (Figure 5.3E). These experiments will have to be repeated to capture the K_{APP} more accurately as maximal stimulation is nearly reached at the first Aha1p concentration used. Increasing the data points, specifically between 0 μM and 4 μM Aha1p, will allow for a stronger conclusion to be made regarding the apparent affinity Aha1p linker truncation variants have for Hsp82p$^{\Delta 211\text{-}263}$.

Overall, when the N-M linker of Hsp82p or the linker of Aha1p was shortened, the affinity between Aha1p and Hsp82p was enhanced while the maximum velocity (V_{MAX}) of the reaction decreased. The decrease in the Aha1p-mediated stimulated rates (V_{MAX}) may be the result of a decrease in the affinity for ATP (K_M), or a change in the rate of catalysis (K_{CAT}) of Hsp82p^{WT} and Hsp82p$^{\Delta 211\text{-}263}$ when bound to Aha1p. From these data, I could conclude that the conformation which Aha1p has the highest affinity may not the most catalytically active one, but without calculating the K_M, I cannot substantiate such a conclusion. By establishing the apparent affinity for ATP (K_M) of Hsp82p^{WT} and Hsp82p$^{\Delta 211\text{-}263}$, with and without the Aha1p linker truncation variants, will allow me to calculate the K_{CAT}

to determine whether the mechanism of stimulation by Aha1p is altered when the linker is absent.

A

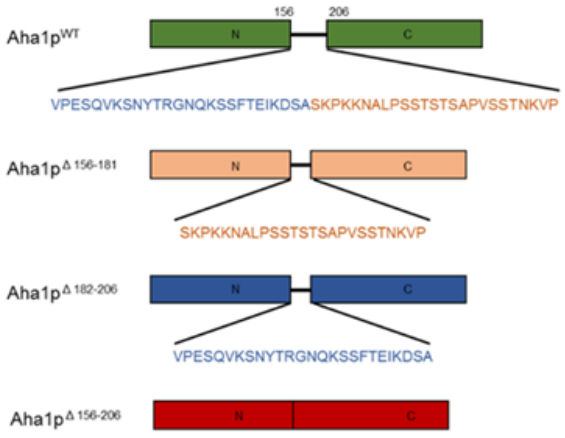

B

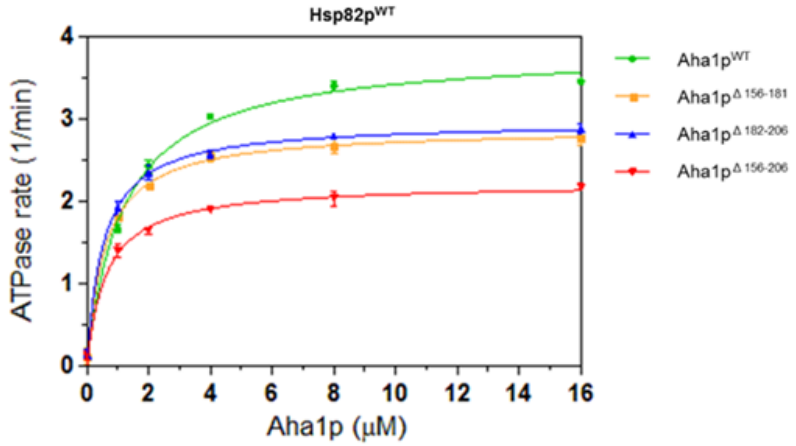

C

	Aha1p^{WT}	Aha1p$^{\Delta 156-181}$	Aha1p$^{\Delta 182-206}$	Aha1p$^{\Delta 156-206}$
V_{MAX}	3.83 ± 0.06	2.88 ± 0.04	2.97 ± 0.04	2.22 ± 0.05
K_{APP}	1.19 ± 0.07	0.60 ± 0.05	0.54 ± 0.05	0.63 ± 0.07

D

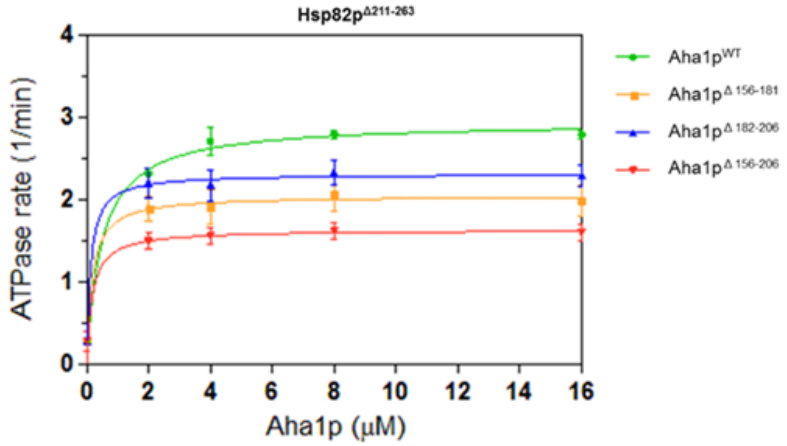

E

	Aha1p^{WT}	Aha1p$^{\Delta 156-181}$	Aha1p$^{\Delta 182-206}$	Aha1p$^{\Delta 156-206}$
V_{MAX}	2.94 ± 0.10	2.05 ± 0.11	2.32 ± 0.10	1.63 ± 0.08
K_{APP}	0.49 ± 0.15	0.18 ± 0.21	0.12 ± 0.16	0.18 ± 0.20

Figure 5.3 ATPase stimulation by Aha1p linker truncation variants. **A**. Schematic representation of the domain structure of wildtype and linker deletion mutant(s) of Aha1p**. B, D.** Aha1p stimulation of Hsp82p^{WT} (B) and Hsp82p$^{\Delta 211\text{-}263}$ (D) by wildtype Aha1p and Aha1p linker truncation variants. Each reaction contained 2 μM Hsp82p^{WT} or Hsp82p$^{\Delta 211\text{-}263}$ and indicated concentration of Aha1p^{WT} (green) or Aha1p linker truncation variants (Aha1p$^{\Delta 156\text{-}181}$ in orange, Aha1p$^{\Delta 182\text{-}206}$ in blue, and Aha1p$^{\Delta 156\text{-}206}$ in red). ATPase rate shown in μM ATP hydrolyzed per minute per μM of enzyme (1/min). This ATPase assay was conducted in triplicate. **C, E.** The V_{MAX} and apparent binding affinities (K_{APP}) of Aha1p for Hsp82p^{WT} (B) and Hsp82p$^{\Delta 211\text{-}263}$ (D), respectively, were calculated using Prism GraphPad.

5.2.4 Sba1p binds to a constrained Hsp82p conformation

Using the Aha1p linker truncations and measuring their effects on the ATPase activity of Hsp82p, structural insight into how Aha1p, and other co-chaperones, regulate Hsp82p can be inferred. Figure 5.2 show that Sba1p inhibits more effectively when Hsp82p is in a constrained conformation ($Hsp82p^{\Delta 211\text{-}263}$). I hypothesized that the addition of Aha1p linker truncation variants to wildtype Hsp82p will induce, and mimic, the constrained conformation. Therefore, I predict to see Sba1p also more effectively inhibit Hsp82p when stimulated by the Aha1p linker truncation variants. Consistent with my hypothesis, upon Sba1p titration, Sba1p is better able to inhibit the ATPase activity of Hsp82p when stimulated by the Aha1p variants (Figure 5.4A). More specifically, the shorter the Aha1p linker, the more easily Sba1p was able to inhibit the stimulated rate.

Sba1p is thought to prevent the release of ADP after ATP hydrolysis, and thus, it does not interfere with the rate of catalysis itself (Graf et al., 2014). Because Sba1p is more effective in inhibiting the ATPase activity in these experiments when stimulated by the Aha1p linker variants, it suggests that Sba1p prolongs the lifetime of the closed, or constrained, conformation to a greater extent than the non-constrained (wildtype) conformation. Sba1p prefers binding to this constrained conformation, suggesting that the linker is involved in acquiring another conformation that results in release of product. Once ATP hydrolysis occurs, this second, post-hydrolysis conformation is required for product release, but is less accessible because of the conformation the Aha1p linker deletions induce in Hsp82p (Figure 5.4A) or the conformation Hsp82p linker deletion acquires (Figure 5.2B).

Knowing that Sti1p is a non-competitive inhibitor and that it inhibits the Aha1p stimulated ATPase activity of both wildtype and $Hsp82p^{\Delta 211\text{-}263}$ in a similar fashion, I hypothesized Sti1p will be able to inhibit the stimulated ATPase activity of wildtype Hsp82p regardless of which Aha1p linker variant is used for stimulation. Upon titration of Sti1p, it appears as though Sti1p was slightly less effective in inhibiting the ATPase rate of Hsp82p when stimulated by the linker variants compared to wildtype Aha1p (Figure 5.4B). This slight difference is most

likely due to the increased binding affinity these Aha1p linker variants have for Hsp82p (Figure 5.3C). Intriguingly, this is evidenced by the curves shifting to the right in Figure 5.4B. To completely inhibit the ATPase rate of Hsp82p when stimulated by Aha1p$^{\Delta 182\text{-}206}$, which had the highest apparent binding affinity for Hsp82p, required the most Sti1p (8 μM) (Figure 5.4B - blue). Conversely, Aha1p^{WT}, which had the lowest apparent binding affinity for Hsp82p, only required 2 μM Sti1p to reach the intrinsic ATPase rate of Hsp82p (Figure 5.4B).

These data indicate that the linker truncations of Hsp82p and Aha1p induces a constrained conformation that Sba1p binds preferentially. This constrained conformation may be a twisted conformation, as Sba1p was crystalized bound to a twisted, closed conformation of Hsp82p (Ali et al., 2006). My results show that Aha1p preferentially bind a constrained Hsp82p conformation, indicated by the higher apparent binding affinity (Figure 5.2 – Figure 5.3). Thus, it stands to reason, that Aha1p binding to a constrained conformation most likely induces a twisted conformation in Hsp82p that Sba1p optimally binds.

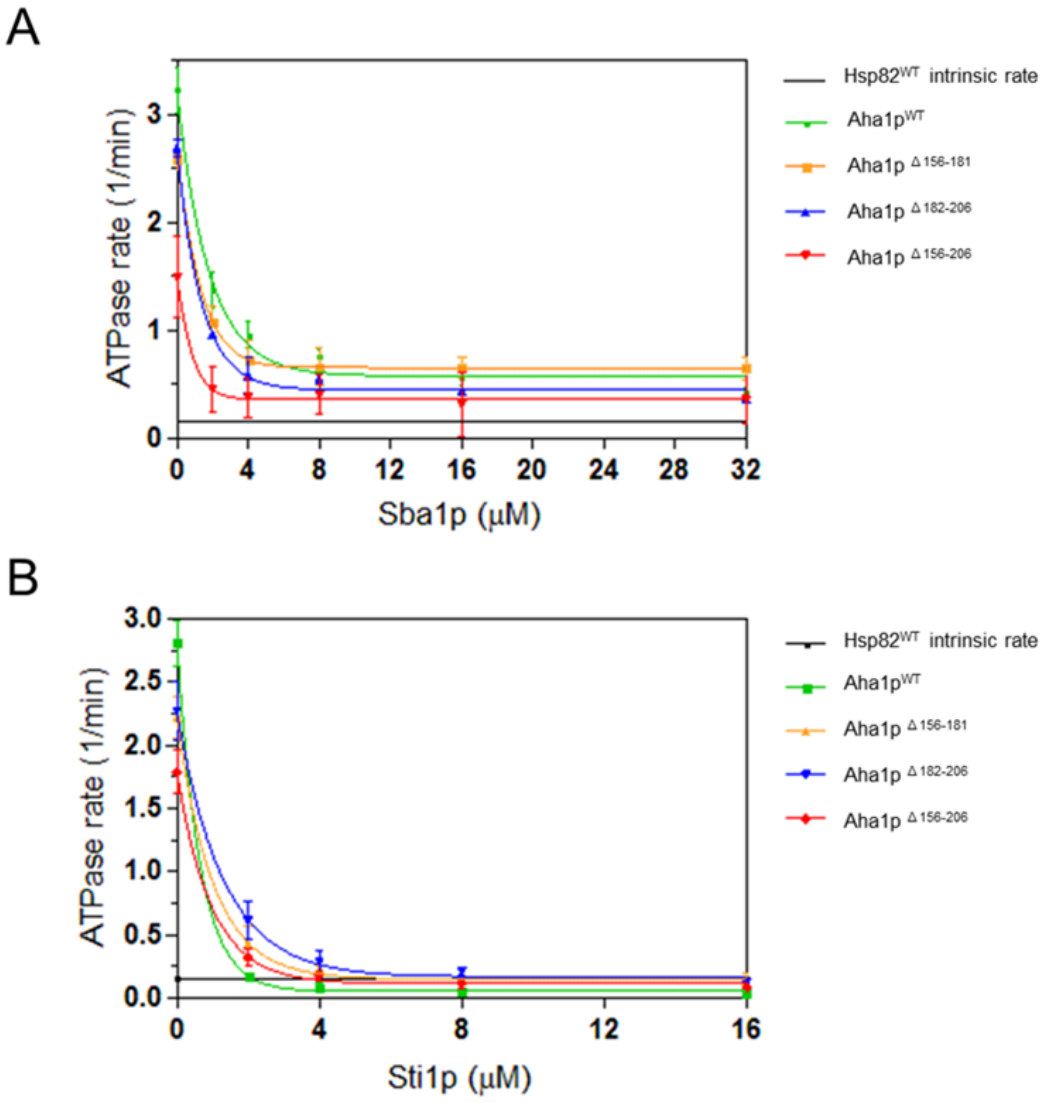

Figure 5.4 Sba1p inhibition of Hsp82p ATPase activity is more severely affected than Sti1p inhibition when stimulated by Aha1p linker variants. Sti1p **(A)** and Sba1p **(B)** inhibition of Aha1p-mediated stimulation of Hsp82p^{WT}. Each reaction contained 2 μM Hsp82p^{WT}, 4 μM Aha1p^{WT} (green) or Aha linker variants (Aha1p$^{\Delta 156\text{-}181}$ in orange, Aha1p$^{\Delta 182\text{-}206}$ in blue, and Aha1p$^{\Delta 156\text{-}206}$ in red), and the indicated concentration of Sti1p or Sba1p. Black solid line indicates intrinsic rate of Hsp82p^{WT}. ATPase rates are shown in μM ATP hydrolyzed per minute per μM of enzyme (1/min).

5.2.5 Co-chaperone switching is maintained with Aha1p linker deletions and the Hsp90 linker deletion

Overall, the apparent binding affinity of all the Aha1p linker truncation variants increased for wildtype Hsp82p and Hsp82p$^{\Delta 211\text{-}263}$, but did not result in an increased stimulated ATPase rate. A possible reason for this observation is that with an increased binding affinity, Aha1p may not dissociate from Hsp82p properly due to the conformation Hsp82p acquires upon binding. I sought out to examine how the increased binding affinity of Aha1p linker truncation variants influence the cycling of Sti1p in the presence of Cpr6p, thereby, indirectly testing how Aha1p cycles on and off Hsp82p (Li et al., 2013). Using this cycling assay with the Hsp82p linker truncation (Hsp82p$^{\Delta 211\text{-}263}$), I specifically tested whether the lack of linker interferes with the necessary conformational transitions of Hsp82p that allow Aha1p and Cpr6p to displace Sti1p. Based on my results in Figure 5.2D, showing that Sti1p can inhibit the Hsp82p-Cpr6p-Aha1p complexes similarly, with or without the linker at equimolar concentrations, I hypothesized that cycling will not be altered with Hsp82p$^{\Delta 211\text{-}263}$.

Sti1p strongly inhibits the Aha1p-mediated ATPase stimulation of Hsp82p^{WT}, and as expected from our Sti1p titrations, it inhibited Aha1p^{WT} the most and Aha1p $^{\Delta 182\text{-}206}$ the least at equimolar concentrations of co-chaperones (Figure 5.5A, lanes 1). This was a similar result for Hsp82p$^{\Delta 211\text{-}263}$ (Figure 5.5B, lanes 1). The addition of Cpr6p to all Aha1p-mediated stimulation of Hsp82p^{WT} and Hsp82p$^{\Delta 211\text{-}263}$ resulted in additional ATPase stimulation compared to Aha1p-mediated stimulation alone, which is expected as previously observed (Panaretou et al., 2002) (Figure 5.5 A&B - lanes 3 compared to lanes 2). Consistent with my hypothesis, cycling using wildtype Aha1p was not altered with Hsp82p$^{\Delta 211\text{-}263}$ (Figure 5.5 A&B – green bars). Interestingly, there is a slight increase in the ATPase recovery rates when using Aha1p linker variants compared to using wildtype Aha1p in reactions containing Sti1p and Cpr6p with Hsp82p^{WT} (Figure 5.5A, lanes 4) or Hsp82p$^{\Delta 211\text{-}263}$ (Figure 5.5B, lanes 4). While the Aha1p linker variants' C-terminal domains were able to participate in co-chaperone switching, an increase in the ATPase recovery was surprising. This result suggests that the

second Hsp82p conformation that is induced by Aha1p, which requires the linker, does not involve the displacement of Sti1p. Rather, to displace Sti1p, the first, high-affinity conformation is required, which is achieved by all Aha1p variants.

It is evident that the stimulated rate by the Aha1p linker variants were not fully inhibited by Sti1p at equimolar concentrations, but Sti1p did inhibit the stimulated ATPase rate when stimulated by wildtype Aha1p (Figure 5.5 – lanes 1). This led me to question whether higher concentrations of wildtype Aha1p would result in a higher ATPase recovery rate of $Hsp82p^{WT}$ in the presence of Sti1p and Cpr6p, as seen with the Aha1p linker variants. At higher concentrations of wildtype Aha1p, a greater increase in recovery was observed (Figure 5.5C). This titration result reveals that the V_{MAX} of the reactions are reached earlier with Aha1p linker variants at the concentrations used in the cycling reactions in Figure 5.5A. This demonstrates that the higher ATPase recovery rates are most likely due to the increased affinity of the Aha1p linker variants.

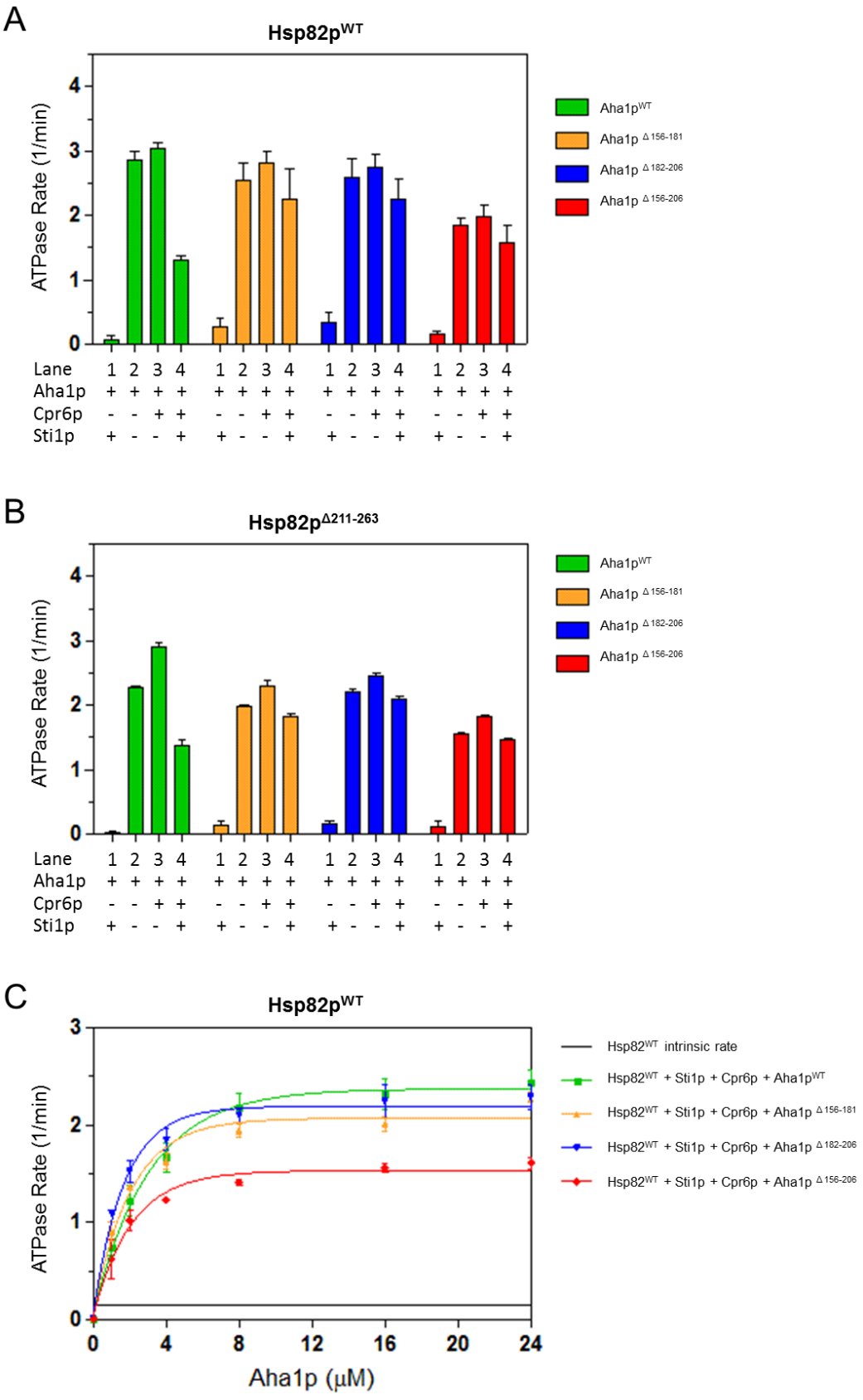
A
Hsp82p^WT
ATPase Rate (1/min)
Aha1p^WT
Aha1p Δ156-181
Aha1p Δ182-206
Aha1p Δ156-206
Lane 1 2 3 4 1 2 3 4 1 2 3 4 1 2 3 4
Aha1p + + + + + + + + + + + + + + + +
Cpr6p - - + + - - + + - - + + - - + +
Sti1p + - - + + - - + + - - + + - - +
B
Hsp82p^Δ211-263
ATPase Rate (1/min)
Aha1p^WT
Aha1p Δ156-181
Aha1p Δ182-206
Aha1p Δ156-206
Lane 1 2 3 4 1 2 3 4 1 2 3 4 1 2 3 4
Aha1p + + + + + + + + + + + + + + + +
Cpr6p - - + + - - + + - - + + - - + +
Sti1p + - - + + - - + + - - + + - - +
C
Hsp82p^WT
ATPase Rate (1/min)
Aha1p (μM)
Hsp82^WT intrinsic rate
Hsp82^WT + Sti1p + Cpr6p + Aha1p^WT
Hsp82^WT + Sti1p + Cpr6p + Aha1p Δ156-181
Hsp82^WT + Sti1p + Cpr6p + Aha1p Δ182-206
Hsp82^WT + Sti1p + Cpr6p + Aha1p Δ156-206

Figure 5.5 Co-chaperone switching with Hsp82p and Aha1p linker truncations. A-B. Co-chaperone cycling of $Hsp82p^{WT}$ (A) and $Hsp82p^{\Delta 211-263}$ (B)**.** Reactions contained 1μM $Hsp82p^{WT}$ (A) or $Hsp82p^{\Delta 211-263}$ (B) and 4 μM Cpr6p, 4 μM Sti1p, and 4 μM $Aha1p^{WT}$ (green), $Aha1p^{\Delta 156-181}$ (orange) $Aha1p^{\Delta 182-206}$ (blue), or $Aha1p^{\Delta 156-206}$ (red). **C.** Aha1p titration into wildtype Hsp82p reactions containing Sti1p and Cpr6p. Each reaction contained 2 μM $Hsp82p^{WT}$, 4 μM Sti1p, 4 μM Cpr6p, and indicated concentration of $Aha1p^{WT}$ (green), $Aha1p^{\Delta 156-181}$ (orange) $Aha1p^{\Delta 182-206}$ (blue), or $Aha1p^{\Delta 156-206}$ (red). Black line represents the intrinsic rate of $Hsp82p^{WT}$. ATPase rates are shown in μM ATP hydrolyzed per minute per μM of enzyme (1/min).

Prior to the incorporation of Aha1p into the cycling model, Li and colleagues proposed that Sba1p was responsible for displacing Sti1p from Hsp82p (Li et al., 2011). My results in chapter 3 show that the C-terminus of Aha1p is required for displacement of Sti1p with Cpr6p and I was curious to investigate how Sba1p would function in the cycling reaction. Due to the fact that both $Aha1p^{C}$ and Sba1p bind to the N-terminally dimerized interface of Hsp82p, it is plausible that Sba1p may function like $Aha1p^{C}$ to some extent. The cycling reaction, as described earlier, depends on the restoration of ATPase activity in the presence of Sti1p, Cpr6p, and Aha1p. Because Sba1p is an inhibitor of the ATPase activity of Hsp82p, unlike Aha1p, testing Sba1p in the cycling reaction instead of Aha1p would not provide a definitive answer to any specific question as no restoration in ATPase activity would result. Therefore, I tested how the addition of Sba1p in Aha1p containing reactions affects the cycling reaction.

My results indicate that Sba1p alone does not result in inhibition of Hsp82p's intrinsic ATPase activity (lane 3), but can inhibit the Aha1p stimulated rate by two-thirds (lane 11) and the Cpr6p-stimulated rate by more than half (lane 6) (Figure 5.6). This is consistent with previous published data showing that Sba1p is not as potent of an inhibitor as Sti1p, which can fully inhibit the intrinsic (lane 2) and stimulated rates of Aha1p (lane 9) and Cpr6p (Figure 5.6) (Panaretou et al., 2002). Lanes 7-10 of Figure 5.6 show Aha1p stimulation and the interplay of Aha1p with Cpr6p or Sti1p, as well as the recovery in ATPase stimulation in the presence of all three co-chaperones, as previously described (chapter 3). When Sba1p was added into the cycling reaction (Figure 5.6- lane 13), only a small decrease is seen from the Sba1p-Aha1p-Hsp82p reaction (Figure 5.6- lane 11). This suggest that Sba1p actually contributes to the displacement of Sti1p. If Sba1p did not participate in displacing Sti1p, a bigger reduction in ATPase activity would be observed, especially since Sba1p and Aha1p compete for binding and because Sba1p inhibited the Aha1p simulated rate by two-thirds (Figure 5.6- lane 11). The missing experiment here would be the resulting Hsp82p ATPase activity in the presence of Sba1p, Sti1p, and Aha1p, where I expect Sti1p will be able to fully inhibit the ATPase activity of Hsp82p. The results presented here show that the addition of

Sba1p to the cycling reaction (Hsp82-Sti1p-Aha1p-Cpr6p) resulted in 65 % ATPase recovery of the Aha1p stimulated rate, which is very similar to the 70 % recovery seen in the absence of Sba1p.

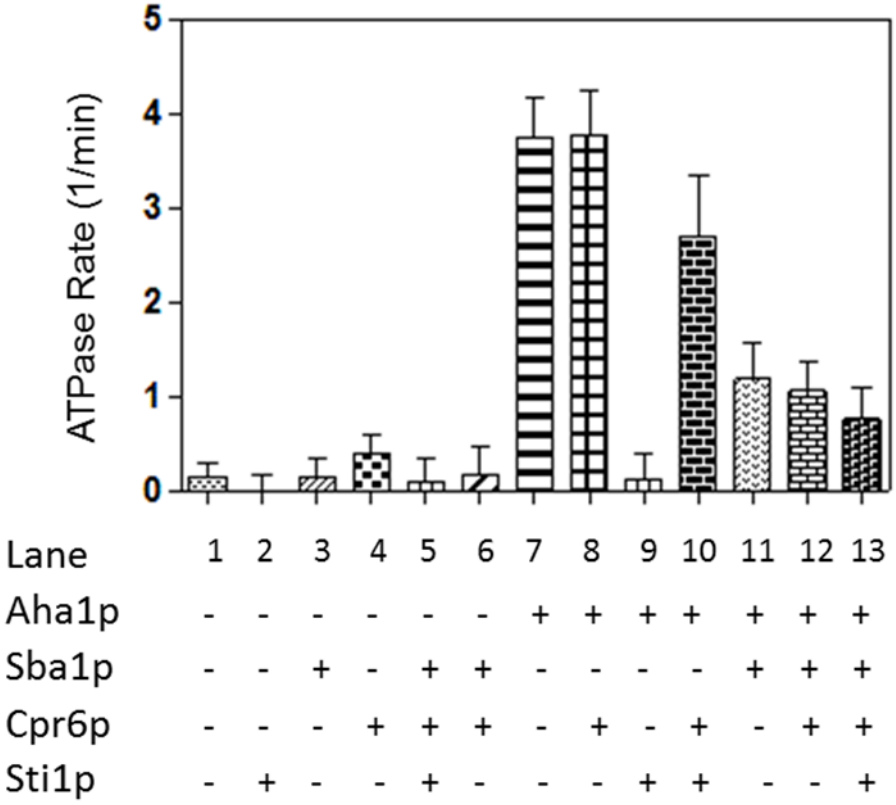

Figure 5.6 Sba1p integration into the cycling reaction. Sba1p alone does not inhibit the ATPase activity of Hsp82p, but can inhibit the Aha1p stimulated rate by two-thirds at equimolar concentrations. In the presence of the Hsp82p, Sti1p, Aha1p, and Cpr6p, the addition of Sba1p only slightly reduced the ATPase activity from the Sba1p-Aha1p-Hsp82p ATPase rate, indicating Sba1p competes for Aha1p binding but also that it can replace Aha1p^{C} in displacing Sti1p. Reactions contained 2 μM Hsp82p^{WT} and 4 μM of the indicated co-chaperones (Aha1p, Sba1p, Cpr6p, and Sti1p). ATPase rate is shown in μM ATP hydrolyzed per minute per μM of enzyme (1/min).

5.3 Summary and model

Aha1p binds preferentially to the constrained Hsp82p conformation

To determine the significance of the linker region of Hsp82p, the length of the linker was shortened and ATPase activity was assessed. Investigating how co-chaperone regulation is affected with the linker deletion constructs has allowed me to further scrutinize the function of the linker region of Hsp82p. Initially, I hypothesized that shortening the distance between the N-terminal and middle domains of Hsp82p will enhance both intrinsic ATPase activity and Aha1p-mediated stimulation, but instead it was impaired. Shortening the linker of Hsp82p enhanced the apparent binding affinity for Aha1p while impairing the magnitude of maximal stimulation. Furthermore, this was synergized by shortening the distance of the linker region of Aha1p. How is it that the binding affinity of Aha1p increases but not the ATPase stimulated rate? This sparked the question of what type of conformation does Hsp82p adopt when the linker region is shortened?

As discussed in the chapter 1, a lot of different rearrangements must occur within the Hsp82p dimer to acquire the ATP-hydrolysis competent state, including opening and closing of the lid, nucleotide binding, N-terminal dimerization, N-terminal strand swap, N-M communication, and twisting of the N-terminal domains (Figure 1.7). Structural data of Hsp90 homologs provides 'snap shots' of the different conformations Hsp90 can acquire throughout its functional cycle (Figure 1.6). In addition to Hsp90 visualized in the flying seagull conformation, the twisted closed state, and in a compact conformation where the N-terminal domains are folded down onto the middle domains, it has also been visualized in an asymmetrically dimerized state (Ali et al., 2006; Bron et al., 2008; Lavery et al., 2014; Southworth and Agard, 2008). How Hsp90 exactly hydrolyzes ATP, and how Aha1p influences the conformational dynamics of Hsp90 to reach the ATP-hydrolysis competent state by advancing/bypassing the rate limiting step, has not been fully elucidated.

For any enzyme, the velocity of a reaction can be altered in two ways: The rate of catalysis (K_{CAT}) can be increased or the affinity for substrate (K_M) can be

increased. By increasing the K_M, the affinity for both the substrate and the product is decreased, which, in the case of Hsp90, is ATP and ADP, respectively. To determine these values, one must determine the maximum velocity of the reaction (V_{MAX}) and the K_M by titrating ATP into the reaction. The K_{CAT} can be calculated by applying the following equation:

$$Kcat = \frac{Vmax}{Km}$$

It is evident from this equation that anything that increases the K_{CAT} or the K_M of the reaction will ultimately result in an increase the reaction velocity (V_{MAX}). Using this equation is one way to 'normalize' the data in order to compare what is truly being tested in these experiments: How is ATP hydrolysis affected by the linker deletion?

Consistently, each time the N-M linker of Hsp82p or the linker of Aha1p was shortened, resulting in a constrained conformation, the affinity between Aha1p and Hsp82p was enhanced while the maximum velocity (V_{MAX}) of the reaction decreased. Although N-M communication is more accessible with the linker deletion constructs, any one of the other conformational transitions, as illustrated in Figure 1.6 and Figure 1.7, may be impaired. My results indicate that Aha1p binds more strongly to a constrained conformation ($Hsp82p^{\Delta 211\text{-}263}$). This suggests that the conformation Aha1p has the highest affinity for is not the most catalytically active one, but without calculating the K_M, such conclusion cannot be made. The decrease in the Aha1p-mediated stimulated rates (V_{MAX}) may be the result of a decrease in the affinity for ATP (K_M) or a change in the rate of catalysis (K_{CAT}) of $Hsp82p^{WT}$ and $Hsp82p^{\Delta 211\text{-}263}$ when bound to Aha1p. By establishing the apparent affinity for ATP (K_M) of $Hsp82p^{WT}$ and $Hsp82p^{\Delta 211\text{-}263}$, with and without the Aha1p linker truncation variants, the catalytic efficiency (K_{CAT}) can be calculated. This type of analysis will bring insight into the mechanistic action of Aha1p-mediated stimulation and the role of the linker of Hsp82p has in acquiring the various conformations it requires in its functional ATPase cycle.

Role of the linker in attaining different conformational states

At the time these experiments were conducted, only a handful of papers investigated the significance of the linker region of Hsp82p. These studies have shown that the charged linker has a role in co-chaperone association and is an important modulator of client activation by providing conformational flexibility (Hainzl et al., 2009; Tsutsumi et al., 2012). There was, however, no mechanistic dissection and assessment of how the linker influences the acquisition of conformational states Hsp82p can adopt. Since the linker truncation of Hsp82p resulted in enhanced affinity for Aha1p, my working hypothesis was that the conformation to which Aha1p binds, is one in which the N-terminal domains are in close proximity to the middle domains. Two articles have since been published and their data brings an insightful perspective to help decipher the results of my ATPase assays. The Hugel group investigated the stability of the various domains and the charged linker region using optical traps and single-molecule mechanic experiments with Hsp82p monomers. Their results demonstrate that the linker actually binds to the N-terminal domain of Hsp82p and that the sequence between amino acids 211 and 263 is crucial for this interaction (Jahn et al., 2014). The linker has a critical role in forming the 'docked state' and this docking/undocking of the linker with the N-terminal domain modulates N-terminal dimerization which they determined by single molecule FRET experiments (Figure 5.7B & Figure 5.8) (Jahn et al., 2014). Furthermore, the N-terminal domains possess a high rotational freedom as crosslinking between D61C Hsp82p can occur (Figure 5.7A- black spheres) (Jahn et al., 2014). In the closed crystal structure of the Hsp82p dimer in complex with Sba1p, the aspartic acid residues at position 61 are found on the opposite sides of the dimerized interface, yet cysteines at these positions can be crosslinked together. They propose a model where the linker acts to prevent certain N-N domain interactions by re-orienting the N-terminal domain through interaction with the linker (Jahn et al., 2014). They hypothesize that undocking of the linker results in rotational freedom of the N-terminal domains to dimerize (Daturpalli et al., 2017; Jahn et al., 2014; Street et al., 2012). In terms of co-chaperone regulation of Hsp82p linker mutants, Aha1p and Sba1p could bind Hsp82p$^{\Delta 211\text{-}263}$ but Sba1p

could not bind Hsp82p$^{\Delta 211\text{-}272}$, possibly because residues 264-272 are required to reach the twisted conformation to which Sba1p binds (Ali et al., 2006; Jahn et al., 2014).

More recently, the Mayer group studied the consequence of shortening the linker region on the conformational dynamics of Hsp90. They too reveal that the N-terminal domains have a high degree of conformational freedom and show that Hsp82p can rotate 180 degrees (Figure 5.7B) (Daturpalli et al., 2017). They determined this rotational flexibility using crosslinking experiments with strategically placed cysteine residues at position 57 (E57C) of the N-terminal domain of Hsp82p. The glutamic acid residues at position 57 are also found on the opposite sides of the dimerized interface, and can crosslink in the presence of homobifunctional thiol-specific crosslinker, BMH (Figure 5.7A – orange spheres) (Daturpalli et al., 2017). This suggests that Hsp82p can acquire this rotated state freely in equilibrium (Figure 5.7B). Interestingly, this rotation was impaired in the presence of AMPPNP and Aha1p, but not with Sba1p (Daturpalli et al., 2017). Sba1p was not able to stabilize the closed state, and thus, crosslinking occurred, indicating that the rotated state was accessed in the presence of Sba1p (Daturpalli et al., 2017). Furthermore, they demonstrated that shortening the linker of Hsp82p compromised the rotational freedom of the N-terminal domain which resulted in reduced intrinsic and stimulated ATPase rates of both yeast and human Hsp90 (Daturpalli et al., 2017). Using Hsp82p linker truncation mutants (Hsp82p$^{\Delta 211\text{-}263}$ and Hsp82p$^{\Delta 211\text{-}266}$), they showed that N-terminal domain rotation was decreased by 50 % which explains why the Hsp82p linker truncation mutant has a decreased intrinsic rate (Daturpalli et al., 2017). They also show that AMPPNP with Aha1p was not able to stabilize the closed conformation of Hsp82p$^{\Delta 211\text{-}266}$, as evidenced by the increased crosslinked product, while Aha1p and AMPPNP was able to decrease the amount of crosslinked product that formed when incubated with wildtype Hsp82p and Hsp82p$^{\Delta 211\text{-}263}$ (Daturpalli et al., 2017). Moreover, Aha1p was unable to stimulate Hsp82p$^{\Delta 211\text{-}266}$, but could stimulate Hsp82p$^{\Delta 211\text{-}263}$ to the same fold rate as Aha1p stimulated wildtype Hsp82p, relative to their own intrinsic rates (Daturpalli et al., 2017). This indicates that the linker plays a role in acquiring

the closed state and that 264-272 is the minimum linker required for the ability of Aha1p and AMPPNP to stabilize the closed conformation. Lastly, Daturpalli *et al.* suggest that the rotated conformation may be the preferred conformation of Hsp82p based on crosslinking data with Hsp82p linker truncation mutants (Daturpalli et al., 2017).

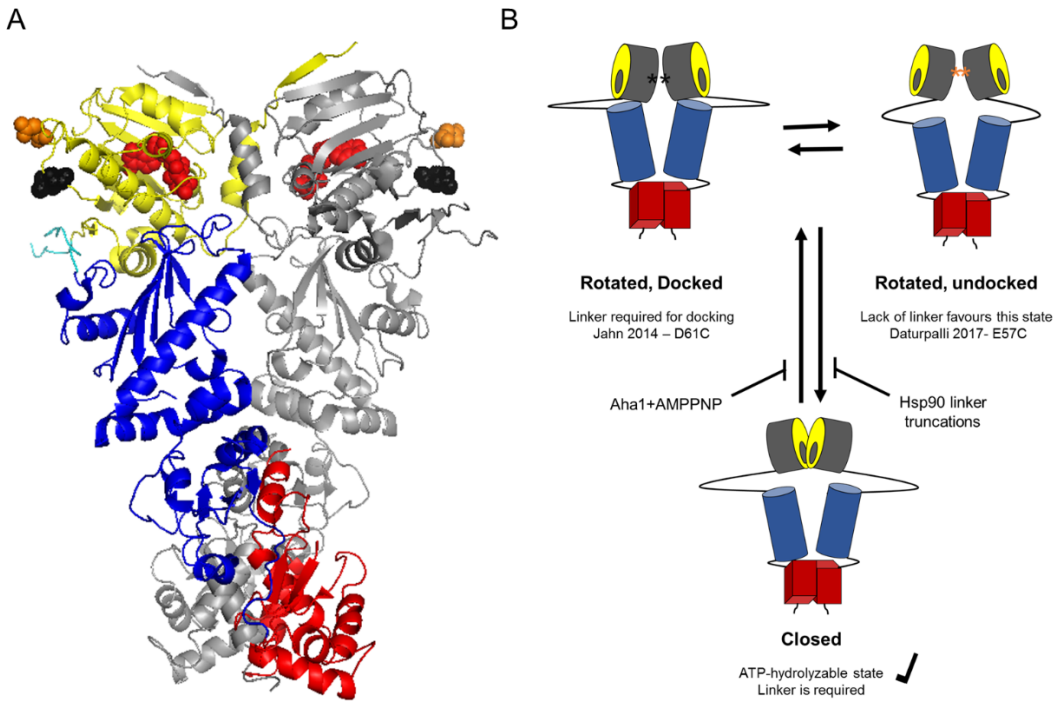

Figure 5.7 Closed and rotated conformation of Hsp82p involving N-terminal domain rotation. A. Crystal structure of an Hsp82p dimer (as shown previously) where bound Sba1p is removed from the dimerized interface, with orange and black spheres representing E57 and D61 residues, respectively. This crystal structure was modified using the PDB file 2CG9 (Ali et al., 2006). **B.** Closed state is the ATPase competent conformation which is stabilized in the presence of Aha1p and AMPPNP. The rotated state can be crosslinked, indicated by the asterisks, where the N-terminal domains rotate nearly 180º from their orientation illustrated in the closed conformation. The linker can be docked or undocked in this rotated state. Hsp82p linker truncations favor the rotated, undocked state. Orange and black asterisks represent E57C and D61C residues where crosslinking occurs. This figure represents a model using data presented in Daturpalli *et al.* (2017) and Jahn *et al.* (2014).

Different conformations that have been described in literature are illustrated in Figure 5.8. Taken together, these publications propose that Hsp82p can exist, and preferentially exist, in a rotated state in which the N-terminal domains are rotated in a position that is not ATPase competent (Figure 5.8B) (Daturpalli et al., 2017; Jahn et al., 2014). Daturpalli *et al.*'s data suggest that Aha1p together with AMPPNP stabilize the closed conformation, meaning that Aha1p and AMPPNP binding induces changes that result in the re-orientation of the N-terminal domains to the closed conformation (Figure 5.8A) (Daturpalli et al., 2017; Jahn et al., 2014). Furthermore, the data implies that when the linker of Hsp82p is shortened past residue 263, the undocked-rotated state is favored and Aha1p action is hindered, as Aha1p is unable to induce the conformational changes that are necessary for attaining the ATPase-competent, closed state (Figure 5.8B) (Daturpalli et al., 2017; Jahn et al., 2014). There seem to be a difference between the linker docked state, described by Jahn *et al.*, and when the N-terminal domain becomes docked to the middle domain (N-M communication), but some aspects of those conformations may be similar (Figure 5.8).

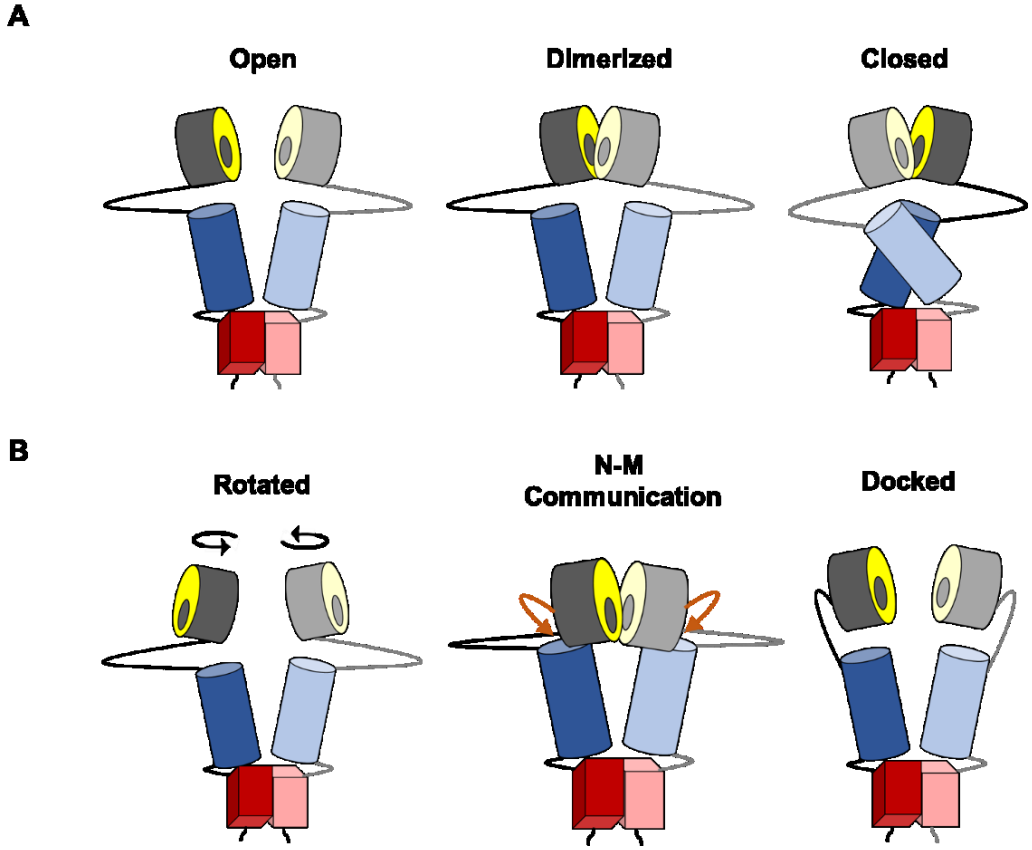

Figure 5.8 Different structural representations of Hsp90 conformations. A. Only in the closed, twisted state is Hsp82p in an ATP-hydrolysis conformation, and not in the open or dimerized state. To reach the closed state, a minimum linker of 264-272 is required. **B.** Hsp90 N-terminal domains can rotate, become docked to the middle domains (N-M communication), and have the linkers docked to it. These events can occur in the open or dimerized conformation shown in (A). Docked refers to the linker being bound to the N-terminal domains. Undocking of the linker allows rotational freedom to the N-terminal domains to acquire the N-terminally dimerized state. N-M communication can be referred to the N-M docked state as the N-terminal domains are in close proximity to the middle domains.

Optimal Aha1p stimulation requires Hsp82p N-M linker and the C-terminus of Aha1p

In light of the new data presented, further insights can be drawn. The linker region of Hsp82p provides conformational flexibility to orient the N-terminal domains between the rotated (docked or undocked) conformation and the closed conformation (Daturpalli et al., 2017; Jahn et al., 2014). My data brings additional information about how co-chaperones regulate the ATPase activity of Hsp82p and the role the linker plays in the conformational transitions that Hsp82p adopts.

When comparing the crosslinking data between Hsp82p$^{\Delta 211\text{-}263}$ and Hsp82p$^{\Delta 211\text{-}266}$, it becomes evident that residues 264-272 are required to reach a conformation that results in Aha1p-mediated stimulation (closed state) (Daturpalli et al., 2017). While Aha1p can bind to either mutant, evidence showing that Aha1p and AMPPNP could stabilize a closed conformation in Hsp82p$^{\Delta 211\text{-}263}$, but not in Hsp82p$^{\Delta 211\text{-}266}$, suggests that the N-M linker provides a certain amount of freedom required by Aha1p to induce a constrained Aha1p-bound conformation, which I described as the high-affinity Aha1p-bound state. It is conceivable that if Aha1p^{C} is not able to induce rearrangement of Hsp82p's N-terminal domains that leads to the closed conformation, due to a lack of freedom when more residues than 211-263 are removed, a lower maximal stimulated ATPase rate (V_{MAX}) will be evident.

Interestingly, Daturpalli *et al*. show that the intrinsic and stimulated rate of Hsp82p$^{\Delta 211\text{-}263}$ was reduced by ~80 % compared to the intrinsic and stimulated rate of wildtype Hsp82p (Daturpalli et al., 2017). This is similar to Hainzl *et al.*'s results showing the intrinsic and stimulated rates of Hsp82p$^{\Delta 211\text{-}263}$ are also affected by the same factor, but reported the intrinsic and stimulated rates were reduced by 50 % compared to the wildtype Hsp82p (Hainzl et al., 2009). These results support Hainzl *et al.*'s data that the efficiency of catalysis of Hsp82p$^{\Delta 211\text{-}263}$ is lower because the mechanism of hydrolysis is hindered without the linker present, as the calculated K_{CAT} of Hsp82p$^{\Delta 211\text{-}263}$ is reduced while the K_M remains the same (Hainzl et al., 2009).

While shortening the Hsp82p linker enhanced the apparent binding affinity for Aha1p and impaired the magnitude of maximal stimulation, this result was

augmented by shortening the distance of the linker region of Aha1p (Figure 5.3D-E). Figure 5.3 shows that Aha1p action, and more precisely, the binding of Aha1p^{C} is affected when the linker of Aha1p is also removed, and thus, step 3 of Aha1p-mediated stimulation is hindered (Wolmarans et al., 2016). This suggests that the linker of Aha1p provides the length required for Aha1p^{C} to bind/act, which is involved in inducing the structural rearrangements leading to the closed conformation and subsequent robust ATPase stimulation. This hypothesis can be tested by measuring the K_M values for Hsp82p in the presence and absence of the Aha1p linker variants. From the equation presented earlier, to change the V_{MAX}, either the K_{CAT} or K_M must change. If the K_M of Hsp82p is changed to more or less the same degree by full-length Aha1p and Aha1p linker variants, then the vast increase in the velocity of the reaction we observe when wildtype Aha1p is added to Hsp82p is because Aha1p^{C} is altering the K_{CAT}.

Because Sba1p more strongly inhibits both the ATPase rates of wildtype Hsp82p and Hsp82p$^{\Delta 211-263}$ when stimulated by the Aha1p linker variants and wildtype Aha1p, respectively, my results reveal a second, post-hydrolysis conformation. This conformation is stalled from forming (due to the constrained conformation Hsp82p), thereby promoting Sba1p association and the appearance of being a more potent inhibitor. If this is the case, then this would suggest that the linker aids in acquiring a conformation involving substrate release.

Regardless of the magnitude of the stimulated rate, or by which Aha1p variant stimulates Hsp82p^{WT} or Hsp82p$^{\Delta 211-263}$, the resulting ATPase inhibition by Sba1p is similar (Figure 5.2B & 5.4A). This suggests that the conformation to which Sba1p binds is the same.

Sba1p displaces Aha1p and binds tighter to a constrained Hsp82p

Both wildtype Hsp82p and the linker mutant Hsp82p$^{\Delta 211-263}$ were able to be stabilized by Aha1p and AMPPNP, but not Sba1p (Daturpalli et al., 2017). It has been reported that Sba1p can bind to Hsp82p$^{\Delta 211-263}$ since the N-terminal domains of Hsp82p$^{\Delta 211-263}$ are able to reach the closed conformation, albeit with half the affinity (Daturpalli et al., 2017; Hainzl et al., 2009; Jahn et al., 2014). In my assays,

however, Sba1p is able to inhibit the stimulated ATPase rate of Hsp82p$^{\Delta 211\text{-}263}$ more effectively than Hsp82p^{WT} in the presence of Aha1p, suggesting Sba1p binding is not negatively affected by the lack of linker (Figure 5.2B). Moreover, Sba1p was also a more effective inhibitor of the ATPase activity of wildtype Hsp82p when stimulated by the Aha1p linker truncations (Figure 5.4A). As previously described, literature has shown that Sba1p binds to the closed, ATP-bound, twisted conformation (Ali et al., 2006; Graf et al., 2014; Johnson et al., 2007). Sba1p was crystalized in a 2:2 complex with Hsp82p (Ali et al., 2006). It was suggested that this closed conformation Hsp82p adopts in this 'inhibited Sba1p-bound conformation' may indeed be the ATPase competent state, although Hsp82p is altered in this structure; it contains no linker segment and harbors the A107D mutation that promotes the N-terminally dimerized state (Ali et al., 2006). It is now understood that Sba1p slow the release of substrate/product when bound to the N-terminally dimerized surface (Graf et al., 2014). Aha1p, on the other hand, also binds the N-terminally dimerized interface and thought to stabilize the ATP-bound, closed conformation (Daturpalli et al., 2017; Johnson et al., 2007; Li et al., 2012; Retzlaff et al., 2010). This closed conformation is very similar to the Sba1p conformation, and indeed, Aha1p and Sba1p have some overlapping binding sites on a portion of the middle domain and the N-terminal dimerized interface, which suggests that binding is mutually exclusive (Ali et al., 2006; Koulov et al., 2010; Retzlaff et al., 2010).

My results suggest that Sba1p and Aha1p binding are in fact mutually exclusive. The constrained conformation that Hsp82p$^{\Delta 211\text{-}263}$ adopts in presence of Aha1p (*C1*) is a conformation to which Sba1p preferentially binds (indicated by the dark arrows of Sba1p displacing Aha1p in the top panel) (Figure 5.9). This conclusion infers that this constrained conformation (*C1*) that Aha1p binding induces, is the twisted state, as that is the state to which Sba1p is shown to bind (Ali et al., 2006; Graf et al., 2014). Aha1p binding induces a closed state that may be ATPase competent, but it does not result in hydrolysis for Sba1p binding must occur before ATP hydrolysis since Sba1p only binds to an ATP-bound Hsp82p (McLaughlin et al., 2006). When the linkers are present, Hsp82p can acquire a

second conformation (*C2*), which is the conformation defined by a high V_{MAX}, K_M, and K_{CAT} in biochemical assays (Figure 5.9). Sba1p binding drives another conformational change that is not compatible with Aha1p binding, displacing Aha1p from the complex, which leads to the acquisition of conformational states *C3* and *C4* (Figure 5.9). I predict that the constrained Hsp82p conformation (*C1*), which Sba1p preferentially binds, is prolonged when bound to Sba1p and thus results in a conformation (*C3*) which appears to have an increased inhibited ATPase rate (Figure 5.9 – top panel). This conformation (*C3*) is short-lived when Hsp82p has its linkers, resulting in product release and the acquisition of the second, post hydrolysis conformation (*C4*) (Figure 5.9 – bottom panel).

Altogether, my results suggest that co-chaperones may be influencing Hsp82p at the level of substrate and product affinity (K_M). Aha1p drives the change in K_M (*C2*) and this change in K_M reloads the reaction thereby allowing for fast release of product (ADP) after hydrolysis (Figure 5.9 – bottom panel). When the linker is deleted ($Hsp82p^{\Delta 211\text{-}263}$), this second conformation where Aha1p perhaps drives the change in K_M to reload the reaction, does not occur, slowing down the cycle (Figure 5.9- top panel).

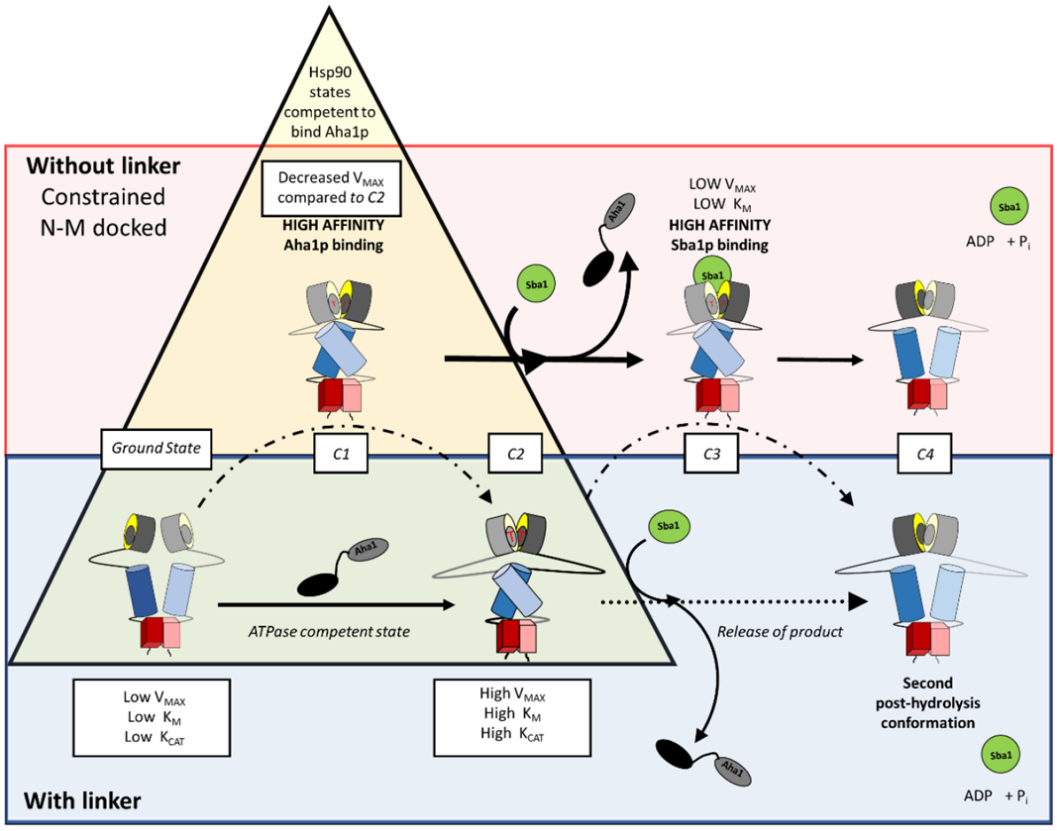
Hsp90 states competent to bind Aha1p
Without linker
Constrained
N-M docked
Decreased V_{MAX} compared to C2
HIGH AFFINITY
Aha1p binding
LOW V_{MAX}
LOW K_M
HIGH AFFINITY
Sba1p binding
Sba1
ADP + P_i
Aha1
Ground State
C1
C2
C3
C4
ATPase competent state
Release of product
Second post-hydrolysis conformation
Low V_{MAX}
Low K_M
Low K_{CAT}
High V_{MAX}
High K_M
High K_{CAT}
With linker

Figure 5.9 A model of how the linker region of Hsp82p limits the conformational dynamics of Hsp82p and subsequent Aha1p and Sba1p regulation. Sba1p and Aha1p is mutually exclusive: Aha1p binds to conformations shown in the triangle, and Sba1p can bind to those conformations, but results in displacement of Aha1p, indicated by the arrows next to the triangle. The yellow triangle shows the conformations that Aha1p induces: Aha1p induces a twisted conformation of Hsp82p that Aha1p and Sba1p preferentially bind (*C1*), and second conformation defined by a high K_M. The top rectangle (red) represents conformations that form in the absence of the linker. The bottom panel (blue) box represents conformations that can only form with the presence of the linker. The dashed arrows from the different conformations (indicated by the labeled white boxes – *ground state, C1, C2, C3, and C4*) shows how Hsp82p with a linker form short-lived, intermediate conformations, where the N-M docked states from. The conformation that Aha1p induces, is an ATP hydrolysis competent conformation (*C1* and *C2*). Sba1 binding occurs before hydrolysis takes place and results in the displacement of Aha1p. The lack of the Hsp82p linker promotes prolonged Sba1p binding, as Sba1p preferentially binds *C1* where Aha1p has not induced an increase in K_M, slowing down the release of ADP. A low K_M and a low V_{MAX} is predicted for the Sba1p-bound Hsp82p conformation (*C3*). When linkers are present on Hsp82p, Aha1p drives the change in K_M resulting in the acquisition of *C4* (indicated by the stippled line), where release of product is favored, while the intermediate conformation (*C3*) is short-lived.

Chapter 6

Discussion of perspectives and future directions

6.1 Aha1p action, recruitment, and interplay with co-chaperones Sba1p and Sti1p

Throughout the course of my doctoral studies, my focus was to understand how co-chaperones modulate the ATPase activity of Hsp90. My goal was to define a mechanical model for the asymmetric interactions of co-chaperones, specifically for Aha1p. I assessed how Aha1p binding results in the stimulation of Hsp82p's ATPase activity and how this stimulation differs from its homolog Hch1p. Further characterization included looking at how Aha1p regulation of the ATPase activity of Hsp82p is influenced in the presence of co-chaperones Sba1p and Sti1p. I also assessed how Aha1p action aids in the cycling of co-chaperones. Using various point mutations in Hsp82p, post-translationally modified Hsp82p, and conformationally restricted Hsp82p in the context of homodimers and heterodimers in ATPase assays, I was able to conduct in-depth analyses of my objectives. My findings provide a framework for integrating subunit-specific co-chaperone interactions and post-translational modifications to better understand how Hsp90 is regulated.

6.1.1 The mechanism of Aha1p action leads to the closed conformation

Chapter 3 represents a clear advance in the mechanistic understanding of Aha1p-mediated stimulation. Aha1p^{N} binding to the middle domain of Hsp82p drives conformational changes to occur in the N-terminal domain in *cis* to the Aha1p^{N} binding event, which allow participation of Aha1p^{C} to occur (Figure 6.1-step 1-2) (Wolmarans et al., 2016). These findings further characterize the asymmetric mechanism of Aha1p stimulation. Not only is one Aha1p molecule sufficient to stimulate the ATPase activity of Hsp82p (Retzlaff et al., 2010), my results demonstrate that Aha1p drives ATPase stimulation in *cis* to the binding of Aha1p^{N}. The hydrolyzing subunit can either be in *cis* or *trans* to Aha1p^{N} binding, but Aha1p^{N} binding drives *cis* conformational rearrangements leading to the ATP-hydrolysis competent state. Furthermore, in combination with newly published data and inferences drawn from chapter 5, I can add more specifics to this model

established in chapter 3 (Wolmarans et al., 2016). My data in chapter 5 suggest that Aha1p^{C} has a role in further modulating the final rearrangements of the N-terminal domains of Hsp82p from a rotated state to the competent ATP-hydrolysis state. The final step involves rearrangements in the N-terminal domains of Hsp82p, where both the linker regions of Aha1p and Hsp82p play a role, as full binding of Aha1p results in twisting Hsp82p into the ATPase competent state (step 3). For this reason, I propose Aha1p^{C} extends to the far side of the N-terminal domain to bind in *cis*. In such a way, Aha1p binding aids in acquiring the twisted, closed state (step 3), stabilizing the ATP-competent state as Aha1p^{C} binds to the dimerized N-terminal domains of Hsp82p (Koulov et al., 2010; Retzlaff et al., 2010).

By separating the different steps of Aha1p action, it becomes clear that there are many conformations of Hsp82p that may be subject to regulation by PTMs or other co-chaperone proteins. Understanding these dynamics will allow for further dissection of the conformational transitions that are necessary for the activation of client proteins.

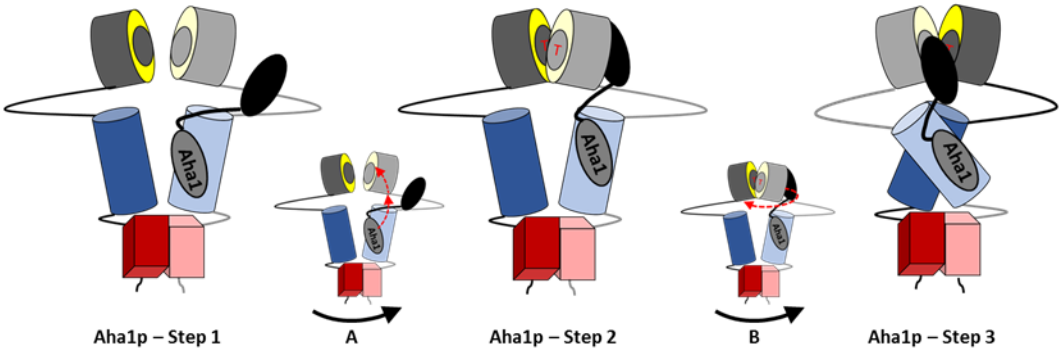

Figure 6.1 Aha1p-mediated stimulation of Hsp82p. Aha1p action consists of a 3-step process. Aha1p^{N} binds to the middle domain of Hsp82p which results in a small stimulation of Hsp82p's ATPase activity (Step 1). This binding event leads to a rearrangement in the N-terminal domain in *cis* allowing Aha1p^{C} to extend and bind to the far end of the N-terminal domain of Hsp82p in *cis* (Step 2). The third step involves final rearrangements in the N-terminal domains of Hsp82p, requiring both linker regions of Aha1p and Hsp82p to allow Aha1p to induce twisting of Hsp82p into the ATPase competent state. Aha1p stabilizes the competent state as Aha1p^{C} can bind to the dimerized N-terminal domains of Hsp82p, leading to robust ATP hydrolysis (Step 3). The red arrows in (A) and (B) indicate the type of rearrangement occurring as a consequence of the previous step. Red arrows in (A) indicate the rearrangement in the N-terminal domain in *cis* due to binding to the middle domain and that this rearrangement requires the linker of Hsp82p. The red arrow in (B) indicate the motion of the N-terminal domains, as Aha1p^{C} induces the closed conformation.

6.1.2 Aha1p and Sba1p interplay

Aha1p and Sba1p interaction was assessed in all my projects in order to determine the interplay of these co-chaperones and to bring insight into how they act within the ATPase cycle of Hsp90. Aha1p and Sba1p are late acting co-chaperones and involved in the progression of the Hsp90 cycle, but it is not known whether Sba1p or Aha1p is primarily responsible for advancing the cycle past the Sti1p-bound conformation. It has been speculated that Sba1p enters the cycle before Aha1p (Bracher and Hartl, 2006; Li et al., 2011), while other studies suggested that Sba1p functions later in the cycle (Li et al., 2011; Li et al., 2012; Panaretou et al., 2002). The most recently published model suggest that Sba1p acts after Aha1p by demonstrating that Aha1p is partially released in a nucleotide-dependent manner by Sba1p in AUC experiments (Li et al., 2013).

6.1.2.1 Hsp90 linker truncation promotes Aha1p and Sba1p binding

Daturpalli *et al.* show that the rotated state of Hsp82p (where residue E57 on each subunit are close together) is easily accessible in the apo state, in the absence of co-chaperones. Furthermore, they show that Sba1p was unable to stabilize the closed conformation, and thus, not able to prevent crosslinking of E57C, despite the fact that Sba1p was shown to stabilize the closed conformation based on the crystalized Sba1p-Hsp82p structure (Alfredson et al., 2006; Ali et al., 2006). It was observed, however, that Aha1p can impair the rotated state as it stabilizes the closed conformation (Figure 5.7B), suggesting that Aha1p is responsible for imparting directionality to the cycle towards the ATP-hydrolysis competent state. My data from chapter 5 suggests that Aha1p induces a conformation that enables Sba1p to bind, thereby allowing Sba1p to inhibit the ATPase activity of Hsp82p in the presence of Aha1p with increased efficiency.

Whether Sba1p binding results in immediate displacement of Aha1p has not been addressed with the Hsp82p linker truncations in the recent publications by Jahn *et al.* or Daturpalli *et al*., but FRET analysis shows that Sba1p competition leads to the dissociation of Aha1p (Li et al., 2013). It is possible, however, that Sba1p binds to the opposite dimerized interface, across from Aha1p, forming a

transient ternary-complex (Sba1p-Hsp82p-Aha1p) (Figure 6.2). In this scenario, the bound Sba1p inhibits the Aha1p-mediated stimulation of the ternary complex. If one Aha1p molecule, acting in *cis*, is involved in rearrangements that lead to a stabilized N-terminal dimerized state, it is possible that Sba1p binding may be primed on the opposite dimerized surface, forming a short-lived transient conformation (Figure 6.2).

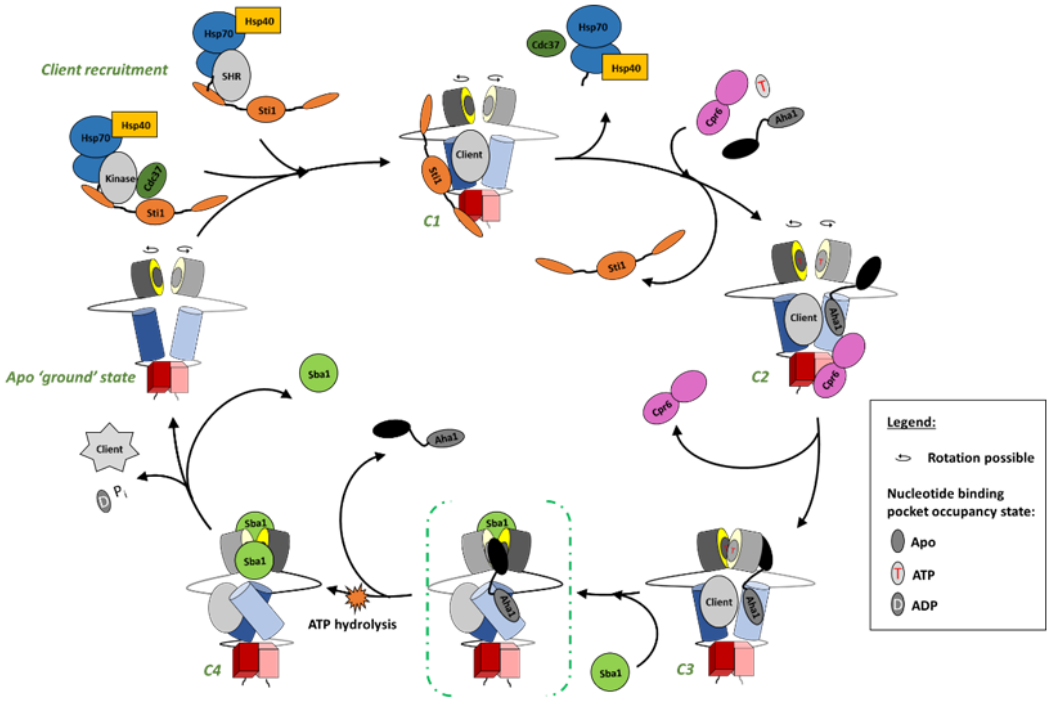

Figure 6.2 Aha1p and Sba1p binding in the late stages of the Hsp90 ATPase cycle. Sti1p inhibits the ATPase activity of Hsp82p by stabilizing the open conformation (C1). Sti1p is cooperatively displaced by Cpr6p, Aha1p, and ATP (C2). Aha1p 'action' first occurs through binding of Aha1p^{N} to the middle domain of Hsp82p, which results in N-terminal rearrangements in *cis* (C3). This rearrangement leads to a conformation that favors Sba1p binding (C4). From C3→C4, I propose a short-lived transient conformation may be acquired, where Aha1p and Sba1p binds at the same time, possibly both contributing to the acquisition or stabilization of the closed state (green brackets). Sba1p displaces Aha1p (C4), and prolongs the closed conformation. Rotation of the N-terminal domains of Hsp82p to the rotated state can occur freely where indicated by the circling arrows above the dimer. The orange star indicates when ATP hydrolysis occurs within the cycle. Ground state and *C1-C4* indicate the different conformational states of Hsp82p previously identified and described in literature.

6.1.2.2 SUMOylation of Hsp90 promotes binding of Aha1p but not Sba1p

Additionally, data discussed in chapters 3, 4, and 5 bring some insight into the effect of Hsp82p SUMOylation on Aha1p stimulation and Sba1p inhibition. It is possible that Aha1p^{N} binding to the middle domain of Hsp82p (which results in a large chemical shift that is observed for Lys178 in the N-terminal domain) may lead to SUMOylation of Lys178 that allow for Aha1p^{C} to bind. This would explain the asymmetric nature of the PTM; Aha1p^{N} binding to one subunit results in SUMOylation of that subunit or SUMOylation of a subunit recruits Aha1p binding to that subunit. This would also explain the increased affinity that Aha1p has for SUMOylated Hsp82p which has been observed *in vivo* (Mollapour et al., 2014). My data from chapter 4 also suggests that Sba1p inhibition is impaired when SUMOylated Hsp82p is stimulated by Aha1p. As discussed earlier, SUMOylation may have an important role in regulating the kinetics of the ATPase cycle. The purpose of the SUMO modification may be to accelerate the cycle by recruiting Aha1p and disfavoring Sba1p inhibition.

It is important to remember, however, that in the *in vitro* SUMOylation experiments, both subunits were SUMOylated, and thus, my data more specifically shows dually SUMOylated Hsp82p interferes with Sba1p inhibition. Considering no difference was evident in the recovered complexes of SUMOylated Hsp82p *in vivo*, one possible explanation for the reduction in Sba1p inhibition is that Sba1p can only inhibit hemi-SUMOylated Hsp82p. This hypothesis can be tested using a heterodimer ATPase strategy, where one subunit is SUMOylated and is mixed with an ATPase dead subunit that harbors the V391E (block Aha1p binding) and D79N mutations (Figure 6.3A). This will specifically test if Sba1p can inhibit the hemi-SUMOylated Hsp82p dimer. The reciprocal assay can also be conducted, where Aha1p is forced to bind to the D79N subunit to determine if Sba1p has a preference from which subunit it inhibits the ATPase activity of Hsp82p (Figure 6.3A). Upon titration of Sba1p, I predict hemi-SUMOylated Hsp82p to be similarly inhibited by Sba1p as wildtype Hsp82p (Figure 6.3B). Another possible explanation could be that once Aha1p^{C} binds to the SUMOylated N-terminal domain, deSUMOylation

is required after Aha1p action to allow binding of Sba1p. If this is the case, Sba1p inhibition of the simulated rate will still be impaired.

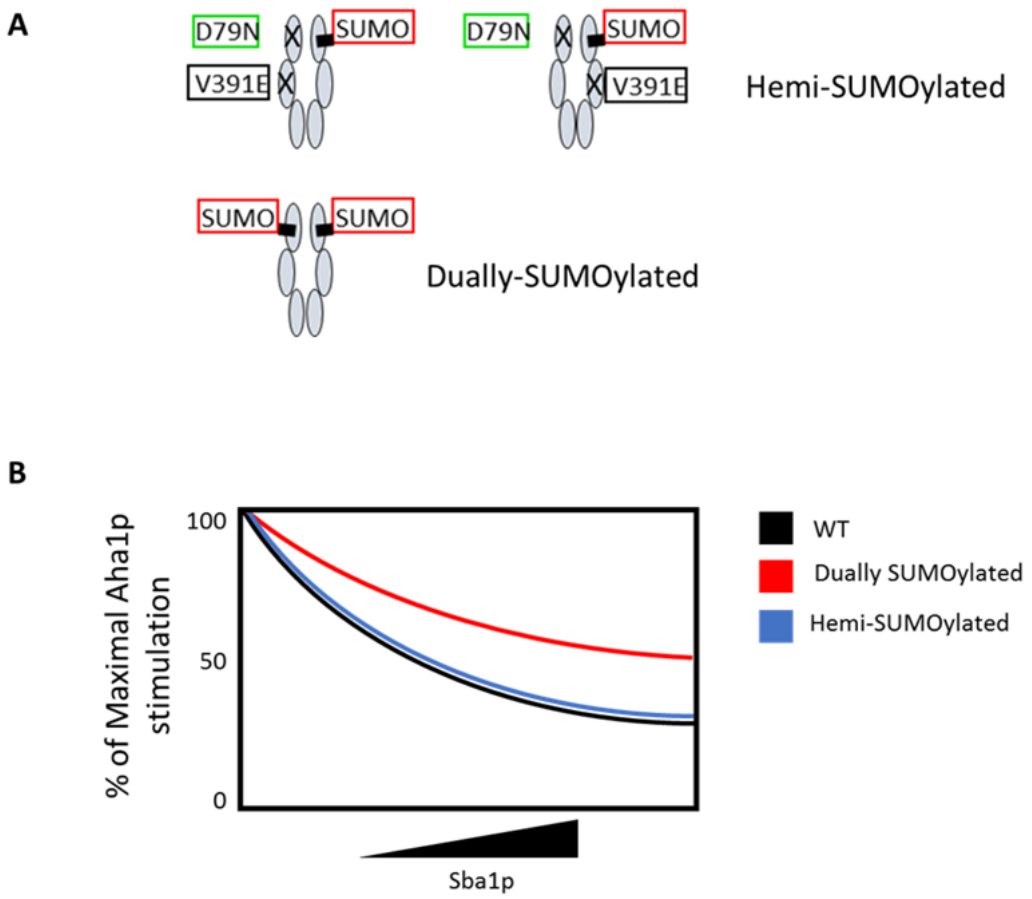

Figure 6.3 Testing Sba1p inhibition of hemi-SUMOylated Hsp82p stimulated by Aha1p. A. Hemi-SUMOylated Hsp82p dimers are formed by either mixing excess Hsp82p$^{D79N/V391E}$ with Hsp82p^{K178C}-Smt3p^{Cys} or mixing excess Hsp82p^{D79N} with Hsp82p$^{V391E/K178C}$-Smt3p^{Cys}. Dually-SUMOylated Hsp82p can also be tested harboring D79N and/or V391E subunits, which represent proper controls **B.** Hypothetical ATPase result, showing that Sba1p can inhibit hemi-SUMOylated Hsp82p, but not dually-SUMOylated Hsp82p to the same degree as wildtype Hsp82p.

6.1.3 Aha1p and Sti1p interplay

Sti1p binds to the MEEVD peptide, and effectively inhibits the ATPase activity of Hsp82p by stabilizing the open conformation (Richter et al., 2003). It is well established that one molecule of Aha1p is sufficient for maximal ATPase stimulation and for displacement of Sti1p in a cycling reaction in cooperation with Cpr6p (Li et al., 2013; Retzlaff et al., 2010). The nature of displacement, however, has not been fully characterized. It has been shown that Cpr6p cannot displace Sti1p but rather forms a ternary complex with Hsp82p (Li et al., 2013). Thus, Cpr6p binds to the opposite subunit that Sti1p binds to I demonstrated that the C-terminal domain of Aha1p is necessary for the displacement of Sti1p, but it is not known to which subunit Aha1p binds. How this displacement occurs can be elucidated by introducing the Hsp82p MEEVD deletion mutant in heterodimer ATPase assays, alongside other Hsp82p mutants to restrict Aha1p binding. First I would show displacement of Sti1p is altered when using Hsp82p:Hsp82p$^{\Delta MEEVD}$ heterodimers. Because Sti1p has such a high affinity for Hsp82p, it will be interesting to see whether displacement of Sti1p occurs when there is only one MEEVD motif present in the dimer. Although the MEEVD motif is the main binding site for both Cpr6p and Sti1p, Sti1p still interacts with Hsp82p by means of other domains, but with much lower affinity (Scheufler et al., 2000). Given that it is not known if Cpr6p binds to other regions of Hsp82p, as Cpr6p did not stably interact with Hsp82p$^{\Delta MEEVD}$, if displacement of Sti1p occurs it would suggest that Cpr6p may bind other regions of Hsp82p (Scheufler et al., 2000). Once a cycling reaction is established, I would then introduce the V391E mutation to block Aha1p binding in *cis* or *trans* to the MEEVD motif to further dissect how Aha1p, along with Cpr6p, displace Sti1p.

6.1.4 Aha1p recruitment to Hsp82p by post-translational modifications

The role of post translational modifications (PTMs) must be considered, for they allow the engagement of binding partners, affect activity of the target protein, and/or alter target protein localization. Studies of Hsp90 *in vivo* have revealed PTMs impart an even greater complexity to the manner in which Aha1 exerts its

effect on Hsp90. As mentioned before, phosphorylation and/or SUMOylation of Hsp90 appears to be a requirement for, or at least stabilize, the interaction between Aha1 and Hsp90 *in vivo* (Mollapour et al., 2014; Mollapour and Neckers, 2011; Mollapour et al., 2010). Phosphorylation of threonine 22 in Hsp82p appears to be required for interaction with Aha1p *in vivo*, however, an *in vivo* immunoprecipitation of the phosphomimetic version of Hsp82p (T22E) did not coprecipitate Aha1p (Mollapour and Neckers, 2011). Similarly, preventing phosphorylation of Hsp82p at tyrosine 24 also prevents Aha1p interaction *in vivo*, but a phosphomimetic substitution at that site (Y24E) lacks ATPase activity (Mollapour et al., 2010). How can an ATPase modifier be recruited to Hsp90 if it does not have ATPase activity? Because these studies were done where both protomers are modified (phosphomimetic), a highly plausible explanation for these observations is that these modifications occur asymmetrically, like it has been shown for SUMOylation (Mollapour et al., 2014).

There has been no examination of the interplay of these different PTMs and how they recruit Aha1p alone or together. Given the substoichiometric levels of co-chaperones to the expression levels of Hsp90 (Ghaemmaghami et al., 2003), it is reasonable that not all these modifications of Hsp90 occur at the same time. Instead, it is more probable that different pools of Hsp90 species exist that are differently modified and regulated. Considering the modular nature of Aha1p binding, it is also reasonable to hypothesize that these PTMs may enhance or restrict the action of one or both domains of Aha1p in a subunit-specific fashion. Analysis of the NMR data, in Section 3.2.4, revealed that Aha1p^{N} binding to the middle domain of Hsp82p elicited a significant chemical shift change for Lys178 in the N-terminal domain, the site of SUMOylation. This was one of the two residues that shifted more than 1 standard deviations (σ) upon Aha1p^{N} binding, compared to the 12 residues than slightly shifted upon Hch1p binding. The binding of Aha1p appears to result in specific N-terminal rearrangements which involves the asymmetric SUMOylation of Lys178 (Mollapour et al., 2014; Wolmarans et al., 2016). Unfortunately, Thr22 and Tyr24 could not be assigned in our NMR spectra. Understanding the mechanism of Aha1p stimulation, and having the tools to dissect

the asymmetric nature of Hsp82p, allows new questions to be proposed to further elucidate how PTMs modify the action of Aha1p. For example, Hsp82p SUMOylation can be further characterized as it is not known which subunit of an asymmetrically SUMOylated dimer is bound by Aha1p^{N}. Our results suggest that this modification would be specific to one subunit. To investigate this, SUMOylated Hsp82p^{V391E} could be mixed with Hsp82p^{D79N} or SUMOylated Hsp82p^{D79N} could be mixed with Hsp82p^{V391E}, to form SUMOylated-Hsp82p^{V391E}:Hsp82p^{D79N} and SUMOylated-Hsp82p^{D79N}:Hsp82p^{V391E} heterodimers, respectively. I could then assess whether Aha1p action occurs from the non-SUMOylated or SUMOylated Hsp82p subunit. The next step towards further characterizing co-chaperone regulation *in vitro* would be to introduce the various PTMs, using the phosphomimetic and non-phosphomimetic mutants. These PTMs will be strategically placed on one subunit or the other, and in combination with SUMOylated Hsp82p, in a heterodimeric context to be assessed in ATPase assays.

The true biological significance of Aha1p interaction with Hsp82p *in vivo* remains unclear. As previously mentioned, different pools of Hsp90 exist and co-chaperones are differentially recruited to these. Furthermore, literature suggests that the different modifications of Hsp82p may be dependent on the client bound. My *in vitro* results show how a couple co-chaperones regulate Hsp82p when they are in direct competition with each other. Thus, it is difficult to assess how post-translational modifications, like SUMOylation, affect co-chaperone dynamics without in depth characterization of all PTMs in the presence of other co-chaperone proteins. More work is required to understand the relationship between PTMs of Hsp90 and co-chaperone function. Experiments such as those outlined above would be the start to unraveling how PTMs specifically and asymmetrically functionalize one subunit and how that relates to altering the mechanism of action and regulation of Hsp90.

6.2 Undocking of the Hsp82p linker

It was demonstrated that docking of the linker occurs in both the open and closed conformation of Hsp82p (Figure 5.8) (Jahn et al., 2014). Revisiting the published results of the Hsp82p linker truncation mutants reveals somewhat opposing results. FRET analysis revealed that Hsp82p$^{\Delta 211\text{-}266}$ could not undergo N-terminal dimerization, yet it displayed roughly the same intrinsic rate as Hsp82p$^{\Delta 211\text{-}263}$ which could N-terminally dimerize (Daturpalli et al., 2017; Hainzl et al., 2009).

Interestingly, when heterodimers consisting of wildtype Hsp82p and Hsp82p$^{\Delta 211\text{-}266}$ were subject to FRET analysis, the heterodimers preferred an N-terminally dimerized conformation compared to homodimers of wildtype Hsp82p (Jahn et al., 2014). This may be a clue into how Hsp82p is initiated to undergo conformational rearrangements necessary to reach the closed state. Hsp82p linker truncations favor the rotated, undocked state and since residues 211-263 are required for docking (Jahn et al., 2014), it would seem that undocking, asymmetrically in this scenario (Hsp82p^{WT}:Hsp82p$^{\Delta 211\text{-}266}$), is driving the closed conformation. Knowing that the linker of Hsp82p is required for accessing the Aha1p-bound closed conformation, since Hsp82p$^{\Delta 211\text{-}266}$ could not be stabilized in the closed conformation or be stimulated by Aha1p (Daturpalli et al., 2017; Hainzl et al., 2009), I predict that asymmetric undocking of the Hsp82p linker is required for Aha1p action. If this is true, then it may explain why Aha1p could bind but not stabilize Hsp82p$^{\Delta 211\text{-}266}$, because both linkers were deleted. Support for asymmetry within the Hsp90 dimer has been documented in how Hsp90 hydrolyze ATP, interact with co-chaperones, as well as forming an asymmetric dimerized conformation (Lavery et al., 2014; Mishra and Bolon, 2014; Mollapour et al., 2014; Retzlaff et al., 2010). Thus, further investigation is required to assess this asymmetric action of undocking.

I propose that Aha1p^{N} binding leads to undocking of the linker or is part of Aha1p action in step 1 (Figure 6.1). This hypothesis can be tested by forming heterodimers harboring the linker mutant (Δ211-266) with the D79N mutation on

one subunit and V391E on the other. It was reported that Hsp82p$^{\Delta 211\text{-}266}$ had 1/5 of the intrinsic rate of wildtype Hsp82p, which is extremely low, but incorporation of the ATPase-dead Hsp82p mutant, D79N, on the same subunit as the linker deletion will ensure it does not interfere with the ATPase readout. Mixing excess of the ATPase dead subunit harboring the double mutant (D79N/Δ211-266) with the V391E subunit, will produce heterodimers that can bind Aha-type co-chaperones in *cis* to the linker deletion (Figure 6.4). I predict that the intrinsic rate will be higher than that of wildtype Hsp82p because one subunit is 'undocked', which has been previously shown to favor a closed conformation (Figure 6.4) (Jahn et al., 2014). I also hypothesize that upon Aha1p titration, stimulation will be recovered, compared to zero Aha1p-mediated stimulation with Hsp82p$^{\Delta 211\text{-}266}$ (Figure 6.4) (Daturpalli et al., 2017; Jahn et al., 2014; Retzlaff et al., 2010). Furthermore, titration of Aha1p^{N} and Hch1p will not increase from the already increased intrinsic rate because the 'undocked' subunit results in a conformation that bypass the stimulations of Aha1p^{N} and Hch1p (Figure 6.4). With the reciprocal assay, heterodimers harboring the triple mutant (D79N, V391E and the linker deletion) on one subunit and wildtype Hsp82p on the other will also have an increased intrinsic rate, but will not be stimulated by Aha1p (Figure 6.4).

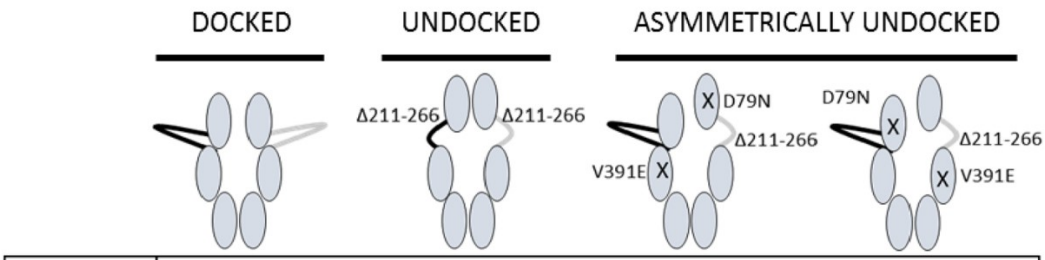

Intrinsic Rate	wt	↓	↑	↑
Aha1p Stimulation	✓	x	✓	x
Aha1p^{N} Stimulation	✓	x	x	x

Figure 6.4 Testing the involvement of Aha1p^{N} in undocking the linker of Hsp82p asymmetrically to drive ATPase stimulation. Structural representation and hypothetical ATPase assay results of the intrinsic, Aha1p stimulated, and Aha1p^{N} stimulated (or Hch1p stimulated) ATPase rates of wildtype Hsp82p, Hsp82p$^{\Delta 211\text{-}266}$, Hsp82p$^{D79N/\Delta 211\text{-}266}$:Hsp82p^{V391E}, and Hsp82p:Hsp82p$^{D79N/V391E/\Delta 211\text{-}266}$ heterodimers.

6.3 Subpopulations of Hsp90 complexes that can be targeted with Hsp90 inhibitors

The Hsp90 system is regulated by the client it activates, co-chaperone interactions, and a multitude of PTMs - all of which shift and alter the conformational equilibria of Hsp90 - during the progression of its ATPase cycle (Martinez-Yamout et al., 2006). It is becoming clear that some co-chaperones are recruited and that this recruitment is dependent on PTMs (Mollapour et al., 2014; Mollapour and Neckers, 2011; Mollapour et al., 2010). Specific co-chaperones are required at specific times during the maturation of certain clients and those which can simultaneously bind are illustrated in Figure 6.5A (Mayer and Le Breton, 2015). This figure also vividly illustrates the magnitude by which Hsp90 is in excess to all the co-chaperones (Figure 6.5B). Aha1p, for example, is expressed at a 10-fold lower concentration than Hsp82p (Ghaemmaghami et al., 2003). This figure is also meant to invoke the idea that many different pools, or subpopulations, of Hsp82p exists in the cell that are all chaperoning different clients and are regulated by different co-chaperones.

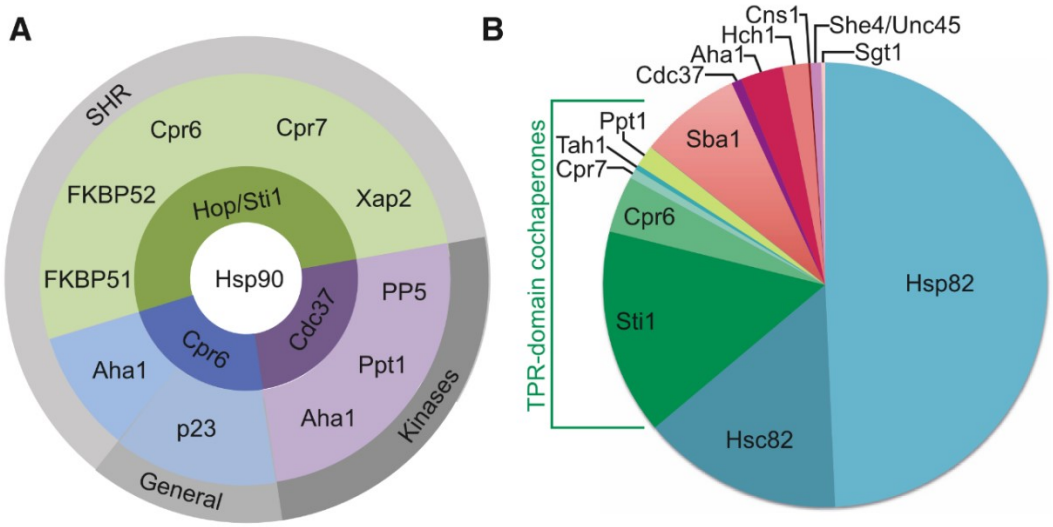

Figure 6.5 Overview of Hsp90 co-chaperones. A. Co-chaperones that can simultaneously bind to Hsp90 during the maturation of kinases, steroid hormone receptors, and other Hsp90 client. **B.** Relative abundance of co-chaperones and Hsp90 in yeast (Ghaemmaghami et al., 2003). Reprinted from Molecular Cell, Vol 58, Mayer M.P. and Le Breton L., Hsp90: Breaking the Symmetry, pg 8-20, 2015, with permission from Elsevier.

The concept of different subpopulations of Hsp90 becomes important when trying to understand how Hsp90 inhibitors function within the cell. In the cell, some Hsp90 are in complex with co-chaperones and clients but there is also another pool of Hsp90 that are in an unbound or 'free' state. It is thought that 'free' Hsp90 can easily bind the Hsp90 ATP-competitive inhibitors. Once Hsp90 binds these inhibitors, Hsp90 is converted into a 'non-functional' Hsp90 pool. These inhibitors prevent Hsp90 from maturating and stabilizing its clients, leading to their degradation (Whitesell and Lindquist, 2005; Whitesell et al., 1994).

It has also been shown, however, that drugs can compete with ATP for binding to an Hsp90 pool that is modified, either by co-chaperones or PTMs like SUMOylation (Mollapour et al., 2014). Altering the mechanism of drug sensitivity in Hsp90 by co-chaperone regulation was shown with Sti1p and Hch1p (Armstrong et al., 2012; Piper et al., 2003). PTMs also influence the mechanism of drug sensitivity in Hsp90 (Mollapour et al., 2014; Mollapour et al., 2010; Mollapour et al., 2011b). The PTMs that recruit Aha1p to Hsp82p are not 'free' but are active within the cycle, chaperoning a client. Conformations associated with these PTMs are identified as Hsp90 conformations to which Hsp90 inhibitors can bind, and understanding how they confer sensitivity is critical for the further advancement of therapeutics against Hsp90.

Mollapour *et al.* show that ATP binding is a prerequisite for SUMOylation of Lys178 and that this PTM is associated with Aha1p recruitment (Mollapour et al., 2014). Increased SUMOylation is also associated with increased sensitivity to Hsp90 inhibitors which means that Hsp90 inhibitors compete with ATP for binding, prior to closure of the ATP lid (Mollapour et al., 2014). This suggests that Hsp90 inhibitors must bind prior to full Aha1p action, for Aha1p stabilization results in ATP lid closure and commitment to hydrolysis. If indeed Aha1p induces the twisted conformation that promotes Sba1p binding, then the conformation that results in step 1 or 2 of Aha1p action (Figure 6.1) may represent the last conformational state that can be targeted by Hsp90 inhibitors.

With the understanding that various subpopulations of Hsp90 exists and that the regulatory effects of co-chaperones are dependent on PTMs, the questions

become: Are all known modifications of Hsp90 required for every client within a single ATPase cycle and are these modifications temporal in nature? Or are they dependent on the workload of the cell and on the client bound? It is unlikely that the modifications are universal for all clientele, but with so many PTMs identified, it is probable that multiple modifications occur on the same Hsp90 molecule. PTMs is a way to regulate directionality within the cycle and I propose that certain PTMs, which are shown to regulate Aha1 interaction with Hsp90, may cooperate temporally together.

As previously mentioned in Section 6.1.4, phosphorylation of T22 and SUMOylation of K178 are involved in recruiting Aha1p (Mollapour et al., 2014; Mollapour et al., 2011a). Interestingly, when expressed in yeast as the sole source of Hsp82p, the phosphomimetic mutant, T22E, resulted in an increase in drug sensitivity to Hsp90 inhibitors (Mollapour et al., 2011a). They demonstrate that ATP binding is a prerequisite for T22 phosphorylation (Mollapour et al., 2011a), and thus, this would suggest that T22 phosphorylation would occur prior to Aha1p action (before the lid is closure), similarly to SUMOylation of K178 (Mollapour et al., 2014). Taking these data together with my findings in chapter 3, if T22 phosphorylation and K178 SUMOylation do in fact occur within the same subpopulation pool of Hsp82p, it may be that Aha1p is recruited upon phosphorylation of T22, leading to $Aha1p^{N}$ binding and subsequent SUMOylation of K178. Dephosphorylation of T22 is most likely required before hydrolysis takes place as its been shown that the phosphomimetic mutation, T22E, interfere with the hydrophobic interaction that is required for N-terminal dimerization (Mollapour et al., 2011b). Altogether, this points to a brief conformational transition of Hsp82p, after SUMOylation and phosphorylation of T22, but before commitment to hydrolysis, that can be targeted by Hsp90 inhibitor drugs (Figure 6.6). By incorporating the various PTMs that affect Aha1p recruitment into heterodimer ATPase assays, it is possible to further pinpoint the Hsp90 conformations that inhibitors can bind to.

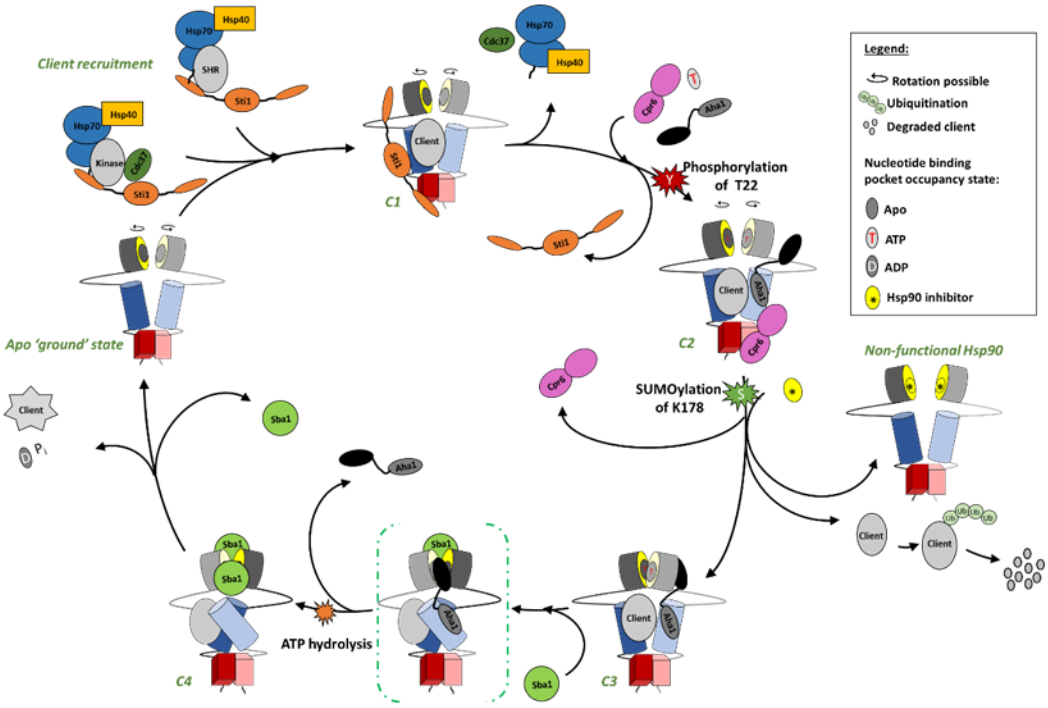

Figure 6.6 Hsp82p ATPase cycle with incorporation of Hsp90 inhibitors and PTMs. Inhibition of Hsp82p results in a non-functional Hsp82p, leading to client degradation by the ubiquitin-proteasome pathway. The red star indicates where phosphorylation of T22 potentially occurs, and the green star indicates where SUMOylation of K178 potentially occurs. The orange star indicates when ATP hydrolysis occurs within the cycle. Hsp90 inhibitor, shown as a yellow molecule with a star, competes with ATP for binding to the N-terminal nucleotide binding pocket, prior to lid closure. Ground state and *C1-C4* indicate the different conformational states of Hsp82p previously identified and described in literature.

6.4 Crystallography trials: Aha1p-Hsp82p complex

One of the major problems we face in the Hsp90 field is that a complete visual representation of Hsp90 has yet to be revealed. Hsp90 is a dynamic chaperone that undergoes large quaternary conformational rearrangements. In order to be crystallized, a protein needs to be in a stable conformation. Sba1p and Aha1p are two co-chaperone proteins that have been shown to stabilize the N-terminally dimerized conformation. Thus, forming Hsp82p complexes with either of these two co-chaperones present possible avenues to pursue structural studies with. The only full-length structure that is available of Hsp82p is in complex with Sba1p. This complex was stabilized and resolved because of two main mutations: an A107N mutant of Hsp82p was used that also stabilizes a N-terminally dimerized conformation, and majority of the linker region of Hsp82p was deleted which restricted the conformational flexibility of Hsp82p (Ali et al., 2006). This structure has since been implicated as the ATP-hydrolysis competent state, but how Hsp90 hydrolyzes ATP is still not fully understood (Graf et al., 2014). We do know how Aha1p^{N} interacts with the middle domain of Hsp82p, but it is not clear how the C-terminal domain of Aha1p interacts with the dimerized N-terminal domains (Meyer et al., 2004a).

My work has identified candidate complexes which stabilizes the Aha1p-Hsp82p interaction, keeping it in a more restricted conformation that can potentially be crystalized. My results show that SUMOylated Hsp82p^{K178C} results in an increased apparent affinity for Aha1p. I have also demonstrated that Hsp82p linker truncation, Hsp82p$^{\Delta 211\text{-}263}$, has an enhanced binding affinity for Aha1p. Using SUMOylated Hsp82p^{K178C} or Hsp82p$^{\Delta 211\text{-}263}$ presents a good strategy to crystalize a stabilized complex with Aha1p. I propose structural studies with these candidate Hsp82p-Aha1p complexes will be a promising avenue to pursue to gain functional insight into how Aha1p regulate/stimulate the ATPase activity of Hsp82p.

6.5 The closed, N-terminally dimerized conformation

Daturpalli *et al.* demonstrated that the N-terminal of Hsp82p can rotate 180º from the conformation illustrated by the Hsp82p-Sba1p dimer structure (Ali et al., 2006; Daturpalli et al., 2017). They reached this conclusion because they were able to crosslink residues E57C, which are on the outside of the N-terminal domains in the Hsp82p-Sba1p structure, to one another, reducing the distance between those residues from 79.9 Å to 13 Å or less.

Interestingly, N-terminal dimerization is determined by using residues close to E57, specifically D61 and I66, in FRET assays (Figure 6.7A). FRET analysis has been widely used to determine the proximity between the N-terminal domain in one subunit and the middle domain of the opposite subunit in the dimer, and how N-terminal dimerization changes with the addition of different co-chaperones. By differentially labelling D61C and E333C/E385C Hsp82p variants with donor and acceptor fluorescent dyes (respectively), heterodimers were formed and tested for the emergence of a FRET signal (Figure 6.7B) (Hessling et al., 2009; Jahn et al., 2014). Hainzl *et al.* conducted similar analysis by using I66C and E381C (Figure 6.7C) (Hainzl et al., 2009). FRET signaling occurs between two fluorophore conjugates when they are in close proximity, between 10-100 Å, depending on the spectral characteristics of the dyes selected (Ha et al., 1996; Leavesley and Rich, 2016; Weiss, 1999; Xiao and Ha, 2017). This raises the question of whether this type of analysis can only differentiate between Hsp82p adopting an open and any type of closed conformation. When a FRET signal is detected between donor and acceptor dyes attached to D61C and E333C (55.1 Å apart), D61C and E385C (40.8 Å apart), and I66 and E381 (37.5 Å apart), it may not necessarily mean Hsp82p is adopting an ATPase-competent conformation. It could suggest that the Hsp82p in question is forming the closed conformation (as visualized by the Hsp82p-Sba1p dimer structure), but it is also possible that Hsp82p is acquiring the rotated conformation.

Comparing how the FRET signal changes upon co-chaperone additions or different ATP analogs can provide a comprehensive picture of the different states

Hsp82p acquires. Caution is needed when interpreting FRET signals, so that a 'closed, N-terminally rotated state' is not mistakenly understood as a 'closed, N-terminally dimerized and ATPase competent' state. Also, caution is required to not translate FRET signal to mean that Hsp82p acquires the closed conformation as visualized by the Sba1p-Hsp82p crystal structure. Furthermore, because the N-terminal domains can rotate 180º, the flexibility that exist between the N-M domains must be considered. It is, therefore, important to support the FRET data with more biochemical analysis to investigate the nature of the N-terminally dimerized state of the Hsp82p construct in question. Analyses that have supported FRET findings have measured the affinity for ATP and the ATPase rate as well as assessed the co-chaperone interactions by AUC (Jahn et al., 2014). All of this data together will provide a more comprehensive assessment of how these different structural components influence and regulate the ATPase-competent conformation of Hsp82p and co-chaperone regulation.

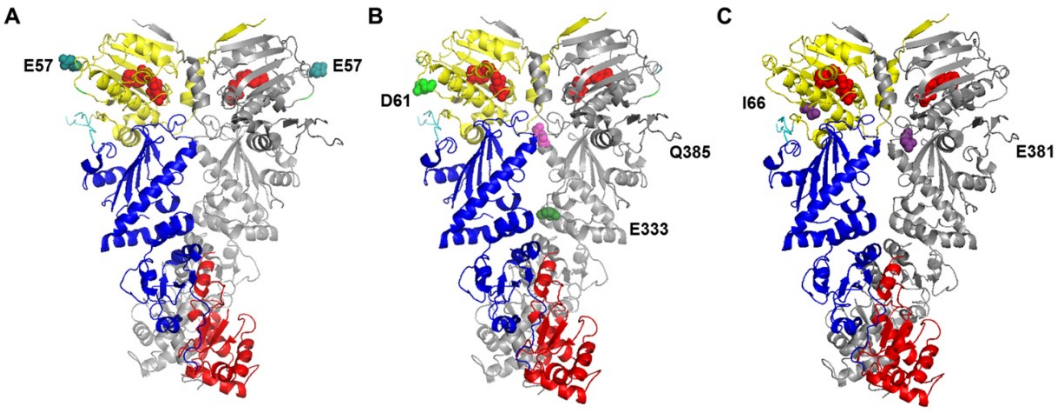

Figure 6.7 Residues used in crosslinking and FRET assays. Cysteine residues were engineered at position E57 for crosslinking experiments (Daturpalli et al., 2017) **(A)**, positions D61 and Q385 or E333 for FRET analysis (Hessling et al., 2009; Jahn et al., 2014) **(B)**, and at positions I66 and E381, also for FRET analysis (Hainzl et al., 2009) **(C)**. The crystal structure was modified using the PDB file 2CG9 (Ali et al., 2006).

6.6 Determining the K_M values for SUMOylated Hsp82p to investigate the mechanism of co-chaperone switching

I established a system to study the enzymology of a SUMOylated Hsp82p, *in vitro,* in a site-specific way. I would next like to investigate and determine the K_M values, with and without different co-chaperones, for SUMOylated Hsp82p. SUMOylated Hsp82p, which has been shown to recruit Aha1p (Mollapour et al., 2014), has a reduced V_{MAX} in the presence of Aha1p. It is not known whether this reduced rate is because SUMO is affecting the catalytic efficiency or substrate release (K_M). Interestingly, the modification did not affect co-chaperone switching. By determining the K_M values, I can start to piece together what is necessary for co-chaperone switching. My findings in chapter 5 indicate that there is a conformation of Hsp82p that results in increased substrate/product release which can increase the cycling reaction of Hsp82p. This led me to ask whether co-chaperone switching has anything to do with acquiring this conformation that can release substrate faster, and thus, make the cycling reaction faster. Analyzing how co-chaperone regulation is altered with SUMOylated Hsp82p^{K178C}, and also by determining how the K_M values of these reactions are altered, will undoubtedly bring insight into how the Hsp82p cycle is regulated. This style of analyses can also be completed with phosphomimetic Hsp82p constructs, to dissect how these PTMs influence the cycling of co-chaperones and the Hsp82p cycle.

6.7 Client activation: Regulated by functionalized Hsp82p subunits and dwell times in certain conformations

It is becoming clear that asymmetric interactions determine many conformational states of Hsp90. Retzlaff and colleagues proposed an asymmetric model where subunits are ‘functionalized’ (Retzlaff et al., 2010). The proposal of functionalized subunits is a plausible scenario, where certain co-chaperones may regulate one subunit or the other, which may be dependent on which subunit is client-bound or is hydrolyzing. If this is the case, then which subunit is post-

translationally modified and which subunit binds co-chaperones? Throughout my discussion, I propose various experiments to answer these questions. By dissecting how asymmetric interactions regulate Hsp90 ATPase activity, a more comprehensive model can be made to include how co-chaperones cycle on and off the functionalized subunits, which will hopefully allow us better to understand how Hsp90 functions.

At the core of the Hsp90 field, which is relevant for all isoforms of Hsp90 in the various compartments in the cell, is the question of how does Hsp90 facilitate the maturation and stabilization of its client proteins? As previously mentioned, numerous studies have shown that yeast expressing Hsp82p^{E33A} (that can bind ATP, but cannot hydrolyze it) as the sole source of Hsp90 is not viable (Mishra and Bolon, 2014; Pearl and Prodromou, 2000; Prodromou et al., 1997). Recently, it was shown that Hsp82p^{E33A} can in fact support viability (Zierer et al., 2016). Although this strain is extremely sick, it is able to support viability without being able to hydrolyze ATP, suggesting that the conformations Hsp82p^{E33A} adopts are sufficient for supporting yeast cell viability (Zierer et al., 2016). Therefore, the relative time spent in certain conformations is critical for client activation. This places greater emphasis on how tightly the conformations of Hsp82p are regulated to ensure proper maturation of clients.

Aha1p stimulates the ATPase activity of Hsp82p by bypassing the rate-limiting conformation to reach the ATPase-competent conformation. By recruiting Aha1p, the cycle is presumably accelerated and does not allow for sufficient 'dwell time' required for proper maturation of these clients (Zierer et al., 2016). This is clearly shown when Aha1p is recruited to SUMOylated Hsp82p, where Aha1p interaction negatively effects the maturation of certain clients, such as CFTR, Ste11, and v-*Src* (Mollapour et al., 2014). This model fits well with the data of CFTR maturation, as it was demonstrated that Aha1 knockdown resulted in an increase in CFTR stabilization (Koulov et al., 2010; Wang et al., 2006b).

My results from chapter 5 suggest that the role co-chaperones have in regulating Hsp90 may be at the level of influencing the affinity for substrate and product (K_M). Aha1p action results in the acquisition of a second conformation that

perhaps drive the change in K_M (Figure 5.9). This change in K_M essentially reloads the reaction: Aha1p binding increases the K_M, and thus, the substrate/product can be released quickly, 'resetting' Hsp82p to partake in another cycle (Figure 5.9 – bottom panel). It is well established that rearrangements occur in response to ATP binding to the N-terminal domain and that co-chaperones guide Hsp90 through different conformational states, ultimately leading to client maturation (Siligardi et al., 2004). If substrate binding and release is basically all that is required to allow Hsp90 to move through the necessary conformations to fulfil its function in stabilizing clients, then it is plausible that the 'dwell times' of various conformations, and not ATP hydrolysis, is essential (Zierer et al., 2016).

Considering all the data, it stands to reason that the best way to get rid of a substrate is to hydrolyze it. When Hsp90 hydrolyze ATP, it allows for fast nucleotide exchange, resetting the cycle efficiently. In the case of $Hsp82p^{E33A}$, although it cannot hydrolyze ATP, ATP can still bind and dissociate which explains why this mutant can support viability as it can undergo all the necessary conformational states to mature clients. This would mean that the conformational transitions associated with co-chaperone regulation may not necessarily be just about stimulating or inhibiting the ATPase activity of Hsp90, but rather, meant to influence substrate affinity (K_M) to progress the cycle through the various states.

6.8 Conclusion

Despite immense work over the last couple of decades, many questions remain to be answered about how exactly Hsp90 hydrolyzes ATP, how co-chaperone proteins modulate the ATPase activity of Hsp90, and how the functional cycle of Hsp90 facilitate the maturation of oncogenic clients. With a mechanistic model of Aha1p-mediated stimulation and the methodologies established in this thesis, including SUMOylation and the use of multiple mutants in heterodimer ATPase assays, a foundation is set to test many specific hypotheses outlined in this discussion. As a broad future direction, it would be of great interest to determine the function of the various Hsp90 conformations, such as the docked conformation,

and determine by what mechanism this conformation actually impair or enhance Hsp90 function. By using the framework established in this thesis, it is possible to expand our knowledge about the role each of the different Hsp90 conformations have and how co-chaperone regulation influence Hsp90 activity during client activation.

References

Alfredson, H., Harstad, H., Haugen, S., and Ohberg, L. (2006). Sclerosing polidocanol injections to treat chronic painful shoulder impingement syndrome-results of a two-centre collaborative pilot study. Knee surgery, sports traumatology, arthroscopy : official journal of the ESSKA. 14(12), 1321-1326. DOI: 10.1007/s00167-006-0205-8.

Ali, M.M., Roe, S.M., Vaughan, C.K., Meyer, P., Panaretou, B., Piper, P.W., Prodromou, C., and Pearl, L.H. (2006). Crystal structure of an Hsp90-nucleotide-p23/Sba1 closed chaperone complex. Nature. 440(7087), 1013-1017. DOI: 10.1038/nature04716.

Alvira, S., Cuellar, J., Rohl, A., Yamamoto, S., Itoh, H., Alfonso, C., Rivas, G., Buchner, J., and Valpuesta, J.M. (2014). Structural characterization of the substrate transfer mechanism in Hsp70/Hsp90 folding machinery mediated by Hop. Nature communications. 5, 5484. DOI: 10.1038/ncomms6484.

Ammirante, M., Rosati, A., Gentilella, A., Festa, M., Petrella, A., Marzullo, L., Pascale, M., Belisario, M.A., Leone, A., and Turco, M.C. (2008). The activity of hsp90 alpha promoter is regulated by NF-kappa B transcription factors. Oncogene. 27(8), 1175-1178. DOI: 10.1038/sj.onc.1210716.

Anfinsen, C.B. (1973). Principles that govern the folding of protein chains. Science. 181(4096), 223-230.

Armstrong, H., Wolmarans, A., Mercier, R., Mai, B., and LaPointe, P. (2012). The co-chaperone Hch1 regulates Hsp90 function differently than its homologue Aha1 and confers sensitivity to yeast to the Hsp90 inhibitor NVP-AUY922. PloS one. 7(11), e49322. DOI: 10.1371/journal.pone.0049322.

Babic, I., Cherry, E., and Fujita, D.J. (2006). SUMO modification of Sam68 enhances its ability to repress cyclin D1 expression and inhibits its ability to induce apoptosis. Oncogene. 25(36), 4955-4964. DOI: 10.1038/sj.onc.1209504.

Bandhakavi, S., McCann, R.O., Hanna, D.E., and Glover, C.V. (2003). Genetic interactions among ZDS1,2, CDC37, and protein kinase CK2 in Saccharomyces cerevisiae. FEBS letters. 554(3), 295-300.

Banerji, U., O'Donnell, A., Scurr, M., Pacey, S., Stapleton, S., Asad, Y., Simmons, L., Maloney, A., Raynaud, F., Campbell, M., et al. (2005). Phase I pharmacokinetic and pharmacodynamic study of 17-allylamino, 17-demethoxygeldanamycin in patients with advanced malignancies. Journal of clinical oncology : official journal of the American Society of Clinical Oncology. 23(18), 4152-4161. DOI: 10.1200/JCO.2005.00.612.

Bansal, P.K., Abdulle, R., and Kitagawa, K. (2004). Sgt1 associates with Hsp90: an initial step of assembly of the core kinetochore complex. Molecular and cellular biology. 24(18), 8069-8079. DOI: 10.1128/MCB.24.18.8069-8079.2004.

Bergerat, A., de Massy, B., Gadelle, D., Varoutas, P.C., Nicolas, A., and Forterre, P. (1997). An atypical topoisomerase II from Archaea with implications for meiotic recombination. Nature. 386(6623), 414-417. DOI: 10.1038/386414a0.

Bettermann, K., Benesch, M., Weis, S., and Haybaeck, J. (2012). SUMOylation in carcinogenesis. Cancer letters. 316(2), 113-125. DOI: 10.1016/j.canlet.2011.10.036.

Birnby, D.A., Link, E.M., Vowels, J.J., Tian, H., Colacurcio, P.L., and Thomas, J.H. (2000). A transmembrane guanylyl cyclase (DAF-11) and Hsp90 (DAF-21) regulate a common set of chemosensory behaviors in caenorhabditis elegans. Genetics. 155(1), 85-104.

Blagg, B.S., and Kerr, T.D. (2006). Hsp90 inhibitors: small molecules that transform the Hsp90 protein folding machinery into a catalyst for protein degradation. Medicinal research reviews. 26(3), 310-338. DOI: 10.1002/med.20052.

Blaser, J., Triebel, S., and Tschesche, H. (1995). A sandwich enzyme immunoassay for the determination of neutrophil lipocalin in body fluids. Clin Chim Acta. 235(2), 137-145.

Borkovich, K.A., Farrelly, F.W., Finkelstein, D.B., Taulien, J., and Lindquist, S. (1989). hsp82 is an essential protein that is required in higher concentrations for growth of cells at higher temperatures. Molecular and cellular biology. 9(9), 3919-3930.

Bracher, A., and Hartl, F.U. (2006). Hsp90 structure: when two ends meet. Nature structural & molecular biology. 13(6), 478-480. DOI: 10.1038/nsmb0606-478.

Brinker, A., Scheufler, C., Von Der Mulbe, F., Fleckenstein, B., Herrmann, C., Jung, G., Moarefi, I., and Hartl, F.U. (2002). Ligand discrimination by TPR domains. Relevance and selectivity of EEVD-recognition in Hsp70 x Hop x Hsp90 complexes. The Journal of biological chemistry. 277(22), 19265-19275. DOI: 10.1074/jbc.M109002200.

Brinkley, M. (1992). A brief survey of methods for preparing protein conjugates with dyes, haptens, and cross-linking reagents. Bioconjug Chem. 3(1), 2-13.

Bron, P., Giudice, E., Rolland, J.P., Buey, R.M., Barbier, P., Diaz, J.F., Peyrot, V., Thomas, D., and Garnier, C. (2008). Apo-Hsp90 coexists in two open conformational states in solution. Biology of the cell. 100(7), 413-425. DOI: 10.1042/BC20070149.

Brough, P.A., Aherne, W., Barril, X., Borgognoni, J., Boxall, K., Cansfield, J.E., Cheung, K.M., Collins, I., Davies, N.G., Drysdale, M.J., et al. (2008). 4,5-diarylisoxazole Hsp90 chaperone inhibitors: potential therapeutic agents for the

treatment of cancer. Journal of medicinal chemistry. 51(2), 196-218. DOI: 10.1021/jm701018h.

Brunet Simioni, M., De Thonel, A., Hammann, A., Joly, A.L., Bossis, G., Fourmaux, E., Bouchot, A., Landry, J., Piechaczyk, M., and Garrido, C. (2009). Heat shock protein 27 is involved in SUMO-2/3 modification of heat shock factor 1 and thereby modulates the transcription factor activity. Oncogene. 28(37), 3332-3344. DOI: 10.1038/onc.2009.188.

Bryngelson, J.D., Onuchic, J.N., Socci, N.D., and Wolynes, P.G. (1995). Funnels, pathways, and the energy landscape of protein folding: a synthesis. Proteins. 21(3), 167-195. Published online 1995/03/01 DOI: 10.1002/prot.340210302.

Bryngelson, J.D., and Wolynes, P.G. (1987). Spin glasses and the statistical mechanics of protein folding. Proceedings of the National Academy of Sciences of the United States of America. 84(21), 7524-7528. Published online 1987/11/01.

Buchner, J. (1996). Supervising the fold: functional principles of molecular chaperones. FASEB J. 10(1), 10-19.

Calderwood, S.K., Khaleque, M.A., Sawyer, D.B., and Ciocca, D.R. (2006). Heat shock proteins in cancer: chaperones of tumorigenesis. Trends Biochem Sci. 31(3), 164-172. DOI: 10.1016/j.tibs.2006.01.006.

Caplan, A.J., Mandal, A.K., and Theodoraki, M.A. (2007). Molecular chaperones and protein kinase quality control. Trends in cell biology. 17(2), 87-92. DOI: 10.1016/j.tcb.2006.12.002.

Chadli, A., Bouhouche, I., Sullivan, W., Stensgard, B., McMahon, N., Catelli, M.G., and Toft, D.O. (2000). Dimerization and N-terminal domain proximity underlie the function of the molecular chaperone heat shock protein 90. Proceedings of the National Academy of Sciences of the United States of America. 97(23), 12524-12529. DOI: 10.1073/pnas.220430297.

Chen, B., Zhong, D., and Monteiro, A. (2006). Comparative genomics and evolution of the HSP90 family of genes across all kingdoms of organisms. BMC genomics. 7, 156. DOI: 10.1186/1471-2164-7-156.

Chen, S., and Smith, D.F. (1998). Hop as an adaptor in the heat shock protein 70 (Hsp70) and hsp90 chaperone machinery. The Journal of biological chemistry. 273(52), 35194-35200.

Chen, S., Sullivan, W.P., Toft, D.O., and Smith, D.F. (1998). Differential interactions of p23 and the TPR-containing proteins Hop, Cyp40, FKBP52 and FKBP51 with Hsp90 mutants. Cell stress & chaperones. 3(2), 118-129.

Chien, C.T., Bartel, P.L., Sternglanz, R., and Fields, S. (1991). The two-hybrid system: a method to identify and clone genes for proteins that interact with a

protein of interest. Proceedings of the National Academy of Sciences of the United States of America. 88(21), 9578-9582.

Chiosis, G., and Neckers, L. (2006). Tumor selectivity of Hsp90 inhibitors: the explanation remains elusive. ACS Chem Biol. 1(5), 279-284. Published online 2006/12/14 DOI: 10.1021/cb600224w.

Citri, A., Harari, D., Shohat, G., Ramakrishnan, P., Gan, J., Lavi, S., Eisenstein, M., Kimchi, A., Wallach, D., Pietrokovski, S., et al. (2006). Hsp90 recognizes a common surface on client kinases. The Journal of biological chemistry. 281(20), 14361-14369. DOI: 10.1074/jbc.M512613200.

Collins, F.S. (1992). Cystic fibrosis: molecular biology and therapeutic implications. Science. 256(5058), 774-779. Published online 1992/05/08.

Cooper, G. (2000). The Cell: A Molecular Approach (Sinauer Associates Inc: Massachusetts, USA).

Csermely, P., Schnaider, T., Soti, C., Prohaszka, Z., and Nardai, G. (1998). The 90-kDa molecular chaperone family: structure, function, and clinical applications. A comprehensive review. Pharmacology & therapeutics. 79(2), 129-168.

Cunningham, C.N., Krukenberg, K.A., and Agard, D.A. (2008). Intra- and intermonomer interactions are required to synergistically facilitate ATP hydrolysis in Hsp90. The Journal of biological chemistry. 283(30), 21170-21178. DOI: 10.1074/jbc.M800046200.

Cunningham, C.N., Southworth, D.R., Krukenberg, K.A., and Agard, D.A. (2012). The conserved arginine 380 of Hsp90 is not a catalytic residue, but stabilizes the closed conformation required for ATP hydrolysis. Protein Sci. 21(8), 1162-1171. DOI: 10.1002/pro.2103.

Daturpalli, S., Kniess, R.A., Lee, C.T., and Mayer, M.P. (2017). Large Rotation of the N-terminal Domain of Hsp90 Is Important for Interaction with Some but Not All Client Proteins. Journal of molecular biology. 429(9), 1406-1423. DOI: 10.1016/j.jmb.2017.03.025.

DeBoer, C., Meulman, P.A., Wnuk, R.J., and Peterson, D.H. (1970). Geldanamycin, a new antibiotic. The Journal of antibiotics. 23(9), 442-447.

Denison, C., Rudner, A.D., Gerber, S.A., Bakalarski, C.E., Moazed, D., and Gygi, S.P. (2005). A proteomic strategy for gaining insights into protein sumoylation in yeast. Molecular & cellular proteomics : MCP. 4(3), 246-254. DOI: 10.1074/mcp.M400154-MCP200.

Dill, K.A., and Chan, H.S. (1997). From Levinthal to pathways to funnels. Nature structural biology. 4(1), 10-19.

Dill, K.A., and MacCallum, J.L. (2012). The protein-folding problem, 50 years on. Science. 338(6110), 1042-1046. DOI: 10.1126/science.1219021.

Dinner, A.R., Sali, A., Smith, L.J., Dobson, C.M., and Karplus, M. (2000). Understanding protein folding via free-energy surfaces from theory and experiment. Trends Biochem Sci. 25(7), 331-339.

Dobson, C.M., and Ellis, R.J. (1998). Protein folding and misfolding inside and outside the cell. The EMBO journal. 17(18), 5251-5254. DOI: 10.1093/emboj/17.18.5251.

Dollins, D.E., Warren, J.J., Immormino, R.M., and Gewirth, D.T. (2007). Structures of GRP94-nucleotide complexes reveal mechanistic differences between the hsp90 chaperones. Molecular cell. 28(1), 41-56. DOI: 10.1016/j.molcel.2007.08.024.

Dunn, D.M., Woodford, M.R., Truman, A.W., Jensen, S.M., Schulman, J., Caza, T., Remillard, T.C., Loiselle, D., Wolfgeher, D., Blagg, B.S., et al. (2015). c-Abl Mediated Tyrosine Phosphorylation of Aha1 Activates Its Co-chaperone Function in Cancer Cells. Cell reports. 12(6), 1006-1018. DOI: 10.1016/j.celrep.2015.07.004.

Dutta, R., and Inouye, M. (2000). GHKL, an emergent ATPase/kinase superfamily. Trends Biochem Sci. 25(1), 24-28.

Dymock, B.W., Barril, X., Brough, P.A., Cansfield, J.E., Massey, A., McDonald, E., Hubbard, R.E., Surgenor, A., Roughley, S.D., Webb, P., et al. (2005). Novel, potent small-molecule inhibitors of the molecular chaperone Hsp90 discovered through structure-based design. Journal of medicinal chemistry. 48(13), 4212-4215. DOI: 10.1021/jm050355z.

Ebong, I.O., Morgner, N., Zhou, M., Saraiva, M.A., Daturpalli, S., Jackson, S.E., and Robinson, C.V. (2011). Heterogeneity and dynamics in the assembly of the heat shock protein 90 chaperone complexes. Proceedings of the National Academy of Sciences of the United States of America. 108(44), 17939-17944. DOI: 10.1073/pnas.1106261108.

Echeverria, P.C., Bernthaler, A., Dupuis, P., Mayer, B., and Picard, D. (2011a). An interaction network predicted from public data as a discovery tool: application to the Hsp90 molecular chaperone machine. PloS one. 6(10), e26044. DOI: 10.1371/journal.pone.0026044.

Echeverria, P.C., Forafonov, F., Pandey, D.P., Muhlebach, G., and Picard, D. (2011b). Detection of changes in gene regulatory patterns, elicited by perturbations of the Hsp90 molecular chaperone complex, by visualizing multiple experiments with an animation. BioData mining. 4(1), 15. DOI: 10.1186/1756-0381-4-15.

Eckl, J.M., and Richter, K. (2013). Functions of the Hsp90 chaperone system: lifting client proteins to new heights. International journal of biochemistry and molecular biology. 4(4), 157-165.

Ellis, E.F., Willoughby, K.A., Sparks, S.A., and Chen, T. (2007). S100B protein is released from rat neonatal neurons, astrocytes, and microglia by in vitro trauma and anti-S100 increases trauma-induced delayed neuronal injury and negates the protective effect of exogenous S100B on neurons. Journal of neurochemistry. 101(6), 1463-1470. DOI: 10.1111/j.1471-4159.2007.04515.x.

Ellis, R.J. (1996). Discovery of molecular chaperones. Cell stress & chaperones. 1(3), 155-160. Published online 1996/09/01.

Ellis, R.J. (2001). Macromolecular crowding: obvious but underappreciated. Trends Biochem Sci. 26(10), 597-604.

Ellis, R.J. (2007). Protein misassembly: macromolecular crowding and molecular chaperones. Advances in experimental medicine and biology. 594, 1-13. DOI: 10.1007/978-0-387-39975-1_1.

Ellis, R.J., and van der Vies, S.M. (1991). Molecular chaperones. Annual review of biochemistry. 60, 321-347. DOI: 10.1146/annurev.bi.60.070191.001541.

Enserink, J.M. (2015). Sumo and the cellular stress response. Cell division. 10, 4. DOI: 10.1186/s13008-015-0010-1.

Falsone, S.F., Leptihn, S., Osterauer, A., Haslbeck, M., and Buchner, J. (2004). Oncogenic mutations reduce the stability of SRC kinase. Journal of molecular biology. 344(1), 281-291. Published online 2004/10/27 DOI: 10.1016/j.jmb.2004.08.091.

Fields, S., and Song, O. (1989). A novel genetic system to detect protein-protein interactions. Nature. 340(6230), 245-246. DOI: 10.1038/340245a0.

Fields, S., and Sternglanz, R. (1994). The two-hybrid system: an assay for protein-protein interactions. Trends Genet. 10(8), 286-292.

Flom, G., Behal, R.H., Rosen, L., Cole, D.G., and Johnson, J.L. (2007). Definition of the minimal fragments of Sti1 required for dimerization, interaction with Hsp70 and Hsp90 and in vivo functions. The Biochemical journal. 404(1), 159-167. DOI: 10.1042/BJ20070084.

Flotho, A., and Melchior, F. (2013). Sumoylation: a regulatory protein modification in health and disease. Annual review of biochemistry. 82, 357-385. DOI: 10.1146/annurev-biochem-061909-093311.

Forafonov, F., Toogun, O.A., Grad, I., Suslova, E., Freeman, B.C., and Picard, D. (2008). p23/Sba1p protects against Hsp90 inhibitors independently of its intrinsic

chaperone activity. Molecular and cellular biology. 28(10), 3446-3456. DOI: 10.1128/MCB.02246-07.

Fraser-Pitt, D., and O'Neil, D. (2015). Cystic fibrosis - a multiorgan protein misfolding disease. Future Sci OA. 1(2), FSO57. Published online 2015/09/01 DOI: 10.4155/fso.15.57.

Freeman, B.C., Felts, S.J., Toft, D.O., and Yamamoto, K.R. (2000). The p23 molecular chaperones act at a late step in intracellular receptor action to differentially affect ligand efficacies. Genes & development. 14(4), 422-434.

Frydman, J., Nimmesgern, E., Ohtsuka, K., and Hartl, F.U. (1994). Folding of nascent polypeptide chains in a high molecular mass assembly with molecular chaperones. Nature. 370(6485), 111-117. DOI: 10.1038/370111a0.

Gaiser, A.M., Kretzschmar, A., and Richter, K. (2010). Cdc37-Hsp90 complexes are responsive to nucleotide-induced conformational changes and binding of further cofactors. The Journal of biological chemistry. 285(52), 40921-40932. DOI: 10.1074/jbc.M110.131086.

Gareau, J.R., and Lima, C.D. (2010). The SUMO pathway: emerging mechanisms that shape specificity, conjugation and recognition. Nature reviews. Molecular cell biology. 11(12), 861-871. DOI: 10.1038/nrm3011.

Geiss-Friedlander, R., and Melchior, F. (2007). Concepts in sumoylation: a decade on. Nature reviews. Molecular cell biology. 8(12), 947-956. DOI: 10.1038/nrm2293.

Ghaemmaghami, S., Huh, W.K., Bower, K., Howson, R.W., Belle, A., Dephoure, N., O'Shea, E.K., and Weissman, J.S. (2003). Global analysis of protein expression in yeast. Nature. 425(6959), 737-741. DOI: 10.1038/nature02046.

Grad, I., Cederroth, C.R., Walicki, J., Grey, C., Barluenga, S., Winssinger, N., De Massy, B., Nef, S., and Picard, D. (2010). The molecular chaperone Hsp90alpha is required for meiotic progression of spermatocytes beyond pachytene in the mouse. PloS one. 5(12), e15770. DOI: 10.1371/journal.pone.0015770.

Graf, C., Lee, C.T., Eva Meier-Andrejszki, L., Nguyen, M.T., and Mayer, M.P. (2014). Differences in conformational dynamics within the Hsp90 chaperone family reveal mechanistic insights. Front Mol Biosci. 1, 4. DOI: 10.3389/fmolb.2014.00004.

Graf, C., Stankiewicz, M., Kramer, G., and Mayer, M.P. (2009). Spatially and kinetically resolved changes in the conformational dynamics of the Hsp90 chaperone machine. The EMBO journal. 28(5), 602-613. DOI: 10.1038/emboj.2008.306.

Gray, P.J., Jr., Stevenson, M.A., and Calderwood, S.K. (2007). Targeting Cdc37 inhibits multiple signaling pathways and induces growth arrest in prostate cancer cells. Cancer research. 67(24), 11942-11950. DOI: 10.1158/0008-5472.CAN-07-3162.

Grbovic, O.M., Basso, A.D., Sawai, A., Ye, Q., Friedlander, P., Solit, D., and Rosen, N. (2006). V600E B-Raf requires the Hsp90 chaperone for stability and is degraded in response to Hsp90 inhibitors. Proceedings of the National Academy of Sciences of the United States of America. 103(1), 57-62. DOI: 10.1073/pnas.0609973103.

Grenert, J.P., Sullivan, W.P., Fadden, P., Haystead, T.A., Clark, J., Mimnaugh, E., Krutzsch, H., Ochel, H.J., Schulte, T.W., Sausville, E., et al. (1997). The amino-terminal domain of heat shock protein 90 (hsp90) that binds geldanamycin is an ATP/ADP switch domain that regulates hsp90 conformation. The Journal of biological chemistry. 272(38), 23843-23850.

Grunow, R., D'Apuzzo, M., Wyss-Coray, T., Frutig, K., and Pichler, W.J. (1994). A cell surface ELISA for the screening of monoclonal antibodies to antigens on viable cells in suspension. J Immunol Methods. 171(1), 93-102.

Guo, C., and Henley, J.M. (2014). Wrestling with stress: roles of protein SUMOylation and deSUMOylation in cell stress response. IUBMB life. 66(2), 71-77. DOI: 10.1002/iub.1244.

Ha, T., Enderle, T., Ogletree, D.F., Chemla, D.S., Selvin, P.R., and Weiss, S. (1996). Probing the interaction between two single molecules: fluorescence resonance energy transfer between a single donor and a single acceptor. Proceedings of the National Academy of Sciences of the United States of America. 93(13), 6264-6268.

Hainzl, O., Lapina, M.C., Buchner, J., and Richter, K. (2009). The charged linker region is an important regulator of Hsp90 function. The Journal of biological chemistry. 284(34), 22559-22567. DOI: 10.1074/jbc.M109.031658.

Harris, S.F., Shiau, A.K., and Agard, D.A. (2004). The crystal structure of the carboxy-terminal dimerization domain of htpG, the Escherichia coli Hsp90, reveals a potential substrate binding site. Structure. 12(6), 1087-1097. DOI: 10.1016/j.str.2004.03.020.

Harst, A., Lin, H., and Obermann, W.M. (2005). Aha1 competes with Hop, p50 and p23 for binding to the molecular chaperone Hsp90 and contributes to kinase and hormone receptor activation. The Biochemical journal. 387(Pt 3), 789-796. DOI: 10.1042/BJ20041283.

Hartl, F.U. (1996). Molecular chaperones in cellular protein folding. Nature. 381(6583), 571-579. DOI: 10.1038/381571a0.

Hartl, F.U. (2011). Chaperone-assisted protein folding: the path to discovery from a personal perspective. Nature medicine. 17(10), 1206-1210. DOI: 10.1038/nm.2467.

Hawle, P., Siepmann, M., Harst, A., Siderius, M., Reusch, H.P., and Obermann, W.M. (2006). The middle domain of Hsp90 acts as a discriminator between different types of client proteins. Molecular and cellular biology. 26(22), 8385-8395. DOI: 10.1128/MCB.02188-05.

Hay, R.T. (2007). SUMO-specific proteases: a twist in the tail. Trends in cell biology. 17(8), 370-376. DOI: 10.1016/j.tcb.2007.08.002.

He, H., Zatorska, D., Kim, J., Aguirre, J., Llauger, L., She, Y., Wu, N., Immormino, R.M., Gewirth, D.T., and Chiosis, G. (2006). Identification of potent water soluble purine-scaffold inhibitors of the heat shock protein 90. Journal of medicinal chemistry. 49(1), 381-390. DOI: 10.1021/jm0508078.

He, W., Wu, L., Gao, Q., Du, Y., and Wang, Y. (2006). Identification of AHBA biosynthetic genes related to geldanamycin biosynthesis in Streptomyces hygroscopicus 17997. Curr Microbiol. 52(3), 197-203. Published online 2006/02/28 DOI: 10.1007/s00284-005-0203-y.

Hecker, C.M., Rabiller, M., Haglund, K., Bayer, P., and Dikic, I. (2006). Specification of SUMO1- and SUMO2-interacting motifs. The Journal of biological chemistry. 281(23), 16117-16127. DOI: 10.1074/jbc.M512757200.

Hessling, M., Richter, K., and Buchner, J. (2009). Dissection of the ATP-induced conformational cycle of the molecular chaperone Hsp90. Nature structural & molecular biology. 16(3), 287-293. DOI: 10.1038/nsmb.1565.

Hickey, C.M., Wilson, N.R., and Hochstrasser, M. (2012). Function and regulation of SUMO proteases. Nature reviews. Molecular cell biology. 13(12), 755-766. DOI: 10.1038/nrm3478.

Holmes, J.L., Sharp, S.Y., Hobbs, S., and Workman, P. (2008). Silencing of HSP90 cochaperone AHA1 expression decreases client protein activation and increases cellular sensitivity to the HSP90 inhibitor 17-allylamino-17-demethoxygeldanamycin. Cancer research. 68(4), 1188-1197. DOI: 10.1158/0008-5472.CAN-07-3268.

Horvat, N.K., Armstrong, H., Lee, B.L., Mercier, R., Wolmarans, A., Knowles, J., Spyracopoulos, L., and LaPointe, P. (2014). A mutation in the catalytic loop of Hsp90 specifically impairs ATPase stimulation by Aha1p, but not Hch1p. Journal of molecular biology. 426(12), 2379-2392. DOI: 10.1016/j.jmb.2014.04.002.

Jacobs, A.M., Nicol, S.M., Hislop, R.G., Jaffray, E.G., Hay, R.T., and Fuller-Pace, F.V. (2007). SUMO modification of the DEAD box protein p68 modulates

its transcriptional activity and promotes its interaction with HDAC1. Oncogene. 26(40), 5866-5876. DOI: 10.1038/sj.onc.1210387.

Jahn, M., Rehn, A., Pelz, B., Hellenkamp, B., Richter, K., Rief, M., Buchner, J., and Hugel, T. (2014). The charged linker of the molecular chaperone Hsp90 modulates domain contacts and biological function. Proceedings of the National Academy of Sciences of the United States of America. 111(50), 17881-17886. DOI: 10.1073/pnas.1414073111.

Johnson, B.D., Schumacher, R.J., Ross, E.D., and Toft, D.O. (1998). Hop modulates Hsp70/Hsp90 interactions in protein folding. The Journal of biological chemistry. 273(6), 3679-3686.

Johnson, J.L. (2012). Evolution and function of diverse Hsp90 homologs and cochaperone proteins. Biochimica et biophysica acta. 1823(3), 607-613. DOI: 10.1016/j.bbamcr.2011.09.020.

Johnson, J.L., Halas, A., and Flom, G. (2007). Nucleotide-dependent interaction of Saccharomyces cerevisiae Hsp90 with the cochaperone proteins Sti1, Cpr6, and Sba1. Molecular and cellular biology. 27(2), 768-776. DOI: 10.1128/MCB.01034-06.

Johnson, J.L., and Toft, D.O. (1994). A novel chaperone complex for steroid receptors involving heat shock proteins, immunophilins, and p23. The Journal of biological chemistry. 269(40), 24989-24993.

Kamal, A., Thao, L., Sensintaffar, J., Zhang, L., Boehm, M.F., Fritz, L.C., and Burrows, F.J. (2003). A high-affinity conformation of Hsp90 confers tumour selectivity on Hsp90 inhibitors. Nature. 425(6956), 407-410. DOI: 10.1038/nature01913.

Kampinga, H.H., and Craig, E.A. (2010). The HSP70 chaperone machinery: J proteins as drivers of functional specificity. Nature reviews. Molecular cell biology. 11(8), 579-592. DOI: 10.1038/nrm2941.

Kim, J.S., Kim, B.H., Jang, J.I., Eom, J.S., Kim, H.G., Bang, I.S., and Park, Y.K. (2014). Functional insight from the tetratricopeptide repeat-like motifs of the type III secretion chaperone SicA in Salmonella enterica serovar Typhimurium. FEMS microbiology letters. 350(2), 146-153. DOI: 10.1111/1574-6968.12315.

Knowles, T.P., Vendruscolo, M., and Dobson, C.M. (2014). The amyloid state and its association with protein misfolding diseases. Nature reviews. Molecular cell biology. 15(6), 384-396. Published online 2014/05/24 DOI: 10.1038/nrm3810.

Koay, Y.C., McConnell, J.R., Wang, Y., Kim, S.J., and McAlpine, S.R. (2014). Chemically accessible Hsp90 inhibitor that does not induce a heat shock response. ACS Med. Chem. Lett. 5, 771-776.

Kobayashi, S., Nantz, R., Kitamura, T., Higashikubo, R., and Horikoshi, N. (2005). Combined inhibition of extracellular signal-regulated kinases and HSP90 sensitizes human colon carcinoma cells to ionizing radiation. Oncogene. 24(18), 3011-3019. DOI: 10.1038/sj.onc.1208508.

Koulov, A.V., LaPointe, P., Lu, B., Razvi, A., Coppinger, J., Dong, M.Q., Matteson, J., Laister, R., Arrowsmith, C., Yates, J.R., 3rd, et al. (2010). Biological and structural basis for Aha1 regulation of Hsp90 ATPase activity in maintaining proteostasis in the human disease cystic fibrosis. Molecular biology of the cell. 21(6), 871-884. DOI: 10.1091/mbc.E09-12-1017.

Kurokawa, M., Zhao, C., Reya, T., and Kornbluth, S. (2008). Inhibition of apoptosome formation by suppression of Hsp90beta phosphorylation in tyrosine kinase-induced leukemias. Molecular and cellular biology. 28(17), 5494-5506. DOI: 10.1128/MCB.00265-08.

Laskey, R.A., Honda, B.M., Mills, A.D., and Finch, J.T. (1978). Nucleosomes are assembled by an acidic protein which binds histones and transfers them to DNA. Nature. 275(5679), 416-420.

Lavery, L.A., Partridge, J.R., Ramelot, T.A., Elnatan, D., Kennedy, M.A., and Agard, D.A. (2014). Structural asymmetry in the closed state of mitochondrial Hsp90 (TRAP1) supports a two-step ATP hydrolysis mechanism. Molecular cell. 53(2), 330-343. DOI: 10.1016/j.molcel.2013.12.023.

Leavesley, S.J., and Rich, T.C. (2016). Overcoming limitations of FRET measurements. Cytometry. Part A : the journal of the International Society for Analytical Cytology. 89(4), 325-327. DOI: 10.1002/cyto.a.22851.

Lee, P., Shabbir, A., Cardozo, C., and Caplan, A.J. (2004). Sti1 and Cdc37 can stabilize Hsp90 in chaperone complexes with a protein kinase. Molecular biology of the cell. 15(4), 1785-1792. DOI: 10.1091/mbc.E03-07-0480.

Lee, S., and Tsai, F.T. (2005). Molecular chaperones in protein quality control. Journal of biochemistry and molecular biology. 38(3), 259-265.

Li, J., and Buchner, J. (2013). Structure, function and regulation of the hsp90 machinery. Biomedical journal. 36(3), 106-117. DOI: 10.4103/2319-4170.113230.

Li, J., Richter, K., and Buchner, J. (2011). Mixed Hsp90-cochaperone complexes are important for the progression of the reaction cycle. Nature structural & molecular biology. 18(1), 61-66. DOI: 10.1038/nsmb.1965.

Li, J., Richter, K., Reinstein, J., and Buchner, J. (2013). Integration of the accelerator Aha1 in the Hsp90 co-chaperone cycle. Nature structural & molecular biology. 20(3), 326-331. DOI: 10.1038/nsmb.2502.

Li, J., Soroka, J., and Buchner, J. (2012). The Hsp90 chaperone machinery: conformational dynamics and regulation by co-chaperones. Biochimica et biophysica acta. 1823(3), 624-635. DOI: 10.1016/j.bbamcr.2011.09.003.

Lindquist, S., and Craig, E.A. (1988). The heat-shock proteins. Annual review of genetics. 22, 631-677. DOI: 10.1146/annurev.ge.22.120188.003215.

Longshaw, V.M., Baxter, M., Prewitz, M., and Blatch, G.L. (2009). Knockdown of the co-chaperone Hop promotes extranuclear accumulation of Stat3 in mouse embryonic stem cells. European journal of cell biology. 88(3), 153-166. DOI: 10.1016/j.ejcb.2008.09.003.

Loo, M.A., Jensen, T.J., Cui, L., Hou, Y., Chang, X.B., and Riordan, J.R. (1998). Perturbation of Hsp90 interaction with nascent CFTR prevents its maturation and accelerates its degradation by the proteasome. The EMBO journal. 17(23), 6879-6887. DOI: 10.1093/emboj/17.23.6879.

Lorenz, O.R., Freiburger, L., Rutz, D.A., Krause, M., Zierer, B.K., Alvira, S., Cuellar, J., Valpuesta, J.M., Madl, T., Sattler, M., et al. (2014). Modulation of the Hsp90 chaperone cycle by a stringent client protein. Molecular cell. 53(6), 941-953. DOI: 10.1016/j.molcel.2014.02.003.

Lotz, G.P., Lin, H., Harst, A., and Obermann, W.M. (2003). Aha1 binds to the middle domain of Hsp90, contributes to client protein activation, and stimulates the ATPase activity of the molecular chaperone. The Journal of biological chemistry. 278(19), 17228-17235. DOI: 10.1074/jbc.M212761200.

Louvion, J.F., Warth, R., and Picard, D. (1996). Two eukaryote-specific regions of Hsp82 are dispensable for its viability and signal transduction functions in yeast. Proceedings of the National Academy of Sciences of the United States of America. 93(24), 13937-13942.

Macario, A.J., and Conway de Macario, E. (2005). Sick chaperones, cellular stress, and disease. The New England journal of medicine. 353(14), 1489-1501. DOI: 10.1056/NEJMra050111.

Maharaj, K.A., Que, N.L., Hong, F., Huck, J.D., Gill, S.K., Wu, S., Li, Z., and Gewirth, D.T. (2016). Exploring the Functional Complementation between Grp94 and Hsp90. PloS one. 11(11), e0166271. DOI: 10.1371/journal.pone.0166271.

Martin, J. (2004). Chaperonin function--effects of crowding and confinement. J Mol Recognit. 17(5), 465-472. DOI: 10.1002/jmr.707.

Martinez-Yamout, M.A., Venkitakrishnan, R.P., Preece, N.E., Kroon, G., Wright, P.E., and Dyson, H.J. (2006). Localization of sites of interaction between p23 and Hsp90 in solution. The Journal of biological chemistry. 281(20), 14457-14464. DOI: 10.1074/jbc.M601759200.

Matts, R.L., Brandt, G.E., Lu, Y., Dixit, A., Mollapour, M., Wang, S., Donnelly, A.C., Neckers, L., Verkhivker, G., and Blagg, B.S. (2011). A systematic protocol for the characterization of Hsp90 modulators. Bioorganic & medicinal chemistry. 19(1), 684-692. DOI: 10.1016/j.bmc.2010.10.029.

Matunis, M.J., Coutavas, E., and Blobel, G. (1996). A novel ubiquitin-like modification modulates the partitioning of the Ran-GTPase-activating protein RanGAP1 between the cytosol and the nuclear pore complex. The Journal of cell biology. 135(6 Pt 1), 1457-1470.

Mayer, M.P., and Bukau, B. (1999). Molecular chaperones: the busy life of Hsp90. Current biology : CB. 9(9), R322-325.

Mayer, M.P., and Le Breton, L. (2015). Hsp90: breaking the symmetry. Molecular cell. 58(1), 8-20. DOI: 10.1016/j.molcel.2015.02.022.

Mayer, M.P., Prodromou, C., and Frydman, J. (2009). The Hsp90 mosaic: a picture emerges. Nature structural & molecular biology. 16(1), 2-6. DOI: 10.1038/nsmb0109-2.

McCarty, J.S., Buchberger, A., Reinstein, J., and Bukau, B. (1995). The role of ATP in the functional cycle of the DnaK chaperone system. Journal of molecular biology. 249(1), 126-137. DOI: 10.1006/jmbi.1995.0284.

McClellan, A.J., Scott, M.D., and Frydman, J. (2005). Folding and quality control of the VHL tumor suppressor proceed through distinct chaperone pathways. Cell. 121(5), 739-748. DOI: 10.1016/j.cell.2005.03.024.

McCollum, A.K., TenEyck, C.J., Stensgard, B., Morlan, B.W., Ballman, K.V., Jenkins, R.B., Toft, D.O., and Erlichman, C. (2008). P-Glycoprotein-mediated resistance to Hsp90-directed therapy is eclipsed by the heat shock response. Cancer research. 68(18), 7419-7427. DOI: 10.1158/0008-5472.CAN-07-5175.

McDowell, C.L., Bryan Sutton, R., and Obermann, W.M. (2009). Expression of Hsp90 chaperone [corrected] proteins in human tumor tissue. International journal of biological macromolecules. 45(3), 310-314. DOI: 10.1016/j.ijbiomac.2009.06.012.

McLaughlin, S.H., Smith, H.W., and Jackson, S.E. (2002). Stimulation of the weak ATPase activity of human hsp90 by a client protein. Journal of molecular biology. 315(4), 787-798. DOI: 10.1006/jmbi.2001.5245.

McLaughlin, S.H., Sobott, F., Yao, Z.P., Zhang, W., Nielsen, P.R., Grossmann, J.G., Laue, E.D., Robinson, C.V., and Jackson, S.E. (2006). The co-chaperone p23 arrests the Hsp90 ATPase cycle to trap client proteins. Journal of molecular biology. 356(3), 746-758. DOI: 10.1016/j.jmb.2005.11.085.

McLaughlin, S.H., Ventouras, L.A., Lobbezoo, B., and Jackson, S.E. (2004). Independent ATPase activity of Hsp90 subunits creates a flexible assembly platform. Journal of molecular biology. 344(3), 813-826. DOI: 10.1016/j.jmb.2004.09.055.

Meyer, P., Prodromou, C., Hu, B., Vaughan, C., Roe, S.M., Panaretou, B., Piper, P.W., and Pearl, L.H. (2003). Structural and functional analysis of the middle segment of hsp90: implications for ATP hydrolysis and client protein and cochaperone interactions. Molecular cell. 11(3), 647-658.

Meyer, P., Prodromou, C., Liao, C., Hu, B., Mark Roe, S., Vaughan, C.K., Vlasic, I., Panaretou, B., Piper, P.W., and Pearl, L.H. (2004a). Structural basis for recruitment of the ATPase activator Aha1 to the Hsp90 chaperone machinery. The EMBO journal. 23(3), 511-519. DOI: 10.1038/sj.emboj.7600060.

Meyer, P., Prodromou, C., Liao, C., Hu, B., Roe, S.M., Vaughan, C.K., Vlasic, I., Panaretou, B., Piper, P.W., and Pearl, L.H. (2004b). Structural basis for recruitment of the ATPase activator Aha1 to the Hsp90 chaperone machinery. The EMBO journal. 23(6), 1402-1410. DOI: 10.1038/sj.emboj.7600141.

Mickler, M., Hessling, M., Ratzke, C., Buchner, J., and Hugel, T. (2009). The large conformational changes of Hsp90 are only weakly coupled to ATP hydrolysis. Nature structural & molecular biology. 16(3), 281-286. DOI: 10.1038/nsmb.1557.

Millson, S.H., Nuttall, J.M., Mollapour, M., and Piper, P.W. (2009). The Hsp90/Cdc37p chaperone system is a determinant of molybdate resistance in Saccharomyces cerevisiae. Yeast. 26(6), 339-347. DOI: 10.1002/yea.1670.

Minty, A., Dumont, X., Kaghad, M., and Caput, D. (2000). Covalent modification of p73alpha by SUMO-1. Two-hybrid screening with p73 identifies novel SUMO-1-interacting proteins and a SUMO-1 interaction motif. The Journal of biological chemistry. 275(46), 36316-36323. DOI: 10.1074/jbc.M004293200.

Mishra, P., and Bolon, D.N. (2014). Designed Hsp90 heterodimers reveal an asymmetric ATPase-driven mechanism in vivo. Molecular cell. 53(2), 344-350. DOI: 10.1016/j.molcel.2013.12.024.

Miyata, Y. (2009). Protein kinase CK2 in health and disease: CK2: the kinase controlling the Hsp90 chaperone machinery. Cellular and molecular life sciences : CMLS. 66(11-12), 1840-1849. DOI: 10.1007/s00018-009-9152-0.

Miyata, Y., and Yahara, I. (1992). The 90-kDa heat shock protein, HSP90, binds and protects casein kinase II from self-aggregation and enhances its kinase activity. The Journal of biological chemistry. 267(10), 7042-7047.

Mollapour, M., Bourboulia, D., Beebe, K., Woodford, M.R., Polier, S., Hoang, A., Chelluri, R., Li, Y., Guo, A., Lee, M.J., et al. (2014). Asymmetric Hsp90 N domain SUMOylation recruits Aha1 and ATP-competitive inhibitors. Molecular cell. 53(2), 317-329. DOI: 10.1016/j.molcel.2013.12.007.

Mollapour, M., and Neckers, L. (2011). Detecting HSP90 phosphorylation. Methods in molecular biology. 787, 67-74. DOI: 10.1007/978-1-61779-295-3_5.

Mollapour, M., and Neckers, L. (2012). Post-translational modifications of Hsp90 and their contributions to chaperone regulation. Biochimica et biophysica acta. 1823(3), 648-655. DOI: 10.1016/j.bbamcr.2011.07.018.

Mollapour, M., Tsutsumi, S., Donnelly, A.C., Beebe, K., Tokita, M.J., Lee, M.J., Lee, S., Morra, G., Bourboulia, D., Scroggins, B.T., et al. (2010). Swe1Wee1-dependent tyrosine phosphorylation of Hsp90 regulates distinct facets of chaperone function. Molecular cell. 37(3), 333-343. DOI: 10.1016/j.molcel.2010.01.005.

Mollapour, M., Tsutsumi, S., Kim, Y.S., Trepel, J., and Neckers, L. (2011a). Casein kinase 2 phosphorylation of Hsp90 threonine 22 modulates chaperone function and drug sensitivity. Oncotarget. 2(5), 407-417. DOI: 10.18632/oncotarget.272.

Mollapour, M., Tsutsumi, S., Truman, A.W., Xu, W., Vaughan, C.K., Beebe, K., Konstantinova, A., Vourganti, S., Panaretou, B., Piper, P.W., et al. (2011b). Threonine 22 phosphorylation attenuates Hsp90 interaction with cochaperones and affects its chaperone activity. Molecular cell. 41(6), 672-681. DOI: 10.1016/j.molcel.2011.02.011.

Morano, K.A. (2007). New tricks for an old dog: the evolving world of Hsp70. Annals of the New York Academy of Sciences. 1113, 1-14. DOI: 10.1196/annals.1391.018.

Morimoto, R.I. (2008). Proteotoxic stress and inducible chaperone networks in neurodegenerative disease and aging. Genes & development. 22(11), 1427-1438. DOI: 10.1101/gad.1657108.

Mukhopadhyay, D., and Dasso, M. (2007). Modification in reverse: the SUMO proteases. Trends Biochem Sci. 32(6), 286-295. DOI: 10.1016/j.tibs.2007.05.002.

Nathan, D.F., and Lindquist, S. (1995). Mutational analysis of Hsp90 function: interactions with a steroid receptor and a protein kinase. Molecular and cellular biology. 15(7), 3917-3925.

Nathan, D.F., Vos, M.H., and Lindquist, S. (1997). In vivo functions of the Saccharomyces cerevisiae Hsp90 chaperone. Proceedings of the National Academy of Sciences of the United States of America. 94(24), 12949-12956.

Nathan, D.F., Vos, M.H., and Lindquist, S. (1999). Identification of SSF1, CNS1, and HCH1 as multicopy suppressors of a Saccharomyces cerevisiae Hsp90 loss-of-function mutation. Proceedings of the National Academy of Sciences of the United States of America. 96(4), 1409-1414.

Neckers, L. (2006). Chaperoning oncogenes: Hsp90 as a target of geldanamycin. Handbook of experimental pharmacology. (172), 259-277.

Nemoto, T., Ohara-Nemoto, Y., Ota, M., Takagi, T., and Yokoyama, K. (1995). Mechanism of dimer formation of the 90-kDa heat-shock protein. European journal of biochemistry. 233(1), 1-8.

Nemoto, T.K., Ono, T., and Tanaka, K. (2001). Substrate-binding characteristics of proteins in the 90 kDa heat shock protein family. The Biochemical journal. 354(Pt 3), 663-670.

Nie, M., and Boddy, M.N. (2015). Pli1(PIAS1) SUMO ligase protected by the nuclear pore-associated SUMO protease Ulp1SENP1/2. The Journal of biological chemistry. 290(37), 22678-22685. DOI: 10.1074/jbc.M115.673038.

Obermann, W.M., Sondermann, H., Russo, A.A., Pavletich, N.P., and Hartl, F.U. (1998). In vivo function of Hsp90 is dependent on ATP binding and ATP hydrolysis. The Journal of cell biology. 143(4), 901-910.

Onuoha, S.C., Coulstock, E.T., Grossmann, J.G., and Jackson, S.E. (2008). Structural studies on the co-chaperone Hop and its complexes with Hsp90. Journal of molecular biology. 379(4), 732-744. DOI: 10.1016/j.jmb.2008.02.013.

Panaretou, B., Prodromou, C., Roe, S.M., O'Brien, R., Ladbury, J.E., Piper, P.W., and Pearl, L.H. (1998). ATP binding and hydrolysis are essential to the function of the Hsp90 molecular chaperone in vivo. The EMBO journal. 17(16), 4829-4836. DOI: 10.1093/emboj/17.16.4829.

Panaretou, B., Siligardi, G., Meyer, P., Maloney, A., Sullivan, J.K., Singh, S., Millson, S.H., Clarke, P.A., Naaby-Hansen, S., Stein, R., et al. (2002). Activation of the ATPase activity of hsp90 by the stress-regulated cochaperone aha1. Molecular cell. 10(6), 1307-1318.

Paraiso, K.H., and Smalley, K.S. (2012). Making sense of MEK1 mutations in intrinsic and acquired BRAF inhibitor resistance. Cancer discovery. 2(5), 390-392. DOI: 10.1158/2159-8290.CD-12-0128.

Pastore, A., and Temussi, P. (2012). Protein aggregation and misfolding: good or evil? J Phys Condens Matter. 24(24), 244101. DOI: 10.1088/0953-8984/24/24/244101.

Pearl, L.H. (2005). Hsp90 and Cdc37 -- a chaperone cancer conspiracy. Current opinion in genetics & development. 15(1), 55-61. DOI: 10.1016/j.gde.2004.12.011.

Pearl, L.H., and Prodromou, C. (2000). Structure and in vivo function of Hsp90. Current opinion in structural biology. 10(1), 46-51.

Pearl, L.H., and Prodromou, C. (2006). Structure and mechanism of the Hsp90 molecular chaperone machinery. Annual review of biochemistry. 75, 271-294. DOI: 10.1146/annurev.biochem.75.103004.142738.

Pearl, L.H., Prodromou, C., and Workman, P. (2008). The Hsp90 molecular chaperone: an open and shut case for treatment. The Biochemical journal. 410(3), 439-453. DOI: 10.1042/BJ20071640.

Picard, D. (2002). Heat-shock protein 90, a chaperone for folding and regulation. Cellular and molecular life sciences : CMLS. 59(10), 1640-1648.

Picard, D. (2006). Intracellular dynamics of the Hsp90 co-chaperone p23 is dictated by Hsp90. Experimental cell research. 312(2), 198-204. DOI: 10.1016/j.yexcr.2005.10.009.

Pimienta, G., Herbert, K.M., and Regan, L. (2011). A compound that inhibits the HOP-Hsp90 complex formation and has unique killing effects in breast cancer cell lines. Molecular pharmaceutics. 8(6), 2252-2261. DOI: 10.1021/mp200346y.

Piper, P.W., and Millson, S.H. (2011). Mechanisms of Resistance to Hsp90 Inhibitor Drugs: A Complex Mosaic Emerges. Pharmaceuticals. 4(11), 1400-1422. DOI: 10.3390/ph4111400.

Piper, P.W., Millson, S.H., Mollapour, M., Panaretou, B., Siligardi, G., Pearl, L.H., and Prodromou, C. (2003). Sensitivity to Hsp90-targeting drugs can arise with mutation to the Hsp90 chaperone, cochaperones and plasma membrane ATP binding cassette transporters of yeast. European journal of biochemistry. 270(23), 4689-4695.

Pirkl, F., and Buchner, J. (2001). Functional analysis of the Hsp90-associated human peptidyl prolyl cis/trans isomerases FKBP51, FKBP52 and Cyp40. Journal of molecular biology. 308(4), 795-806. DOI: 10.1006/jmbi.2001.4595.

Porstmann, T., and Kiessig, S.T. (1992). Enzyme immunoassay techniques. An overview. J Immunol Methods. 150(1-2), 5-21.

Powers, M.V., and Workman, P. (2006). Targeting of multiple signalling pathways by heat shock protein 90 molecular chaperone inhibitors. Endocrine-related cancer. 13 Suppl 1, S125-135. DOI: 10.1677/erc.1.01324.

Proctor, C.J., and Lorimer, I.A. (2011). Modelling the role of the Hsp70/Hsp90 system in the maintenance of protein homeostasis. PloS one. 6(7), e22038. DOI: 10.1371/journal.pone.0022038.

Prodromou, C. (2012). The 'active life' of Hsp90 complexes. Biochimica et biophysica acta. 1823(3), 614-623. DOI: 10.1016/j.bbamcr.2011.07.020.

Prodromou, C. (2016). Mechanisms of Hsp90 regulation. The Biochemical journal. 473(16), 2439-2452. DOI: 10.1042/BCJ20160005.

Prodromou, C., Panaretou, B., Chohan, S., Siligardi, G., O'Brien, R., Ladbury, J.E., Roe, S.M., Piper, P.W., and Pearl, L.H. (2000). The ATPase cycle of Hsp90 drives a molecular 'clamp' via transient dimerization of the N-terminal domains. The EMBO journal. 19(16), 4383-4392. DOI: 10.1093/emboj/19.16.4383.

Prodromou, C., Roe, S.M., O'Brien, R., Ladbury, J.E., Piper, P.W., and Pearl, L.H. (1997). Identification and structural characterization of the ATP/ADP-binding site in the Hsp90 molecular chaperone. Cell. 90(1), 65-75.

Prodromou, C., Siligardi, G., O'Brien, R., Woolfson, D.N., Regan, L., Panaretou, B., Ladbury, J.E., Piper, P.W., and Pearl, L.H. (1999). Regulation of Hsp90 ATPase activity by tetratricopeptide repeat (TPR)-domain co-chaperones. The EMBO journal. 18(3), 754-762. DOI: 10.1093/emboj/18.3.754.

Proisy, N., Sharp, S.Y., Boxall, K., Connelly, S., Roe, S.M., Prodromou, C., Slawin, A.M., Pearl, L.H., Workman, P., and Moody, C.J. (2006). Inhibition of Hsp90 with synthetic macrolactones: synthesis and structural and biological evaluation of ring and conformational analogs of radicicol. Chemistry & biology. 13(11), 1203-1215. DOI: 10.1016/j.chembiol.2006.09.015.

Rain, J.C., Selig, L., De Reuse, H., Battaglia, V., Reverdy, C., Simon, S., Lenzen, G., Petel, F., Wojcik, J., Schachter, V., et al. (2001). The protein-protein interaction map of Helicobacter pylori. Nature. 409(6817), 211-215. DOI: 10.1038/35051615.

Ran, F., Bali, M., and Michels, C.A. (2008). Hsp90/Hsp70 chaperone machine regulation of the Saccharomyces MAL-activator as determined in vivo using noninducible and constitutive mutant alleles. Genetics. 179(1), 331-343. DOI: 10.1534/genetics.107.084921.

Ratzke, C., Berkemeier, F., and Hugel, T. (2012). Heat shock protein 90's mechanochemical cycle is dominated by thermal fluctuations. Proceedings of the

National Academy of Sciences of the United States of America. 109(1), 161-166. DOI: 10.1073/pnas.1107930108.

Ratzke, R., Moreno, D.H., Gorenstein, C., and Moreno, R.A. (2011). Validity and reliability of the Structured Clinical Interview for Mood Spectrum: Brazilian version (SCIMOODS-VB). Revista brasileira de psiquiatria. 33(1), 64-67.

Retzlaff, M., Hagn, F., Mitschke, L., Hessling, M., Gugel, F., Kessler, H., Richter, K., and Buchner, J. (2010). Asymmetric activation of the hsp90 dimer by its cochaperone aha1. Molecular cell. 37(3), 344-354. DOI: 10.1016/j.molcel.2010.01.006.

Richter, K., and Buchner, J. (2001). Hsp90: chaperoning signal transduction. Journal of cellular physiology. 188(3), 281-290. DOI: 10.1002/jcp.1131.

Richter, K., Moser, S., Hagn, F., Friedrich, R., Hainzl, O., Heller, M., Schlee, S., Kessler, H., Reinstein, J., and Buchner, J. (2006). Intrinsic inhibition of the Hsp90 ATPase activity. The Journal of biological chemistry. 281(16), 11301-11311. DOI: 10.1074/jbc.M510142200.

Richter, K., Muschler, P., Hainzl, O., and Buchner, J. (2001). Coordinated ATP hydrolysis by the Hsp90 dimer. The Journal of biological chemistry. 276(36), 33689-33696. DOI: 10.1074/jbc.M103832200.

Richter, K., Muschler, P., Hainzl, O., Reinstein, J., and Buchner, J. (2003). Sti1 is a non-competitive inhibitor of the Hsp90 ATPase. Binding prevents the N-terminal dimerization reaction during the atpase cycle. The Journal of biological chemistry. 278(12), 10328-10333. DOI: 10.1074/jbc.M213094200.

Richter, K., Reinstein, J., and Buchner, J. (2002). N-terminal residues regulate the catalytic efficiency of the Hsp90 ATPase cycle. The Journal of biological chemistry. 277(47), 44905-44910. DOI: 10.1074/jbc.M208457200.

Richter, K., Soroka, J., Skalniak, L., Leskovar, A., Hessling, M., Reinstein, J., and Buchner, J. (2008). Conserved conformational changes in the ATPase cycle of human Hsp90. The Journal of biological chemistry. 283(26), 17757-17765. DOI: 10.1074/jbc.M800540200.

Richter, K., Walter, S., and Buchner, J. (2004). The Co-chaperone Sba1 connects the ATPase reaction of Hsp90 to the progression of the chaperone cycle. Journal of molecular biology. 342(5), 1403-1413. DOI: 10.1016/j.jmb.2004.07.064.

Riggs, D.L., Roberts, P.J., Chirillo, S.C., Cheung-Flynn, J., Prapapanich, V., Ratajczak, T., Gaber, R., Picard, D., and Smith, D.F. (2003). The Hsp90-binding peptidylprolyl isomerase FKBP52 potentiates glucocorticoid signaling in vivo. The EMBO journal. 22(5), 1158-1167. DOI: 10.1093/emboj/cdg108.

Riordan, J.R. (2005). Assembly of functional CFTR chloride channels. Annual review of physiology. 67, 701-718. DOI: 10.1146/annurev.physiol.67.032003.154107.

Ritossa, F. (1962). A new puffing pattern induced by temperature shock and DNP in drosophila. Experientia. 18(12), 571-573.

Rodriguez, M.S., Dargemont, C., and Hay, R.T. (2001). SUMO-1 conjugation in vivo requires both a consensus modification motif and nuclear targeting. The Journal of biological chemistry. 276(16), 12654-12659. DOI: 10.1074/jbc.M009476200.

Roe, S.M., Ali, M.M., Meyer, P., Vaughan, C.K., Panaretou, B., Piper, P.W., Prodromou, C., and Pearl, L.H. (2004). The Mechanism of Hsp90 regulation by the protein kinase-specific cochaperone p50(cdc37). Cell. 116(1), 87-98.

Roe, S.M., Prodromou, C., O'Brien, R., Ladbury, J.E., Piper, P.W., and Pearl, L.H. (1999). Structural basis for inhibition of the Hsp90 molecular chaperone by the antitumor antibiotics radicicol and geldanamycin. Journal of medicinal chemistry. 42(2), 260-266. DOI: 10.1021/jm980403y.

Rohl, A., Rohrberg, J., and Buchner, J. (2013). The chaperone Hsp90: changing partners for demanding clients. Trends Biochem Sci. 38(5), 253-262. DOI: 10.1016/j.tibs.2013.02.003.

Rudiger, S., Buchberger, A., and Bukau, B. (1997). Interaction of Hsp70 chaperones with substrates. Nature structural biology. 4(5), 342-349.

Sanchez, E.R., Redmond, T., Scherrer, L.C., Bresnick, E.H., Welsh, M.J., and Pratt, W.B. (1988). Evidence that the 90-kilodalton heat shock protein is associated with tubulin-containing complexes in L cell cytosol and in intact PtK cells. Molecular endocrinology. 2(8), 756-760. DOI: 10.1210/mend-2-8-756.

Sarto, C., Binz, P.A., and Mocarelli, P. (2000). Heat shock proteins in human cancer. Electrophoresis. 21(6), 1218-1226. DOI: 10.1002/(SICI)1522-2683(20000401)21:6<1218::AID-ELPS1218>3.0.CO;2-H.

Sato, T., Hanada, M., Bodrug, S., Irie, S., Iwama, N., Boise, L.H., Thompson, C.B., Golemis, E., Fong, L., Wang, H.G., et al. (1994). Interactions among members of the Bcl-2 protein family analyzed with a yeast two-hybrid system. Proceedings of the National Academy of Sciences of the United States of America. 91(20), 9238-9242.

Scheibel, T., Siegmund, H.I., Jaenicke, R., Ganz, P., Lilie, H., and Buchner, J. (1999). The charged region of Hsp90 modulates the function of the N-terminal domain. Proceedings of the National Academy of Sciences of the United States of America. 96(4), 1297-1302.

Scheibel, T., Weikl, T., and Buchner, J. (1998). Two chaperone sites in Hsp90 differing in substrate specificity and ATP dependence. Proceedings of the National Academy of Sciences of the United States of America. 95(4), 1495-1499.

Scheufler, C., Brinker, A., Bourenkov, G., Pegoraro, S., Moroder, L., Bartunik, H., Hartl, F.U., and Moarefi, I. (2000). Structure of TPR domain-peptide complexes: critical elements in the assembly of the Hsp70-Hsp90 multichaperone machine. Cell. 101(2), 199-210. DOI: 10.1016/S0092-8674(00)80830-2.

Schneider, C., Sepp-Lorenzino, L., Nimmesgern, E., Ouerfelli, O., Danishefsky, S., Rosen, N., and Hartl, F.U. (1996). Pharmacologic shifting of a balance between protein refolding and degradation mediated by Hsp90. Proceedings of the National Academy of Sciences of the United States of America. 93(25), 14536-14541.

Scroggins, B.T., and Neckers, L. (2007). Post-translational modification of heat-shock protein 90: impact on chaperone function. Expert opinion on drug discovery. 2(10), 1403-1414. DOI: 10.1517/17460441.2.10.1403.

Shao, J., Prince, T., Hartson, S.D., and Matts, R.L. (2003). Phosphorylation of serine 13 is required for the proper function of the Hsp90 co-chaperone, Cdc37. The Journal of biological chemistry. 278(40), 38117-38120. DOI: 10.1074/jbc.C300330200.

Shiau, A.K., Harris, S.F., Southworth, D.R., and Agard, D.A. (2006). Structural Analysis of E. coli hsp90 reveals dramatic nucleotide-dependent conformational rearrangements. Cell. 127(2), 329-340. DOI: 10.1016/j.cell.2006.09.027.

Sidera, K., and Patsavoudi, E. (2014). HSP90 inhibitors: current development and potential in cancer therapy. Recent patents on anti-cancer drug discovery. 9(1), 1-20.

Siligardi, G., Hu, B., Panaretou, B., Piper, P.W., Pearl, L.H., and Prodromou, C. (2004). Co-chaperone regulation of conformational switching in the Hsp90 ATPase cycle. The Journal of biological chemistry. 279(50), 51989-51998. DOI: 10.1074/jbc.M410562200.

Siligardi, G., Panaretou, B., Meyer, P., Singh, S., Woolfson, D.N., Piper, P.W., Pearl, L.H., and Prodromou, C. (2002). Regulation of Hsp90 ATPase activity by the co-chaperone Cdc37p/p50cdc37. The Journal of biological chemistry. 277(23), 20151-20159. DOI: 10.1074/jbc.M201287200.

Smith, D.F. (1993). Dynamics of heat shock protein 90-progesterone receptor binding and the disactivation loop model for steroid receptor complexes. Molecular endocrinology. 7(11), 1418-1429. DOI: 10.1210/mend.7.11.7906860.

Smith, V., Sausville, E.A., Camalier, R.F., Fiebig, H.H., and Burger, A.M. (2005). Comparison of 17-dimethylaminoethylamino-17-demethoxy-geldanamycin (17DMAG) and 17-allylamino-17-demethoxygeldanamycin (17AAG) in vitro: effects on Hsp90 and client proteins in melanoma models. Cancer chemotherapy and pharmacology. 56(2), 126-137. DOI: 10.1007/s00280-004-0947-2.

Solit, D.B., Osman, I., Polsky, D., Panageas, K.S., Daud, A., Goydos, J.S., Teitcher, J., Wolchok, J.D., Germino, F.J., Krown, S.E., et al. (2008). Phase II trial of 17-allylamino-17-demethoxygeldanamycin in patients with metastatic melanoma. Clinical cancer research : an official journal of the American Association for Cancer Research. 14(24), 8302-8307. DOI: 10.1158/1078-0432.CCR-08-1002.

Solit, D.B., Zheng, F.F., Drobnjak, M., Munster, P.N., Higgins, B., Verbel, D., Heller, G., Tong, W., Cordon-Cardo, C., Agus, D.B., et al. (2002). 17-Allylamino-17-demethoxygeldanamycin induces the degradation of androgen receptor and HER-2/neu and inhibits the growth of prostate cancer xenografts. Clinical cancer research : an official journal of the American Association for Cancer Research. 8(5), 986-993.

Southworth, D.R., and Agard, D.A. (2008). Species-dependent ensembles of conserved conformational states define the Hsp90 chaperone ATPase cycle. Molecular cell. 32(5), 631-640. DOI: 10.1016/j.molcel.2008.10.024.

Southworth, D.R., and Agard, D.A. (2011). Client-loading conformation of the Hsp90 molecular chaperone revealed in the cryo-EM structure of the human Hsp90:Hop complex. Molecular cell. 42(6), 771-781. DOI: 10.1016/j.molcel.2011.04.023.

Stebbins, C.E., Russo, A.A., Schneider, C., Rosen, N., Hartl, F.U., and Pavletich, N.P. (1997). Crystal structure of an Hsp90-geldanamycin complex: targeting of a protein chaperone by an antitumor agent. Cell. 89(2), 239-250.

Stepanova, L., Leng, X., Parker, S.B., and Harper, J.W. (1996). Mammalian p50Cdc37 is a protein kinase-targeting subunit of Hsp90 that binds and stabilizes Cdk4. Genes & development. 10(12), 1491-1502.

Street, T.O., Lavery, L.A., Verba, K.A., Lee, C.T., Mayer, M.P., and Agard, D.A. (2012). Cross-monomer substrate contacts reposition the Hsp90 N-terminal domain and prime the chaperone activity. Journal of molecular biology. 415(1), 3-15. DOI: 10.1016/j.jmb.2011.10.038.

Sullivan, W., Stensgard, B., Caucutt, G., Bartha, B., McMahon, N., Alnemri, E.S., Litwack, G., and Toft, D. (1997). Nucleotides and two functional states of hsp90. The Journal of biological chemistry. 272(12), 8007-8012.

Supko, J.G., Hickman, R.L., Grever, M.R., and Malspeis, L. (1995). Preclinical pharmacologic evaluation of geldanamycin as an antitumor agent. Cancer chemotherapy and pharmacology. 36(4), 305-315. DOI: 10.1007/BF00689048.

Sydor, J.R., Normant, E., Pien, C.S., Porter, J.R., Ge, J., Grenier, L., Pak, R.H., Ali, J.A., Dembski, M.S., Hudak, J., et al. (2006). Development of 17-allylamino-17-demethoxygeldanamycin hydroquinone hydrochloride (IPI-504), an anti-cancer agent directed against Hsp90. Proceedings of the National Academy of Sciences of the United States of America. 103(46), 17408-17413. DOI: 10.1073/pnas.0608372103.

Szabo, A., Langer, T., Schroder, H., Flanagan, J., Bukau, B., and Hartl, F.U. (1994). The ATP hydrolysis-dependent reaction cycle of the Escherichia coli Hsp70 system DnaK, DnaJ, and GrpE. Proceedings of the National Academy of Sciences of the United States of America. 91(22), 10345-10349.

Taipale, H.T., Hartikainen, S., and Bell, J.S. (2010). A comparison of four methods to quantify the cumulative effect of taking multiple drugs with sedative properties. The American journal of geriatric pharmacotherapy. 8(5), 460-471. DOI: 10.1016/j.amjopharm.2010.10.004.

Taipale, M., Jarosz, D.F., and Lindquist, S. (2010). HSP90 at the hub of protein homeostasis: emerging mechanistic insights. Nature reviews. Molecular cell biology. 11(7), 515-528. DOI: 10.1038/nrm2918.

Tan, J.A., Sun, Y., Song, J., Chen, Y., Krontiris, T.G., and Durrin, L.K. (2008). SUMO conjugation to the matrix attachment region-binding protein, special AT-rich sequence-binding protein-1 (SATB1), targets SATB1 to promyelocytic nuclear bodies where it undergoes caspase cleavage. The Journal of biological chemistry. 283(26), 18124-18134. DOI: 10.1074/jbc.M800512200.

Thorsness, P.E., and Koshland, D.E., Jr. (1987). Inactivation of isocitrate dehydrogenase by phosphorylation is mediated by the negative charge of the phosphate. The Journal of biological chemistry. 262(22), 10422-10425.

Trepel, J., Mollapour, M., Giaccone, G., and Neckers, L. (2010). Targeting the dynamic HSP90 complex in cancer. Nature reviews. Cancer. 10(8), 537-549. DOI: 10.1038/nrc2887.

Tsutsumi, S., Mollapour, M., Prodromou, C., Lee, C.T., Panaretou, B., Yoshida, S., Mayer, M.P., and Neckers, L.M. (2012). Charged linker sequence modulates eukaryotic heat shock protein 90 (Hsp90) chaperone activity. Proceedings of the National Academy of Sciences of the United States of America. 109(8), 2937-2942. DOI: 10.1073/pnas.1114414109.

Uehara, Y., Murakami, Y., Mizuno, S., and Kawai, S. (1988). Inhibition of transforming activity of tyrosine kinase oncogenes by herbimycin A. Virology. 164(1), 294-298.

Uetz, P., Giot, L., Cagney, G., Mansfield, T.A., Judson, R.S., Knight, J.R., Lockshon, D., Narayan, V., Srinivasan, M., Pochart, P., et al. (2000). A comprehensive analysis of protein-protein interactions in Saccharomyces cerevisiae. Nature. 403(6770), 623-627. DOI: 10.1038/35001009.

Ulrich, H.D. (2009). The SUMO system: an overview. Methods in molecular biology. 497, 3-16. DOI: 10.1007/978-1-59745-566-4_1.

van der Straten, A., Rommel, C., Dickson, B., and Hafen, E. (1997). The heat shock protein 83 (Hsp83) is required for Raf-mediated signalling in Drosophila. The EMBO journal. 16(8), 1961-1969. DOI: 10.1093/emboj/16.8.1961.

Vaughan, C.K., Gohlke, U., Sobott, F., Good, V.M., Ali, M.M., Prodromou, C., Robinson, C.V., Saibil, H.R., and Pearl, L.H. (2006). Structure of an Hsp90-Cdc37-Cdk4 complex. Molecular cell. 23(5), 697-707. DOI: 10.1016/j.molcel.2006.07.016.

Vaughan, C.K., Mollapour, M., Smith, J.R., Truman, A., Hu, B., Good, V.M., Panaretou, B., Neckers, L., Clarke, P.A., Workman, P., et al. (2008). Hsp90-dependent activation of protein kinases is regulated by chaperone-targeted dephosphorylation of Cdc37. Molecular cell. 31(6), 886-895. DOI: 10.1016/j.molcel.2008.07.021.

Vaughan, C.K., Piper, P.W., Pearl, L.H., and Prodromou, C. (2009). A common conformationally coupled ATPase mechanism for yeast and human cytoplasmic HSP90s. FEBS J. 276(1), 199-209. DOI: 10.1111/j.1742-4658.2008.06773.x.

Verghese, J., Abrams, J., Wang, Y., and Morano, K.A. (2012). Biology of the heat shock response and protein chaperones: budding yeast (Saccharomyces cerevisiae) as a model system. Microbiology and molecular biology reviews : MMBR. 76(2), 115-158. DOI: 10.1128/MMBR.05018-11.

Vertegaal, A.C., Andersen, J.S., Ogg, S.C., Hay, R.T., Mann, M., and Lamond, A.I. (2006). Distinct and overlapping sets of SUMO-1 and SUMO-2 target proteins revealed by quantitative proteomics. Molecular & cellular proteomics : MCP. 5(12), 2298-2310. DOI: 10.1074/mcp.M600212-MCP200.

Voss, A.K., Thomas, T., and Gruss, P. (2000). Mice lacking HSP90beta fail to develop a placental labyrinth. Development. 127(1), 1-11.

Wandinger, S.K., Richter, K., and Buchner, J. (2008). The Hsp90 chaperone machinery. The Journal of biological chemistry. 283(27), 18473-18477. DOI: 10.1074/jbc.R800007200.

Wang, X., Khaleque, M.A., Zhao, M.J., Zhong, R., Gaestel, M., and Calderwood, S.K. (2006a). Phosphorylation of HSF1 by MAPK-activated protein kinase 2 on serine 121, inhibits transcriptional activity and promotes HSP90 binding. The Journal of biological chemistry. 281(2), 782-791. DOI: 10.1074/jbc.M505822200.

Wang, X., Venable, J., LaPointe, P., Hutt, D.M., Koulov, A.V., Coppinger, J., Gurkan, C., Kellner, W., Matteson, J., Plutner, H., et al. (2006b). Hsp90 cochaperone Aha1 downregulation rescues misfolding of CFTR in cystic fibrosis. Cell. 127(4), 803-815. DOI: 10.1016/j.cell.2006.09.043.

Wayne, N., and Bolon, D.N. (2007). Dimerization of Hsp90 is required for in vivo function. Design and analysis of monomers and dimers. The Journal of biological chemistry. 282(48), 35386-35395. DOI: 10.1074/jbc.M703844200.

Wayne, N., and Bolon, D.N. (2010). Charge-rich regions modulate the anti-aggregation activity of Hsp90. Journal of molecular biology. 401(5), 931-939. DOI: 10.1016/j.jmb.2010.06.066.

Wegele, H., Muller, L., and Buchner, J. (2004). Hsp70 and Hsp90--a relay team for protein folding. Reviews of physiology, biochemistry and pharmacology. 151, 1-44. DOI: 10.1007/s10254-003-0021-1.

Wegele, H., Wandinger, S.K., Schmid, A.B., Reinstein, J., and Buchner, J. (2006). Substrate transfer from the chaperone Hsp70 to Hsp90. Journal of molecular biology. 356(3), 802-811. DOI: 10.1016/j.jmb.2005.12.008.

Weikl, T., Muschler, P., Richter, K., Veit, T., Reinstein, J., and Buchner, J. (2000). C-terminal regions of Hsp90 are important for trapping the nucleotide during the ATPase cycle. Journal of molecular biology. 303(4), 583-592. DOI: 10.1006/jmbi.2000.4157.

Weiss, S. (1999). Fluorescence spectroscopy of single biomolecules. Science. 283(5408), 1676-1683.

Whitesell, L., and Lindquist, S.L. (2005). HSP90 and the chaperoning of cancer. Nature reviews. Cancer. 5(10), 761-772. DOI: 10.1038/nrc1716.

Whitesell, L., Mimnaugh, E.G., De Costa, B., Myers, C.E., and Neckers, L.M. (1994). Inhibition of heat shock protein HSP90-pp60v-src heteroprotein complex formation by benzoquinone ansamycins: essential role for stress proteins in oncogenic transformation. Proceedings of the National Academy of Sciences of the United States of America. 91(18), 8324-8328.

Wolmarans, A., Lee, B., Spyracopoulos, L., and LaPointe, P. (2016). The Mechanism of Hsp90 ATPase Stimulation by Aha1. Sci Rep. 6, 33179. DOI: 10.1038/srep33179.

Workman, P., Burrows, F., Neckers, L., and Rosen, N. (2007). Drugging the cancer chaperone HSP90: combinatorial therapeutic exploitation of oncogene addiction and tumor stress. Annals of the New York Academy of Sciences. 1113, 202-216. DOI: 10.1196/annals.1391.012.

Xiao, J., and Ha, T. (2017). Flipping nanoscopy on its head. Science. 355(6325), 582-584. DOI: 10.1126/science.aam5409.

Xie, Q., Wondergem, R., Shen, Y., Cavey, G., Ke, J., Thompson, R., Bradley, R., Daugherty-Holtrop, J., Xu, Y., Chen, E., et al. (2011). Benzoquinone ansamycin 17AAG binds to mitochondrial voltage-dependent anion channel and inhibits cell invasion. Proceedings of the National Academy of Sciences of the United States of America. 108(10), 4105-4110. DOI: 10.1073/pnas.1015181108.

Xu, W., Mimnaugh, E., Rosser, M.F., Nicchitta, C., Marcu, M., Yarden, Y., and Neckers, L. (2001). Sensitivity of mature Erbb2 to geldanamycin is conferred by its kinase domain and is mediated by the chaperone protein Hsp90. The Journal of biological chemistry. 276(5), 3702-3708. DOI: 10.1074/jbc.M006864200.

Xu, W., Mollapour, M., Prodromou, C., Wang, S., Scroggins, B.T., Palchick, Z., Beebe, K., Siderius, M., Lee, M.J., Couvillon, A., et al. (2012). Dynamic tyrosine phosphorylation modulates cycling of the HSP90-P50(CDC37)-AHA1 chaperone machine. Molecular cell. 47(3), 434-443. DOI: 10.1016/j.molcel.2012.05.015.

Xu, W., and Neckers, L. (2007). Targeting the molecular chaperone heat shock protein 90 provides a multifaceted effect on diverse cell signaling pathways of cancer cells. Clinical cancer research : an official journal of the American Association for Cancer Research. 13(6), 1625-1629. DOI: 10.1158/1078-0432.CCR-06-2966.

Xu, W., Yuan, X., Xiang, Z., Mimnaugh, E., Marcu, M., and Neckers, L. (2005). Surface charge and hydrophobicity determine ErbB2 binding to the Hsp90 chaperone complex. Nature structural & molecular biology. 12(2), 120-126. DOI: 10.1038/nsmb885.

Xu, Y., and Lindquist, S. (1993). Heat-shock protein hsp90 governs the activity of pp60v-src kinase. Proceedings of the National Academy of Sciences of the United States of America. 90(15), 7074-7078. Published online 1993/08/01.

Yang, K., Shi, H., Qi, R., Sun, S., Tang, Y., Zhang, B., and Wang, C. (2006). Hsp90 regulates activation of interferon regulatory factor 3 and TBK-1 stabilization in Sendai virus-infected cells. Molecular biology of the cell. 17(3), 1461-1471. DOI: 10.1091/mbc.E05-09-0853.

Yang, Y., Fiskus, W., Yong, B., Atadja, P., Takahashi, Y., Pandita, T.K., Wang, H.G., and Bhalla, K.N. (2013). Acetylated hsp70 and KAP1-mediated Vps34 SUMOylation is required for autophagosome creation in autophagy. Proceedings

of the National Academy of Sciences of the United States of America. 110(17), 6841-6846. DOI: 10.1073/pnas.1217692110.

Young, J.C., Hoogenraad, N.J., and Hartl, F.U. (2003). Molecular chaperones Hsp90 and Hsp70 deliver preproteins to the mitochondrial import receptor Tom70. Cell. 112(1), 41-50.

Young, J.C., Moarefi, I., and Hartl, F.U. (2001). Hsp90: a specialized but essential protein-folding tool. The Journal of cell biology. 154(2), 267-273.

Young, J.C., Obermann, W.M., and Hartl, F.U. (1998). Specific binding of tetratricopeptide repeat proteins to the C-terminal 12-kDa domain of hsp90. The Journal of biological chemistry. 273(29), 18007-18010.

Zhao, R., Davey, M., Hsu, Y.C., Kaplanek, P., Tong, A., Parsons, A.B., Krogan, N., Cagney, G., Mai, D., Greenblatt, J., et al. (2005). Navigating the chaperone network: an integrative map of physical and genetic interactions mediated by the hsp90 chaperone. Cell. 120(5), 715-727. DOI: 10.1016/j.cell.2004.12.024.

Zhou, W., Ryan, J.J., and Zhou, H. (2004). Global analyses of sumoylated proteins in Saccharomyces cerevisiae. Induction of protein sumoylation by cellular stresses. The Journal of biological chemistry. 279(31), 32262-32268. DOI: 10.1074/jbc.M404173200.

Zierer, B.K., Rubbelke, M., Tippel, F., Madl, T., Schopf, F.H., Rutz, D.A., Richter, K., Sattler, M., and Buchner, J. (2016). Importance of cycle timing for the function of the molecular chaperone Hsp90. Nature structural & molecular biology. 23(11), 1020-1028. DOI: 10.1038/nsmb.3305.

Zou, J., Guo, Y., Guettouche, T., Smith, D.F., and Voellmy, R. (1998). Repression of heat shock transcription factor HSF1 activation by HSP90 (HSP90 complex) that forms a stress-sensitive complex with HSF1. Cell. 94(4), 471-480.

Zuehlke, A.D., Beebe, K., Neckers, L., and Prince, T. (2015). Regulation and function of the human HSP90AA1 gene. Gene. 570(1), 8-16. DOI: 10.1016/j.gene.2015.06.018.

Zuehlke, A.D., and Johnson, J.L. (2012). Chaperoning the chaperone: a role for the co-chaperone Cpr7 in modulating Hsp90 function in Saccharomyces cerevisiae. Genetics. 191(3), 805-814. DOI: 10.1534/genetics.112.140319.

Zungu, M., Schisler, J., and Willis, M.S. (2011). All the little pieces. -Regulation of mitochondrial fusion and fission by ubiquitin and small ubiquitin-like modifer and their potential relevance in the heart. Circulation journal : official journal of the Japanese Circulation Society. 75(11), 2513-2521.